Development of new methodologies for dating in the forensic field, combining analytical techniques with multivariate regression treatments

Laura Ortiz Herrero

March 2021

eman ta zabal zazu
Universidad del País Vasco
Euskal Herriko Unibertsitatea
CAMPUS OF INTERNATIONAL EXCELLENCE

Development of new methodologies for dating in the forensic field, combining analytical techniques with multivariate regression treatments

Presented by

Laura Ortiz Herrero

Supervisors

Miren Itxaso Maguregui Olabarria

Luis Bartolomé Moro

A dissertation presented in candidacy for the degree of International Doctor of Philosophy from the University of the Basque Country (UPV/EHU)

March 2021

Analytical Chemistry Department

Faculty of Science and Technology

CAMPUS OF INTERNATIONAL EXCELLENCE

A mi familia

A Dani

Acknowledgments

The completion of this thesis has been possible thanks to the recruitment grant for the training of research staff (PIF16/114), the research mobility and dissemination grant (MOV18/93) and the research group grants (GIU16/04 and GIU19/068) awarded by the University of the Basque Country (UPV/EHU). Likewise, to the support of the Fundação para a Ciência e a Tecnologia (FCT) through the Projects UIDB/00313/2020 and UIDP/00313/2020. Finally, thanks to the income from the analyses performed in real-life settings under the application of the DATINK method with the collaboration of LEYAS Investigaciones Forenses Documentales S.L. [1].

[1] I. San Román, L. Bartolomé, M.L. Alonso, R.M. Alonso, M. Ezcurra, DATINK pilot study: an effective methodology for ballpoint pen ink dating in questioned documents, *Anal. Chim. Acta* 892 (2015) 105–114. https://doi.org/10.1016/j.aca.2015.08.038.

Cuando comencé este proyecto me pareció que cuatro años eran mucho tiempo, a pesar de ello, y casi sin darme cuenta ya me encuentro en la recta final. Quiero mostrar mi agradecimiento a todos aquellos que de uno u otro modo me han ayudado a crecer como persona e investigadora, contribuyendo, cada uno a su manera, a que esta tesis haya sido posible.

Mis primeras palabras van dirigidas a mis directores de tesis doctoral. Al Dr. Luis Bartolomé, Txesko para sus compañeros, por depositar su confianza en mí desde el primer año de prácticas en SGIker. Por enseñarme, por darme la oportunidad de trabajar bajo su dirección y por tener la capacidad de guiarme positivamente tanto en la realización de esta tesis como en mi formación investigadora. A la Dra. Itxaso Maguregui por su inestimable ayuda y dedicación, experiencia, disponibilidad y paciencia para resolver siempre mis dudas. Y a la Dra. Mariluz Alonso por su amabilidad y ayuda fundamental en el laboratorio cuando más necesario era.

Asimismo, quiero agradecer a la profesora Rosa María Alonso el haberme dado la oportunidad de pertenecer a su grupo de investigación FARMARTEM, de lo que estoy muy orgullosa. Sus importantes consejos y constantes ánimos para presentarme a cualquier conferencia, curso o jornada han ayudado a superarme y a ampliar mi formación.

Irene, gracias por tu colaboración en esta tesis. Fue una suerte coincidir contigo en la conferencia celebrada en Brujas y compartir unos buenos ratos de turismo y diversión.

Gracias a todos los integrantes del laboratorio, a los que están y a los que ya se fueron, por crear el mejor ambiente de trabajo. Oskar, gracias por tu ayuda y consejos que siempre he tenido muy en cuenta tanto en el laboratorio como en docencia. Gracias a mis compañeras con las que he

estado desde el comienzo de la tesis; Oihane por tu disposición a ayudarme en todo y Bea siempre por tu compañía, has hecho que me sintiera muy bien acogida en Burdeos y para nada sola en Granada. Gracias Ruth por los buenos ratos compartidos este último año en el laboratorio, aunque cortos, siempre guardaré un buen recuerdo de ellos. Finalmente, quiero tener unas palabras de agradecimiento especiales para ti, Omaira, por tu apoyo, tus buenos consejos, nuestras conversaciones dentro y fuera del laboratorio y por tu visita a Coimbra que me hizo sentir como si volviera a casa. Espero que sigamos siendo amigas por mucho tiempo.

En este punto, quiero reconocer la colaboración de la Sección de Documentoscopia de la Comisaría General de Policía Científica, la Sección de Documentoscopia y Grafística de la Unidad de la Policía Científica de la Ertzaintza, el Centro de Instrumentación Científica (CIC) y el Departamento de Medicina Legal, Toxicología y Antropología Física de la Universidad de Granada, el equipo de Investigación en Química Forense (INQUIFOR) de la Universidad de Alcalá, a los artistas Jesús Mari Lazkano y Luis Candaudap y a los Servicios Generales de Investigación (SGIker) de la Unidad de Bizkaia de la UPV/EHU que han hecho posible esta tesis proporcionándome las muestras y el equipamiento necesarios.

Me gustaría agradecer a la Universidad de Coimbra en Portugal y en especial al profesor J. Sérgio Seixas de Melo el haberme aceptado en su grupo de investigación. Su ayuda y acogida durante mi estancia en Coimbra fueron clave en el progreso de este trabajo. A todos los compañeros del laboratorio que estuvieron siempre pendientes de mí, especialmente a Catarina y a Ana Clara que me ayudaron en todo momento con el funcionamiento de los equipos, con los análisis y mis dudas, también les dedico estas líneas de agradecimiento. Para finalizar y de forma sincera quiero agradecer a Ana Cristina de Almeida Assis,

experta forense de la Polícia Judiciária de Lisboa, su ayuda en la realización de los análisis que fueron fundamentales para el desarrollo de esta tesis y el haberme permitido acceder al equipo Vis-MSP. A todos ellos, MUITO OBRIGADA!

A mis amigos de Coimbra, Fany, Roberto, Emilio, Dani, Danielle, Aingeru, Denisse, Martina y Poonam, que me arroparon sin dudar. No olvidaré nunca los momentos que pasamos juntos fuera de la universidad, nuestras barbacoas, nuestros viajes por Portugal, los sitios curiosos que me enseñasteis de Coimbra, que absolutamente todos, me encantaron. Mil gracias por vuestra amistad sincera que empezó allí y que espero sea para toda la vida. Fany, gracias porque tú fuiste la culpable de conocerles. Por todos tus consejos y ayuda antes, durante y después de mi estancia en Coimbra, tanto dentro como fuera del laboratorio. No pude tener más suerte cuando Sérgio me puso en contacto contigo.

A mis compañeros de carrera por todas las horas compartidas, que no han sido pocas. Y a mis amigas de siempre y de ahora, Ainhize, Silvia, Raquel, Arrate, Lorea y Sara, gracias por estar siempre a mi lado y conseguir hacerme desconectar cuando más duro era el trabajo.

Por último, y más importante, quiero reconocer el apoyo y el ánimo que me ha dado mi familia durante todos estos años. Ama y aita, gracias por sentiros orgullosos de cada paso que he dado para alcanzar mis metas, por vuestra infinita paciencia, por recorrer cientos de kilómetros para visitarme en Coimbra y por haber sido también parte de esta tesis. Adri y Amaia, gracias por haberme acompañado en este largo camino. Habéis sido un pilar fundamental durante esta etapa y sin vosotros nunca habría llegado hasta aquí. Por ello, os dedico también esta tesis.

Dani, lo mejor de estos cuatro años sin duda has sido tú. Fue una suerte conocerte en Coimbra y que te convirtieras en un apoyo imprescindible durante mi estancia allí. No sabes lo importante que han sido tus consejos y tu ayuda a lo largo de esta tesis, especialmente en esta última etapa. Siempre has estado a mi lado, animándome a seguir y enseñándome a creer en mi misma y a que puedo hacer todo lo que me proponga o se me ponga por medio. Por supuesto, esta tesis también va dedicada a ti.

“¿Qué es el tiempo? Si nadie me lo pregunta, lo sé. Pero si tuviese que explicárselo a alguien no sabría cómo hacerlo”

San Agustín

“Todos nacemos siendo originales y la mayoría acaban siendo copias”

Carl Jung

Table of contents

Summary

Whenever a crime is committed, there is always a unity of time, place and action that forensic experts will aim to demonstrate throughout the investigation. Determining the succession, simultaneity, frequency or duration of criminal activities as well as the age of objects, persons and traces is therefore one of the most important goals of forensics in reconstructing the crime scene or in finding and understanding the connections between the evidence and the suspects involved therein. However, time has been largely unexplored due to the complexity of the overall challenge at hand, not yet successfully overcome by single cutting-edge techniques. The coupling of such techniques with chemometrics, more specifically with multivariate regression methods, could turn this situation upside down thanks to the development of age quantitation methodologies based on the modelling of the modifications experienced by the evidence in its properties with respect to time. The potential applicability of these chemometric tools, however, remains poorly understood and underexploited due to their recent introduction into forensic dating research and the statistical background required for their optimal application. That is why this thesis focuses on highlighting the usefulness of multivariate regression methods in several forensic fields, such as questioned documents, art forgery and medico-legal death investigation, through the development and validation of dating methodologies in which non-destructive and micro-destructive techniques are applied together with the (orthogonal) partial least squares regression ((O)PLSR) method.

Chapter 1 presents a general introduction, covering the main aspects of forensic dating and the application of multivariate regression methods thereto. A theoretical framework is also included in which the methodology to be adopted in forensic dating and how to overcome the most common

drawbacks are presented, starting with the pre-processing of data, followed by chemometric modelling and validation and ending with the external validation of the methodology developed.

Chapter 2 presents two complementary approaches, direct and indirect, to estimate the age of relatively old documents through micro-destructive analysis of the paper support by pyrolysis-gas chromatography/mass spectrometry (Py-GC/MS). The applicability of both approaches was evaluated by studying several office documents under police custody. On the one hand, the direct approach, based on a multivariate regression model built from pyrolytic profiles of artificially aged paper samples, successfully estimated the age of relatively old documents (up to 30 years old) and established the equivalence of 5 h in a combined climatic test chamber with one natural year under police custody conditions, for further studies. This approach could be applied to paper supports with the same or similar composition and stored under storage conditions comparable to those of the study. On the other hand, the indirect approach, based on the identification of compounds characteristic of the time of production of the paper support, was a valuable complementary tool to ratify the age of the documents estimated by the direct approach. Both approaches could be a promising alternative and/or complementary methodologies to those used to estimate the age of a questioned document based on the ink strokes found on it, especially when no ink entry is present or when the documents are between 5 and 30 years old, exceeding the scope of application of such methodologies.

Chapter 3 explores the feasibility of dating ballpoint pen ink brushstrokes by monitoring the modifications in the UV-Vis-NIR diffuse reflectance spectra of artificially aged Inoxcrom® brand inks and their subsequent modelling with respect to time using the PLSR method. The PLS model was applied to five brands and predicted accurate dates with a 25% error

for two of the studied brands, while for the other three, there was a lack of fit to the model due to the different chromatographic profile they showed with respect to that of the Inoxcrom® ink brand. It was also possible to define the region of the UV-Vis-NIR spectrum directly related to the ink ageing processes. Moreover, one hour of artificial ageing was established to be equivalent to approximately 143 hours of natural ageing under the conditions studied, so the methodology could have applicability in the non-destructive dating of ballpoint pen inks up to 5 years old, sharing a common chromatographic profile with the Inoxcrom® ink brand. Advantage would be gained over existing methods that rely on solvent analysis for ink age estimation, as they are destructive and, for the most part, with a temporal scope of up to two years.

Chapter 4 presents a non-invasive methodology for dating ink strokes on handwritten documents made with different ballpoint pen and gel pen brands by applying Vis-microspectrophotometry (Vis-MSP) combined with OPLSR. The methodology was externally validated against blind samples provided by the Forensic Science Unit of the Basque Country Police Department, reinforcing the strength and reliability of the methodology. The methodology was able to predict the age with an error of less than 25% for handwritten documents made with different pen ink brands and exposed to the same or slightly different storage conditions than those applied in the study, whenever the established pre-requirements were met. In addition, the methodology was able to detect those documents above or below its temporal application range. This methodology is a breakthrough in the field of ink dating, as it is applicable to cases of document falsification of up to at least 2 years when kept under regular police custody conditions. Furthermore, the method provides micro-level analysis of ink strokes without damaging the integrity of the document, ensuring accurate predictions of the ink age with 95% confidence with which to make firm decisions in court.

Chapter 5 is devoted to contemporary artistic paint dating with a scope on forgery detection. It describes the development of multivariate OPLS regressions from Fourier transform infrared-attenuated total reflectance (FTIR-ATR) spectra of artificially aged Liquitex® and Hyplar® brand paints for application to contemporary artwork dating. In spite of the fact that the OPLS models of both paint brands were characterised throughout the ageing process by the modifications of the same paint components, it was not possible to develop a universal OPLS model due to the different ageing trends that each one presented, thus requiring the development of individual models for each brand. The applicability of the OPLS model of the Liquitex® paint brand was tested in artworks provided by internationally recognised contemporary Basque artists. Approximately 50 hours of accelerated ageing under the applied conditions were equivalent to one natural year. By means of this correlation, artworks up to at least 22 years old preserved under comparable conditions and created with the same paint formulation could be dated. This methodology sets a precedent in the potential application of multivariate regression methods to the dating of contemporary artworks, in addition to providing valuable information on the processes involved in the ageing of acrylic paints, fundamental for the development of conservation and restoration strategies.

Chapter 6 presents an extension study on the robustness and applicability of multivariate regression models, built for the Liquitex® brand, to the age estimation of three colours of acrylic paints from two different manufacturers, subjected to accelerated ageing. The influence of the pigment in the ageing process of the paints, the type and quantity of additives present in them as well as the ageing conditions to which they were subjected were decisive in the short-term model, which resulted in a lack of fit of the samples to the model and, therefore, high inaccuracies in the predicted age values. But, on the other hand, the slower degradation processes and the stabilisation of the paints at higher stages of ageing

made the long-term model robust and applicable to the estimation of the age of different colours of the same brand of acrylic paint as well as of acrylic paints of different brands that were artificially long-term aged under slightly different conditions. We concluded that the long-term model could be applied to the dating of contemporary artworks from 14 to at least 22 years of age with an error of less than 23%, created with any acrylic paint regardless of the brand or paint colour used by the artist or the conditions under which they were preserved.

Chapter 7 focuses on the field of medico-legal death investigation and describes the OPLS modelling of Raman spectral modifications experienced by human skeletal remains with respect to the post-mortem interval (PMI). The proposed methodology aims to provide a reliable quantification of the PMI as well as an invaluable tool for the identification and characterisation of the most influential spectral regions during the burial period, which in turn would provide additional important information for the estimation of the PMI. In order to fulfil these scopes and be applicable in real scenarios, the OPLS model was externally validated with bone samples coming from cemetery niches with a large inter-individual variability. The coupling of Raman spectroscopy with multivariate regression methods had previously demonstrated its effectiveness in synthetic laboratory samples and now it has done so with real human skeletons, presenting itself as an additional and/or complementary tool to those already existing for the determination of the PMI. Moreover, the great inter-individual variability of the skeletons and the large number of external and internal factors that influence their diagenesis have been decisive to fail in the construction of an OPLS model capable of estimating with acceptable accuracy the PMI of all the samples in the validation set. Nevertheless, the estimates were highly promising for those samples to which the OPLS model was able to respond, opening up the possibility of determining the PMI of human skeletal remains (15 years ≤ PMI ≤ 87 years)

that have been buried in similar or equal conditions to those of the cemetery niches and in a geographic location with a Mediterranean climate.

Chapter 8 presents a general discussion of the work developed in this thesis as well as the prospects for the implementation of emerging imaging techniques together with multivariate regression methods to forensic dating.

Finally, **Chapter 9** draws the main conclusions from the results of this thesis.

Resumen

Siempre que se comete un delito, existe una unidad de tiempo, lugar y acción cuya demostración será el objetivo de los peritos forenses a lo largo de la investigación correspondiente. Determinar la sucesión, la simultaneidad, la frecuencia o la duración de las actividades delictivas, así como la antigüedad de los objetos, las personas y los rastros es, por lo tanto, uno de los propósitos más importantes de la ciencia forense. Estas revelaciones permitirán la reconstrucción del lugar del delito o el descubrimiento y la comprensión de las conexiones entre las pruebas y los sospechosos implicados en el mismo. Sin embargo, el tiempo ha permanecido prácticamente inexplorado debido a la complejidad del reto global que plantea, aún no superado con éxito mediante la utilización individual de técnicas analíticas de vanguardia. El acoplamiento de dichas técnicas con la quimiometría, más específicamente, con los métodos de regresión multivariante, podría revertir esta situación gracias al desarrollo de metodologías de estimación de edad basadas en la modelización de las modificaciones temporales experimentadas por las propiedades de las evidencias. No obstante, la aplicabilidad potencial de estas herramientas quimiométricas sigue siendo poco conocida y explotada debido a su reciente introducción en el campo de la datación forense y a la relativa complejidad de los conocimientos estadísticos necesarios para su aplicación óptima. Por ello, la investigación descrita en esta tesis se ha centrado en poner de relieve la utilidad de los métodos de regresión multivariante (regresión de mínimos cuadrados parciales (ortogonales), (O)PLSR) en diferentes campos forenses, como el de los documentos cuestionados, las falsificaciones en el arte y las investigaciones médico-legales, con el fin de realizar dataciones mediante la aplicación de técnicas no destructivas y/o microdestructivas.

En el **capítulo 1** se presenta una introducción general que abarca los principales aspectos de la datación forense y la aplicación de los métodos de regresión multivariante a la misma. También se incluye un marco teórico en el que se presenta la metodología que se ha de seguir en la datación forense y cómo superar los inconvenientes más comunes, comenzando por el pretratamiento de los datos, seguido de la modelización y validación quimiométrica y finalizando con la validación externa de la metodología desarrollada.

En el **capítulo 2** se presentan dos enfoques complementarios, directo e indirecto, para estimar la edad de documentos relativamente antiguos mediante el análisis microdestructivo del papel por pirólisis-cromatografía de gases/espectrometría de masas (Py-GC/MS). La aplicabilidad de ambos enfoques se evaluó estudiando varios documentos bajo custodia policial. Por una parte, el enfoque directo, basado en un modelo de regresión multivariante construido a partir de perfiles pirolíticos de muestras de papel envejecidas artificialmente, estimó con éxito la edad de documentos relativamente antiguos (hasta 30 años de edad) y estableció para su aplicación en estudios posteriores la equivalencia de 5 h en cámara climática de ensayo combinado respecto a un año natural bajo condiciones de custodia policial. Este enfoque podría aplicarse a los soportes de papel de composición igual o similar y almacenados en condiciones de almacenamiento comparables a las del estudio. Por otra parte, el enfoque indirecto, basado en la identificación de los compuestos característicos y distintivos del momento de la producción del papel, constituyó una valiosa herramienta complementaria para ratificar la edad de los documentos. Ambos enfoques podrían ser una alternativa prometedora y/o complementaria a las metodologías utilizadas habitualmente para estimar la edad de un documento cuestionado, basadas en el análisis de los trazos de tinta realizados en el mismo. Las metodologías propuestas resultarían de especial interés cuando el

documento no presente entradas de tinta o tenga una antigüedad de entre 5 y 30 años, excediendo el alcance de aplicación de las metodologías tradicionales.

El **capítulo 3** explora la viabilidad de la datación de tintas viscosas mediante la monitorización de las modificaciones en los espectros de reflectancia difusa UV-Vis-NIR de las tintas de la marca Inoxcrom® envejecidas artificialmente y su posterior modelización con respecto al tiempo mediante el método PLSR. El modelo PLS estimó el tiempo de envejecimiento con un error del 25% para dos de las cinco marcas de tinta de bolígrafo estudiadas. Para las otras tres marcas de tinta de bolígrafo, hubo una falta de ajuste al modelo debido al diferente perfil cromatográfico que mostraron con respecto al de la marca de tinta Inoxcrom®. También fue posible delimitar la región del espectro UV-Vis-NIR relacionada con el proceso de envejecimiento de la tinta. Además, se estableció que una hora de envejecimiento artificial equivalía a aproximadamente 143 horas de envejecimiento natural bajo las condiciones estudiadas, de modo que la metodología podría tener aplicabilidad en la datación no destructiva de tintas de bolígrafo de hasta 5 años de edad que compartan un perfil cromatográfico común con la marca de tinta Inoxcrom®. Las ventajas sobre los métodos existentes basados en el análisis de disolventes para la estimación de la edad de la tinta son evitar la destrucción de la muestra y un mayor alcance temporal superando la barrera de los dos años.

En el **capítulo 4** se presenta una metodología no invasiva para datar los trazos de tinta en documentos manuscritos realizados con diferentes marcas de bolígrafo de tinta viscosa y gel mediante la aplicación de la técnica microespectrofotometría visible (Vis-MSP) combinada con el método OPLSR. La metodología fue validada externamente frente a muestras ciegas proporcionadas por la Unidad de Ciencias Forenses del Departamento de Policía del País Vasco, reforzando así su solidez y

fiabilidad. El método desarrollado fue capaz de estimar la edad con un error inferior al 25% en documentos manuscritos realizados con diferentes marcas de tinta de bolígrafo y expuestos a condiciones de almacenamiento iguales o ligeramente diferentes a las empleadas en el estudio, siempre y cuando se cumplieran los requisitos previos establecidos. Además, se pudo detectar aquellos documentos por encima o por debajo del rango de aplicación temporal del método, pudiéndose así establecer límites inferiores y superiores respecto a la posible datación de dichos documentos. Esta metodología constituye un gran avance en el campo de la datación de tintas, ya que es aplicable a los casos de falsificación de documentos de hasta, por lo menos, 2 años de edad cuando son conservados bajo condiciones normales de custodia policial. Además, el método proporciona un análisis a nivel micro de los trazos de tinta sin dañar la integridad del documento, garantizando predicciones exactas de la edad de la tinta con un 95% de confianza, constituyendo así un respaldo importante en la toma de decisiones judiciales.

El **capítulo 5** está dedicado a la datación de la pintura artística contemporánea con proyección a la detección de falsificaciones. Describe el desarrollo de regresiones multivariantes OPLS a partir de espectros obtenidos por espectroscopia infrarroja con transformada de Fourier-reflectancia total atenuada (FTIR-ATR) de pinturas de la marca Liquitex® e Hyplar® envejecidas artificialmente, para su aplicación a la datación de obras de arte contemporáneo. A pesar de que los modelos OPLS de ambas marcas de pintura se caracterizaron a lo largo del proceso de envejecimiento por las modificaciones de componentes comunes en la pintura, no fue posible desarrollar un modelo OPLS universal debido a las diferentes tendencias de envejecimiento que presentó cada una de ellas, requiriendo por tanto el desarrollo de modelos individuales para cada marca. La aplicabilidad del modelo OPLS de la marca de pintura Liquitex® se puso a prueba en obras de arte proporcionadas por artistas vascos

contemporáneos de renombre internacional. Aproximadamente 50 horas de envejecimiento acelerado bajo las condiciones aplicadas fueron equivalentes a un año natural. Por medio de esta correlación, se podrían datar obras de arte de al menos 22 años de antigüedad conservadas en condiciones comparables y creadas con la misma formulación de pintura. Esta metodología sienta un precedente en la posible aplicación de métodos de regresión multivariante a la datación de obras de arte contemporáneo, además de proporcionar una valiosa información sobre los procesos que intervienen en el envejecimiento de las pinturas acrílicas, fundamental para el desarrollo de estrategias de conservación y restauración.

En el **capítulo 6** se presenta un estudio ampliado sobre la robustez y aplicabilidad de los modelos de regresión multivariante construidos a partir de la marca Liquitex® a la estimación de la edad de tres colores de pinturas acrílicas de dos fabricantes diferentes, sometidas a envejecimiento acelerado. La influencia del pigmento en el proceso de envejecimiento de las pinturas, el tipo y la cantidad de aditivos presentes en ellas, así como las condiciones de envejecimiento a las que fueron sometidas, fueron decisivas en el modelo a corto plazo, lo que dio lugar a una falta de ajuste de las muestras al modelo y, por consiguiente, a elevadas imprecisiones en los valores de edad predichos. Sin embargo, los procesos de degradación más lentos y la estabilización de las pinturas en etapas más avanzadas de envejecimiento hicieron que el modelo a largo plazo fuera robusto y aplicable a la estimación de la edad de diferentes colores de la misma marca de pintura acrílica, así como de pinturas acrílicas de diferentes marcas que fueron envejecidas artificialmente a largo plazo en condiciones ligeramente diferentes. Concluimos que el modelo a largo plazo es robusto y podría aplicarse a la datación de obras de arte contemporáneo de edades iguales o superiores

a los 14-22 años, con un error inferior al 23%, con independencia de la marca empleada, los colores y las condiciones de almacenamiento.

El **capítulo 7** se centra en el campo de la investigación médico-legal de restos mortales y describe el modelado OPLS de las modificaciones espectrales Raman experimentadas por restos óseos humanos en relación al intervalo post-mortem (PMI). La metodología propuesta tiene por objeto proporcionar una cuantificación fiable del PMI, así como constituir una herramienta inestimable para la identificación y caracterización de las regiones espectrales más influyentes durante el período de enterramiento, lo que a su vez proporcionaría información adicional importante para la estimación del PMI. Para cumplir estos objetivos y ser aplicable en escenarios reales, el modelo OPLS fue validado externamente con muestras óseas procedentes de nichos de cementerio con una gran variabilidad interindividual. El acoplamiento de la espectroscopia Raman con los métodos de regresión multivariante ya había demostrado anteriormente su eficacia en muestras sintéticas de laboratorio y ahora lo ha hecho con esqueletos humanos reales, presentándose como una herramienta adicional y/o complementaria a las ya existentes para la determinación del PMI. Por otra parte, la gran variabilidad interindividual de los esqueletos y el gran número de factores externos e internos que influyen en su diagénesis han sido decisivos para fracasar en la construcción de un modelo OPLS capaz de estimar con una precisión aceptable el PMI de todas las muestras del conjunto de validación. Sin embargo, las estimaciones fueron altamente prometedoras para aquellas muestras a las que el modelo OPLS pudo responder, abriendo la posibilidad de determinar el PMI de restos óseos humanos (15 años ≤ PMI ≤ 87 años) que han sido enterrados en condiciones similares o iguales a las de nichos y en una ubicación geográfica con clima mediterráneo.

En el **capítulo 8** se presenta una discusión general de los trabajos realizados y descritos en esta tesis, así como las perspectivas que presentan las técnicas de imagen emergentes junto a los métodos de regresión multivariante para la datación forense.

Finalmente, en el **capítulo 9** se extraen las principales conclusiones de los resultados de esta tesis.

List of abbreviations

AART	Automatic adjustment of retention time
ANN	Artificial neural networks
CMYK	Cyan, magenta, yellow and key
E	Predictive accuracy error
FTIR-ATR	Fourier transform infrared-attenuated total reflectance
HCA	Hierarchical cluster analysis
HPLC-DAD	High-performance liquid chromatography-diode-array detector
HSI	Hyperspectral imaging
IR	Infrared
kNN	k-nearest neighbour
LDA	Linear discriminant analysis
LS-SVM	Least squares-support vector machine
LV	Latent variable
MCR	Multivariate curve resolution
MLR	Multiple linear regression
MSC	Multiplicative scatter correction
NIR	Near-infrared
(O)PLS-DA	(Orthogonal) partial least squares-discriminant analysis
(O)PLSR	(Orthogonal) partial least squares regression
PB29	Ultramarine blue
PCA	Principal component analysis
PCR	Principal component regression
p(EA-MMA)	poly(ethyl acrylate-methyl methacrylate)
PEO	Poly(ethylene oxide)
PG7	Chlorinated copper phthalocyanine green
PMI	Post-mortem interval
p(nBA-MMA)	poly(n-butyl acrylate-methyl methacrylate)

PY3	Hansa yellow 10G
Py-GC/MS	Pyrolysis-gas chromatography/mass spectrometry
Q^2	Goodness-of-prediction
R^2 CV	Coefficient of determination of cross-validation
R^2 P	Coefficient of determination of prediction
R^2X/Y	Goodness-of-fit
RGB	Red, green and blue
RMSECV	Root mean square error of cross-validation
RMSEE	Root mean square error of estimation
RMSEP	Root mean square error of prediction
RT	Retention time
RTL	Retention time locking
SG	Savitzky-Golay
SIMCA	Soft independent modelling of class analogy
SNV	Standard normal variate
SVM	Support vector machines
UV	Ultraviolet
UV	Unit variance
Vis	Visible
Vis-MSP	Vis-microspectrophotometry

Objectives

The role that state-of-the-art techniques along with multivariate regression methods play in the estimation of the age of forensic evidence remains largely unexplored. Therefore, the main objective of this thesis was to highlight their usefulness in the field of questioned documents, art forgery and medico-legal death investigation through the development and validation of dating methodologies applying non-destructive and micro-destructive techniques together with the (O)PLSR method. The specific objectives undertaken to achieve this goal were:

I: Selection and setting up of sampling and artificial ageing procedures in combined climatic test chambers under controlled conditions with which to cover wide intervals of time.

II: Direct dating by building (O)PLS models that correlate the spectral/chromatographic modifications undergone by the different samples with their age as well as indirect dating by identifying compounds within the samples that are characteristic of specific time periods.

III: Optimisation of (O)PLS models and development of a guideline for the fine-tuning of multivariate regression methods in forensic dating.

IV: Optimisation of different analytical techniques according to the objectives pursued.

V: Application of the chemometric-based methodologies developed in this work to real-life scenarios by collaborating with artists, scientific police units and academic institutions in order to establish reliable correlations between accelerated ageing and their natural equivalents as well as to conduct external validation.

VI: Extraction of supplementary time-related information from chemometric tools with which to study and understand the modifications that the different samples undergo throughout the ageing process.

Thesis structure

This thesis is structured in nine chapters.

Chapter 1, which is a part of a scientific paper, presents a general introduction that includes the main aspects of forensic dating and the application of multivariate regression methods thereto. This chapter also covers the theoretical framework, outlining the methodological approach followed throughout this thesis for the optimal use of multivariate regression methods in forensic dating as well as describing how to overcome the most frequent drawbacks found in each work, which will be further developed in the corresponding chapters.

Chapters 2 to 7 present six scientific papers in the area of questioned documents, art forgery and medico-legal death investigation that gather the experimental work and results of this thesis. **Chapter 2** deals with the development of two complementary approaches, direct and indirect, to estimate the age of the paper support in handwritten documents using Py-GC/MS. **Chapter 3** addresses a non-destructive methodology for pen ink brushstroke dating by applying the PLS regression method to UV-Vis-NIR reflectance spectra. One drawback is that the large size of the ink samples used in the work reported in this chapter is not representative of the handwritten strokes present in real-life document examinations. Therefore, **Chapter 4** presents the transition from this methodology to real-life scenarios using the Vis-MSP technique. **Chapter 5** deals with counterfeiting in contemporary painting and describes the development of multivariate OPLS regressions from FTIR-ATR spectra of acrylic paints for age estimation of contemporary artworks. **Chapter 6** is an extension study in which the robustness and applicability of such multivariate regressions are proved by applying them to acrylic paints from various manufacturers containing different pigments and exposed to slightly varying preservation

conditions. **Chapter 7** deals with the medico-legal death investigation field and covers a post-mortem interval estimation methodology using Raman spectroscopy together with OPLS regression.

Chapter 8 presents a general discussion of the work developed and described in this thesis as well as the prospects for the implementation of emerging imaging techniques together with multivariate regression methods to forensic dating.

In **Chapter 9**, the main conclusions are drawn from the results of this thesis.

The annex contains the list and the cover of the scientific publications included in this thesis.

CHAPTER 1

General introduction and theoretical framework

An adapted version of

Multivariate regression methods in forensic dating

L. Ortiz-Herrero, M.I. Maguregui, L. Bartolomé

TrAC Trends in Analytical Chemistry, **2021** (under review)

Q1, IF: 9.801, 2/86, Chemistry, Analytical

1.1 General introduction

1.1.1 Forensic dating

The aim of forensics is to provide all persons involved in an investigation and criminal proceedings with the scientific evidence and tools necessary to reconstruct a crime and deliver a fair sentence. Thus, forensic chemistry may be defined as the chemistry exercised in the service of the law. Although analytical chemistry is the ground discipline of forensic chemistry, other chemical disciplines, auxiliary sciences and forensic science disciplines are increasingly applied to overcome scientific and legal constraints [1], e.g. questioned documents, art forgery, medico-legal death investigation, bloodstain pattern analysis, firearms and tool marks, fire and arson investigation, impression and pattern evidence, trace evidence, etc.. In this regard, dating is widely applied and reported in the aforementioned forensic science disciplines (Figure 1) [2-8].

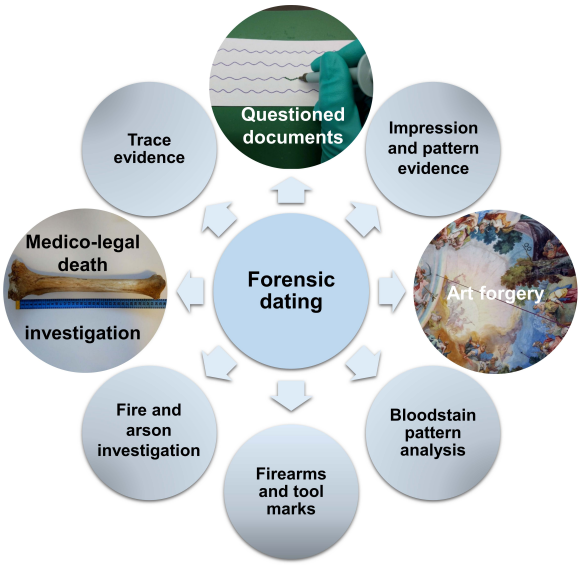

Figure 1. The most common forensic science disciplines in which dating is reported.

When a crime is committed, there is always a unity of time, place and action that the investigation will aim to demonstrate. Situating criminal activities, objects, persons and traces in time is therefore one of the most important goals of forensics. Succession, simultaneity, frequency, duration and age are highlighted as important aspects of time. On this basis, forensics reconstructs the crime scene through the dating of evidence of a physical nature that is indicative of or associated with the criminal event [9]. Thus, estimating the age of the bloodstains found at the crime scene could help determine the approximate period in which the crime was committed as well as link the suspect to the criminal act [2, 10]. In addition, with the knowledge of the victim's post-mortem interval (PMI), an accurate chronology of events could be established with respect to the victim, which would be useful in narrowing the search for missing persons, identifying or eliminating a suspect and directing the investigation [11]. While fingermarks deposited at the crime scene have been widely used for identification purposes, the estimation of their age could determine the time of their transfer, i.e. whether or not the suspect left them during the crime and, therefore, be crucial to the resolution of the case [3]. Moreover, the analysis of evidence from the remains of an arson attack could provide critical information when the deliberate use of flammable liquids to start a fire is suspected. Estimating the length of time an ignitable liquid has been exposed to the effects of weather prior to a fire may help determine its cause and intent [4]. In firearms-related crimes, the estimation of the time that has elapsed since the last discharge or expenditure of ammunition elements could be aimed at identifying the elements most likely to have been used to commit the crime or at situating the discharge of the various firearms-related elements in time in order to reconstruct the course of events [5]. In the case of fraud offences, the legitimacy of an ink entry is often an important issue during the forensic examination of questioned documents. Estimating the approximate time that the ink was deposited on the support could help solve this problem [6]. Likewise, counterfeit or

misattributed artworks could be detected by characterising and estimating the age of the paint used, since its knowledge would make it possible to determine when the artwork was made and whether or not the paint used is representative of the artist's period [8]. Each of these cases highlights the importance of situating an evidence in time across multiple disciplines of forensic science, being of significant added value to the criminal investigation and providing supporting information to investigators and solid evidence to reach unequivocal conclusions in a trial. However, time has been largely unexplored due to the complexity of the overall challenge. Furthermore, the time period studied in forensics is usually considerably short and, therefore, errors of similar size have a greater impact [9]. Thanks to the intrinsic adaptability of forensic chemistry and its continuous innovation and advancement with the support of science, technology and instrumentation, new state-of-the-art analytical techniques are being introduced with which to address the aforementioned drawbacks [1]. Nevertheless, the increasing amount of complex and multi-dimensional data that these techniques generate has made their coupling with chemometrics indispensable in forensic dating [1, 12].

1.1.2 Chemometrics applied to forensic dating

Chemometrics in forensic dating uses mathematical and statistical operations to provide additional information in complex crime cases and to improve the processes of handling and interpreting high-dimensional data [12]. Moreover, the implementation of chemometric tools enables the achievement of more objective and significant results in a fast time domain, while decreasing human error for subsequent decision-making [13]. That is why chemometrics is not a minor tool in forensics and its use is dynamically increasing over the last few years [1, 12-14]. The most widely used chemometric methods in forensics are shown in Figure 2. The choice of

method to be applied will depend on the objective pursued at each crime scene under investigation [12-14].

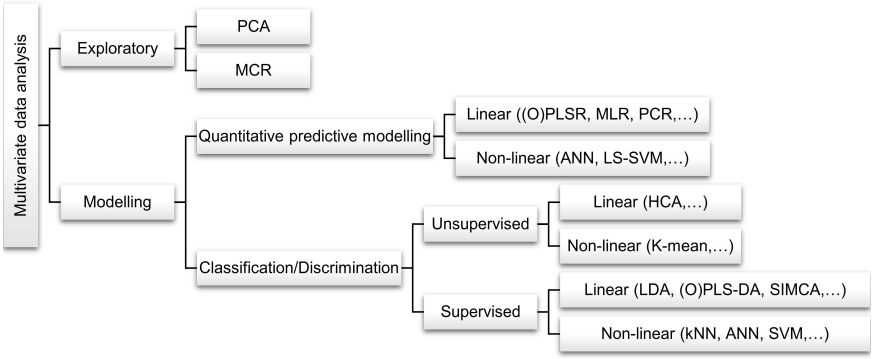

* ANN, artificial neural networks; HCA, hierarchical cluster analysis; kNN, k-nearest neighbour; LDA, linear discriminant analysis; LS-SVM, least squares-support vector machine; MCR, multivariate curve resolution; MLR, multiple linear regression; (O)PLS-DA, (orthogonal) partial least squares-discriminant analysis; (O)PLSR, (orthogonal) partial least squares regression; PCA, principal component analysis; PCR, principal component regression; SIMCA, soft independent modelling of class analogy; SVM, support vector machines.

Figure 2. Chemometric methods used in forensics.

Regression methods model one or several dependent variables (responses, **Y**) through a set of predictor variables (**X**) [15]. Multiple studies have employed these methods to relate **Y** = the characteristics of the samples [2-4, 6-8, 10, 11, 16, 17], the circumstances related to the forensic cases [5, 18] or the quantity of compounds [19-26] to **X** = the analytical response. The aim of multivariate regression methods is therefore to replace the measurement of the property of interest (**Y**), which is often expensive, difficult, time consuming, dangerous, ethically undesirable, etc., by an experimentally measurable signal which, in turn, can be cheaper, faster and more accurately measured by analytical techniques applied to the forensic evidence found at the crime scene [27, 28]. In spite of the various regression methods available, PLSR has been one of the most predominant in forensics. PLSR is a quantitative multivariate analysis method, which uses the two-block predictive PLS model to model the linear relation between two data matrices, **X** and **Y**. It also models the structure

of **X** and **Y**. The usefulness of the PLSR is its ability to analyse data with many, noisy, strongly collinear (correlated) and incomplete **X** and **Y** variables. Moreover, the greater the number of significant variables and observations, the more accurate the model parameters are [15]. Thus, the PLSR enables the investigation of complex forensic issues and the analysis of the collected data in an objective manner. In recent years, it has undergone several extensions and improvements to cope with nonlinearities, multiple variables and systematic but **Y**-irrelevant regularities in the **X** data [29]. OPLSR is a modification of the PLSR method, which separates the systematic variation in **X** into two parts, one that is linearly related (predictive) to **Y** and another that is not related (orthogonal) to **Y**. The OPLSR method can therefore be considered as a modelling and pre-processing method, reducing the complexity of the model and thus improving its interpretation and predictive power. For a single **Y** variable, the OPLS model will always be reduced to a single predictive component [29-31]. Furthermore, the PLS and its extensions can be adapted for classification purposes, such as the (O)PLS-DA [15].

Ageing is a characteristic of all individuals and materials, i.e. their components and, consequently, their properties are altered as a function of time. The monitoring of such modifications with subsequent modelling with respect to time under controlled conditions would allow the evidence found at crime scenes to be situated in time. The (O)PLSR method has been widely and successfully applied in the construction of these age estimation models [2-8, 16, 17]. Despite the potential that this chemometric tool has in dating as well as chemometric methods in general in forensics, the development of standard operating procedures of these methods and their application to real caseworks are still very recent [6, 32]. In short, their implementation in forensic laboratories is still limited. Due to the need for statistical background and the challenge of developing robust, fast and reliable models applicable to real scenarios, forensic experts are reluctant

to use chemometrics on a daily basis. Although this situation is expected to change over the years thanks to the growing number of publications in this field and the collaboration between academic institutions and scientific police units [13, 14].

1.2 Theoretical framework

Throughout this section we will address the methodological approach to be adopted in forensic dating, starting with the pre-treatment of the data, followed by the construction and validation of the (O)PLS models and ending with the external validation of the developed methodology. In addition, the most common difficulties encountered throughout the chapters of this thesis and in recent studies in which the (O)PLSR method has been applied to forensic dating will be presented, as well as how to overcome them. Finally, this approach will be outlined in a flow chart that will serve as an aid and guide on how and what the forensic expert does step-by-step to optimally pre-process the data and use the (O)PLSR method in forensic dating and that will also set the methodological basis for Chapters 2 to 7 of this thesis.

1.2.1 Pre-processing of analytical signals

Evidence taken from crime scenes that need to be dated can range from questioned documents and artworks to explosives and gunshot residues, body fluids, skeletal remains, etc. The wide range of materials encountered at the crime scenes is therefore diverse, complex and often of an unknown nature. In addition, since maintaining material integrity is a legal requirement for counterproof analysis, the insufficient quantity of evidence often available to perform multiple analyses is a major drawback [14]. Due to the limited availability and legal implications of forensic evidence, the analytical techniques applied to forensic dating are mainly characterised

as being micro-destructive or non-destructive [1]. Spectroscopy and chromatography are the most commonly used analytical techniques [2-4, 6-8, 10, 11, 17, 33]. Their choice will depend on the questions posed. Moreover, the technique selected must cover the selectivity, specificity, reproducibility and robustness required for that purpose. Thus, the variety of chemical data with which forensics works when attempting to date evidence is extremely large. These data usually consist of measurements over a continuous range, e.g., spectroscopic data in which the spectrum of a forensic sample is measured over a range of wavelengths or wavenumbers [6, 8], and chromatographic signals in which measurements are made over retention time [17]. They are made up of multiple **X** variables, each of which represents a measurement point in one of the continuous domain mentioned above. These **X** variables are strongly correlated, but do not in themselves represent any defined feature of the measured sample. Information about the composition of the forensic sample, which is usually a mixture of components, and the modifications that these compounds undergo over time is contained in the correlations between these **X** variables. The response of the individual compounds and the ageing processes experienced by each of them is therefore not isolated, as the data include the contributions of all the components present in the forensic sample and the modifications they undergo throughout the ageing process [12]. All this information is used in multivariate modelling for dating purposes. However, irrelevant information from instrumental variation, scattering or spurious radiation and even irrelevant variations from samples can also be found in the high-dimensional data that mask and diminish the weight of time-related **X** variables in the modelling stage, thus causing inaccurate predictions for new samples and affecting the robustness of the model. These data must therefore be pre-processed prior to multivariate modelling to eliminate systematic variation in **X** unrelated to the **Y** vector, in this case the time, while enhancing what is relevant to its prediction [14, 27, 31]. Although data pre-processing is a critical

stage for the achievement of robust and simple models, it is impossible to establish some preliminary rules that guarantee the suitability of a pre-processing for specific data. Which pre-processing is applied will depend on the objective set, the type of data collected and the previous experience of the researcher [27, 34, 35]. In addition, data pre-processing must be applied with caution, as there is a risk of losing relevant time-related information and thus worsening model performance if inappropriate methods are used [32]. Therefore, although the previous search and exhaustive evaluation of the impact of a wide range of pre-processing methods on the data at hand is time-consuming and computationally intensive, it opens up the possibility of finding the most appropriate ones for subsequent optimal modelling [36]. These pre-processing methods are divided into four groups: spectral signal transformation methods, scaling and data distribution transformation methods, variable selection and dimensionality reduction methods, and alignment methods.

1.2.1.1 Spectral signal transformation methods

Spectral signal transformation methods remove unwanted physical phenomena. These methods are specifically designed to process the data gathered by means of spectroscopic techniques [6-8, 16], even though a few cases of their application to chromatographic data have been reported [4, 17]. Two subgroups are distinguished within this group. The first subgroup is that of normalisation methods, which correct for shifts and trends in baseline and curvilinearity as well as for multiplicative effects, all of which are mainly caused by scattering. Standard normal variate (SNV) and multiplicative scatter correction (MSC) are normalisation methods included in this subgroup. These methods give equal weight to all **X** variables. The SNV normalises each spectrum by subtracting the mean and dividing it by the standard deviation. In contrast, the MSC normalises each spectrum by regressing it against the average spectrum. Thus, while the SNV is applied

individually to each spectrum, the MSC considers the spectra of the whole data set at once to compute the correction factors. Both methods are linearly related and tend to give similar results in data pre-processing [27, 28, 31, 34, 36]. A case study could be that of Ortiz-Herrero *et al.* [6], who used the SNV and MSC normalisation methods to correct the scattering effects in the visible spectra of pen ink samples, thus minimising non-**Y**-related spectral variations and reinforcing those linked to the modifications of the ink dyes throughout the ageing process (Figure 3). In this way, the robustness and performance of the OPLS models were improved. Information on this pre-processing will be expanded in Chapter 4 of this thesis.

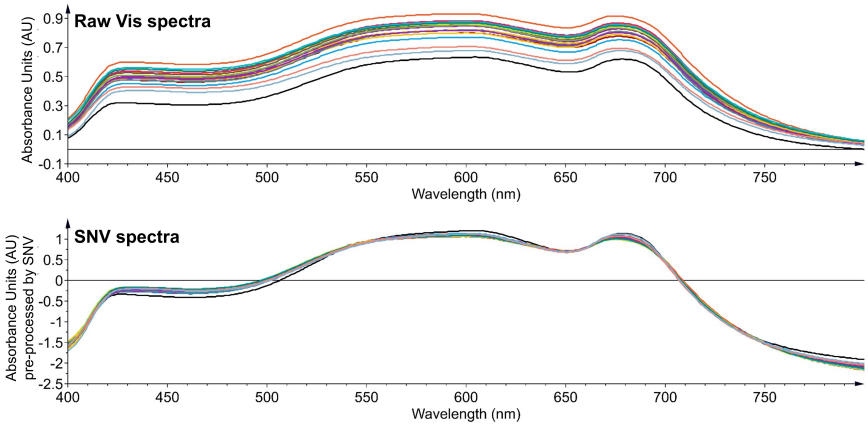

Figure 3. Raw and SNV-treated visible spectra of Bic® brand pen inks.

It is worth noting that the SNV normalisation method has succeeded in pre-processing various analytical signals, such as pyrograms, UV-Vis-NIR spectra and visible spectra, unlike other spectral signal transformation methods in which unsatisfactory statistical values and high predictive inaccuracies have been obtained at the modelling and validation stage. The ability of this spectral signal transformation method to efficiently pre-process various analytical signals was demonstrated in forensic applications through Table 1, in which the statistical values obtained when applying the SNV normalisation method and the smoothing and differentiation methods to the data collected in Chapters 2, 3 and 4 of this thesis were compared.

The second subgroup is that of smoothing and differentiation methods. Smoothing methods reduce noise, whereas differentiation methods, such as first and second derivatives, resolve peak overlap and remove constant or linear baseline drift [27, 28, 31, 34, 36]. A case study could be that of Ortiz-Herrero *et al.* [8], who used the first derivative to process the IR spectra of acrylic paint samples, thus eliminating baseline variations, while improving the spectral resolution by making the position of the bands more accurate (Figure 4). In this way, the modelling of the modifications given in the IR spectra of the acrylic paint samples over time was improved. Chapter 5 of this thesis will provide further information on this pre-processing.

Table 1. Statistical values obtained in the modelling and validation stage from different analytical signals pre-processed by various spectral signal transformation methods.

Analytical signal	Signal transformation method	LV	R^2Y	Q^2	RMSEE	RMSECV	R^2 CV	RMSEP	R^2 P	E (%)
Pyrograms [17]	SNV	3	0.93	0.53	0.18	0.51	0.93	0.28	0.93	30
	2nd derivative	3	0.78	0.40	0.31	0.47	0.78	5	0.76	100
Uv-Vis-NIR spectra [16]	SNV	2	0.95	0.93	0.08	0.09	0.95	0.09	0.95	17
	2nd derivative	2	0.97	0.87	0.06	0.14	0.97	0.22	0.95	59
Vis spectra [6]	SNV	1+3	0.87	0.74	0.08	0.10	0.87	0.05	0.96	10
	Savitzky-Golay	1+0	0.07	-0.45	0.20	0.23	0.07	0.28	<0.01	55

* E, predictive accuracy error; LV, latent variable; Q^2, goodness-of-prediction; R^2 CV, coefficient of determination of cross-validation; R^2 P, coefficient of determination of prediction; R^2X/Y, goodness-of-fit; RMSECV, root mean square error of cross-validation; RMSEE, root mean square error of estimation; RMSEP, root mean square error of prediction.

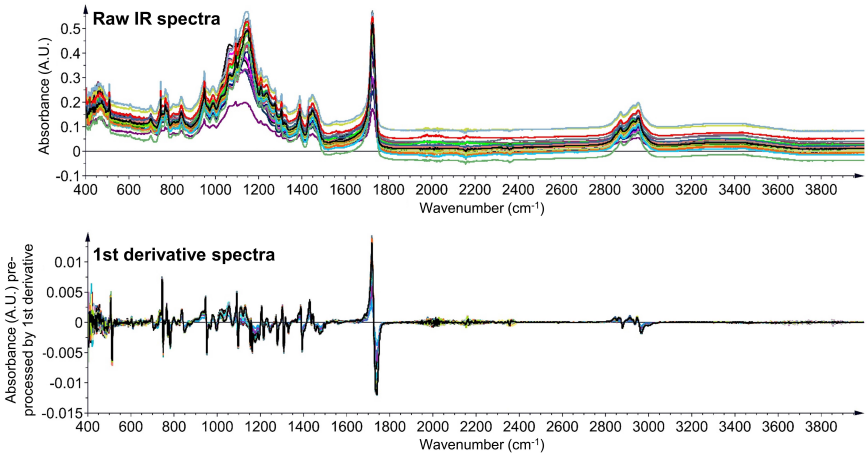

Figure 4. Raw and 1st derivate-treated IR spectra of short-term aged Liquitex® paints.

The application of differentiation methods could, however, decrease the signal-to-noise ratio. In order to cope with this drawback, the Savitzky-Golay (SG) smoothing and differentiation filter is used, which is based on the fitting of a piecewise low degree polynomial function (quadratic or cubic degree) to the data, followed by the calculation of the first derivative or the second derivative from the resulting polynomial at the defined points [37]. Thus, the SG filter supresses amplified high-frequency noise by a smoothing operation, while simultaneously removing the additive (offset) and linear baseline in the low-frequency region of the spectrum by differentiation [27]. It is worth noting that both the first- and second-order derivative filters and the SG smoothing and differentiation filter have successfully processed FTIR spectra of a wide range of forensic evidence, including bloodstains, fingermarks, human skeletal remains and counterfeit artworks [2, 3, 8, 11]. All the spectral signal transformation methods that have been mentioned can be used individually or in combination, in addition to the possibility of modifying the order in which they are applied [34].

1.2.1.2 Scaling methods and X and Y variable distribution transformation methods

Scaling, although not directly related to the elimination of signal artefacts, unifies the statistical scale of the variables by making them equally important, thus preventing one variable from dominating another in the modelling due to its greater numerical range, i.e. due to its higher variance. This is called auto-scaling, which is based on centring each variable by subtracting the average and scaling it to the unit variance by dividing it by the standard deviation. All scaled variables therefore have equal variance and a mean value of zero. Auto-scaling is the most objective approach and is applied when no prior information on the data is available [15, 36], as is the case with forensic dating. Due to the fact that it is often unknown which **X** variables are the most informative for time modelling, the data tend to be auto-scaled so that no variable is highlighted nor overshadowed by its weight [4, 6, 8, 16, 33]. In addition to auto-scaling, there is the Pareto scaling, which differs from the former in that each variable is scaled to the Pareto variance by dividing it by the square root of the standard deviation. The scaled data are less modified with respect to the raw data than in auto-scaling [37]. Since the magnitude of the scaling effect can be reduced after the application of the spectral signal transformation methods, it must be used in the last stage of pre-processing [34]. The variables can also be centred but not scaled [17]. This is called centring, which is based on subtracting the mean of the data from each variable so that the new variables have a mean of zero. This way the interpretability of the model is improved.

Furthermore, the **X** and **Y** variables may have a highly skewed and non-normal distribution due to the presence of outliers, the combination of multimodal distributions in the data or the insufficient sample size available [37]. Throughout the work on this thesis, we have come across these non-

normal distributions in the data, negatively impacting the modelling. An example is that of Figure 5 which shows the **Y** distribution of the human skeleton samples from Chapter 7. This is often due to the limited number of samples available for the construction of the model, which will be further discussed in section 1.2.2. Therefore, the **Y** variable is transformed into a logarithmic function to fit a normal distribution and thus minimise the accuracy error of (O)PLS models [6-8, 16, 17].

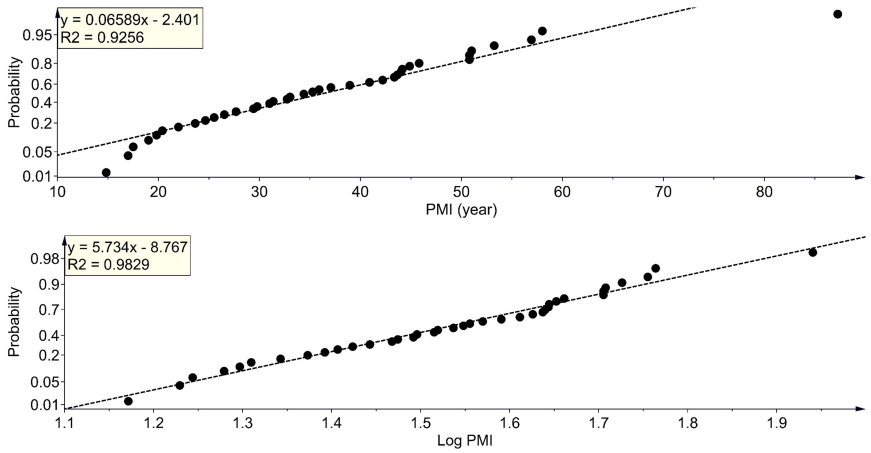

Figure 5. Normal probability plots for the untransformed **Y** variable (PMI) and for the **Y** variable transformed into a logarithmic function.

1.2.1.3 Variable selection and dimensionality reduction methods

Variable selection and dimensionality reduction methods provide simpler interpretation and improve the predictive performance of multivariate regression models [38]. Dimensionality reduction methods replace the original high-dimensional **X** variable space by a low-dimensional space containing **Y**-related variations. This way, in the data set there are various combinations of variables that are strongly correlated to each other and by capturing these underlying correlation patterns, the data can be

represented in a smaller dimensional space with fewer variables that are linear combinations of the original ones [27]. Projection methods, such as the (O)PLSR, are dimensionality reduction methods. The PLSR method extracts from the predictors a set of orthogonal factors called LVs that account for the maximum possible covariance between **X** and **Y**, thus having the best predictive power [39]. The complexity of the model is defined by the number of these LVs. The OPLSR method, on the other hand, filters out the structured noise in the data set by separately modelling the variation in **X** that is correlated and uncorrelated to **Y**. That is, the first LV explains the maximum covariance and the rest of the LVs captures the variance in **X** that is orthogonal to **Y**. In this way, the complexity of the model is reduced by decreasing the number of LVs needed to fit it [28-30]. We can find multiple case studies focused on forensic dating in which the PLSR and OPLSR methods have enabled the reduction of hundreds or thousands of **X** variables of the data set to one or a few LVs, thus overcoming the problem of high dimensionality [6-8, 17].

Moreover, variable selection methods aim to select a subset of **Y**-related variables by eliminating non-informative (noise) and interfering variables, but without increasing the predictive error due to the enhancement of the importance of irrelevant variables, the elimination of interference correcting variables or the elimination of useless variables that when taken with others improve the model's performance [12, 28, 35, 38]. They are classified into filter-, wrapper- and embedded-methods. Yun *et al.* [38], Zeaiter *et al.* [28] and Mehmood *et al.* [35] reported on the basis and the most widely used examples of each of these methods in the multivariate regressions. They are fundamental in the pre-processing of high-dimensional data used in the construction of (O)PLS models focused on forensic dating, since the variables that constitute them are intended to be related to time, eliminating all those that are not or that could interfere detrimentally with them [7, 11]. The loading weight vectors (**w***) is an example of filter-methods used for

the selection of variables in PLSR. The PLS analysis outputs model coefficients for the variables, called PLS-weights or loadings. While the loadings for the **X** variables (**w**) represent the importance of these variables, i.e. their contribution to the modelling of **Y**, the loadings for the **Y** variables (**c**) indicate which **Y** variables are modelled in the respective dimensions of the PLS model. These coefficients are represented in a **w*c** plot, which shows the relationships between **X** and **Y**, the most important **X** variables or which **Y** variables are related to which **X**. **X** variables with large positive or negative values in **w*** are highly correlated with **U** (**Y**) [37]. Thus, the **w*** can be used as a measure of importance to select the **X** variables. To do this, an absolute threshold value is set for the loading weight that the variables must exceed in order to be selected [35]. The OPLSR, on the contrary, plots the predictive and orthogonal in **X** loading vectors. The predictive loading vectors are **p** for the **X** block and **q** for the **Y** block. **X** loading weight **p** and **Y** loading weight **q** are combined into a **pq** vector. The orthogonal in **X** loading vectors are **po** for the **X** block and **so** for the **Y** block. Orthogonal loading **po** of the **X** part and the projection of **to** onto **Y**, **so**, are combined into a **poso** vector. The predictive loading vector for the **X** block, **p**, accounts for the variation in **X** related to **Y**. Therefore, the **X** variables that have a high positive or negative value of **p** will be those selected for the construction of the model [37]. A case study could be that of Ortiz-Herrero *et al.* [7], who used this filter-method to select which Raman shifts accounted for the maximum variation related to the PMI of human skeletons. An absolute threshold value of 0.04 was set for the **X**-**Y**-loading vector **pq[1]** of the predictive component and for the **X** loading vector **poso[1]** of the orthogonal in **X** component, eliminating the **X** variables that were below this threshold. The data set was thus reduced from 1651 **X** variables to 295. The elimination of the non-informative and noisy variables enable an improvement in the robustness and performance of the OPLS model. Information on the application of this filter-method will be expanded in Chapter 7 of this thesis.

1.2.1.4 Chromatographic signal alignment methods

Unlike spectroscopic techniques, an additional problem of the application of chromatographic techniques coupled with chemometrics is that when working with the whole chromatographic profile of forensic samples the possibility of small run-to-run variations in the retention times of the analytes is high, which, if not corrected, can have a negative effect on the multivariate model built up. In these cases, the time axes must be precisely aligned prior to modelling so that the signal of each analyte is recorded at the same coordinates in the data matrix for all the forensic samples analysed [40]. Sinkov *et al.* [40] and Goicoechea *et al.* [41] reported on the basis and the pros and cons of various pre-processing methods of time shift alignment. Moreover, Agilent Technologies' and Shimadzu Scientific Intruments' gas chromatography (GC) equipment has a retention time locking (RTL) or automatic adjustment of retention time (AART) software installed to fix retention times, which could be used alternatively to the above-mentioned computationally time-consuming and statistically complex alignment algorithms. This software is used when changes are made to the chromatographic system, a transfer is made to an entirely different GC unit or a degradation in chromatographic performance is detected. Its ability to block retention times of chromatographic peaks displaced from one run to another makes it possible to optimise laboratory resources and still provide a reproducible response that saves time and money, in addition to increasing productivity [42]. However, when working in the pyrolysis injection mode, neither RTL nor AART can be used, so as a fast and simple alternative means, the chromatographic experimental conditions are optimised to overcome measurement reproducibility problems. A case study could be that of Ortiz-Herrero *et al.* [17], who used pyrolysis-gas chromatography/mass spectrometry (Py-GC/MS) together with PLSR to develop a paper dating methodology based on two approaches. Due to the coupling of a pyrolyser to the chromatographic

equipment, the injection mode affected the pneumatic control of the chromatographic system, causing a shift of the chromatographic peaks with a low retention time, as shown in Figure 6A. Using a chromatographic column offering greater retention for polar compounds could delay their elution, thus increasing chromatographic reproducibility (Figure 6B). Chapter 2 of this thesis will deepen on the optimisation of the chromatographic experimental conditions.

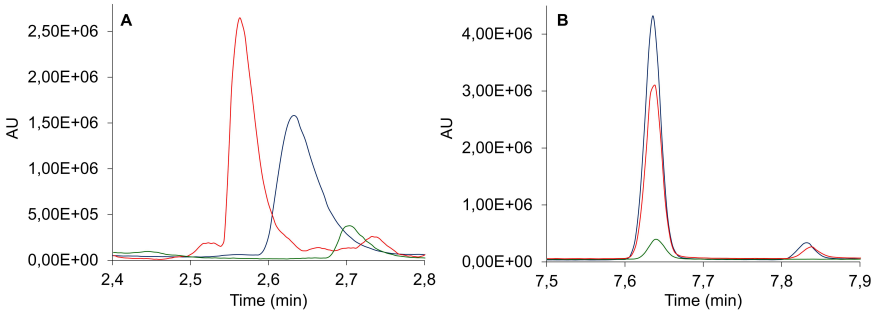

Figure 6. Run-to-run shifts of the chromatographic peak of 1-hydroxy-2-propanone obtained from paper pyrolysis using an HP-5 column (A) and a ZB-WAX column (B). Pyrolysis temperature of 400 °C.

1.2.2 Construction and validation of multivariate regression models

Having sets of samples representative of the characteristics and variability of the evidence than can be found in forensic scenarios is one of the main constraints for the implementation of robust and high predictive performance models. It is important to note that forensic police units, medical-legal and academic institutions, artists, etc., have access to large collections of real samples, so their collaboration is indispensable to give greater credibility and practicality to the models to be built and validated [6-8, 17]. However, although the availability or access to large collections and sample providers could overcome the problem of representativeness, forensic dating has an added drawback related to the wide temporal ageing

intervals of the samples needed in order to be able to build models that cover any required dating interval in a specific forensic case, thus making sampling much more complex. In view of this situation, a set of own samples are artificially made by the researchers by storing them under controlled environmental conditions for defined time periods that imitate those at the scene of the crime or by exposing them to scheduled accelerated ageing in chambers to immediately achieve longer aged samples [2-6, 8, 10, 11, 16, 17]. Even so, the size of the sample set is usually limited in both sample preparation methods, either because the former is extremely time-consuming, or because the latter can provide a number of samples restricted by the dimensions of the chamber used.

In any case, once the data collected from the analysis of these sample sets is pre-processed, modelling and subsequent validation is carried out. To do this, the entire sample set is split into two sets, training set (calibration samples) and test set (validation samples). Although random split is commonly applied, it has the drawbacks that the models are modifiable according to the split chosen and that an optimal split representing the whole sample set is not guaranteed. That is why sample split algorithms, such as the Kennard-Stone, are used. The Kennard-Stone algorithm allows selecting samples with a uniform distribution over the entire set. To this end, the algorithm finds the two most separated samples at a Euclidean distance in the sample set and adds them to the training set. For each candidate sample, it finds the smallest distance to any sample already selected and chooses the sample that has the largest of these smallest distances by adding it to the training set. These steps are repeated until the desired number of samples is reached in the training set, whereas the remaining samples will constitute the test set [43]. The test set is generally composed of fewer samples than the training set, representing in various forensic dating studies from 20% to 40% of the total samples (Table 2). This percentage, though, must be high enough to be able to

optimally evaluate the model's performance metrics. The importance of having validation samples independent from those used in the construction of the model must be emphasised, since it allows the performance of the model to be evaluated more reliably, thus avoiding overestimation and optimistic assessments that could be provided by the samples used both for the construction and for the validation of the model. However, as stated above, a representative and independent test set is not always possible due to the difficulty often encountered in forensics in achieving a large enough number of samples [14, 32].

A further issue to be considered in the construction of (O)PLS models focused on forensic dating is that when modelling the modifications of the sample components over time there is a possibility that short-term aged samples will behave differently than long-term aged ones, as is the case of paints and hydrocarbon compound mixtures. The consequence would be a non-linear trend over time that the (O)PLS model by itself is not able to model successfully, so individual models need to be built for the short- and long-term aged samples [4, 8]. The (O)PLS score scatter graph plotted from the whole sample set enables the visualisation of sample behaviours and trends over time, making it possible to decide whether or not to perform multiple models in order to achieve greater linearity in the data trend. It is therefore recommended to perform it prior to the splitting of the entire data set. A case study could be that of Ortiz-Herrero *et al.* [8], who saw a displacement of the acrylic paint samples over the accelerated ageing time in the OPLS score scatter plot, resulting in two groups: one consisting of short-term aged paint samples that moved to the right in the predictive component and another consisting of long-term aged paint samples that moved down in the orthogonal component. Therefore, an OPLS model was built for each group. Information on the observation of such multimodal distributions and the consequent need to build multiple models will be further developed in Chapter 5 of this thesis.

Table 2. Number of samples used for the construction and validation of (O)PLS models in various forensic dating studies.

Total number of samples	Training set	Test set	Sample split algorithm	Reference
15 paper micro-samples x 3 replicas	15 paper micro-samples x 3 replicas	15 paper micro-samples x 3 replicas	None	Ortiz-Herrero *et al.* [17]
45 ballpoint pen ink samples	35 ballpoint pen ink samples	10 ballpoint pen ink samples	Kennard-Stone	Ortiz-Herrero *et al.* [16]
48 samples per paint brand 31 short-term and 17 long-term aged Liquitex® paint samples 28 short-term and 20 long-term aged Hyplar® paint samples	21 short-term and 12 long-term aged Liquitex® paint samples 18 short-term and 12 long-term aged Hyplar® paint samples	10 short-term and 5 long-term aged Liquitex® paint samples 10 short-term and 8 long-term aged Hyplar® paint samples	Kennard-Stone	Ortiz-Herrero *et al.* [8]
20-30 samples per pen ink brand	15-23 samples per pen ink brand	5-7 samples per pen ink brand	Kennard-Stone	Ortiz-Herrero *et al.* [6]
47 human bone samples	33 human bone samples	14 human bone samples	Kennard-Stone	Ortiz-Herrero *et al.* [7]
53 unburied and 55 buried human bone samples	38 unburied and 40 buried human bone samples	15 unburied and 15 buried human bone samples	Kennard-Stone	Wang *et al.* [11]
Class 1: 72 samples of a hydrocarbon mixture for the individual study and 144 samples for the combined study Class 2: 48 samples of a hydrocarbon mixture for the individual study and 96 samples for the combined study	Class 1: 48 samples of a hydrocarbon mixture for the individual study and 96 samples for the combined study Class 2: 32 samples of a hydrocarbon mixture for the individual study and 64 samples for the combined study	Class 1: 24 samples of a hydrocarbon mixture for the individual study and 48 samples for the combined study Class 2: 16 samples of a hydrocarbon mixture for the individual study and 32 for the combined study	Random	Zorzetti *et al.* [4]
312 human bloodstain samples	248 human bloodstain samples	64 human bloodstain samples	Random	Kumar *et al.* [2]

After splitting the whole sample set into training and test sets, the former is used to build the multivariate regression model. One of the arising questions is whether to use the PLSR method instead of the OPLSR method or vice versa for its construction. The dimensionality of the model may give some hint. To this end, a study was conducted in which the dimensionality and performance statistics of the models from Chapters 4, 5 and 7 of this thesis built using the OPLSR method were compared with those that would have been obtained if the models had been built using the PLSR method. The data from this study, in addition to the reduction of the number of **X** variables to one or a few LVs mentioned in section 1.2.1.3, are shown in Table 3. It has been theoretically discussed that PLS models with more LVs than the true rank of **Y**, in this case a single **Y** variable, which is the time, would benefit from using the OPLSR method so that the orthogonal variation in **X** could be filtered out, thus decreasing the complexity of the model to a single LV [29, 30]. Nevertheless, the OPLS models from various research studies in Table 3 had to be fitted to more than one LV for optimal time modelling. The number of LVs was in fact the same or slightly higher when the OPLSR method was used than when the PLSR method was applied. Theoretically, the construction of PLS and OPLS models with a single **Y** variable using the SIMCA 15.0.2 Umetrics® software (Umeå, Sweden) results in the same total number of LVs. However, due to the fact that the PLSR method is based on sequential cross-validation and the OPLSR method on full cross-validation, slight differences in the Q^2 values may occur and, therefore, a different number of components may be considered significant [37]. In spite of this, both the OPLSR and the PLSR methods showed almost identical performance statistics and, therefore, provided similar predictions for each of the various research studies listed in Table 3.

Table 3. Number of **X** variables constituting the data and the LVs needed to fit the PLS and OPLS models of each study, in addition to the statistical values obtained in the construction and validation stage with each multivariate regression method.

Reference	No. of X variables	Multivariate regression method	LV	R^2X	R^2Y	Q^2	RMSEE	RMSECV	R^2 CV	RMSEP	R^2 P	E (%)
Ortiz-Herrero *et al.* [8] Short-term model of the Liquitex® paint brand	7455	OPLSR	1+3	0.46	1	0.69	0.02	0.28	1	0.19	0.86	32
		PLSR	3	0.42	0.99	0.87	0.05	0.26	0.99	0.19	0.84	31
Ortiz-Herrero *et al.* [8] Long-term model of the Liquitex® paint brand	7455	OPLSR	1+4	0.73	1	0.74	<0.01	0.05	1	0.04	0.89	8
		PLSR	4	0.69	1	0.96	0.01	0.05	1	0.04	0.89	8
Ortiz-Herrero *et al.* [7] Model of human skeletal remains	295	OPLSR	1+2	0.43	0.89	0.67	0.06	0.10	0.89	0.17	<0.01	34
		PLSR	3	0.43	0.89	0.68	0.06	0.09	0.89	0.17	<0.01	34
Ortiz-Herrero *et al.* [6] Model of the Bic® ballpoint pen brand from France	401	OPLSR	1+3	0.98	0.87	0.74	0.08	0.10	0.87	0.05	0.96	10
		PLSR	1	0.30	0.52	0.32	0.14	0.16	0.52	0.24	0.31	60
Ortiz-Herrero *et al.* [6] Model of the Paper Mate® gel pen brand	401	OPLSR	1+2	0.94	0.70	0.41	0.09	0.11	0.70	0.10	0.54	13
		PLSR	1	0.35	0.51	0.13	0.11	0.14	0.51	0.08	0.63	14

* The OPLSR method was used in the research studies and the PLSR method was used as a comparative test.

On the other hand, theoretically when a single LV constitutes the PLS model, there is no need to apply the OPLSR method, as there is no disturbing latent orthogonal variation present [29, 30]. However, this is not always the case in practise, as the PLSR may not have enough fitting and predictive capacity to incorporate more LVs than one, as shown in Table 3 of the research study conducted by Ortiz-Herrero *et al.* [6] for the PLS model of the Bic® ballpoint pen brand from France. In this case, it is imperative to check the operation of the OPLSR method, since although its use may imply that the model is fitted with a higher number of LVs, the statistical values can be improved, thus obtaining a robust and well-performing model.

Due to discrepancies between theory and practice, it is impossible to know in advance which of the two multivariate regression methods would work best for forensic dating. That is why the PLSR method is first used for the construction of the model. The assessment of its complexity and the performance statistics provided will determine whether it is suitable or whether the use of the OPLSR method is required. To do this, the first step is to set the number of LVs that will make up the model. The amount of variance explained by a LV indicates its importance in predicting **Y**, although it will only be relevant if it improves the prediction of **Y** for new forensic samples. This opens up a new problem about how many LVs the model needs to be built to achieve optimal predictions for new real caseworks [39]. It must be emphasised that when working with a large amount of data there is a risk of over-fitting, i.e. a well-fitted model but with low or no predictive ability [15]. This is the case when as the number of LVs increases the quality of the prediction decreases, thus the model would be over-fitting the data [39]. The selection of the optimal dimensionality of the model would avoid an over-fitting that would be detrimental to the performance of the model, since it would not only be incorporating the predictive features of the data, but also the noise [44]. The number of LVs

is optimised by internal cross-validation method, which is performed by dividing the training set data into various groups and then building several parallel models from the reduced data with one of the omitted groups. Once a model is built, the omitted data are used as a test set and the differences between the real and predicted values are calculated for the test set [37]. The statistical parameters used to evaluate this step are the RMSECV and the R^2 CV. RMSECV is calculated using the following Eq. 1:

$$\text{RMSECV} = \sqrt{\frac{\sum_{i=1}^{n}(y_i - \hat{y}_i)^2}{n}} \qquad \text{(Eq. 1)}$$

Where y_i is the real value, $\hat{y}_i$ is the value predicted by the model fitted to a certain number of LVs and *n* is the total number of samples used in the training set [8]. Each model fitted to a certain number of LVs will result in an RMSECV value. Thus, the minimum RMSECV value will determine the optimum dimensionality of the model. It must be emphasised that a small decrease in the RMSECV value resulting from the fit of an additional LV must be thoroughly studied to determine whether it is worthwhile or not, since the greater the dimensionality of the model, the less robust it is [44]. Two additional statistical parameters used to optimise the number of LVs are R^2X/Y and Q^2. A model with a defined dimensionality will have a R^2X/Y value, which indicates its fitness and which varies from 1 to 0 according to whether it fits perfectly or not, and a Q^2 value, which indicates its robustness and predictive ability, being good when $Q^2 > 0.5$ and excellent when $Q^2 > 0.9$ [8]. A model with a low or negative value of R^2X/Y and Q^2 is indicative of inhomogeneity in the data, in addition to being poor and not predicting better than chance [15].

Moreover, due to factors such as instrumental artifacts, variations in the samples, etc., the recorded spectra or chromatographic profiles of some of the forensic samples may differ significantly from the whole set. These samples are considered outliers and impact negatively on the robustness and performance of the model, so they must be identified and removed. To this end, the Hotelling's T2 and distance-to-model tests with 95% confidence level are used. Any samples that exceed the critical limits (level 0.05) are potential outliers. It must be taken into account that the processes of variable selection and outlier detection influence each other, in addition to the fact that their conduction orders influence the results of the modeling [27, 38]. Emphasising on forensic dating, PLS models have been found to perform worse in the shortest time periods, obtaining high inaccuracies in the estimates. This may be due to the non-linear trend of some forensic samples in the initial stage of ageing, which is inappropriately modeled by the PLS algorithm [33]. Furthermore, the limited number of samples available at this initial stage may reinforce this trend and make them outliers [16]. A case study could be that of Ortiz-Herrero *et al.* [16], who detected three outliers using the Hotelling's T2 control chart with 95% confidence (Figure 7). These were the pen ink samples with the lower accelerated ageing times. Their UV-Vis-NIR spectra showed visual modifications in the UV range, unlike the older pen inks, due to the evaporation of the volatile components in the initial period of the ageing process. These modifications in the initial ageing period of the pen inks, in addition to the low number of samples available, distorted the PLS model, resulting in high accuracy errors in the estimates, so the youngest samples had to be eliminated to improve its performance. Information on the elimination of these outliers will be expanded in Chapter 3 of this thesis.

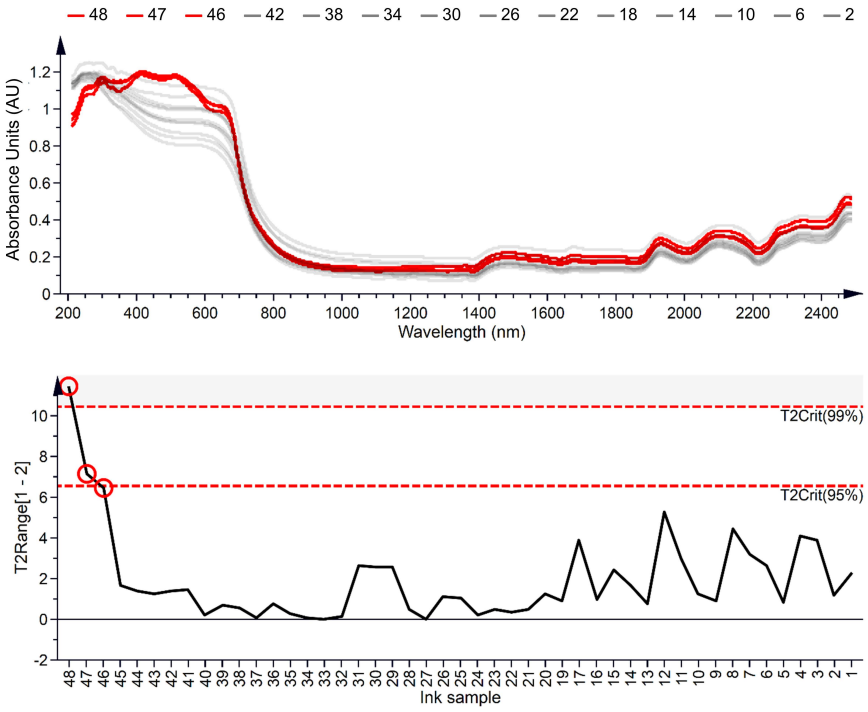

Figure 7. UV-Vis-NIR spectra of the three pen ink samples detected as outliers by the Hotelling's T2 chart with 95% confidence (marked in red).

The built model is subsequently validated externally using the samples from the test set. The model's predictive ability is assessed by the RMSEP and the R^2 P. The RMSEP is calculated using Eq. 2:

$$\text{RMSEP} = \sqrt{\frac{\sum_{i=1}^{n_t}(y_{t,i}-\hat{y}_{t,i})^2}{n_t}} \qquad \text{(Eq. 2)}$$

Where $y_{t,i}$ is the real value, $\hat{y}_{t,i}$ is the value predicted by the model fitted to a certain number of LVs and n_t is the total number of samples in the test set. RMSEP is a measure of the average error expected in future predictions when the regression model is applied to unknown samples, so the robustness of the model can be evaluated by this statistical parameter.

A robust model will have a high predictive accuracy and, therefore, a minimum RMSEP value [8]. The number of LVs that make up the model could also be optimised by means of the RMSEP. Thus, the lowest RMSEP value calculated among the models fitted to different LVs tested will determine the optimal dimensionality of the model [44]. Moreover, it is worth noting that when the selection of variables is performed during data pre-processing, the risk of over-fitting is extremely high, thus, the validation stage is indispensable as a final evaluation of the selected variables [35]. An additional statistical parameter is the accuracy error made by the model in the prediction, which is calculated by Eq. 3:

$$\text{Error (\%)} = \left(\frac{(y_r - y_p)}{y_r}\right) x\ 100 \qquad \text{(Eq. 3)}$$

Where, y_r is the real value and y_p is the value predicted by the model fitted to a certain number of LVs for that sample.

The entire modelling and validation process is performed on data to which a certain pre-processing method is previously applied. However, the pre-processing method must also be optimised by evaluating the performance and robustness of each model built from the data processed by various pre-processing methods and from the raw data [36]. This is done by the trial and error method. The optimal data pre-processing method selected will be that which results in a model that have high R^2X/Y and Q^2 values as well as low RMSECV and RMSEP values and a small difference between the last two statistical parameters. A large difference between RMSECV and RMSEP would indicate the possibility that too many LVs are being used in the model (over-fitting) and that the noise is being modelled. The number of LVs is therefore intended to be as low as possible.

Moreover, in the case of using accelerated ageing samples for the construction of a multivariate regression model, an additional step is required so that it can be applied to real forensic scenarios. Since the model predicts **Y** in accelerated time units, its natural time equivalent must be determined. To do this, the **Y** values of known forensic samples are predicted from their **X** values. From the predicted **Y** values and the real **Y** values of the samples a regression is performed from which an equation is obtained that determines the correlation between the accelerated time and the natural age. Thus, the predicted **Y** values of unknown new forensic samples are transformed into natural time units taking into account this correlation [8, 16, 17]. A case study could be that of Ortiz-Herrero *et al.* [8], who built OPLS models for artwork dating based on artificially aged paint samples. Various contemporary artists provided them with artworks dated in different years, enabling the correlation between artificial ageing and its natural equivalent. To this end, the OPLS models were used to predict the equivalent accelerated age of the artworks. The predicted accelerated age was plotted against the real age of the artworks, thus obtaining a regression line. The correlation was determined by the equation of this regression line, in which approximately 50 h of accelerated ageing were equivalent to one natural year under the studied storage conditions. This correlation would therefore make it possible to date artworks up to at least 22 years old, to be used for attribution purposes, for example, whenever the questioned artworks have been preserved under comparable conditions and created with the same paint formulation as that of the study, in spite of the fact that the OPLS models have been constructed from artificially aged paint samples. In Chapter 5 of this thesis, the information on the establishment of this correlation will be expanded.

1.2.3 External validation of the methodology for implementation in real scenarios

When new analytical methodologies are implemented in laboratories, they require multi-laboratory intercomparison and blind testing exercises to provide them with an independent external evaluation. These international intercomparison exercises have been widely used in classical analytical methods to guarantee the quality and reliability of the results provided. Following the same line, not only in forensic dating, but also in all forensic areas, the developed chemometric-based methodology has to undergo strict validation procedures prior to its implementation in forensic laboratories for routine work, so such multi-laboratory intercomparison and blind testing exercises can also be used for this purpose. In spite of the fact that the multivariate regression model may have been externally validated with samples independent from those of the construction set, these samples are also prepared under controlled conditions, so the performance of the methodology when applied to real caseworks is not guaranteed. This uncertainty and lack of reliability can cause the results presented by the forensic expert at the trial to be rejected by the judge. The methodology should therefore be subjected to multi-laboratory intercomparison and blind testing exercises in which a law enforcement agency provides the forensic evidence through which to assess its robustness and performance in real scenarios. A case study could be that of Ortiz-Herrero *et al.* [6], who used blind pen ink samples from document entries for method validation. In addition to setting out the pros and cons of this methodology, the blind testing exercise enabled the researchers to establish a procedure to be followed in order to obtain reliable results under statistical criteria that would be defensible in court. Further information on this intercomparison study will be provided in Chapter 4 of this thesis.

1.2.4 Methodological proposal for the use of multivariate regression methods in forensic dating

Taking into account the aforementioned sections, the steps that the forensic expert follows to develop and validate any chemometric-base dating methodology have been outlined in a flow chart (Figure 8), which likewise is the methodological basis of Chapters 2 to 7 of this thesis. The flow chart is structured in 3 main blocks: the first block represents the scope of the method, the sampling and the choice of the analytical technique, the second block is the data pre-processing and multivariate regression analysis and the last block corresponds to the external validation of the methodology.

The first question raised in the first block is the temporal scope that the methodology must cover, which depends on the crime scene that the forensic expert is dealing with. Once the objective has been set, real samples of an equal or similar nature to that of the forensic evidence found at the crime scene are sought. Having a large number of real samples covering the required time interval is often complicated, so an alternative of preparing synthetic samples and ageing them in a combined climatic test chamber under controlled conditions should be considered. Analytical techniques with advantages such as being non-destructive, fast, reliable, cost-effective, reproducible and multi-element analysis are at the forefront of forensics. That is why spectroscopic techniques are the first choice when it comes to age estimation. However, the complexity of the forensic samples that the expert deals with may require techniques that perform a more thorough analysis even if they are destructive. In these cases, chromatographic techniques need alignment methods, either as data processing or already installed in the instrumental equipment, or the optimisation of chromatographic experimental conditions to cope with run-to-run reproducibility problems.

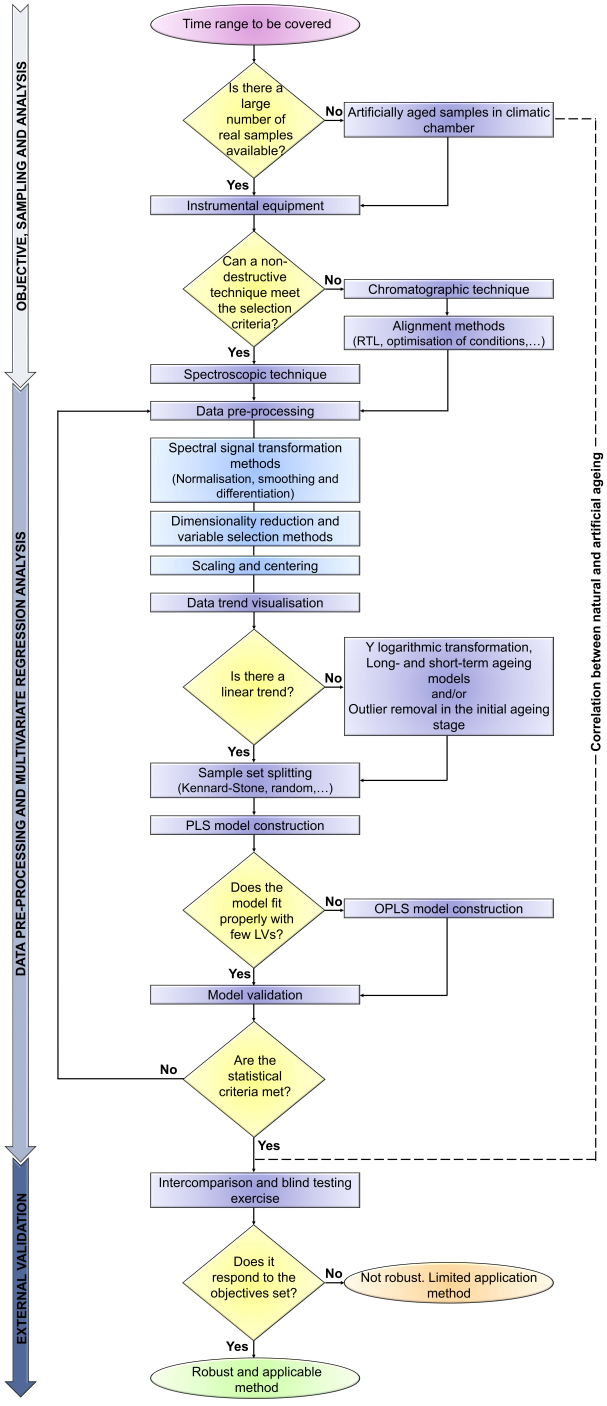

Figure 8. Flow chart for any chemometric-based dating methodology.

After data acquisition, the forensic expert moves on to the second block, related to data pre-processing and multivariate regression analysis. The pre-processing of the data is the most arduous and time-consuming step, since in spite of the fact that there are various methodologies that are more suitable for processing certain data and fulfilling certain objectives, it is impossible to establish beforehand those that guarantee optimal processing of the set of data that the forensic expert has to deal with. Different pre-processing methodologies are therefore selected and evaluated by trial and error until that which improves the signal and eliminates the largest non-time related systematic variation is found. As guidance for the forensic expert, the SNV normalisation method has successfully pre-processed a wide range of analytical signals, such as pyrograms, visible spectra and UV-Vis-NIR spectra. However, SNV has not provided optimal results for FTIR spectra, for which differentiation and smoothing methods were more suitable. The next step is to visualise the trend of the data set. (O)PLSR is a linear multivariate regression method, so a non-linear trend in the data would impair its performance. Minor non-linearities in data distribution are overcome by transforming the **Y** variable into a logarithmic function or by eliminating outliers from the initial ageing stage, for example. However, the various modifications that sample components undergo throughout ageing can cause multimodal distributions that require the construction of individual models for long- and short-term ageing samples so that a clearer linear data distribution can be achieved. The data set is subsequently split into two sets by using sample split logarithms, whenever possible: a training set for the construction of the (O)PLS model and a test set for its validation. The use of one multivariate regression method or another for the construction of the model depends on its complexity and the performance statistics it provides. Although in practice it has been found that various models fit with an equal or minimal difference in the number of LVs and have almost identical performance statistics when the PLSR or OPLSR method is applied

indistinctly, the latter is recommended for priority and optimal modelling of systematic variation in **X** related to time, putting aside all orthogonal variation. This predictive component also enables easier identification of the most influential **X** variables and, therefore, the regions of the chromatogram or spectrum that are modified over time and which in turn correspond to certain components of the forensic evidence, providing supplementary information to the criminal investigation. Moreover, the main source of orthogonal variation can be subsequently identified and analysed. A robust and well performing (O)PLS model has high R^2X/Y and Q^2 values, low RMSECV and RMSEP values and a small difference between these last two statistical parameters. Failure to meet these statistical criteria returns the forensic expert to the data pre-processing stage. Prior to moving on to the last block concerning the external validation of the methodology and in the event that the forensic expert has built the (O)PLS model from artificially aged samples, the expert establishes the correlation between accelerated ageing and its natural equivalent so that the model has real applicability.

Finally, the forensic expert participates in multi-laboratory intercomparison and blind testing exercises with the aim of implementing the methodology in the standardised work of forensic laboratories. By means of these exercises, the expert validates the methodology developed through the simulation of real forensic scenarios with which he/she sets the scope of the methodology and evaluates the reliability of the results provided.

References

[1] L.S. Castillo-Peinado, M.D. Luque de Castro, An overview on forensic analysis devoted to analytical chemists, *Talanta* 167 (2017) 181–192. http://dx.doi.org/10.1016/j.talanta.2017.01.087.

[2] R. Kumar, K. Sharma, V. Sharma, Bloodstain age estimation through infrared spectroscopy and Chemometric models, *Sci. Justice* (2020). https://doi.org/10.1016/j.scijus.2020.07.004.

[3] A. Girod, L. Xiao, B. Reedy, C. Roux, C. Weyermann, Fingermark initial composition and aging using Fourier transform infrared microscopy (m-FTIR), *Forensic Sci. Int.* 254 (2015) 185–196. http://dx.doi.org/10.1016/j.forsciint.2015.07.022.

[4] B.M. Zorzetti, J.M. Shaver, J.J. Harynuk, Estimation of the age of a weathered mixture of volatile organic compounds, *Anal. Chim. Acta* 694 (2011) 31-37. https://doi.org/10.1016/j.aca.2011.03.021.

[5] M.D. Gallidabino, C. Weyermann, Time since last discharge of firearms and spent ammunition elements: state of the art and perspectives. *Forensic Sci. Int.* 311 (2020) 110290. http://dx.doi.org/10.1016/j.forsciint.2020.110290.

[6] L. Ortiz-Herrero, A.C. de Almeida Assis, L. Bartolomé, M.L. Alonso, M.I. Maguregui, R.M. Alonso, J.S. Seixas de Melo, A novel, non-invasive, multi-purpose and comprehensive method to date inks in real handwritten documents based on the monitoring of the dye ageing processes, *Chemom. Intell. Lab. Syst.* 207 (2020) 104187. https://doi.org/10.1016/j.chemolab.2020.104187.

[7] L. Ortiz-Herrero, B. Uribe, L. Hidalgo Armas, M.L. Alonso, A. Sarmiento, J. Irurita, R.M. Alonso, M.I. Maguregui, F. Etxeberria, L. Bartolomé, Estimation of the post-mortem interval of human skeletal remains using Raman spectroscopy and chemometrics, *Forensic Sci. Int.* (2021) (under review).

[8] L. Ortiz-Herrero, I. Cardaba, S. Setien, L. Bartolomé, M.L. Alonso, M.I. Maguregui, OPLS multivariate regression of FTIR-ATR spectra of acrylic paints for age estimation in contemporary artworks, *Talanta* 205 (2019) 120114. https://doi.org/10.1016/j.talanta.2019.120114.

[9] C. Weyermann, O. Ribaux, Situating forensic traces in time, *Sci. Justice* 52 (2012) 68-75. http://dx.doi.org/10.1016/j.scijus.2011.09.003.

[10] T. Das, A. Harshey, K. Nigam, V.K. Yadav, A. Srivastava, Analytical approaches for bloodstain aging by vibrational spectroscopy: Current trends and future perspectives, *Microchem. J.* 158 (2020) 105278. https://doi.org/10.1016/j.microc.2020.105278.

[11] Q. Wang, Y. Zhang, H. Lin, S. Zha, R. Fang, X. Wei, S. Fan, Z. Wang, Estimation of the late postmortem interval using FTIR spectroscopy and chemometrics in human skeletal remains, *Forensic Sci. Int.* 281 (2017) 113-120. https://doi.org/10.1016/j.forsciint.2017.10.033.

[12] M. Bovens, B. Ahrens, I. Alberink, A. Nordgaard, T. Salonen, S. Huhtala, Chemometrics in forensic chemistry — Part I: Implications to the forensic workflow, *Forensic Sci. Int.* 301 (2019) 82–90. https://doi.org/10.1016/j.forsciint.2019.05.030.

[13] R. Kumar, V. Sharma, Chemometrics in forensic science, *TrAC Trends Anal. Chem.* 105 (2018) 191-201. https://doi.org/10.1016/j.trac.2018.05.010.

[14] C.S. Silva, A. Braz, M.F. Pimentel, Vibrational Spectroscopy and Chemometrics in Forensic Chemistry: Critical Review, Current Trends and Challenges, *J. Braz. Chem. Soc.* 30 (11) (2019) 2259-2290. http://dx.doi.org/10.21577/0103-5053.20190140.

[15] S. Wold, M. Sjöström, L. Eriksson, PLS-regression: a basic tool of chemometrics, *Chemom. Intell. Lab. Syst.* 58 (2001) 109–130.

[16] L. Ortiz-Herrero, L. Bartolomé, I. Durán, I. Velasco, M.L. Alonso, M.I. Maguregui, M. Ezcurra, DATUVINK pilot study: A potential non-invasive methodology for dating ballpoint pen inks using multivariate

chemometrics based on their UV–vis-NIR reflectance spectra, *Microchem. J.* 140 (2018) 158-166. https://doi.org/10.1016/j.microc.2018.04.019.

[17] L. Ortiz-Herrero, M.E. Blanco, C. García-Ruiz, L. Bartolomé, Direct and indirect approaches based on paper analysis by Py-GC/MS for estimating the age of documents, *J. Anal. Appl. Pyrolysis* 131 (2018) 9-16. https://doi.org/10.1016/j.jaap.2018.02.018.

[18] K.L. Miranda, F.E. Ortega-Ojeda, C. García-Ruíz, P.S. Martínez, Shooting distance estimation based on gunshot residues analyzed by XRD and multivariate analysis, *Chemom. Intell. Lab. Syst.* 193 (2019) 103831. https://doi.org/10.1016/j.chemolab.2019.103831.

[19] R.B. Godinho, M.C. Santos, R.J. Poppi, Determination of fragrance content in perfume by Raman spectroscopy and multivariate calibration, *Spectrochim. Acta A Mol. Biomol. Spectrosc.* 157 (2016) 158-163. http://dx.doi.org/10.1016/j.saa.2015.12.025.

[20] S. Farres, L. Srata, F. Fethi, A. Kadaoui, Argan oil authentication using visible/near infrared spectroscopy combined to chemometrics tools, *Vib. Spectrosc.* 102 (2019) 79-84. https://doi.org/10.1016/j.vibspec.2019.04.003.

[21] F.R. Doucet, G. Lithgow, R. Kosier, P. Bouchard, M. Sabsabi, Determination of isotope ratios using Laser-Induced Breakdown Spectroscopy in ambient air at atmospheric pressure for nuclear forensics, *J. Anal. At. Spectrom.* 26 (2011) 536-541. https://doi.org/10.1039/c0ja00199f.

[22] S.J. Mazivila, A.C. Olivieri, Chemometrics coupled to vibrational spectroscopy and spectroscopic imaging for the analysis of solid-phase pharmaceutical products: A brief review on non-destructive analytical methods, *TrAC Trends Anal. Chem.* 108 (2018) 74-87. https://doi.org/10.1016/j.trac.2018.08.013.

[23] R. Chauhan, R. Kumar, V. Sharma, Soil forensics: A spectroscopic examination of trace evidence, *Microchem. J.* 139 (2018) 74-84. https://doi.org/10.1016/j.microc.2018.02.020.

[24] S. Materazzi, A. Gregori, L. Ripani, A. Apriceno, R. Risoluti, Cocaine profiling: Implementation of a predictive model by ATR-FTIR coupled with chemometrics in forensic chemistry, *Talanta* 166 (2017) 328-335. http://dx.doi.org/10.1016/j.talanta.2017.01.045.

[25] S.P. Stewart, S.E.J. Bell, D. McAuley, I. Baird, S.J. Speers, G. Kee, Determination of hydrogen peroxide concentration using a handheld Raman spectrometer: Detection of an explosives precursor, *Forensic Sci. Int.* 216 (2012) e5-e8. http://dx.doi.org/10.1016/j.forsciint.2011.08.002.

[26] E. Deconinck, R. Van Campenhout, C. Aouadi, M. Canfyn, J.L. Bothy, L. Gremeaux, P. Blanckaert, P. Courselle, Combining attenuated total reflectance- infrared spectroscopy and chemometrics for the identification and the dosage estimation of MDMA tablets, *Talanta* 195 (2019) 142-151. https://doi.org/10.1016/j.talanta.2018.11.027.

[27] R. Gautam, S. Vanga, F. Ariese, S. Umapathy, Review of multidimensional data processing approaches for Raman and infrared spectroscopy, *EPJ Techniques and Instrumentation* 2 (2015) 1-38. https://doi.org/10.1140/epjti/s40485-015-0018-6.

[28] M. Zeaiter, J.-. Roger, V. Bellon-Maurel, Robustness of models developed by multivariate calibration. Part II: The influence of pre-processing methods, *TrAC Trends Anal. Chem.* 24 (5) (2005) 437-445. https://doi.org/10.1016/j.trac.2004.11.023.

[29] S. Wold, J. Trygg, A. Berglund, H. Antti, Some recent developments in PLS modeling, *Chemom. Intell. Lab. Syst.* 58 (2001) 131-150.

[30] J. Trygg, S. Wold, Orthogonal projections to latent structures (O-PLS), *J. Chemom.* 16 (2002) 119-128. https://doi.org/10.1002/cem.695.

[31] J. Gabrielsson, J. Trygg, Recent Developments in Multivariate Calibration, *Crit. Rev. Anal. Chem.* 36 (2006) 243-255. http://dx.doi.org/10.1080/10408340600969924.

[32] T. Salonen, B. Ahrens, M. Bovens, J. Eliaerts, S. Huhtala, A. Nordgaard, I. Alberink, Chemometrics in forensic chemistry — Part II: Standardized applications – Three examples involving illicit drugs, *Forensic Sci. Int.* 307 (2020) 110138. http://dx.doi.org/10.1016/j.forsciint.2019.110138.

[33] M. Gallidabino, F.S. Romolo, C. Weyermann, Time since discharge of 9 mm cartridges by headspace analysis, part 2: Ageing study and estimation of the time since discharge using multivariate regression, *Forensic Sci. Int.* 272 (2017) 171–183. http://dx.doi.org/10.1016/j.forsciint.2016.12.027.

[34] C. Mas, L. Rubio, L. Valverde-Som, L.A. Sarabia, M.C. Ortiz, Impact of the pretreatment of ATR-FTIR signals on the figures of merit when PLS is used, *Chemom. Intell. Lab. Syst.* 201 (2020) 104006. https://doi.org/10.1016/j.chemolab.2020.104006.

[35] T. Mehmood, K.H. Liland, L. Snipen, S. Sæbø, A review of variable selection methods in Partial Least Squares Regression, *Chemom. Intell. Lab. Syst.* 118 (2012) 62-69. http://dx.doi.org/10.1016/j.chemolab.2012.07.010.

[36] L.C. Lee, C. Liong, A.A. Jemain, A contemporary review on Data Preprocessing (DP) practice strategy in ATR-FTIR spectrum, *Chemom. Intell. Lab. Syst.* 163 (2017) 64-75. http://dx.doi.org/10.1016/j.chemolab.2017.02.008.

[37] L. Eriksson, T. Byrne, E. Johansson, J. Trygg, C. Vikström, Multi- and Megavariate Data Analysis. Basic Principles and Applications, third ed., Umetrics Academy, 2013.

[38] Y. Yun, H. Li, B. Deng, D. Cao, An overview of variable selection methods in multivariate analysis of near-infrared spectra, *TrAC*

Trends Anal. Chem. 113 (2019) 102-115. https://doi.org/10.1016/j.trac.2019.01.018.

[39] H. Abdi, Partial least squares regression and projection on latent structure regression (PLS Regression), *WIREs Comp. Stat.* 2 (2010) 97-106. https://doi.org/10.1002/wics.051.

[40] N.A. Sinkov, B.M. Johnston, P.M.L. Sandercock, J.J. Harynuk, Automated optimization and construction of chemometric models based on highly variable raw chromatographic data, *Anal. Chim. Acta* 697 (2011) 8-15. https://doi.org/10.1016/j.aca.2011.04.029.

[41] H.C. Goicoechea, M.J. Culzoni, M.D.G. García, M.M. Galera, Chemometric strategies for enhancing the chromatographic methodologies with second-order data analysis of compounds when peaks are overlapped, *Talanta* 83 (2011) 1098-1107. https://doi.org/10.1016/j.talanta.2010.07.057.

[42] N. Etxebarria, O. Zuloaga, M. Olivares, L.J. Bartolomé, P. Navarro, Retention-time locked methods in gas chromatography, *J. Chromatogr. A* 1216 (2009) 1624-1629. https://doi.org/10.1016/j.chroma.2008.12.038.

[43] R.W. Kennard, L.A. Stone, Computer Aided Design of Experiments, *Technometrics* 11 (1969) 137-148. http://dx.doi.org/10.1080/00401706.1969.10490666.

[44] N.M. Faber, R. Rajkó, How to avoid over-fitting in multivariate calibration—The conventional validation approach and an alternative, *Anal. Chim. Acta.* 595 (2007) 98-106. http://dx.doi.org/10.1016/j.aca.2007.05.030.

CHAPTER

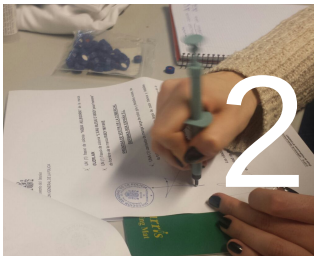

Direct and indirect approaches based on paper analysis by Py-GC/MS for estimating the age of documents

L. Ortiz-Herrero, M.E. Blanco, C. García-Ruiz, L. Bartolomé

Journal of Analytical and Applied Pyrolysis, **2018**; 131: 9–16

Q1, IF: 3.470, 17/84, Chemistry, Analytical

Abstract

The age of a relatively old document is one of the outstanding issues in the field of forensic document examination. Although several analytical methodologies exist today that focus on the analysis of inks to estimate the age of documents, paper analysis has received little attention. This study aims to develop two complementary approaches to estimate the age of documents based on paper analysis by pyrolysis coupled with gas chromatography with mass spectrometry detection (Py-GC/MS): (i) a direct approach using a multivariate regression model constructed from the pyrolytic profiles of artificially aged samples, and (ii) an indirect approach based on the identification of compounds characteristic of the document period. The direct approach has successfully allowed the age estimation of relatively old documents under police custody (up to 30 years of age) and the determination of a correlation between the natural and the accelerated ageing of paper under controlled conditions. This approach is applicable to papers that have the same (or similar) composition and have been stored under comparable storage conditions. Additionally, the indirect approach is presented as an interesting perspective to ratify valuable information of the document age.

Key words: Questioned document, paper, Py-GC/MS, age estimation, multivariate regression.

2.1 Introduction

The analysis of documents is a matter of great interest in the field of forensic analysis. From handwritten texts and signatures to printed papers, a broad range of document types may be subject to analysis (e.g. identity cards, commercial documents or industrial and intellectual property documents). These are commonly legal documents of mandatory compliance and/or with economic, administrative, labour and social implications. The wide variety and complexity of documents hinders their analysis and, therefore, several aspects of the forensic science aimed to study documents (so-called documentoscopy) remain so far unsolved. Estimating the age of a document is one of these unresolved issues [1].

Although the body of a document may be made up of many different materials—as for example granodiorite in the famous Rosetta Stone—for many centuries paper has been the main component used in documentation throughout the world [2]. Since the first paper manufactured in China before 105 CE, composed of fabric fragments or silk threads, different materials have been used. In 751, Arabs varied and improved the composition of paper to reduce the cost of manufacture, employing mixtures of linen, hemp and cotton. In the tenth century, a mixture of linen seeds was used in the Armenian paper [3]. In 1450, the supply problems that arose with the invention of the printing press drove the production of new types of paper, mainly based on the use of plants. Currently, paper is made mainly from cellulose and hemicellulose fibres and from wood fibres with various impurities, such as lignin, pectins, traces of resins, tannins, carbohydrates and waxes [2, 4, 5]. In addition, small amounts of organic and inorganic additives, such as inks, adhesives, fillers and bleaching agents, are commonly added to improve the properties of the paper.

By analysing the composition of the paper, it is possible to characterise its origin through its trace elements, which may differ from one manufacturer to another [4, 5]. This way, a unique chemical fingerprint can be identified for each batch or sheet of paper [2]. Therefore, the paper could provide crucial information on the production of manuscripts that may not be found in any other type of evidence [2, 5, 6].

Nevertheless, paper does not remain unaltered over time, as it deteriorates through physicochemical and biological processes [7]. The severity of these deterioration is influenced not only by the chemical composition of the paper, but also by some environmental factors involved in its storage and preservation (e.g. the presence of microorganisms and contaminants, humidity, temperature and light) [2, 4, 8-10].

Moreover, components such as inks are generally found in documents. The forensic examination of inks is mainly focused on the analysis of any written entry that may be added or altered, and their study is one of the most widespread tools for document dating [11-16]. However, document dating remains one of the most burdensome tasks in the field of forensic document examination [12, 13, 17-19]. Ink analysis presents several difficulties, since not all documents under investigation have ink entries and the range of application of the existing methods is quite limited ($0 < x < 5$ years) [16, 17, 19, 20]. In this study, paper analysis is proposed as a possible alternative to ink studies to estimate the age of relatively old documents (around 5-30 years).

Two main approaches can be applied when studying the age of a questioned document: direct and indirect. The first approach follows the degradation of known compounds over time, whereas the second one is based on the analysis of the ink or paper composition by comparison with other papers, ink strokes or inks of known age [1]. In both approaches,

artificial ageing treatments (using controlled UV radiation, temperature, humidity and environmental contaminants) can be used to mimic the degradation processes, providing reference materials similar to naturally aged documents [21, 22].

Currently, several analytical techniques have been applied to estimate the age of documents [1]. Spectroscopic techniques are one of the most powerful tools used in this field due to their non-destructive nature. These techniques can directly analyse the materials under investigation, without requiring the collection of samples, and even portable instruments have been developed [1, 2]. Due to their microscopic applications, Fourier transform infrared spectroscopy (FTIR) [2, 23, 24], Raman spectroscopy [2, 25], X-ray spectroscopy (XRF) [2, 24] and laser ablation inductively coupled plasma mass spectrometry (LA-ICP-MS) [2, 26] have been widely used. However, despite their effectiveness in obtaining preliminary information, their results often need to be confirmed or complemented with other analyses.

The complexity of the samples under investigation and the interest in obtaining more extensive information has led to the use of destructive techniques. Gas chromatography coupled to mass spectrometry (GC/MS) is widely recognised as the best approach to investigate organic materials in artworks and archaeological objects [22, 27, 28]. However, many of the organic materials encountered in the cultural heritage or forensic field are complex polar compounds with high molecular weight and low volatility that cannot be analysed by this technique. In those cases, their analysis by GC/MS can be achieved by coupling it to pyrolysis (Py-GC/MS) [8, 22, 27-31]. Py-GC/MS has been used for the characterisation and identification of organic materials in cultural heritage, art, conservation and restoration and archaeological fields with different purposes: to address attribution and dating issues, to characterise materials used in different manufacturing

stages, to establish the various chemical and physical changes that take place in materials as they age, to assess the best conditions for long-term preservation and plan restoration, etc. [9, 22, 28, 32].

Py-GC/MS is a micro-destructive technique that can be applied directly to a solid or liquid sample, without any previous treatment [33]. By applying this technique, the chemical structures of the thermal decomposition products can be identified with the aim of characterising the paper. This information enables the determination of different organic materials, such as waxes, resins, oils, binders, pigments and dyes [31, 34-36]. The fragments observed provide a characteristic fingerprint of each particular sample in terms of the nature of the fragment and its relative distribution [4, 36]. The chemical composition of the original components of a sample can be reconstructed by performing a detailed interpretation of the chromatographic molecular profile of the thermal degradation products. However, this can be an arduous task for complex matrices [22, 27, 28, 30, 31, 35]. Chemometric methods together with analytical techniques are powerful tools that are increasingly being used to overcome these difficulties. Principal component analysis (PCA), cluster analysis (CA) and discriminant analysis (DA) have already been used in ink differentiation and characterisation [37, 38]. In addition, multivariate regression methods, such as partial least squares (PLS) regression, have attracted researchers' attention for ink and paper dating purposes [23, 39, 40], as they can be used to correlate spectral or chromatographic data with modifications in sample composition over time.

In this work, Py-GC/MS is used to estimate the age of the document through two different approaches based on paper analysis: (i) a direct method using a multivariate regression of the pyrolytic profiles of synthetic samples correlated with their ageing time in chamber, and (ii) an indirect method for the identification of the characteristic components of the paper

during different time periods. The applicability of these approaches was assessed by studying several office-type documents held under police custody and registered between 1986 and 2011.

2.2 Experimental procedure

2.2.1 Analytical method

2.2.1.1 Pyrolysis temperature

In order to study the influence of the pyrolysis temperature on the fragmentation of the paper components and, consequently, the resolution of the obtained pyrogram, 3, 5 and 10 micro-samples were taken. Fewer micro-samples were not tested to avoid lack of representativeness of the sampled document. A Harris Micro-Punch (1.00 mm in diameter) was used for sampling white paper sheets (SelectOne, Australia, 100 g m^{-2}). 3, 5 and 10 micro-samples were pyrolysed at 280, 400, 600, 750 and 1000 ºC and analysed by GC/MS. The representativeness of the entire sample (document) and the sensitivity of the analysis were examined.

2.2.1.2 Study of document age

Sheets of three types of paper were selected to construct and validate the calibration model: white paper (SelectOne, Australia, 100 g m^{-2}), recycled paper (Steinbeis, Germany, 80 g m^{-2}) and notebook paper (Oxford-Optik Paper, 90 g m^{-2}, 4 mm squared). Paper tests of 3 x 2 cm were artificially aged using xenon light based Solarbox 1500 equipment (CO.FO.ME.GRA., Italy). The spectral range between 300 and 850 nm was used and the irradiance, temperature and relative humidity were set at 550 W m^{-2}, 55 °C and 50%, respectively. The temperature was controlled by a BST (Black Standard Thermometer) probe. The three types of paper were

exposed to a maximum of 475 h of chamber ageing under controlled conditions. 15 tests for each type of paper were aged following an isochronous timetable (475, 411, 387, 363, 339, 315, 282, 256, 239, 219, 194, 163, 89, 48 and 2 h). A vial with 3 micro-samples of each aged paper was analysed by Py-GC/MS applying a pyrolysis temperature of 400 ºC. A quality control sample (QC) made up of 3 micro-samples of white paper (100 g m^{-2}) was added after every 6 samples.

2.2.1.3 Py-GC/MS analysis

The analysis of the micro-samples was carried out in a microfurnace pyrolyser (5250 pyrolyser, CDS Analytical, United States (USA)) connected directly to the injector of a gas chromatograph coupled to the mass spectrometer (5975C GC/MS system with Triple-Axis Detector, Agilent Technologies, USA). A ZB-WAX capillary column (30 m x 0.25 mm x 0.25 µm) was used for the chromatographic separation. The carrier gas was helium (99.999%) with a constant flow of 1.7 mL min^{-1} and a pressure of 13.7 psi. The injector and transfer line temperatures were set at 300 °C. The injector operated in split mode (split ratio 1:10) and a solvent delay of 2.10 min was set. The oven temperature program started at 40 °C, keeping this temperature for 2 min, and then increased at 12 °C min^{-1} up to 250 ºC, temperature that was held for 1 min. The operation conditions for the electron impact (EI) mass spectrometer were: an ionising voltage of 70 eV and a SCAN range from m/z 40 to m/z 550. The structural identification of the fragments was performed by comparison with the NIST 11 mass spectra library.

2.2.1.4 Documents studied

The Documentoscopy section of the Spanish General Commissary of Scientific Police (Madrid) provided 6 report documents under police custody registered in 1986, 1991, 1996, 2002, 2006 and 2011. Each of them was made up of 5 sheets stapled at the top left, with the exception of the document from 1991, which consisted of 2 stapled sheets. The sheets employed were white commercial paper of 90 g m^{-2} in A4 size, typical of office stationery. It was not possible to ensure the same manufacturer for all of them. Each report was printed in black ink on a single face. The logo of the Ministry of the Interior was placed on the upper left side of each sheet. On the left margin of the pages and on the bottom of the last sheet of the documents, the stamp of this department and the signatures of the head of section and the experts (made with black and blue ink writing tools) were located. The storage conditions from printing to analysis were similar for all the documents. After a brief period under office conditions, the reports were all kept together in classification boxes for several weeks. Afterwards, they were stored in files for about 6 years on shelves in an archive with controlled humidity, temperature and lighting conditions. In 2012, documents from 2000 onwards were kept in the archive, while those from earlier dates were moved to a basement warehouse in dark and low temperature conditions. The documents were delivered to the laboratory in transparent plastic covers. A micro-sample was taken from each of the top, middle and bottom pages of each document. A total of 15 micro-samples (5 sheets x 3 micro-samples per page) were taken per document, except for the one from 1991 (2 sheets x 3 micro-samples per page). They were stored and transported to another laboratory in closed glass vials until their subsequent analysis. A vial with 3 micro-samples of each page of the document was analysed by Py-GC/MS applying a pyrolysis temperature of 400 and 600 ºC, which were the optimal ones in terms of chromatographic resolution. QC samples were also added for every 6 samples. The

documents were used to test the regression models developed and to identify the characteristic compounds of each of the dates studied.

2.2.2 Data pre-processing and multivariate statistical analysis

In order to examine the differences between each type of artificially aged paper, an unsupervised exploratory analysis of the chromatographic data was performed by means of a PCA using SIMCA 13.0 software (Umetrics, Umeå, Sweden). The intensities of the chromatographic signals recorded at each retention time were used as **X** variables. The best grouping of quality control samples was the criterion used for the choice of data processing. Data were centred prior to analysis and no scaling or transformation algorithm was applied.

A predictive model was built by applying PLS regression after examining the data through PCA. Retention times from 7 to 19.5 min were used, since the direct injection of volatile fragments obtained in the pyrolyser affects the pneumatic control of the chromatographic system, causing a lack of reproducibility in early retention times (2 min < RT < 7 min). The pyrograms were treated as spectra. A calibration set consisting of 45 micro-samples (3 micro-samples of white paper for each artificial ageing time, n = 15) was used for the construction of the model. The ageing time in chamber (as dependent **Y** variable) was regressed against the intensities of the chromatographic signals of each retention time recorded in the pyrograms (as independent **X** variables). A leave-one-out cross-validation was performed to internally validate the PLS model. The chromatographic data of one sample of the calibration set was removed from this set and a model was constructed with the remaining chromatographic data of the calibration set. The deleted sample was predicted with this model and the procedure was repeated leaving each sample out of the calibration set. The PLS model was also externally validated using a validation set of 18 micro-

samples (3 micro-samples for each notebook and recycled paper with accelerated ageing of 475, 282 and 2 h). Different mathematical pre-treatments of the chromatographic data, including mean centering, unit variance (UV) and Pareto scaling as well as logarithm and power transformations, were tested. Spectral filters, such as first and second derivative transformations, multiplicative scatter correction (MSC), Savitzky-Golay, standard normal variate (SNV), row center, exponentially weighted moving average (EWMA) and combinations thereof, were also applied in order to minimise baseline noise and maximise the differences found in the chromatographic signals. A logarithmic transformation was applied to the **Y** variable, resulting in a significant decrease in the root mean square error of estimation (RMSEE) and cross-validation (RMSECV) values. No outliers were detected in the Hotelling's T2 control graph for 95% confidence in any PLS model. Although two samples (2 and 475 h) were detected in the distance-to-model graph as possible moderate outliers, they were not excluded to avoid the lack of information of the extreme times.

2.3 Results and discussion

In the chromatograms obtained using the HP-5 capillary column several compounds were eluted within the first minutes of analysis, while for the ZB-WAX column fewer chromatographic signals were detected before 7 min. The pyrolysis injection mode caused a displacement of the chromatographic signals of poorly retained compounds, therefore, the ZB-WAX capillary column was selected, increasing the chromatographic resolution and reproducibility.

No improvement in chromatographic sensitivity was achieved with 5 or 10 micro-samples. Thus, 3 micro-samples of each aged paper and each page of the documents were analysed.

Among the different pyrolysis temperatures studied, the temperature of 280 °C resulted in a pyrogram with weak chromatographic signals and few pyrolytic products. According to previous research in which temperatures above 300 ºC are recommended [3, 4], the application of 400 ºC increased the intensity of the chromatographic signals and produced new compounds due to the decomposition of cellulose, whereas at a temperature of 600 ºC a greater number of pyrolysis products were created. Most intensities of the chromatographic signals increased at higher pyrolysis temperatures (750 and 1000 ºC), but a large number of small and non-specific products were formed, causing a drastic decrease in chromatographic resolution. Based on the good chromatographic resolution and sensitivity obtained at a pyrolysis temperature of 400 ºC, such temperature was applied to carry out the multivariate regression analysis (direct approach). For the indirect approach, pyrolysis temperatures of 400 ºC and 600 ºC were used.

The reproducibility of the sampling was tested to ensure that all analyses were carried out by taking the same amount of micro-samples. In this test, the Micro-Punch tool used always extracted an equal quantity of paper (4% in terms of relative standard deviation (RSD) by testing 10 replicas by weighing).

The pyrograms of each type of paper (white, recycled and notebook paper) were visually examined prior to carrying out the multivariate regression study. The pyrograms and the main compounds identified on each type of paper after an accelerated ageing of 475, 282 and 2 h and at a pyrolysis temperature of 400 °C are shown in Figure 1 and Table 1.

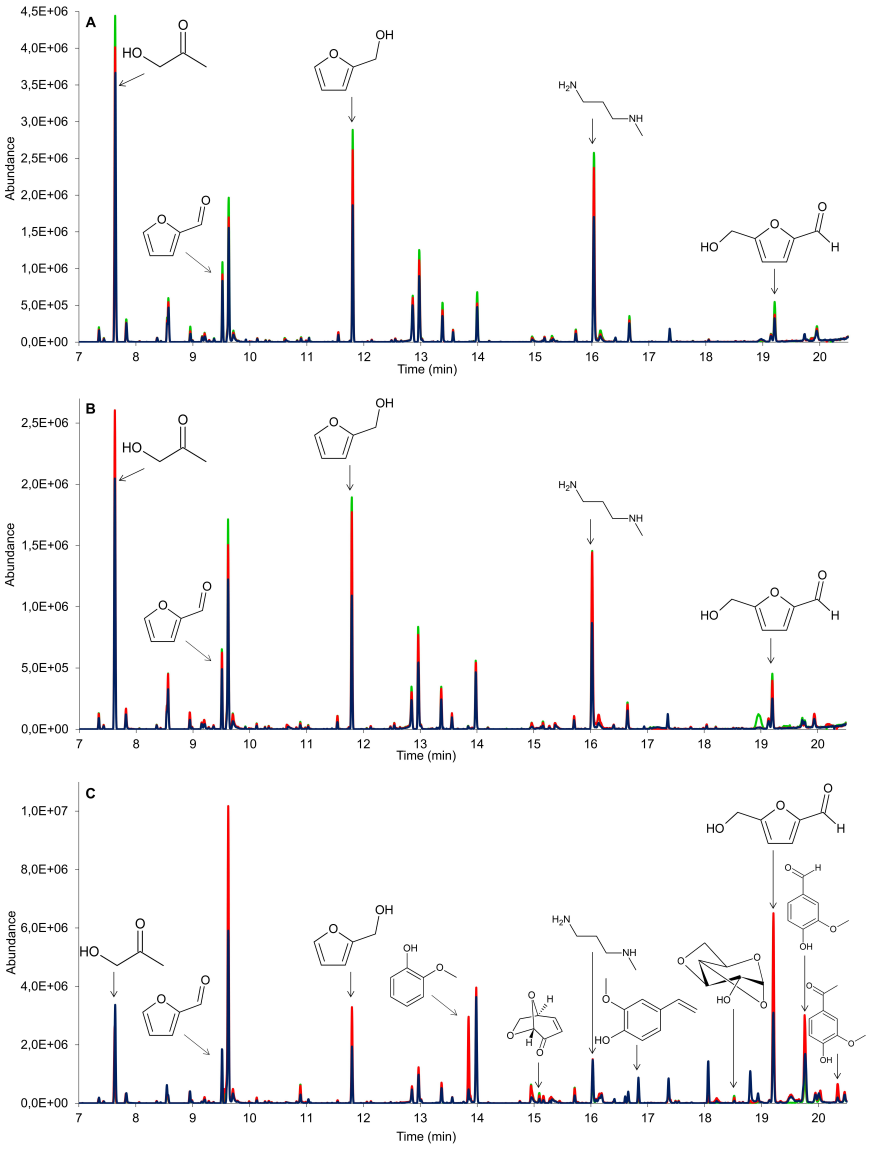

Figure 1. Pyrolysis products identified in the pyrograms of white paper (A), notebook paper (B) and recycled paper (C) after an accelerated ageing of 475 (green line), 282 (red line) and 2 (blue line) h. Pyrolysis temperature of 400 ºC. GC/MS conditions: ZB-WAX column (30 m x 0.25 mm x 0.25 µm), split injection (1:10), injection temperature of 300 °C, temperature gradient: 40 °C kept for 2 min, 12 °C min^{-1} to 250 ºC and 250 ºC hold for 1 min.

Table 1. Pyrolysis products identified in artificially aged white, notebook and recycled paper. More than 90% match for the NIST 11 mass spectra library. Pyrolytic and chromatographic conditions as in Figure 1.

Compound	RT (min)	M (g/mol)	White paper	Notebook paper	Recycled paper
1-Hydroxy-2-propanone	7.65	74.08	×	×	×
Furfural	9.60	96.09	×	×	×
2-Furanmethanol	11.80	98.10	×	×	×
2-Methoxy-phenol	13.84	124.14			×
Levoglucosenone	15.10	126.11			×
N-methyl-1,3-propanediamine	16.04	88.15	×	×	×
2-Methoxy-4-vynilphenol	16.85	150.18			×
1,4:3,6-dianhydro-α-d-glucopyronose	18.52	144.13			×
5-Hydroxymethylfurfural	19.20	126.11	×	×	×
Vanillin (4-hydroxy-3-methoxybenzaldehyde)	19.78	152.15			×
Apocynin (1-(4-hydroxy-3-methoxyphenyl)ethanone)	20.34	166.17			×

The chromatographic profiles of white paper and notebook paper were practically identical. In general, the older was the paper, the higher was the intensity of the chromatographic signals. This may be due to the fact that the breakage of the cellulose chains of the paper made up of β-D-glucose molecules increases with age, releasing a greater number of compounds and thus obtaining chromatographic signals of greater intensity. In contrast, the pyrogram of recycled paper was completely different to that of white paper and notebook paper, the increase in the intensity of the chromatographic signals with artificial ageing being less evident. It was possible to identify characteristic compounds of the recycled paper known as 4-substituted-2-methoxyphenols formed by the acid-base and redox reactions of lignin and sugars, for example, levoglucosone and 1,4:3,6-dianhydro-α-d-glucopyranose created by the decomposition of hemicellulose and cellulose [41].

The recycled paper differed strongly from the white paper and notebook paper in the first component of the PCA model's scores plot (Figure 2A), in agreement with the large difference already detected by visual inspection of the chromatographic profiles. The white paper and notebook paper samples were separated from each other along the second component. Moreover, the **X** variables (RT) corresponding to furfural and 5-hidroxymethylfurfural with retention times of 9.60 and 19.20 min, respectively, were positively correlated with the first component in the loadings plot (Figure 2B), having a great influence on the differentiation of white, recycled and notebook paper according to the intensity of the chromatographic signals that such compounds show on each type of paper. The chromatographic signals of furfural and 5-hidroxymehtylfurfural were found to be more intense in the samples of the recycled paper.

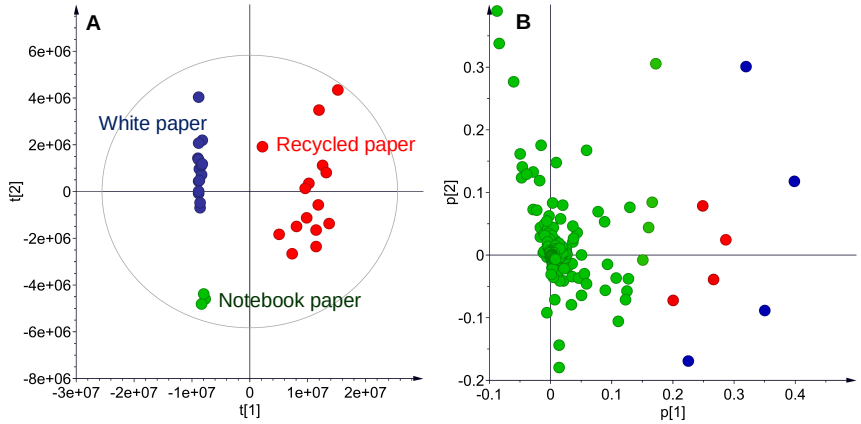

Figure 2. A - Scores plot of the first two components of the PCA model with the Hotelling's T2 control ellipse (95% confidence). B - Loadings plot of the PCA model. The points represent the **X** variables (RT). The variables corresponding to furfural and 5-hidroxymethylfurfural are coloured in blue and red, respectively.

The optimal PLS models were obtained by applying SNV, EWMA and row center filters (Table 2). The models were established with 3 components (PCs), explaining a variation of 88-92% (R^2X) and 80-93% (R^2Y) in the data with predictive properties of 37-53% (Q^2). The fit of the PLS models was perfect with acceptable predictive capabilities. The RMSECV and RMSEE values of the PLS model with SNV filter were 0.51 and 0.18, respectively, indicative of the model's good predictive accuracy. Likewise, the RMSE of prediction (RMSEP) value was 0.28, implying that its predictive ability was valid. The RMSECV, RMSEE and RMSEP values were much larger for the PLS models in which EWMA and row center filters were applied.

Table 2. Data of the PLS models applying centering and spectral filter transformations with 3 PCs.

Espectral Filter	R^2X	R^2Y	Q^2	RMSEE	RMSECV	R^2CV	RMSEP
First derivative transformation (15 points in filter and quadratic order polynomial fit)	0.94	0.80	0.43	0.30	0.49	0.80	3
Second derivative transformation (15 points in filter and quadratic order polynomial fit)	0.95	0.78	0.40	0.31	0.47	0.78	5
Multiplicative Scatter Correction (MSC)	0.90	0.92	0.63	0.20	0.47	0.92	0.28
Standard Normal Variate (SNV)	0.88	0.93	0.53	0.18	0.51	0.93	0.28
Row Center	0.92	0.81	0.38	0.30	0.47	0.80	0.38
Savitzky-Golay	0.94	0.80	0.40	0.30	0.49	0.80	2
Exponentially Weighted Moving Average (EWMA)	0.92	0.80	0.37	0.30	0.47	0.80	0.39

The predictions for the white paper were similar in terms of precision in the three models. In terms of accuracy, the PLS model with SNV filter got a higher accuracy (30% relative error) compared to the results obtained with the EWMA and row center filters (35% relative error), as shown in Table 3. Therefore, the application of the SNV filter was optimal for the white paper (the most commonly used in questioned documents). The predictions for notebook paper, on the contrary, were more accurate when applying the PLS models with EWMA and row center filters, with identical precisions (Table 3). The recycled paper was excluded from the analysis, since the differences in the chemical composition of this type of paper made it impossible to predict a date with an acceptable error (results not shown).

The **Y** variable (logarithm of accelerated ageing time) and the **X** variables (RT) corresponding to 2-furanmethanol and n-methyl-1,3-propanediamine with retention times of 11.80 and 16.04 min, respectively, had a large contribution and were positively correlated with the first component of the loadings plot of the PLS model with SNV filter (Figure 3), while 1-hydroxy-2-propanone with a retention time of 7.65 min was negatively correlated with age. This indicates that the intensities of the chromatographic signals of 2-furanmethanol and n-methyl-1,3-propanediamine increase with age, whereas the intensity of 1-hydroxy-2-propanone decreases. The monitoring of the behaviour and influence of these compounds on the ageing process of white paper would be strongly recommended in further analyses.

Table 3. Predicted ageing time (h) ± error for the white and notebook paper samples by applying the PLS models with SNV, EWMA and row center filters.

Paper type	Real ageing time (h)	Predicted ageing time (h)		
		Model with SNV filter	Model with EWMA filter	Model with row center filter
White	48	32 ± 1	42 ± 1	41 ± 1
	89	61 ± 1	38 ± 2	39 ± 2
	194	285 ± 1	170 ± 1	173 ± 1
	219	325 ± 1	410 ± 2	408 ± 2
	239	316 ± 1	129 ± 2	133 ± 2
	282	182 ± 2	119 ± 2	120 ± 2
	363	367 ± 1	424 ± 1	421 ± 1
	387	425 ± 1	376 ± 1	379 ± 1
	475	240 ± 2	415 ± 1	408 ± 1
Notebook	2	78 ± 39	13 ± 6	13 ± 6
	282	1322 ± 5	203 ± 1	201 ± 1
	475	2120 ± 4	427 ± 1	419 ± 1

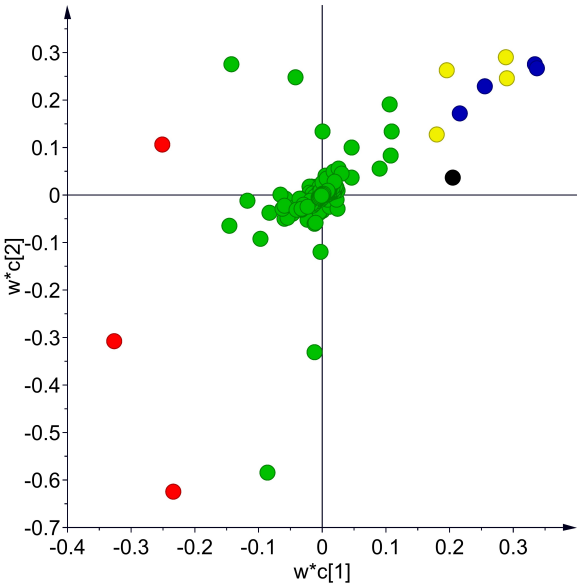

Figure 3. Loadings plot of the PLS model with SNV filter. The first component (R^2X 21%) was plotted against the second component (R^2X 62%). The green and black points represent the **X** and **Y** variables, respectively. The **X** variables (RT) corresponding to 2-furanmethanol and N-methyl-1,3-propanediamine are coloured in yellow and blue, respectively, while 1-hidroxy-2-propanone is coloured in red.

In order to determine the correlation between artificial ageing and its equivalent in real ageing under police custody conditions, the PLS model with SNV filter was used. Throughout this study, a great variability between the different pages of the same document was observed. The abundances of some of the compounds obtained from the different pages that make up the document of the same year had a dispersion measured as RSD of 21-54% for the document of 1986, 5-44% for the document of 1991, 7-16% for the document of 2006 and 17-22% for the document of 2011. This variability was not a consequence of the technique applied, since the same test performed on the control samples showed a RSD of 6-8%, but of the environmental conditions to which they may have been exposed. Due to this variability, the fourth sheet of each document whose ageing process was the most uniform was chosen to construct the regression line (Figure

4). The documents of 2011, 2006, 2002 and 1986 showed a good fit, whereas the documents of 1996 and 1991 displayed a greater deviation. This may be due to the different preservation environments that during their custody they passed through, as explained in the description of the documents. The correlation between the natural ageing and the accelerated ageing of the selected papers was determined by the equation in Figure 4, in which 5 h in chamber under the conditions studied were equivalent to one natural year under police custody conditions. From this regression model, other documents kept under the same conditions and made with a similar type of paper could have been dated. Currently, given the impossibility of having more samples for this study from the Spanish General Commissary of Scientific Police, each of the samples used to build the regression was taken as a real sample. To do this, the age of each of the samples was estimated from the regression obtained with the data set (n = 3), leaving out the test sample. An acceptable estimation date was calculated (red triangle) with accuracy error values between 1.8% and 7.4%, as shown in Figure 4.

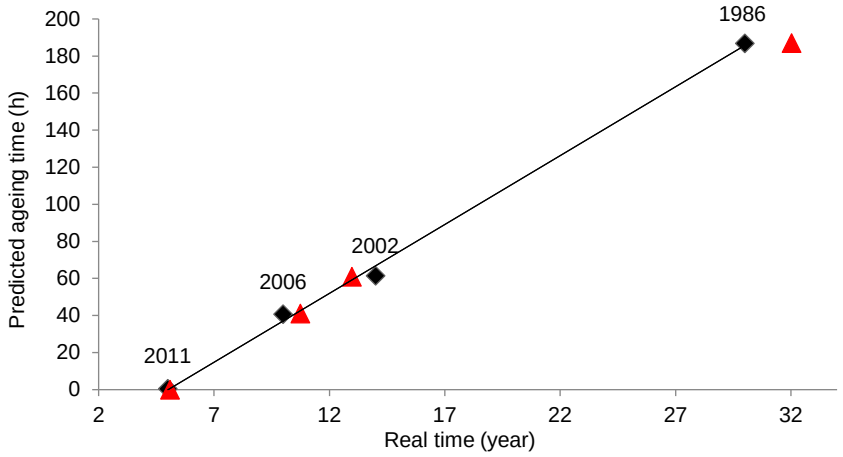

Figure 4. Graph of real time (year) versus predicted ageing time (h) from the PLS model with SNV filter. Equation Y = 7.43 X - 37.25, R^2 = 0.99. The red triangle represents the predicted date from the regression obtained with the data set (n = 3), leaving out the test sample.

Finally, an indirect approach based on the identification of compounds characteristic of the period of the document was explored. In a visual examination of the pyrograms at a pyrolysis temperature of 400 °C, a similar profile was observed in all the documents (Figure 5). In general, the greater the ageing, the greater the intensity of the chromatographic signals, as was also observed in the study of artificial ageing. The main compounds identified in the pyrograms of each document are listed in Table 4. 4-hydroxybutanoic acid and 2-hydroxy-3,4-dimethyl-2-cyclopenten-1-one were detected in all the documents analysed, except in the sample from 1986. The absence of these compounds in the oldest document may be due to a change in paper manufacture [7, 24]. If confirmed, the targeted analysis of these compounds could help to determine the age of the document indirectly. In addition, propanoic acid was found at a pyrolysis temperature of 600 °C in all the oldest documents: 1986, 1991 and 1996. 4-hydroperoxy-1-phenyl-1-cyclohexene, 2-methyl benzofuran and naphthalene, formed by the thermal decomposition of cellulose [41], were also detected in all the sheets constituting the document from 1986, but not in the rest of the documents (Table 4).

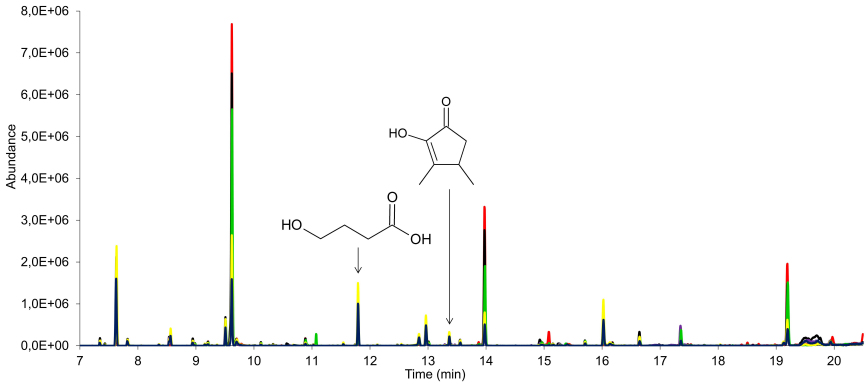

Figure 5. Pyrograms of the documents under police custody: 2011 (blue line), 2006 (yellow line), 2002 (green line), 1996 (purple line), 1991 (black line) and 1986 (red line). Pyrolytic and chromatographic conditions as in Figure 1.

Table 4. Pyrolysis products identified on the sheets of each document under police custody. More than 90% match for the NIST 11 mass spectra library. Pyrolytic and chromatographic conditions as in Figure 1.

Pyrolysis temperature	Compound	RT (min)	M (g/mol)	1986 document	1991 document	1996 document	2002 document	2006 document	2011 document
400 ºC	4-Hydroxybutanoic acid	11.54	104.11		×	×	×	×	×
	2-Hydroxy-3,4-dimethyl-1,2-cyclopenten-1-one	13.21	126.15		×	×	×	×	×
600 ºC	Propanoic acid	10.53	74.08	×	×	×			
	4-Hydroperoxy-1-phenyl-1-cyclohexene	11.11	191.25	×					
	2-Methyl benzofuran	11.18	132.16	×					
	Naphtalene	12.74	128.17	×					

2.4 Conclusions

The estimation of the document age based on the analysis of paper applying Py-GC/MS has proven to be a promising approach to be taken into account for forensic purposes. It is a micro-destructive approach, requiring a small portion of document and no sample treatment prior to the pyrolysis stage.

The direct approach by means of a PLS model with SNV filter obtained acceptable accuracy and precision values of ageing estimation for white paper samples. However, this method presented difficulties in finding a universal model for samples with a completely different profile and composition. This direct approach requires that the compared documents were kept under similar conservation conditions. From this direct approach, a correlation between the natural and artificial ageing was established, in which 5 h in the ageing chamber were equivalent to one natural year under policy custody conditions.

Moreover, this chemometric treatment enabled to obtain interesting information about the transformations that the paper matrix undergoes during the ageing process. The abundance of the chromatographic signals increased with ageing (both natural and accelerated). In addition, it was possible to identify the paper components that most influenced this ageing process: 2-furanmethanol, n-methyl-1,3-propanediamine and 1-hydroxy-2-propanone.

Complementarily, although further studies will be necessary, the indirect approach allowed to identify some characteristic compounds of the different dates studied. The presence or absence of some identified compounds (4-hydroxybutanoic acid, 2-hydroxy-3,4-dimethyl-2-cyclopenten-1-one, propanoic acid, 4-hydroperoxy-1-phenyl-1-

cyclohexene, 2-methyl benzofuran and naphthalene) may be related with the age estimation determined by the direct approach.

The two methodologies for estimating the age of documents based on paper analysis here presented can be considered as promising alternative and/or complementary tools to the more commonly used ink analyses. Although the two proposed approaches lack of universal applicability due to the influence of relevant factors, such as the type of paper and the conservation conditions, they open a promising horizon for dating moderately old documents.

Acknowledgments

The authors would like to thank the Documentoscopy section of the General Commissary of Scientific Police (Madrid) for providing the documents under police custody and explaining their forensic needs. The authors also thank Dr. Carlos Martín Alberca from the Research Group in Forensic Chemistry (INQUIFOR) of the University of Alcalá for his useful discussion. Likewise, we thank Dr. Enara Artetxe and Dr. Itxaso Maguregui from the Faculty of Fine Arts of the University of the Basque Country (UPV/EHU) for the technical support with the accelerated ageing chamber. The authors would also like to thank the Advanced Research Facilities (SGIker) of the UPV/EHU for the technological support in the development of this work. Finally, L. Ortiz-Herrero thanks the UPV/EHU for the pre-doctoral fellowship.

References

[1] M. Calcerrada, C. García-Ruiz, Analysis of questioned documents: A review, *Anal. Chim. Acta.* 853 (2015) 143-166. http://doi.org/10.1016/j.aca.2014.10.057.

[2] M. Manso, M.L. Carvalho, Application of spectroscopic techniques for the study of paper documents: A survey, *Spectrochim. Acta Part B At. Spectrosc.* 64 (6) (2009) 482–490. http://doi.org/10.1016/j.sab.2009.01.009.

[3] Y. Keheyan, V. Aharonian, Proceedings 4th International Congress on Science and Technology for the Safeguard of Cultural Heritage in the Mediterranean Basin, v. 2, pp. 542-551, 6-8 December 2009, Cairo Egypt.

[4] Y. Keheyan, Py/GC/MS analyses of historical papers, *BioRes.* 3 (3) (2008) 829-837.

[5] C. Avataneo, M. Sablier, New criteria for the characterisation of traditional East Asian papers, *Environ. Sci. Pollut. Res.* 24 (2017) 2166-2181. http://doi.org/10.1007/s11356-016-6545-0.

[6] B. Han, G. Daheur, M. Sablier, Py-GCxGC/MS in cultural heritage studies: An illustration through analytical characterisation of traditional East Asian handmade papers, *J. Anal. Appl. Pyrolysis* 122 (2016) 458–467. http://doi.org/10.1016/j.jaap.2016.10.018.

[7] M.C. Area, H. Cheradame, Paper ageing and degradation: recent findings and research methods, *BioRes.* 6 (4) (2011) 5307-5337.

[8] Y. Keheyan, G. Eliazyan, P. Engel, B. Rittmeier, Py/GC/MS characterisation of naturally and artificially aged inks and papers, *J. Anal. Appl. Pyrolysis* 86 (2009) 192-199. http://doi.org/10.1016/j.jaap.2009.06.004.

[9] H. Ohtani, T. Komura, N. Sonoda, Y. Taguchi, Evaluation of acidic paper deterioration in library materials by pyrolysis-gas

chromatography, *J. Anal. Appl. Pyrolysis* 85 (2009) 460-464. http://doi.org/10.1016/j.jaap.2008.11.037.

[10] S. Manente, A. Micheluz, R. Ganzerla, G. Ravagnan, A. Gambaro, Chemical and biological characterisation of paper: A case study using a proposed methodological approach, *Int. Biodeterior. Biodegrad.* 74 (2012) 99-108. http://doi.org/10.1016/j.ibiod.2012.03.008.

[11] A. Koenig, C. Weyermann, Ink dating part II: Interpretation of results in a legal perspective, *Sci. Justice* 58 (1) (2017) 31-46. http://doi.org/10.1016/j.scijus.2017.08.003.

[12] A. Koenig, S. Magnolon, C. Weyermann, A comparative study of ballpoint ink ageing parameters using GC/MS, *Forensic Sci. Int.* 252 (2015) 93-106. http://doi.org/10.1016/j.forsciint.2015.03.027.

[13] A. Koenig, J. Bügler, D. Kirsch, F. Köhler, C. Weyermann, Ink Dating Using Thermal Desorption and Gas Chromatography/Mass Spectrometry: Comparison of Results Obtained in Two Laboratories, *J. Forensic Sci.* 60 (S1) (2015) 52-61. http://doi.org/10.1111/1556-4029.12603.

[14] G.M. LaPorte, J.D. Wilson, A.A. Cantu, S.A. Mancke, S.L. Fortunato, The identification of 2-phenoxyethanol in ballpoint inks using gas chromatography/mass spectrometry-relevance to ink dating, *J. Forensic Sci.* 49 (2004) 1–5. http://doi.org/10.1520/JFS2003217.

[15] A. Koenig, C. Weyermann, Ink dating, part I: Statistical distribution of selected ageing parameters in a ballpoint inks reference population, *Sci. Justice* 58 (1) (2018) 17-30. http://doi.org/10.1016/j.scijus.2017.08.002.

[16] J. Bügler, H. Buchner, A. Dallmayer, Age determination of ballpoint pen ink by thermal desorption and gas chromatography-mass spectrometry, *J. Forensic Sci.* 53 (4) (2008) 982–988. http://doi.org/10.1111/j.1556-4029.2008.00745.x.

[17] C. Weyermann, J. Almog, J. Bügler, A.A. Cantu, Minimum requirements for application of ink dating methods based on solvent

analysis in casework, *Forensic Sci. Int.* 210 (1) (2011) 52-62. http://doi.org/10.1016/j.forsciint.2011.01.034.

[18] C. Weyermann, B. Schiffer, P. Margot, A logical framework to ballpoint ink dating interpretation, *Sci. Justice* 48 (2008) 118–125. http://doi.org/10.1016/j.scijus.2007.10.009.

[19] C. Weyermann, D. Kirsch, C. Vera, B. Splenger, A GC/MS study of the drying of ballpoint pen ink on paper, *Forensic Sci. Int.* 168 (2007) 119-127. http://doi.org/10.1016/j.forsciint.2006.06.076.

[20] I. San Román, L. Bartolomé, M.L. Alonso, R.M. Alonso, M. Ezcurra, Datink pilot study: a powerful methodology for ballpoint pen ink dating in questioned documents, *Anal. Chim. Acta* 892 (2015) 105-114. http://doi.org/10.1016/j.aca.2015.08.038.

[21] C. Weyermann, B. Spengler, The potential of artificial ageing for modelling of natural ageing processes of ballpoint ink, *Forensic Sci. Int.* 180 (2008) 23-31. http://doi.org/10.1016/j.forsciint.2008.06.012.

[22] M.P. Colombini, A. Andreotti, I. Bonaduce, F. Modugno, E. Ribechini, Analytical strategies for characterising organic paint media using gas chromatography/mass spectrometry, *Acc. Chem. Res.* 43 (6) (2010) 715-727. http://doi.org/10.1021/ar900185f.

[23] T. Trafela, M. Strlic, J. Kolar, D.A. Lichtblau, M. Anders, D.P. Mencigar, B. Pihlar, Nondestructive analysis and dating of historical paper based on IR spectroscopy and chemometric data evaluation, *Anal. Chem.* 79 (16) (2007) 6319-6323. http://doi.org/10.1021/ac070392t.

[24] V. Causin, C. Marega, A. Marigo, R. Casamassina, G. Peluso, L. Ripani, Forensic differentiation of paper by X-ray diffraction and infrared spectroscopy, *Forensic Sci. Int.* 197 (2010) 70-74. http://doi.org/10.1016/j.forsciint.2009.12.056.

[25] M.R. López-Ramírez, N. Navas, L.R. Rodríguez-Simón, J.C. Otero, E. Manzano, Study of modern artistic materials using combined spectroscopic and chromatographic techniques. Case study: painting

with the signature “Picasso”, *Anal. Methods* 7 (2015) 1499-1508. http://doi.org/10.1039/c4ay02365j.

[26] T. Trejos, A. Flores, J.R. Almirall, Micro-spectrochemical analysis of document paper and gel inks by laser ablation inductively coupled plasma mass spectrometry and laser induced breakdown spectroscopy. *Spectrochim. Acta Part B At. Spectrosc.* 65 (11) (2010) 884-895. http://doi.org/10.1016/j.sab.2010.08.004.

[27] S. Prati, S. Smith, G. Chiavari, Characterisation of siccative oils, resins and pigments in art works by thermochemolysis coupled to thermal desorption and pyrolysis GC and GC-MS, *Chromatographia* 59 (3) (2004) 227-231. http://doi.org/10.1365/s10337-003-0141-4.

[28] I. Bonaduce, E. Ribechini, F. Modugno, M.P. Colombini, Analytical approaches based on gas chromatography mass spectrometry (GC/MS) to study organic materials in artwork and archaeological objects, *Top. Curr. Chem.* 374 (2016) 1-6. http://doi.org/10.1007/s41061-015-0007-x.

[29] T. Learner, The analysis of synthetic paints by pyrolysis-gas chromatography-mass spectrometry (PY-GC/MS), *Stud. Conserv.* 46 (2001) 225-241. http://doi.org/10.1179/sic.2001.46.4.225.

[30] P. Schossler, I. Fortes, J.C. D’ Ars de Figueiredo Júnior, F. Carazza, L.A. Cruz Souza, Acrylic and vinyl resins identification by pyrolysis-gas chromatography/mass spectrometry: a study of cases in modern art conservation, *Anal. Lett.* 46 (12) (2013) 1869-1884. http://doi.org/10.1080/00032719.2013.777925.

[31] G. Chiavari, S. Prati, Analytical pyrolysis as diagnostic tool in the investigation of works of art, *Chromatographia* 58 (2003) 543-554. https://doi.org/10.1365/s10337-003-0094-7.

[32] R. Ganzerla, A. Gambaro, E. Cappelletto, M. Fantin, S. Montalbani, M. Orlandi, Characterisation of selected paper documents from the archives of Palazzo Ducale (Venice), Italy using various analytical

techniques, *Microchem. J.* 91 (2009) 70-77. https://doi.org/10.1016/j.microc.2008.08.003.

[33] J. Rusell, B.W. Singer, J.J. Perry, A. Bacon, The identification of synthetic organic pigments in modern paints and modern paintings using pyrolysis-gas chromatography-mass spectrometry, *Anal. Bioanal. Chem.* 400 (2011) 1473-1491. https://doi.org/10.1007/s00216-011-4822-9.

[34] I.D. Van der Werf, G. Germinario, F. Palmisano, L. Sabbatini, Characterisation of permanent markers by pyrolysis gas chromatography-mass spectrometry, *Anal. Bioanal. Chem.* 399 (2011) 3483-3490. https://doi.org/10.1007/s00216-011-4714-z.

[35] G. Chiavari, S. Montalbani, S. Prati, Y. Keheyan, S. Baroni, Application of analytical pyrolysis for the characterisation of old inks, *J. Anal. Appl. Pyrolysis* 80 (2007) 400-405. https://doi.org/10.1016/j.jaap.2007.04.011.

[36] L. Keheyan, L. Giulianelli, Identification of historical ink ingredients using pyrolysis-GC-MS. A model study, *Preserv. Sci.* 3 (2006) 5-10.

[37] R. Kumar, V. Sharma, A novel combined approach of diffuse reflectance UV–Vis-NIR spectroscopy and multivariate analysis for non-destructive examination of blue ballpoint pen inks in forensic application, *Spectrochim. Acta Mol. Biomol. Spectrosc.* 175 (2017) 67-75. http://doi.org/10.1016/j.saa.2016.12.008.

[38] N.C. Thanasoulias, N.A. Parisis, N.P. Evmiridis, Multivariate chemometrics for the forensic discrimination of blue ballpoint pen inks based on their vis spectra, *Forensic Sci. Int.* 138 (2003) 75-84. http://doi.org/10.1016/j.forsciint.2003.08.014.

[39] V.S. Amador, H.V. Pereira, M.M Sena, R. Augusti, E. Piccin, Paper Spray Mass Spectrometry for the Forensic Analysis of Black Ballpoint Pen Inks, *J. Am. Soc. Mass Spectrom.* (2017) 1-12. http://doi.org/10.1007/s13361-017-1686-z.

[40] V. Sharma, R. Kumar, Dating of ballpoint pen writing inks via spectroscopic and multiple linear regression analysis: A novel approach, *Microchem. J.* 134 (2017) 104-113. http://doi.org/10.1016/j.microc.2017.05.014.

[41] M. Chávez-Sifontes, M.E. Dominel, Lignin, structure and applications: depolymerisation methods for obtaining aromatic derivatives of industrial interest, *Av. Cienc. Ing.* 4 (4) (2013) 15-46.

CHAPTER 3

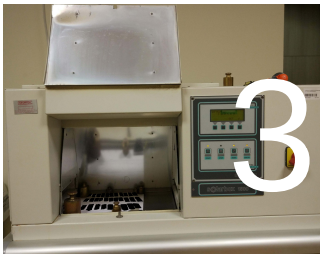

DATUVINK pilot study: A potential non-invasive methodology for dating ballpoint pen inks using multivariate chemometrics based on their UV-Vis-NIR reflectance spectra

L. Ortiz-Herrero, L. Bartolomé, I. Durán, I. Velasco, M.L. Alonso, M.I. Maguregui, M. Ezcurra

Microchemical Journal, **2018**; 140: 158–166

Q1, IF: 3.206, 20/84, Chemistry, Analytical

Adapted version

Abstract

The main methods for dating ballpoint pen inks in questioned documents used up to day are based on the analysis of ink volatile components. These methods have some limitations still unresolved, such as the impossibility of dating documents older than two to five years and the partial or total destruction of the questioned document after analysis. This study aims to overcome these drawbacks by exploring the feasibility of dating inks based on the monitoring of their UV-Vis-NIR diffuse reflectance spectra combined with a partial least squares (PLS) multivariate modelling. Inoxcrom® ink samples were exposed to accelerated ageing, their reflectance spectra were measured and a multivariate regression was applied. The spectroscopic data were pre-processed to improve the model's predictive ability and the characterisation of the spectra. The optimal model was the one obtained with the SNV filter. Accurate predictions with 25% error were obtained for two of the five ballpoint pen inks studied and a correlation between natural and artificial ageing could be established. Moreover, the region of the spectrum most closely related to the ink ageing process could be delimited. Young inks were characterised by modifications in the region of the visible and NIR spectra, while after ageing the most influential region was the NIR spectrum. The mismatch with the other three ballpoint pen inks studied could be attributed to consistent differences in the formulations of the inks. Inks sharing a common chromatographic profile proved to fit correctly into the predictive model, indicating that the methodology has great potential for future applications in the field of questioned document dating.

Key words: Ballpoint pen ink, ink dating, UV-Vis-NIR spectroscopy, diffuse reflectance, PLS.

3.1 Introduction

The proofs received in document examination cases are often on paper with ink entries. Hence, studies are carried out on both the printing system and the writing tool to look for signs of alteration and falsification and to determine or discard authorship. A way to determine the legitimacy of a document is to date it [1]. Most of the analytical methods used so far are destructive, being the widest used methodology the one based on the analysis of the volatile components of inks (2-phenoxyethanol) by gas chromatography coupled to mass spectrometry (GC/MS) [2-7]. However, this methodology has several drawbacks, such as the total or partial loss of the sample, which is a major problem in court cases, since it requires that the documents analysed be kept for a certain period of time. The scope of the method is also limited, as it can only establish an approximate date for the inks that have been deposited in the document for a maximum of two years [7-9]. An exception is the DATINK method, which dates ballpoint pen inks up to five years with a mean relative error of 21% using multiple headspace solid-phase microextraction (MHS-SPME) coupled to GC/MS [10]. Moreover, the methodology is based on the ageing kinetics of the volatile components, which varies according to the initial composition of the ink, the support on which it is deposited and the storage conditions to which it has been exposed [3, 4, 8, 9, 11]. Another disadvantage is the mass dependency, since the method depends on the amount of ink sampled, which can vary due to the heterogeneity of the ink stroke and the writing pressure applied. Therefore, the result of the analysis is dependent on these variations, which can sometimes lead to erroneous conclusions [8, 9]. The aforementioned issues have led researchers to employ other analytical techniques, such as UV-Vis-NIR spectroscopy, to address the great challenge of ink dating. This technique focuses on the study of the resins that make up the inks, in particular on the polymerisation and degradation processes linked to them and related to the age and/or drying

time of the ink. The resins deposited on the paper, once dry, create chemical bonds between the ink and the paper. They undergo degradation processes over time that result in the polymerisation and cross-linking of these bonds, causing changes in the structure and properties of the resins. Some of these modifications cause variations in the optical properties of the molecules, which can be measured by diffuse reflectance and absorbance. In addition, the dyes that make up the inks also undergo these processes and contribute to the signal detected. In summary, the UV-Vis-NIR spectroscopy technique measures the variations in the refractive index due to a greater or lesser polymerisation, a factor highly related to the degradation processes and, therefore, to the age of the ink [12].

The combination of analytical techniques with chemometrics has been widely used in recent years to extract the maximum and most meaningful information from the acquired data in an interpretable way. In the field of ink characterisation, differentiation and classification, several applications of exploratory analysis methods (principal component analysis (PCA) [13-17]) and classification and discrimination methods (hierarchical cluster analysis (HCA) [13], partial least squares-discriminant analysis (PLS-DA) [13, 18] and linear discriminant analysis (LDA) [15, 17, 19]) have been reported. Furthermore, although still limited, it is increasingly common to find scientific papers that have used chemometrics for ink dating. Senior *et al.* [16] used UV-Vis spectroscopy and high-performance thin layer chromatography (HPTLC) combined with PCA to characterise and date ballpoint pen inks. Ink lines extracted from the paper at different times were applied to a PCA, displaying different PCA loadings that were correlated over time by multiple linear correlation analysis. The equations obtained could be used to estimate the time at which a document of up to 4 months was written with accurate predictions within 10 days. Sharma *et al.* [20] subsequently reported the use of UV-Vis spectroscopy in conjunction with multiple linear regression (MLR) to model the fading of dyes in inks of a

particular ballpoint pen brand of up to approximately one year old. The model was able to estimate the age of the ink with an accuracy of ± 10 days. Diaz-Santana *et al.* [21] also applied gas chromatography-mass spectrometry and high performance liquid chromatography-diode array detection (HPLC-DAD) together with MLR. The modifications in the concentration of solvents and dyes in Montblanc® ballpoint pen inks of up to 4 years old were modelled, obtaining a maximum error estimate of 4 to 7 months. The above-mentioned research studies highlight the potential applicability of chemometrics to ink dating, however, several drawbacks still need to be resolved. Most methodologies require the extraction of the ink in a solvent, rather than an in-situ analysis on the paper support. Moreover, they have a limited scope, as they are applied either to inks of a particular pen brand or to inks that have been deposited in the document for a few months.

The aim of this study was to develop a universal and non-destructive ink dating method (DATUVINK) based on the monitoring of diffuse reflectance modifications in writing inks as they age. In order to do this, a chemometric model was performed using artificially aged black ink samples, based on a multivariate regression of the gathered diffuse reflectance data. The UV-Vis-NIR reflectance analysis allowed determining the refractive index variations occurred due to changes in the ink components as they age (loss of volatile components, fading of dyes and/or polymerisation of resins). Factors related to the ink degradation processes and, therefore, to the age of the ink. In this way, a predictive model capable of determining the age of the ink was developed. However, the model was carried out using artificially aged ink samples, so in order to improve applicability it was necessary to establish a previous correlation between natural and accelerated ageing.

3.2 Materials and methods

3.2.1 Chemicals and materials

Ethanol (EtOH) was purchased from Scharlab (Scharlab Chemie S.A., Barcelona, Spain). Methanol (MeOH) was acquired from Romil Pure Chemistry (Cambridge, England, United Kingdom (UK)). Ammonium acetate (AmAc) was from Merck (Darmstadt, Germany). Milli-Q water from a Millipore filtration system (Millipore, Bedford, MA, United States (USA)) was used. A bottle of Inoxcrom® brand black ink supplied by the company was used for the multivariate regression model. Four different black ballpoint pens and one blue ballpoint pen from different brands were used for method validation: Milan® P1 Touch black pen (Spain), Paper Mate® Write Bros.® black pen (USA), Staedtler® Ball 432F black pen (Germany), Sierra IB-B® Fine black pen (Spain) and Bic® Cristal Medium blue pen (France). Inks were sampled using individual paint brushes (da Vinci, Germany). Many trademarks manufacture their own inks under patent, so the exact composition is unknown. Ink brushstrokes were made on wood and chlorine-free paper from Inacopia® (80 g m^{-2}, DINA4 format, Portugal).

3.2.2 Accelerated and natural ageing procedures

A total of 48 samples of a commercial ink (Inoxcrom®) were exposed to artificial ageing in a time range from 1 to 257 h and their reflectance measurements were applied to the multivariate regression (Table 1). The samples were previously prepared by spreading a thin film of ink, with the help of a paint brush, on a piece of white paper (80 g m^{-2}). All training and test samples were prepared with the same paint brush and Inoxcrom® ink. For the subsequent UV-Vis-NIR reflectance analysis, a minimum area equivalent to 0.79 cm^2 (a circle of 1 cm diameter) was required. All samples were prepared just at the time of introduction into the accelerated ageing

chamber in order to prevent previous natural ageing. On the other hand, blank samples (pieces of paper without ink application) were introduced to determine the contribution of the ageing of the blank paper to the model. For the validation of the method, the ink was extracted from four different black ballpoint pens and one blue ballpoint pen, applied on paper and subjected to four ageing intervals (211, 98, 48 and 16 h), as shown in Table 1. To extract the ink from the pens, the cartridges were cut at one end and spread on white paper using a different paint brush for each ink. The paint brushes were cleaned with EtOH and air-dried to avoid the contamination between inks of different ageing intervals.

The ink samples were fixed in the climate chamber with adhesive tape, leaving a small space between them. A Solarbox 1500e RH purchased from Neurtek Instruments (Spain) was used to artificially accelerate the ageing of the ink samples. The parameters were controlled and programmed as follows: 40% relative humidity, 600 W m^{-2} irradiance with a xenon lamp, an indoor light filter to simulate indirect exposure to sunlight and 50 ºC temperature controlled by a BST (Black Standard Thermometer) probe.

In addition, a sample of each black ballpoint pen ink was exposed to natural ageing during 216, 264 and 1080 h (Table 2) and subsequently analysed by UV-Vis-NIR spectroscopy in order to establish a correlation between natural and artificial ageing. The ink-impregnated pieces of paper, in the same way as it was explained above, were left on a free surface, uncovered and under general local room conditions (70% humidity, 20 ºC). The room was located in the ground floor without direct sunlight.

Table 1. Accelerated ageing time of each Inoxcrom® (ID1-ID48), Milan®, Paper Mate®, Staedtler®, Sierra IB-B® and Bic® brand ink samples.

Ink sample	Accelerated ageing time (h)	Ink sample	Accelerated ageing time (h)	Ink sample	Accelerated ageing time (h)
ID1	256.5	ID19	166	ID37	48
ID2	241.5	ID20	163	Milan3	48
ID3	240	ID21	160	Paper Mate3	48
ID4	238	ID22	145	Staedtler3	48
ID5	235	ID23	139	Sierra IB-B3	48
ID6	232	ID24	121	Bic3	48
ID7	218	ID25	115	ID38	46
ID8	216	ID26	98	ID39	43
ID9	214	Milan2	98	ID40	40
ID10	211	Paper Mate2	98	ID41	26
Milan1	211	Staedtler2	98	ID42	24
Paper Mate1	211	Sierra IB-B2	98	ID43	22
Staedtler1	211	Bic2	98	ID44	19
Sierra IB-B1	211	ID27	96	ID45	16
Bic1	211	ID28	94	Milan4	16
ID11	208	ID29	91	Paper Mate4	16
ID12	194	ID30	88	Staedtler4	16
ID13	192	ID31	74	Sierra IB-B4	16
ID14	190	ID32	72	Bic4	16
ID15	187	ID33	70	ID46	3
ID16	184	ID34	67	ID47	2
ID17	170	ID35	64	ID48	1
ID18	168	ID36	50		

Ink sample	Natural ageing time (h)
InoxcromN1	1080
InoxcromN2	264
MilanN	216
Paper MateN	216
StaedtlerN	216
Sierra IB-BN	216

Table 2. Natural ageing time of each Inoxcrom®, Milan®, Paper Mate®, Staedtler®, Sierra IB-B® and Bic® brand ink samples.

3.2.3 Reflectance measurements

After the accelerated ageing, ink samples were analysed at the same time using a Cary 5000 UV-Vis-NIR spectrophotometer (Varian, Inc., Palo Alto, Canada) coupled to an integrating sphere (DRA-CA-5500, Labsphere, Inc., Brossard, Qc, Canada) to measure diffuse reflectance. All spectra recorded from 200 to 2500 nm with a resolution of 0.1 nm (600 nm min^{-1} scanning speed) were smoothed (1:50) and transformed to absorbance by means of Kubelka-Munk function (Eq. 1).

$$A = \frac{(1 - Reflectance)\ x\ 2}{2\ x\ Reflectance} \qquad \text{(Eq. 1)}$$

A baseline sample of polytetrafluoroethene (PTFE) and blank paper were used to obtain the optical reference standard for the system. In order to stabilise the light sources (deuterium and tungsten) of the spectrophotometer, they were warmed up for a period of 30 min prior to any reflectance measurement. In addition, an internal diagnosis of the instrument in terms of wavelength accuracy, repeatability and noise characteristics was performed according to manufacturer's specifications prior to analysis.

3.2.4 Chemometrics

SIMCA 13.0 Umetrics® (Umeå, Sweden) was used for statistical analysis. Partial least squares (PLS) relate two data matrices, **X** and **Y**, to each other using a multivariate linear model. It is capable of analysing data with many variables, noisy, collinear and even incomplete on both **X** and **Y**. That is why PLS was used in this study for multivariate regression. **X** (predictors) contained N UV-Vis-NIR spectra at K wavelengths, and **Y** (response) the value of the accelerated ageing time of N samples in the set [22].

All artificially aged Inoxcrom® ink samples (ID1 to ID48, Table 1) were used for preliminary studies. Different mathematical pre-treatments of the spectroscopic data, such as mean centering, scaling (unit variance (UV) and Pareto), logarithm and power transformations and spectral filters (first and second derivative transformations, multiplicative scatter correction (MSC), Savitzky-Golay, standard normal variate (SNV), row center, exponentially weighted moving average (EWMA) and combinations thereof), were tested to optimise the predictive ability of the model and improve the characterisation of the spectra. The Hotelling's T2 and distance-to-model tests with a 95% confidence level were applied to check for outliers.

After selecting the best pre-treatments for the optimisation of the PLS model, the entire set of artificially aged Inoxcrom® ink samples was split into two sets: 35 training samples and 10 test samples (ID3, ID7, ID12, ID13, ID18, ID29, ID31, ID33, ID43 and ID45), selected by the Kennard-Stone algorithm [23]. The training set was used for the construction of the model. The number of latent variables (LVs) was selected by internal validation with the cross-validation method. The main statistical parameters used for evaluating this step were the root mean square error of cross-validation (RMSECV) and the coefficient of determination of

cross-validation (R^2 CV). External validation of the model was performed with the test set. The RMSE of prediction (RMSEP) and the R^2 of prediction (R^2 P) were used as statistical measures to assess the model's predictive ability. RMSEP expresses the average error to be expected in future predictions when the model is applied to unknown samples [22]. The predictive performance in terms of accuracy was thus evaluated by the RMSECV and RMSEP parameters and calculated using the Eq. (2):

$$\text{RMSECV, RMSEP} = \sqrt{\frac{\sum_{i=1}^{n} (y_{r,i} - y_{p,i})^2}{n}} \qquad \text{(Eq. 2)}$$

Where, $y_{r,i}$ and $y_{p,i}$ are the reference and predicted values for the total ink samples (n) used in the training and test sets, respectively. The robustness of the model was established by applying it to an independent predictive set of samples (artificially and naturally aged inks from five different brands of black and blue ballpoint pens) that were not used in the construction or validation of the model.

Taking into account the above statistical parameters, the optimal model would have high determination coefficient (R^2) and predictive square correlation coefficient (Q^2) values as well as low RMSECV and RMSEP values and a small difference between the last two statistical parameters. A large difference between RMSECV and RMSEP indicates the possibility that too many LVs are used in the model (over-fitting) and noise is modelled. The number of LVs is intended to be as low as possible, as larger number of LVs may include some irrelevant information. The R^2 parameter varies from 0 to 1, indicating the degree of adjustment to perfect fitting, and the Q^2 parameter shows the robustness and predictive capacity of the model, being good when $Q^2 > 0.5$ and excellent when $Q^2 > 0.9$ [22].

3.2.5 HPLC-DAD analysis

In order to characterise the inks and identify possible differences in composition between them, a chromatographic analysis was performed. 0.1 mg of fresh ink from each ballpoint pen were weighed (Sartorius CP2245 Analytical balance, Gottingen, Germany) and 1 ml MeOH was added. For complete extraction of dyes, they were vigorously shaken for 1 min, and then sonicated in an ultrasonic bath (Elmasonic S 60 H, Elma Ultrasonic, Singen, Germany) for 5-10 min at room temperature. They were filtered through a 0.45 µm PTFE filter and an aliquot of 10 µl of the solutions was injected into the HPLC. In the case of the naturally and artificially aged inks, 7 micro-samples were extracted from each with a Harris Micro-Punch (1.20 mm diameter, Sigma-Aldrich, USA), and then the previous steps were followed. All HPLC work was carried out on a Waters™ 2690 separations module with a Waters™ 996 PDA detector (Milford, MA, USA). The data acquisition software was Empower 3. The chromatographic separation was achieved with a Waters™ Atlantis dC18 column (100 x 3.9 mm, 3 µm) operating at 30 ºC. A gradient elution was run for 14 min at a flow rate of 0.8 ml min^{-1} (Table 3). Prior to the ink analysis, the column was eluted with the initial composition of the mobile phases for at least 10 min until a stable pressure and background signal was achieved. The chromatograms as well as the UV spectra (200-800 nm) of the eluted analytes along the whole run were recorded.

Time (min)	% A (10 mM AmAc)	% B (MeOH)
0	80	20
1	80	20
3	30	70
5.9	19	81
6	19	81
8	10	90
12	10	90
12.1	80	20
14	80	20

Table 3. Elution gradient for HPLC-DAD analysis.

3.3 Results and Discussion

3.3.1 UV-Vis-NIR spectrum characterisation

Although no significant differences in the NIR region (720-2500 nm) of the spectra of the artificially aged Inoxcrom® ink samples were visualised, the main NIR bands characteristic of the resins could be identified (Figure 1).

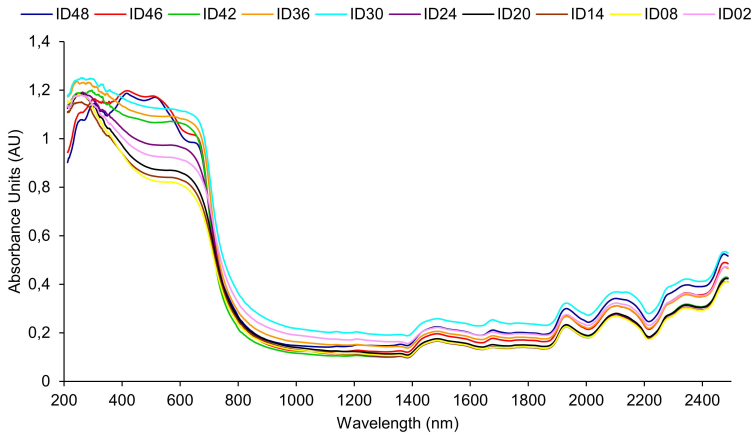

Figure 1. Smoothed UV-Vis-NIR absorption spectra of artificially aged Inoxcrom® inks.

The bands at 1240-1450 nm attributed to the young inks may be due to the C-H second overtone, O-H and N-H first overtones and C-H first overtone combinations. The bands at 1575-1895 nm could be assigned to the C-H first overtone and C=O second overtone. The bands at 715-950 nm attributed to the old inks could be characteristic of the N-H, O-H and C-H third overtones, C-H fourth overtone and O-H second overtone. The bands at 2130-2150 nm and 2435-2488 nm may be due to N-H and O-H combinations and C-H and C-C combinations, respectively. Moreover, the young inks (ID48, ID47 and ID46) showed a different UV-Vis spectral profile (200-780 nm). It is known that after depositing ink on a substrate, changes in composition can occur rapidly due to loss of solvents and/or

fading of dyes. These processes could be the cause of changes in the UV-Vis profile.

3.3.2 Data pre-processing and multivariate statistical analysis

The entire sample set (artificially aged Inoxcrom® inks (ID1 to ID 48)) was first used to select the combination of pre-processing strategies that would yield the lowest RMSECV value with which to optimise the PLS model. The RMSECV value was reduced with the application of the logarithmic function to the **Y** variable (accelerated ageing time). Therefore, the **Y** variable was transformed to a logarithmic function in the following tested models. Three outliers were found using Hotelling's T2 control graph for 95% of confidence. The outliers were the ink samples with fewer ageing hours, i.e. ID48, ID47 and ID46. As shown in Figure 1, the impact of the evaporation of the volatile components of the ink manifested itself in the initial period of the ink ageing process (in the first 5 h of accelerated ageing) with significant modifications in the UV region. This phenomenon could distort the PLS model due to the low number of ink samples used in this period, so the youngest samples were eliminated. In any case, a larger sampling within the initial time range could perhaps overcome it. Testing different pre-processings (Table 4), the best PLS model was obtained by applying the UV scaling and the SNV spectral filter transformation. The SNV filter is applied to reduce from the spectra most of the variability that may be caused by the effects of scattering. The spectral transformation was carried out from the smoothed spectrum. In order to remove non-informative regions and minimise the influence of spectral noise, the UV-Vis-NIR spectra were examined. The RMSECV value worsened as non-significant UV-Vis-NIR regions were eliminated. The entire spectrum was therefore used for the optimisation of the PLS model.

Table 4. PLS model data applying UV scaling and different spectral filters.

Sample set	Espectral Filter	LV	R^2X	R^2Y	Q^2	RMSEE	RMSECV	R^2CV
Whole	No spectral filter	4	0.99	0.98	0.95	0.08	0.20	0.98
	1st derivative transformation (15 points in filter and quadratic order polynomial fit)	2	0.55	0.99	0.98	0.07	0.09	0.99
	2nd derivative transformation (15 points in filter and quadratic order polynomial fit)	2	0.22	0.98	0.92	0.08	0.18	0.98
	2nd derivative transformation (5 points in filter and quadratic order polynomial fit)	2	0.11	0.99	0.83	0.05	0.24	0.99
	2nd derivative subtraction (5 points in filter and quadratic order polynomial fit)	4	0.99	0.98	0.95	0.08	0.20	0.98
	MSC	2	0.62	0.96	0.91	0.11	0.17	0.96
	SNV	2	0.64	0.96	0.92	0.11	0.16	0.96
	Row Center	3	0.98	0.95	0.93	0.12	0.16	0.95
	Savitzky-Golay	4	0.99	0.98	0.96	0.08	0.20	0.98
	EWMA	4	0.99	0.98	0.95	0.08	0.20	0.98
	2nd derivative transformation (5 points in filter and quadratic order polynomial fit) and SNV	2	0.12	0.99	0.86	0.05	0.25	0.99
	2nd derivative subtraction (5 points in filter and quadratic order polynomial fit) and SNV	2	0.64	0.96	0.92	0.11	0.17	0.96
Young inks excluded (ID46, ID47 and ID48)	No spectral filter	3	0.98	0.97	0.96	0.06	0.09	0.97
	1st derivative transformation (15 points in filter and quadratic order polynomial fit)	2	0.52	0.99	0.97	0.04	0.08	0.99
	2nd derivative transformation (15 points in filter and quadratic order polynomial fit)	2	0.20	0.97	0.87	0.06	0.14	0.97
	MSC	2	0.66	0.95	0.93	0.08	0.09	0.95
	SNV	2	0.67	0.95	0.93	0.08	0.09	0.95
	Row Center	3	0.97	0.96	0.95	0.08	0.08	0.96
	Savitzky-Golay	3	0.98	0.97	0.96	0.06	0.09	0.97
	EWMA	3	0.98	0.97	0.96	0.06	0.09	0.97

These selected treatments were applied to a new PLS model using the training and test sets separately. The model was built using the training set and the RMSECV statistical parameter was used to evaluate its predictive accuracy. The optimised PLS model with SNV filter was thus established with 2 LVs, explaining 73% (R^2X) and 95% (R^2Y) variation in the data with predictive properties of 94% (Q^2), indicating that the fit of the PLS model was quite good with excellent predictability. The RMSECV and RMSEE values were 0.09 and 0.07, respectively, with a R^2 CV value of 0.95, indicative of the model's high predictive accuracy. The PLS model was subsequently validated externally using the test set. The value of the RMSEP statistical parameter was taken into account to establish the expected prediction error when applying the model to unknown samples. The RMSEP value was 0.09 with a R^2 P value of 0.95, implying that its predictive capacity was valid according to the predictive accuracy required in potential real samples. The non-discrepancy between the RMSECV and RMSEP values indicates a no over-fitted model within the training set.

In addition, the accuracy error of the predicted values for the test set was calculated according to the following equation (Eq. 3):

$$\text{Error (\%)} = \left(\frac{(y_r - y_p)}{y_r}\right) x\ 100 \qquad \text{(Eq. 3)}$$

Where, y_p is the accelerated ageing value predicted by the model and y_r the real age of the ink sample. The predicted values were fairly accurate with a 17% error for the entire time range studied, as shown in Table 5.

Table 5. Predicted artificial ageing time and deviation values obtained by the PLS model for the test set.

Ink sample	Real accelerated ageing time (h)	Predicted accelerated ageing time (h)
ID45	16	23 ± 1
ID43	22	26 ± 1
ID33	70	74 ± 1
ID31	74	73 ± 1
ID29	91	94 ± 1
ID18	168	111 ± 2
ID13	192	234 ± 1
ID12	194	158 ± 1
ID7	218	236 ± 1
ID3	240	285 ± 1

Moreover, the influence of the **X** variables (the wavelengths recorded in the spectrum) on the ink ageing process was studied based on the information obtained from the PLS model. The ink samples followed a spatial distribution from left to right in the first component of the scores plot according to their artificial ageing time. The youngest inks were on the left of the plot, whereas the oldest were on the right. The loadings plot of the PLS model was also studied. The **Y** variable (the logarithmic function of the artificial ageing time) was found on the right side of the graph with a value of 0.03. On the left side of the loadings plot, linked to the youngest inks, the spectrum ranges between 405-670 nm, 1240-1450 nm and 1575-1895 nm were placed, while on the right side, associated to the oldest inks, the most influential ranges of the spectrum were between 715-950 nm, 2435-2488 nm and 2130-2150 nm. In order to explain this behaviour, a colour scale based on the values of the loadings plot was made. The different spectrum ranges were strongly related to the different ages of the inks, as shown in Figure 2. The NIR region (1240-1450 and 1575-1895 nm, light blue) had the greatest influence on the youngest ink samples. It must be taken into account that a large impact of the UV region was also found on them. The most influential region for the medium-term aged inks was in the visible range (405-670 and 715-950 nm, blue), whereas the oldest inks were influenced by the NIR region (2130-2150 and 2435-2488 nm, dark blue). The young inks were therefore characterised by the first and second overtone regions of the NIR spectrum, while the old inks by those of the

third overtone and combination band regions. This change in the influence of the spectrum over time can be explained by the ageing processes that the different components of the ink undergo. The main ink components (solvents, dyes and resins) have different degradation mechanisms and rates. While the evaporation of the volatile components takes place practically in the first moments immediately after the ink has been deposited on the paper, the changes undergone by the dyes and resins take place in the medium- and long-term [24, 25]. This phenomenon could be observed in the significant impact of the UV region on the youngest ink samples due to solvent evaporation, followed by the influence of the visible and NIR regions on medium- and long-term aged inks due to dye fading and resin hardening.

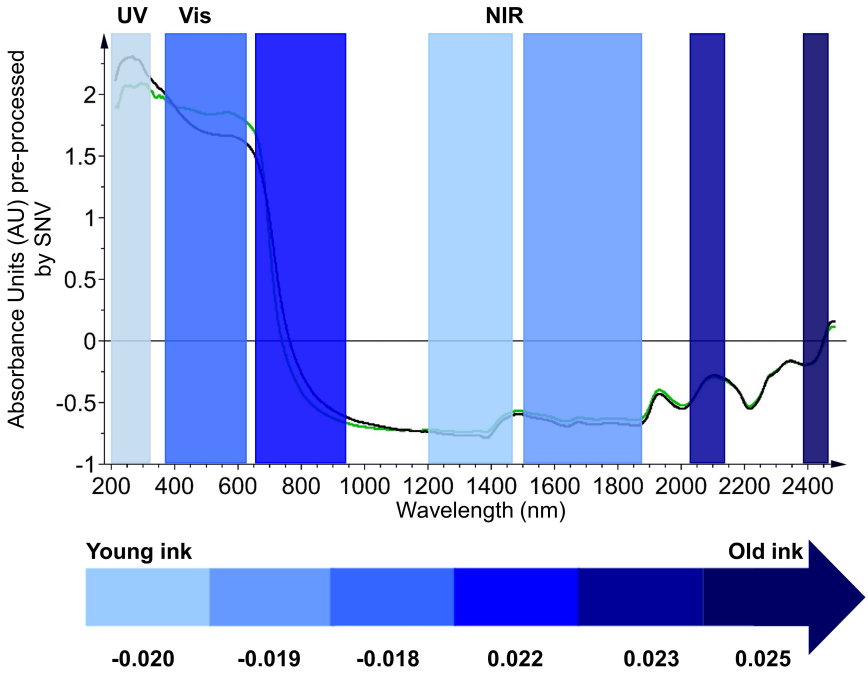

Figure 2. The influence of the **X** (wavelengths (nm) recorded in the SNV pre-processed spectrum) and **Y** (logarithmic function of the accelerated ageing time) variables on the ageing process of young (green line) and old (black line) inks in the first component. The row represents the values of the loadings plot. The logarithmic function of the accelerated ageing time has a value of 0.03.

3.3.3 PLS model application to artificially aged inks

The PLS model was applied to the age prediction of artificially aged Inoxcrom® inks, different black ballpoint pen inks and a blue ballpoint pen ink (Table 6). Accurate predictions were obtained for two of the five commercial pens studied, Milan® and Paper Mate® black ink pens, with 16% and 29% error, respectively. The error was 48% for the oldest Sierra IB-B® black pen ink samples, whereas the deviation increased significantly for the youngest ones. The Staedtler® black pen ink also did not fit the model well, obtaining high predictive deviations for both young and old ink samples. In addition, the Bic® blue pen ink had a greater mismatch, so the model did not give a good approximation. In these cases of mismatch, other ink components could be affecting the reflectance of the ink and thus increasing the deviation of the prediction.

Table 6. Ageing time values predicted by the PLS model for the predictive set.

Type of ageing	Ink sample	Real ageing time (h)	Predicted ageing time (h)
Artificial	Milan1	211	201
	Paper Mate1	211	175
	Staedtler1	211	680
	Sierra IB-B1	211	340
	Bic1	211	11803
	Milan2	98	65
	Paper Mate2	98	70
	Staedtler2	98	345
	Sierra IB-B2	98	142
	Bic2	98	13924
	Milan3	48	43
	Paper Mate3	48	35
	Staedtler3	48	303
	Sierra IB-B3	48	66
	Bic3	48	6801
	Milan4	16	13
	Paper Mate4	16	9
	Staedtler4	16	104
	Sierra IB-B4	16	53
	Bic4	16	2169
Natural	InoxcromN1	1080	16
	InoxcromN2	264	4
	MilanN	216	2
	Paper MateN	216	1
	StaedtlerN	216	14
	Sierra IB-BN	216	9

The dyes were therefore analysed by HPLC to account for the differences observed between the inks studied. The most mismatched inks, Staedtler® black and Bic® blue pen inks, had a different HPLC profile and were easily differentiated from other inks, as shown in the chromatograms in Figure 3. Bic® blue pen ink was characterised by the chromatographic peaks at 4.1, 4.5, 5.0 and 5.2 min that the remaining inks did not show. Staedtler® and Bic® pen inks had the same chromatographic peak at 7.4 min, while Inoxcrom® and Bic® pen inks showed another one at 4.4 min. In addition, the chromatographic peaks at 7.8, 8.2 and 8.8 min for Inoxcrom® black pen ink gave a different ratio to Staedtler® and Bic® pen inks. The differences in both the chromatographic peaks and the peak ratios between the various inks highlighted the differences in their composition, thus facilitating their discrimination.

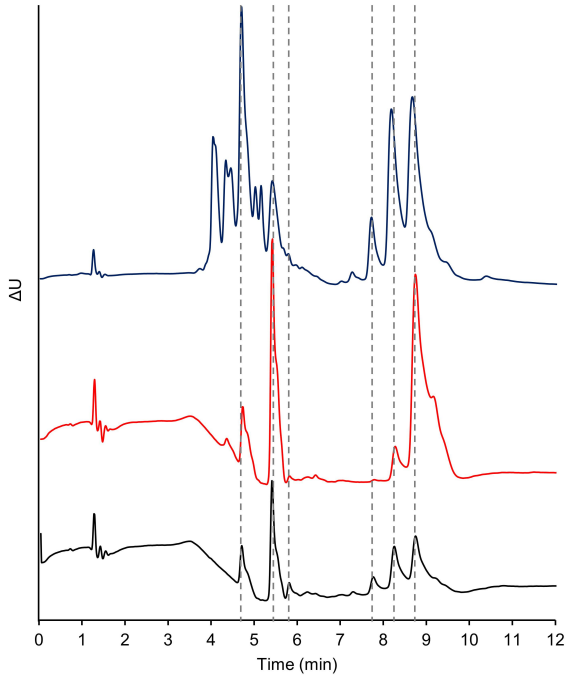

Figure 3. Chromatograms of fresh pen inks from Bic® (blue line), Inoxcrom® (red line) and Staedtler® (black line) at 200-800 nm. Sierra IB-B®, Milan® and Paper Mate® pen inks showed an identical chromatogram to that of Inoxcrom®.

These results were contrasted through research conducted by Adam *et al.* [26], who classified and discriminated black ballpoint pen inks using a PCA from their UV-Vis absorption spectra. Differences in the dyes within each pen brand were detected, enabling a questioned ink to be assigned to a particular class of ink composition. Sierra®, Paper Mate® and Staedtler® black pen inks were identified in different ink classes and were well discriminated against each other.

This would mean that the methodology can be universal, but the PLS model cannot be recognised as such and would only work with ballpoint pens using Inoxcrom® type inks, such as Milan® and Paper Mate® brands. Additional models would need to be developed for each ink class with a similar chemical composition so that predictions can be obtained for each of them.

3.3.4 Correlation between artificial and natural ageing

Naturally aged Inoxcrom® and black ballpoint pen inks were analysed to establish the range of application of the PLS model. A regression line was performed from the natural age and the predicted artificial age of the Inoxcrom®, Milan® and Paper Mate® black pen inks in order to determine the correlation between the artificial exposure time and its equivalent in real time ageing (Table 6 and Figure 4), in which one hour in the artificial ageing chamber would correlate with 143 h of natural ageing under the conditions studied. The developed methodology could therefore be useful for dating naturally aged inks up to approximately 5 years and may be applicable as a multivariate regression model to samples with the same ink typology analysed and exposed to the conditions studied.

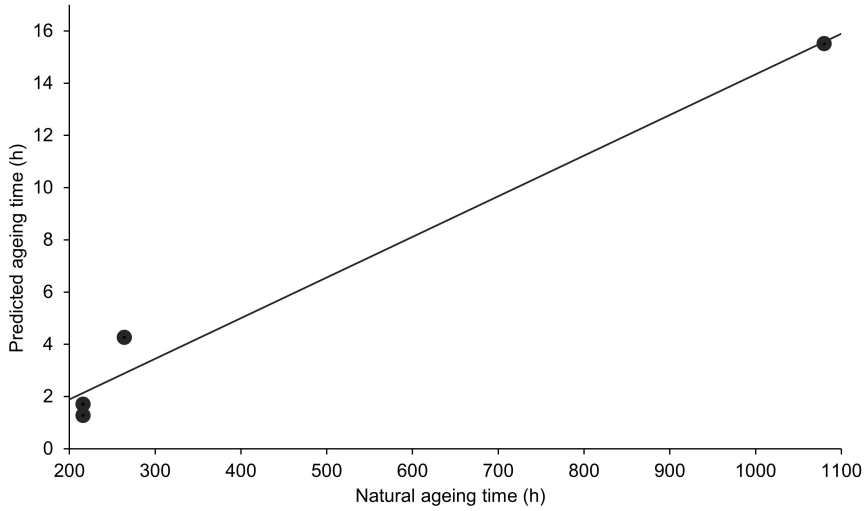

Figure 4. Graph of natural ageing time (h) versus predicted ageing time (h). Equation Y = 0.02 X – 1.22, R^2 = 0.98.

3.4. Conclusions

UV-Vis-NIR spectroscopy together with PLS regression as ink dating method reported in this paper, called DATUVINK, demonstrates that UV-Vis-NIR diffuse reflectance spectroscopy combined with chemometrics is a powerful tool for predicting the age of inks deposited on paper. In addition, it is worth noting the advantage of this methodology in this type of analysis, since it would be fast and non-destructive, needing little to no sample treatment.

Despite the advantages of this method, the large ink surfaces prepared in the study are unlikely to be representative of real samples, such as handwriting strokes and thus in a casework scenario. Equivalent UV-Vis-NIR reflectance spectra would need to be acquired using a microspectrophotometer with a smaller sample aperture.

The DATUVINK method can be universal, but the developed PLS model cannot be recognised as such, since it cannot be applied to any ballpoint pen brand. The predictions obtained for some of the different brands of artificially aged ballpoint pen inks were not accurate enough. An example was the predicted age of Sierra IB-B® black pen ink that shared the same base as Inoxcrom® ink, but did not fit as well as the samples in the training set. This could indicate that there are other factors, such as the composition of the dyes, affecting the reflectance of the ink, as shown in the HPLC-DAD analyses. Therefore, taking into account the differences observed in the chemical composition of the inks and the previous research studies that corroborate this fact, it would be necessary to develop new individualised predictive models for each type of ink, while the model developed would be effective for those inks that show affinity with the chemical composition of Inoxcrom® inks.

Although predictive models based on naturally aged ink samples would be more suitable, the correlation between natural and artificial ageing, in which one hour of artificial ageing was correlated with approximately 143 h of natural ageing under the conditions studied, allowed for a faster and more flexible method development. The methodology could be useful for dating naturally aged Inoxcrom® type inks up to 5 years, giving us an advantage over the existing ink dating methods, which are destructive and limited to a maximum prediction time of 2 years, with the exception of the DATINK method that reaches to date ink entries up to 5 years.

In addition, the method showed that the youngest inks were characterised by modifications in the ranges of 405-670 nm of the visible spectrum and 1240-1450 nm and 1575-1895 nm of the NIR spectrum, whereas after ageing the most influential regions were the ranges of 715-950 nm, 2435-2488 nm and 2130-2150 nm of the NIR spectrum.

In conclusion, there is great potential in the development of chemometric models based on the variation of the optical properties of inks induced by the degradation degree of their resins and dyes. However, it would be necessary to know the chromatographic profile of the ink in order to assign a valid predictive model to each type of ink. These new methods developed from diffuse reflectance measurements could complement the existing ink dating methods based on the analysis of volatile components, restricted to ink samples with less than 2 years, with the exception of the DATINK method, by extending the time prediction range and ensuring old and young ink dating without destruction of the sample.

Acknowledgments

The author would like to thank the General Research Services (SGIker) of the UPV/EHU for the technological support with the UV-Vis-NIR spectrophotometer, supported by the National Program for the Promotion of Human Resources in the National Plan for Scientific Research, Development and Innovation, Ministry of Science and Innovation, European Social Fund (ESF) and Basque Government, Scientific Political Management. Finally, L. Ortiz-Herrero thanks the UPV/EHU for the pre-doctoral fellowship.

References

[1] M. Calcerrada, C. García-Ruiz, Analysis of questioned documents: a review, *Anal. Chim. Acta* 853 (2015) 143-166. https://doi.org/10.1016/j.aca.2014.10.057.

[2] A. Koenig, C. Weyermann, Ink dating part II: Interpretation of results in a legal perspective, *Sci. Justice* 58 (1) (2017) 31-46. https://doi.org/10.1016/j.scijus.2017.08.003.

[3] A. Koenig, S. Magnolon, C. Weyermann, A comparative study of ballpoint ink ageing parameters using GC/MS, *Forensic Sci. Int.* 252 (2015) 93-106. https://doi.org/10.1016/j.forsciint.2015.03.027.

[4] A. Koenig, J. Bügler, D. Kirsch, F. Köhler, C. Weyermann, Ink Dating Using Thermal Desorption and Gas Chromatography/Mass Spectrometry: Comparison of Results Obtained in Two Laboratories, *J. Forensic Sci.* 60 (S1) (2015) 52-61. https://doi.org/10.1111/1556-4029.12603.

[5] G.M. LaPorte, J.D. Wilson, A.A. Cantu, S.A. Mancke, S.L. Fortunato, The identification of 2-phenoxyethanol in ballpoint inks using gas chromatography/mass spectrometry-relevance to ink dating, *J. Forensic Sci.* 49 (2004) 1-5. https://doi.org/10.1520/jfs2003217.

[6] A. Koenig, C. Weyermann, Ink dating, part I: Statistical distribution of selected ageing parameters in a ballpoint inks reference population, *Sci. Justice* 58 (1) (2018) 17-30. http://dx.doi.org/10.1016/j.scijus.2017.08.002.

[7] J. Bügler, H. Buchner, A. Dallmayer, Age determination of ballpoint pen ink by thermal desorption and gas chromatography-mass spectrometry, *J. Forensic Sci.* 53 (4) (2008) 982-988. https://doi.org/10.1111/j.1556-4029.2008.00745.x.

[8] C. Weyermann, J. Almog, J. Bügler, A.A. Cantu, Minimum requirements for application of ink dating methods based on solvent

analysis in casework, *Forensic Sci. Int.* 210 (1) (2011) 52-62. https://doi.org/10.1016/j.forsciint.2011.01.034.

[9] C. Weyermann, D. Kirsch, C. Vera, B. Splenger, A GC/MS study of the drying of ballpoint pen ink on paper, *Forensic Sci. Int.* 168 (2007) 119-127. https://doi.org/10.1016/j.forsciint.2006.06.076.

[10] I. San Román, L. Bartolomé, M.L. Alonso, R.M. Alonso, M. Ezcurra, DATINK pilot study: An effective methodology for ballpoint pen ink dating in questioned documents, *Anal. Chim. Acta* 892 (2015) 105-114. http://dx.doi.org/10.1016/j.aca.2015.08.038.

[11] C. Weyermann, B. Schiffer, P. Margot, A logical framework to ballpoint ink dating interpretation, *Sci. Justice* 48 (2008) 118-125. https://doi.org/10.1016/j.scijus.2007.10.009.

[12] M. Ezcurra, Avances Analíticos en la Datación Forense de Tintas y Documentos, Universidad del País Vasco (UPV/EHU), Doctoral Thesis, 2012.

[13] F. de Souza Lins Borba, R. Saldanha Honorato, A. de Juan, Use of Raman spectroscopy and chemometrics to distinguish blue ballpoint pen inks, *Forensic Sci. Int.* 249 (2015) 73-82. http://dx.doi.org/10.1016/j.forsciint.2015.01.027.

[14] R. Kumar, V. Sharma, A novel combined approach of diffuse reflectance UV–Vis-NIR spectroscopy and multivariate analysis for non-destructive examination of blue ballpoint pen inks in forensic application, *Spectrochim. Acta A Mol. Biomol. Spectrosc.* 175 (2017) 67-75. http://dx.doi.org/10.1016/j.saa.2016.12.008.

[15] G. Sauzier, P. Giles, S.W. Lewis, W. van Bronswijk, In situ studies into the characterisation and degradation of blue ballpoint inks by diffuse reflectance visible spectroscopy, *Anal. Methods* 7 (2015) 4892-4900. http://dx.doi.org/10.1039/c5ay00761e.

[16] S. Senior, E. Hamed, M. Masoud, E. Shehata, Characterisation and Dating of Blue Ballpoint Pen Inks Using Principal Component Analysis of UV–Vis Absorption Spectra, IR Spectroscopy, and HPTLC, *J.*

Forensic Sci. 57 (4) (2012) 1087-1093. http://dx.doi.org/10.1111/j.1556-4029.2012.02091.x.

[17] V. Sharma, R. Kumar, Fourier transform infrared spectroscopy and high performance thin layer chromatography for characterisation and multivariate discrimination of blue ballpoint pen ink for forensic applications, *Vib. Spectrosc.* 92 (2017) 96-104. https://doi.org/10.1016/j.vibspec.2017.05.006.

[18] V.A.G. da Silva, M. Talhavini, I.C.F. Peixoto, J.J. Zacca, A.O. Maldaner, J.W.B. Braga, Non-destructive identification of different types and brands of blue pen inks in cursive handwriting by visible spectroscopy and PLS-DA for forensic analysis, *Microchem. J.* 116 (2014) 235–243. https://doi.org/10.1016/j.microc.2014.05.013.

[19] A. Kher, M. Mulholland, E. Green, B. Reedy, Forensic classification of ballpoint pen inks using high performance liquid chromatography and infrared spectroscopy with principal components analysis and linear discriminant analysis, *Vib. Spectrosc.* 40 (2016) 270-277. https://doi.org/10.1016/j.vibspec.2005.11.002.

[20] V. Sharma, R. Kumar, Dating of ballpoint pen writing inks via spectroscopic and multiple linear regression analysis: A novel approach, *Microchem. J.* 134 (2017) 104-113. https://doi.org/10.1016/j.microc.2017.05.014.

[21] O. Díaz-Santana, D. Vega-Moreno, F. Conde-Hardisson, Gas Chromatography-Mass Spectrometry and High Performance Liquid Chromatography-Diode Array Detection for Dating of Paper Ink, *J. Chromatogr. A* 1515 (2017) 187-195. http://dx.doi.org/10.1016/j.chroma.2017.07.093.

[22] L. Eriksson, T. Byrne, E. Johansson, J. Trygg, C. Vikström, Multi- and Megavariate Data Analysis. Basic Principles and Applications, third ed., Umetrics Academy, 2013.

[23] R.W. Kennard, L.A. Stone, Computer Aided Design of Experiments, *Technometrics* 11 (1969) 137-148. http://dx.doi.org/10.1080/00401706.1969.10490666.

[24] N.M. Grechukha, K.O. Gorshkova, M.S. Panov, I.I. Tumkin, E.O. Kirillova, V.V. Lukianov, N.P. Kirillova, V.A. Kochemirovsky, Analysis of the ageing processes of writing ink: Raman spectroscopy versus gas chromatography aspects, *Appl. Sci.* 7 (10) (2017) 991. https://doi.org/10.3390/app7100991.

[25] K.O. Gorshkova, I.I. Tumkin, L.A. Myund, A.S. Tverjanovich, A.S. Mereshchenko, M.S. Panov, V.A. Kochemirovsky, The investigation of dye ageing dynamics in writing inks using Raman spectroscopy, *Dyes Pigm.* 131 (2016) 239-245. http://dx.doi.org/10.1016/j.dyepig.2016.04.009.

[26] C. Adam, S. Sherratt, V. Zholobenko, Classification and individualization of black ballpoint pen inks using principal component analysis of UV–Vis absorption spectra, *Forensic Sci. Int.* 174 (2008) 16-25. http://dx.doi.org/10.1016/j.forsciint.2007.02.029.

CHAPTER 4

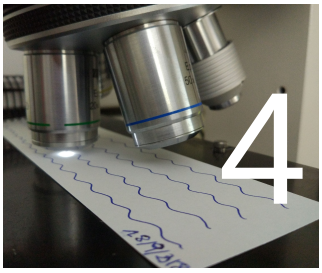

A novel, non-invasive, multi-purpose and comprehensive method to date inks in real handwritten documents based on the monitoring of the dye ageing processes

L. Ortiz-Herrero, A.C. de Almeida Assis, L. Bartolomé, M.L. Alonso, M.I. Maguregui, R.M. Alonso, J.S. Seixas de Melo

Chemometrics and Intelligent Laboratory Systems, **2020**; 207: 104187

Q1, IF: 2.895, 13/124, Statistics & Probability

Abstract

Blue ink strokes belonging to 11 types of writing tools from 7 different brands were naturally aged in the darkness for 2 years and characterised by Vis-microspectrophotometry (Vis-MSP). Ink clustering and classification was performed by applying principal component analysis (PCA) and hierarchical cluster analysis (HCA) in order to subsequently assign an optimal orthogonal partial least squares (OPLS) model capable to predict the age of different inks. This method was found applicable to the exact dating of forged documents with ink strokes of up to 2 years old. The method was tested with blind samples supplied by the Forensic Science Unit of the Basque Country Police Department. Age predictions ($p < 0.05$) with an accuracy error below 25% were obtained whenever: (i) the two ink replicas were placed inside the ellipse of the predicted score graph, (ii) the age of the ink was within the temporal application range of the OPLS model, and (iii) the ink was found to fit correctly in any of the classifications of the pen brands studied. The OPLS model was also able to detect those inks out of its temporal application range, if the ink samples were correctly clustered in the PCA model and/or classified in the HCA model with one of the pen brands studied, but one of the two ink replicas was placed outside the ellipse of the predicted score graph. Thus, these inks were temporarily above or below the application limit of the OPLS model of the corresponding pen brand.

Keywords: Ballpoint pen, gel pen, ink dating, dyes, Vis-microspectrophotometry, OPLS, forensic chemistry, questioned documents.

4.1 Introduction

Forgery of documents and the fight against this type of illegal activity is an everyday reality, which is increasing and can have serious and far-reaching negative implications for companies, individuals and political entities. This crime is not only for profit, but may also constitute a means to other ends, such as terrorism, smuggling of migrants and trafficking in persons. The different units of law enforcement agencies have therefore been forced to collaborate and develop new methodologies to deal with these crimes [1].

Counterfeit material may consist of contracts, wills, titles and deeds, bank checks, suicide notes, agreements, ID cards, handwritten correspondence, etc. The study of these materials implies their chemical analysis as well as the use of physical and optical techniques either to determine their authorship, the alterations made to them or to date them. The dating of documents is one of the most studied tasks, but also one of the most challenging due to the great variety of pen brands and ink formulations on the market. Moreover, the lack of knowledge of the conditions under which the documents were exposed and the lack of inter-laboratory validation and applicability assessment of the methodologies developed are also critical issues in the reliability of the results [2-6], and rightfully questioned when presented in court cases [7].

The most commonly used writing tools are ballpoint pens, which contain viscous oil-based inks, as well as rollerball pens, containing either water-based liquid inks or gel inks. Ink is a complex homogeneous medium, consisting of solvents, pigments and dyes, resins, lubricants, solubilisers, surfactants, particulate matter, fluorescents and other materials. The components contained in this mixture are implied in the colour, in

controlling density or flow, in modifying the drying kinetics and in providing the final appearance [8, 9].

The ink undergoes modifications once deposited on the paper: (I) the ink dries due to solvent evaporation, solvent absorption on the surface of the support and solvent diffusion within it, immediately decreasing its quantity, (II) the ink fades due to dye degradation when exposed to light, and (III) the ink solidifies due to the polymerisation of resins, decreasing their solubility and making them more difficult to extract. These processes achieve stability over time without further ink modifications [8, 9].This dynamic ink profile has been studied using different techniques for ink dating.

GC/MS is the predominant technique for quantifying 2-phenoxyethanol solvent loss over time by using liquid extraction [3, 4, 10, 11], thermal desorption [12] and SPME (Solid-phase Microextraction) [13] as sample preparation methods. However, the methodologies developed have some drawbacks. Most of the ink solvents evaporate within a few minutes after depositing the ink in the support and the rest continues to evaporate gradually over approximately 2 years [4]. Thus, the temporal application range of these methodologies is limited to recent documents except for the DATINK methodology, which is applied to documents up to 5 years old with a mean relative error of 21% [13]. Moreover, the initial ink quantity and composition variation between the different pen brands, the writing pressure applied and the paper support can modify the results of ink dating analysis [2-5, 11]. Finally, the methodologies are based on mass-dependent measurements, so the amount of ink extracted must always be almost the same [13].

In the last few years, research has focused on other ink components, such as dyes [14]. This is due to the fact that dyes are more stable over time, so their degradation is much slower than that of other ink components [15]. Exposure to light is the main factor in the long-term degradation of dyes [16]. This process can last several years under natural conditions, making it possible to date relatively old documents [15]. However, a certain dispute exists when attempting to date the ink by measuring dye degradation, as ink ageing is highly dependent on the initial composition of the ink, storage conditions and the type of support, and are generally unknown in case investigations [16]. Díaz-Santana *et al*. [17] proposed a combined method applying GC-MS and HPLC-DAD for the quantitative analysis of solvents and dyes over time, enabling the dating of Montblanc® ballpoint pen inks up to 4 years with a maximum error of 4-7 months. For forensic application, however, non-destructive methods are much better techniques, since the analysis is carried out directly on the document without destroying part of it, which guarantees the preservation of evidence in court and the possibility of counterproof. Grechukha *et al*. [18] demonstrated the possibility of using Raman spectroscopy separately or together with gas chromatography as a technique to estimate the age of inks up to 10 years by studying the ageing dynamics of solvents and dyes. Recent studies have investigated the feasibility of ink dating using spectroscopic techniques in combination with chemometrics. Sharma *et al*. [19] demonstrated the application of UV-vis spectroscopy with multiple linear regression (MLR) to date a blue ballpoint pen brand by measuring the ink fade over time. The methodology is capable of dating inks up to approximately 1 year with an accuracy of ± 10 days. Sauzier *et al*. [20] subsequently developed individualised chemometric models for naturally aged inks using in-situ visible spectroscopy with PLS regression. Age estimation was effective on multiple ink types, such as ballpoint and gel inks, up to 2 years with a maximum error of 6 months. However, an unresolved issue is that the size of the ink sample used in this study does

not reflect the real samples presented in document examination cases. The transition from this approach to casework would imply the use of micro-techniques.

In a previous study by Ortiz-Herrero *et al*. [21] a non-destructive ink dating methodology (DATUVINK) was developed by applying partial least squares (PLS) to the recorded UV-vis-NIR spectroscopic data of artificially aged Inoxcrom® black ballpoint pen inks. The PLS model could be applied to the dating of inks up to 5 years old that have a chromatographic dye profile common to Inoxcrom® inks (Milan® and Paper Mate®) with an accuracy error of about 25%. However, several limitations of the methodology must be highlighted. The large size of the ink sample required by this technique is not representative of real samples, such as handwriting strokes in a casework scenario. In addition, the fact that the PLS model was built with a particular brand of ballpoint pen ink made its application to inks with a significantly different formulation impossible.

In this work, we present a non-invasive multipurpose methodology for dating ink strokes by monitoring the modifications in the visible spectrum of the dyes over time. Thus, an averaged visible reflectance spectrum was acquired from each pen ink brand using a microspectrophotometer with a smaller sample aperture than in our previous work and a subsequent ink clustering and classification was carried out using PCA and HCA. Moreover, the modifications undergone by the inks were related to natural ageing under controlled conditions by applying multivariate regression analysis. Predictive models capable of predicting the age of the ink from 7 different pen brands were built and validated. Finally, the methodology was applied to real cases using blind samples supplied by the Forensic Science Unit of the Basque Country Police Department in order to provide an external assessment of the laboratory's performance.

4.2 Material and methods

4.2.1 Ink samples

Blue ink ballpoint pens of 6 different brands (Bic® Cristal Medium, Staedtler® Stick 430 M, Paper Mate® Flex Grip Elite 1.4 M, Pilot® Super Grip M, Faber-Castell® Medium and Uni-Ball® Jetstream Sport) and blue liquid ink pens of 4 different brands (Uni-Ball® Signo Broad, Pilot® G-1, Paper Mate® gel 0.7mm and Inoxcrom® TC Ball Stainless Steel Tip M) were acquired in national and international markets. Bic® Cristal Medium ballpoint pens were selected from the United States (USA) and France, as they have been reported to have a different ink formulation [22]. Thus, a total of 11 types of writing tools from 7 different brands were studied. Four ink strokes of each writing tool were made every month between 2017 and 2019 on white paper of A4 size and 80 g/m^2 (Inacopia® Elite, Portugal) and left to age under local room conditions (60% humidity, 20 ºC and in the dark). A total of 20-30 ink samples were obtained for each writing tool, achieving a maximum ageing of 27 natural months for the oldest one.

4.2.2 Vis-microspectrophotometry analysis

Ink strokes of each writing tool were fixed to a microscope base slide and placed in the microscope stage within the microspectrophotometer instrument. For the spectra acquisition, a TIDAS MSP-800 microspectrophotometer consisting of a microscope (Zeiss®, Axiotech 100) coupled to a spectrophotometer (J&M Tidas®) was used [23]. The ink strokes were analysed in the visible region between 400 and 800 nm in reflectance mode. For each writing tool and age, as shown in Table 1, a measurement was obtained for each of the 4 ink strokes.

Table 1. Number and age of ink samples of each writing tool analysed by Vis-microspectrophotometry. Those highlighted in bold made up the validation set.

Sample No.	Ink age (days)										
	Ballpoint pen							Gel pen			
	Bic® France	Bic® USA	Faber-Castell®	Pilot®	Paper Mate®	Uni-Ball®	Staedtler®	Inoxcrom®	Pilot®	Paper Mate®	Uni-ball®
1	122	152	98	122	98	121	98	189	243	248	137
2	**152**	**168**	121	136	163	**163**	100	248	**273**	295	167
3	181	181	**163**	189	188	188	121	265	**304**	**311**	203
4	243	243	168	**218**	**202**	247	163	**295**	318	340	228
5	273	265	188	247	**247**	265	**169**	**311**	335	359	266
6	295	273	203	294	318	309	188	340	359	371	295
7	**304**	304	**218**	309	**339**	318	203	371	361	403	318
8	335	318	227	**339**	359	**384**	218	403	390	458	360
9	359	**335**	247	370	370	401	228	**415**	424	**491**	**385**
10	361	359	294	385	**401**	427	**247**	430	443	**520**	**415**
11	390	361	309	401	427	443	**266**	**458**	453	536	444
12	424	**390**	318	**427**	443	456	309	491	**507**	**549**	507
13	443	424	339	**443**	490	490	318	566	**566**	566	536
14	453	443	359	456	581	519	339	**582**	567	582	567
15	482	**453**	**370**	519	598	536	360	610	607	610	599
16	515	482	401	548	609	**548**	**370**	625	625	625	626
17	543	515	414	567	673	581	401	634	653	**653**	**654**
18	**566**	536	427	581	686	673	415	653	686	686	**674**
19	567	543	**443**	623	**715**	**686**	427	674	715	715	702
20	**607**	**566**	456	633	744	**734**	**444**	686	**744**	744	716
21	624	567	489	652		762	456	715			**735**
22	636	607	505	673			489	744			745
23	668	623	**535**	686			506				763
24	**696**	636	566	715			**567**				
25	744	652	597	**744**			**624**				
26		**668**	**623**				653				
27		696	652				686				
28		726	**685**								
29		744									
30		**805**									

A diaphragm was used to select each measurement area under the following conditions: for the microscope (Diaphragm dimensions 220.0 x 127.0 µm, image resolution 640 x 80, objective with 20x magnification and microscope light intensity 10) and for the spectrophotometer (Interpolation yes, 1 nm resolution, absorbance representation (AU), single scan, 3 accumulations and 1 pixel bunching). A white area without ink from the same sheets where the ink strokes were made was used as a reference. The average of the 4 measurements recorded for each ink stroke type was applied to the classification and dating study.

4.2.3 Chemometrics

For statistical analysis, SIMCA 15.0.2 Umetrics® (Umeå, Sweden) was used. The first stage of data analysis was conducted using PCA and HCA for exploratory and classification analysis.

PCA is a multivariate projection method designed to extract and display systematic variation in an **X** data matrix. The most important use of PCA is to represent a multivariate data table as a low-dimensional plane so that an overview of the data is obtained. This overview may uncover groups of observations, trends, outliers and relationships between observations and variables [24].

A PCA was performed using the absorbance values of the entire spectral region acquired by microspectrophotometry as **X** variables. The data were pre-treated by applying scaling and spectral filters to transform them so that they could be analysed. The score plot was examined to observe whether ink groupings between the different pen brands existed.

There is a risk that grouping in a data set may not be fully observed using PCA when the clusters are many, less distinct, partially overlapped or captured by higher order latent variables. In these cases, HCA can detect subtle and prominent groupings between observations and variables in large and complex datasets. The distances between the observations (or variables) are calculated and compared in HCA. When the distances between observations are relatively small, this implies that the observations are similar in some way, while when they are larger the observations are significantly different. The aim is to organise the data points into smaller and more homogeneous groups in which the variability within the group is minimised and the variability between groups is maximised. The HCA result will depend on the distance metric used and the linkage criterion selected [24].

HCA was applied in the search for new clusters as well as to contrast those detected by the PCA. To do this, the Euclidean distance method and the Ward's linkage method, in which groups are formed so that the sum of the squares within the group is minimised, were used.

Orthogonal partial least squares (OPLS) was applied after the classification of the inks. OPLS is an extension of PLS that splits the systematic variation in the **X** block into two parts, one that models the correlation between **X** and **Y** (predictive) and another that shows the systematic **X** variation not related (orthogonal) to **Y**. Orthogonalisation can reduce the complexity of the model, as it eliminates the systematic variation in the **X** matrix that is not correlated with the property to predict [24]. Thus, mathematical models were constructed for each writing tool in which the spectroscopic data (**X** matrix) was related to the natural ageing time (**Y** vector). The predictive models were used to predict the age of inks in questioned documents from their spectroscopic data.

The **X** matrix was made up of the spectroscopic data of the entire range of the recorded visible spectrum of the aged inks of each writing tool. The average of the absorbance values recorded at each wavelength of the four ink strokes analysed was calculated for each ink sample. The **X** matrix was split into two sets, calibration samples (training set) and validation samples (test set), as shown in Table 1, using Kennard-Stone algorithm [25]. The training set was used for the construction of the OPLS model. Spectral pre-processing techniques, such as Savitzky-Golay, multiplicative scatter correction (MSC), standard normal variate (SNV), row center, exponentially weighted moving average (EWMA) and first and second derivatives, were applied in order to correct unwanted effects related to noise and scattering. The **Y** variable was transformed to logarithmic function. The number of latent variables (LVs) was optimised by internal validation with cross-validation method. The main statistical parameters used for evaluating this step were the root mean square error of cross-validation (RMSECV) and the coefficient of determination of cross-validation (R^2 CV). RMSECV is calculated using Eq. 1:

$$\text{RMSECV} = \sqrt{\frac{\sum_{i=1}^{n}(y_i - \hat{y}_i)^2}{n}} \qquad \text{(Eq. 1)}$$

Where y_i is the measured value (natural ageing), $\hat{y}_i$ is the value predicted by the model and n is the total number of samples used in the training set. The external validation of the model was carried out using the spectra of the validation samples as a set, and then the predictive ability was evaluated by the RMSE of prediction (RMSEP) and the R^2 of prediction (R^2 P). The RMSEP was calculated using Eq. 2:

$$\text{RMSEP} = \sqrt{\frac{\sum_{i=1}^{n_t}\left(y_{t,i} - \hat{y}_{t,i}\right)^2}{n_t}} \qquad \text{(Eq. 2)}$$

Where $y_{t,i}$ is the measured value, $\hat{y}_{t,i}$ is the age predicted by the model, and n_t is the number of samples in the test set. RMSEP expresses the average error to be expected in future predictions when the calibration model is applied to unknown samples. Moreover, the accuracy error of the predictions obtained for the validation samples and questioned documents was calculated according to Eq. 3:

$$\text{Error (\%)} = \left(\frac{(y_r - y_p)}{y_r}\right) x\ 100 \qquad \text{(Eq. 3)}$$

Where, y_p is the age predicted by the OPLS model and y_r the real age of the ink sample. Taking into account the above statistical parameters, the optimal model would have high R^2 and Q^2 values as well as low RMSECV and RMSEP values and a small difference between the last two statistical parameters. A large difference between RMSECV and RMSEP indicates the possibility that too many LVs are used in the model (over-fitting) and noise is modelled. The number of LVs is intended to be as low as possible, as larger number of LVs may include some irrelevant information. The R^2 parameter varies from 0 to 1, indicating the degree of adjustment to perfect fitting, and the Q^2 parameter shows the robustness and predictive capacity of the model, being good when $Q^2 > 0.5$ and excellent when $Q^2 > 0.9$ [24, 26]. The Hotelling's T2 and distance-to-model tests with a 95% confidence level were applied to check for outliers.

4.2.4 Case documents

Samples of ink entries from blind documents were used for method validation. The entries belonged to 4 documents provided by the Documentoscopy and Graphistics Section of the Forensic Science Unit of the Basque Country Police Department (Ertzaintza) and corresponded to the period 2018-2019: a sheet with handwritten annotations (SDG-Q6), two

Post-it® with handwritten annotations (SDG-Q7 and SDG-Q8) and a handwritten telephone notice (SDG-Q9). Each document was transported to the laboratory in individual folders and delivered according to the chain of custody. All the documents showed single-sided ink entries made with a blue ballpoint pen. The exact date on which the ink entries were made, the conditions to which the documents were exposed and the pen brand and paper manufacturer used were initially unknown for the laboratory. Once the ink prediction for each case document was made, the police disclosed the real date of the documents against which to contrast and evaluate the OPLS models, thus assessing the applicability of the method.

Four invoices from 2017, 2018 and 2019 were also provided. The first document from 2019 was made up of two stapled sheets printed in black ink on one side with a signature made with a blue ink gel pen on the bottom of each sheet (F12019 and F22019). The second document from 2018 consisted of two stapled sheets printed in black ink on one side with two signatures made with a blue ink ballpoint pen (F12018 and F32018) and a blue ink gel pen (F22018 and F42018) on the bottom of each sheet. The last two documents were from 2017, out of the temporal application range of the OPLS models. The first was made up of three stapled sheets printed in black ink on one side with two signatures on the bottom of the first sheet (F12017) and a signature on the other two sheets (F32017 and F42017) made with a blue ink ballpoint pen. The second consisted of two stapled sheets printed in black ink on one side with a signature made with a blue ink gel pen on the bottom of the first sheet (F52017). The documents were stored in folders under normal room conditions (60% humidity, 20 ºC). The pen brand and paper manufacturer used were unknown.

The analysis was carried out by Vis-microspectrophotometry following the procedure described in section 4.2.2. Two replicas were taken for each document.

4.3 Results and discussion

4.3.1 Multipurpose and comprehensive method development

Ink clustering and classification was performed by applying PCA and HCA in order to subsequently assign an optimal OPLS model that predicts the age of a certain ink.

4.3.1.1 Ink clustering and classification by PCA and HCA

A PCA and an HCA were performed with the spectroscopic data of all the ink samples of 11 types of writing tools from 7 different brands and aged at different time intervals with the aim of classifying and discriminating them (Table 1).

The PCA-X was built using all recorded wavelengths of the visible spectrum as **X** variables. The absorbance values of each wavelength were scaled with Pareto scaling and transformed into the first derivative to highlight the maxima and minima of the visible spectra. The PCA-X was set up with 3 PCs, accounting for 81.1% of total variation in the data. No outliers were found in the distance-to-model graph or in the Hotelling's T2 control graph with a 95% confidence level.

The PCA scores graph discriminated the writing tools into seven clusters (Figure 1). This discrimination was mainly along the first and second components, as they explained a total variance of 68%. The Inoxcrom® gel pen brand was strongly differentiated from the others in the extreme right area of the first component. The Uni-Ball® and Paper-Mate® gel pen brands were grouped at the top end of the second component. The rest of the pen ink brands were clustered in the central area of the graph with more or less differentiation between them.

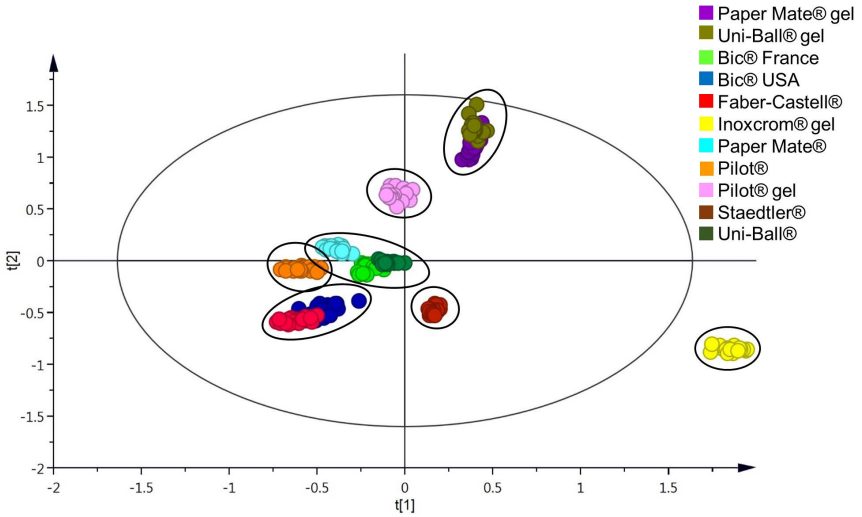

Figure 1. PCA scores graph. Clusters of 11 writing tools from 7 different brands along the first and second components.

The loadings graph of the PCA model was studied to establish which wavelengths of the visible spectrum had the most influence along the first and second components and, therefore, caused the discrimination of each type of pen ink brand. The wavelengths ascribed to violet-blue in the range 423-465 nm and red-purple in the range 666-698 nm had a negative influence on the first component, while the wavelength ranges corresponding to violet at 407-411 nm, yellow-green at 538-568 nm and purple at 718-746 nm influenced positively and, therefore, made the Inoxcrom® gel pen brand discriminate from the others. Likewise, the wavelength ranges attributed to blue in the range 446-458 nm and purple in the range 749-793 nm had a negative influence on the second component, whereas the wavelength ranges that influenced positively were those ascribed to yellow-green at 521-552 nm and red-purple at 656-719 nm, discriminating the ballpoint and gel pen brands from each other.

This discrimination was contrasted by performing an HCA. Applying the same data processing as in the PCA, the HCA dendogram (Figure 2) classified the writing tools into four main groups at a Euclidean distance of 15.

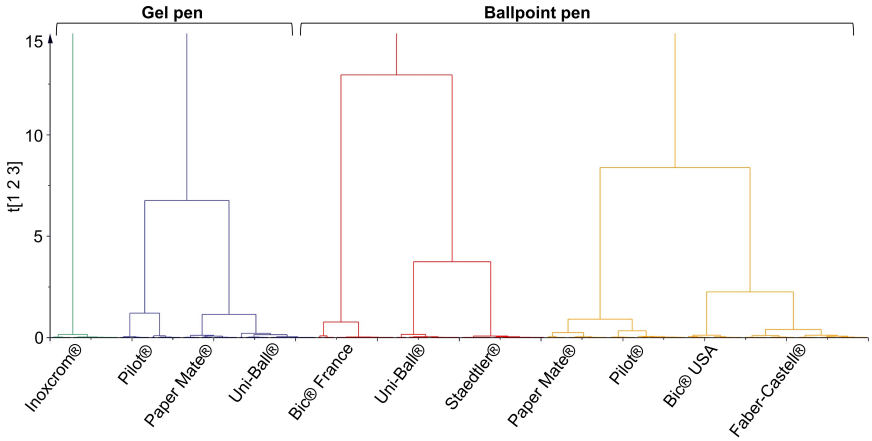

Figure 2. HCA dendogram. Classification of 11 writing tools from 7 different brands into 4 clusters. Euclidean distance 15.

As was done in the case above, the wavelengths of the visible spectrum that had the greatest influence on the classification of each pen brand group were studied from the loadings graph. The first class included the Inoxcrom® gel pen brand. The ink of this brand was characterised by the absorption of yellow in the range of 555-574 nm, purple in the range of 732-752 nm and orange in the range of 593-620 nm. The second class covered the Pilot®, Paper Mate® and Uni-Ball® gel pen brands. The absorption of red-purple at 705-716 and 632-645 nm as well as violet at 416-422 nm distinguished these pen ink brands. The third class included the Bic® from France, Uni-Ball® and Staedtler® ballpoint pen brands. The inks of these brands were characterised by the absorption of red in the range of 630-640 nm, blue-green in the range of 495-509 nm and violet in the range of 414-420 nm. The fourth class covered the Paper Mate®, Pilot®, Bic® from the USA and Faber-Castell® ballpoint pen brands. The

absorption of red at 634-645 nm, blue-green at 470-505 nm and violet at 417-422 nm differentiated these pen ink brands.

No differences were observed with the naturally aged ink samples of each writing tool and all of them were grouped with their corresponding brands. This is consistent with the research carried out by Sauzier *et al*. [20], as they observed that the overall classification of inks stored in dark and polypropylene archive sleeves and those stored away from light but open to air remained unchanged over time and thus the inks were grouped with their fresh equivalents after 28 and 32 months.

Both PCA and HCA can be applied as complementary pre-clustering and -classification tools to inks for which the writing tool used is unknown. While the PCA makes it possible to visualise in which group of writing tools the ink could be found, the HCA ratifies this clustering at a Euclidean distance of 1. At this Euclidean distance, the 11 writing tools were separated from each other, but classified with their corresponding group, and would therefore allow an unknown ink to be classified in one of them.

4.3.1.2 OPLS models construction and validation

The RMSECV and R^2 values and the number of LVs in the calibration set were evaluated to optimise and justify the type of spectral pre-treatment to be applied. The model was applied to the validation set once the best pre-treatment was chosen, in which the RMSEP value was assessed to determine the expected prediction error when the model is applied to unknown samples.

The predictive model of the Bic® ballpoint pen brand from the USA was made up of 30 samples split into 23 for the calibration set and 7 for the validation set using the Kennard-Stone algorithm. The application of centering and SNV filtering for the entire range of the visible spectrum showed the best statistical parameters (Table 2). The model was set up with 4 LVs, explaining 86% for R^2Y and predicting 74% for Q^2 of the data variation in the calibration set, which implies that the model has a high fit and predictive capacity. No outliers were found in either the distance-to-model graph or the Hotelling's T2 control graph with a 95% confidence level. In addition, values of 0.10 (1.3 days) for RMSECV and 0.86 for R^2 CV were obtained. The low RMSECV value indicates the high accuracy of the predictive model. It also showed an excellent predictive capacity, achieving values of 0.05 (1.12 days) for RMSEP and 0.94 for R^2 P in the validation set. High predictive accuracy with 10% error was obtained.

The same procedure was followed for the remaining writing tools. The pre-treatments applied and the statistical data obtained in the OPLS model for each writing tool are shown in Table 2. The Q^2 values were above 50% for the ballpoint pen brands, indicating a high predictive ability, whereas for the gel pen brands it was around 30% and 45%. The models also showed valid predictive accuracy and capacity on RMSECV and RMSEP terms to be applied to real cases. Accuracy errors of less than 15% were obtained, except for the Paper Mate® and Uni-Ball® ballpoint pen brands and Uni-Ball® gel pen brand that were 20 to 25%.

Table 2. Data of the OPLS models of each writing tool.

Ink type	Pen brand	No. calibration /validation samples	Pre-treatment	LV	R^2X	R^2Y	Q^2	RMSEE (days)[a]	RMSECV (days)[a]	R^2CV	RMSEP (days)[a]	R^2P	Accuracy error (%)[b]
Ballpoint	Bic® France	20/5	UV scaling and SNV filter	4	0.98	0.87	0.74	0.08 (1.2)	0.10 (1.3)	0.87	0.05 (1.1)	0.96	10
	Bic® USA	23/7	Centering and SNV filter	4	1.00	0.86	0.74	0.08 (1.2)	0.10 (1.3)	0.86	0.05 (1.1)	0.94	10
	Faber-Castell®	21/7	UV scaling and MSC filter	2	0.72	0.71	0.52	0.13 (1.4)	0.15 (1.4)	0.71	0.09 (1.2)	0.97	15
	Staedtler®	20/7	UV scaling and 1st derivative filter	6	0.96	0.95	0.83	0.07 (1.2)	0.10 (1.3)	0.95	0.07 (1.2)	0.88	15
	Pilot®	20/5	UV scaling and SNV filter	1	0.44	0.65	0.55	0.14 (1.4)	0.15 (1.4)	0.65	0.06 (1.2)	0.91	12
	Paper Mate®	15/5	UV scaling and 1st derivative filter	3	0.77	0.78	0.53	0.13 (1.4)	0.17 (1.5)	0.78	0.10 (1.3)	0.84	18
	Uni-Ball®	16/5	UV scaling and MSC filter	3	0.95	0.82	0.63	0.10 (1.3)	0.12 (1.3)	0.82	0.11 (1.3)	0.91	22
Gel	Paper Mate®	15/5	UV scaling and SNV filter	3	0.94	0.70	0.41	0.09 (1.2)	0.11 (1.3)	0.70	0.10 (1.3)	0.54	13
	Uni-Ball®	18/5	UV scaling and 1st derivative filter	2	0.82	0.58	0.41	0.16 (1.5)	0.18 (1.5)	0.58	0.15 (1.4)	0.91	25
	Pilot®	15/5	UV scaling and MSC filter	1	0.53	0.60	0.45	0.09 (1.2)	0.10 (1.3)	0.60	0.11 (1.3)	0.60	16
	Inoxcrom®	17/5	UV scaling and MSC filter	3	0.96	0.50	0.31	0.14 (1.4)	0.15 (1.4)	0.50	0.07 (1.2)	0.84	15

[a] Values given in logarithmic function and those in brackets in antilogarithmic function in days.
[b] Mean value calculated from the total number of ink samples of each pen brand.

Moreover, the visible spectrum ranges that characterise young and old inks in the predictive model of each writing tool were studied using the loadings graph (Figure 3), as it was visually impossible to observe shifts or changes in the absorption maxima of each pen ink brand over time.

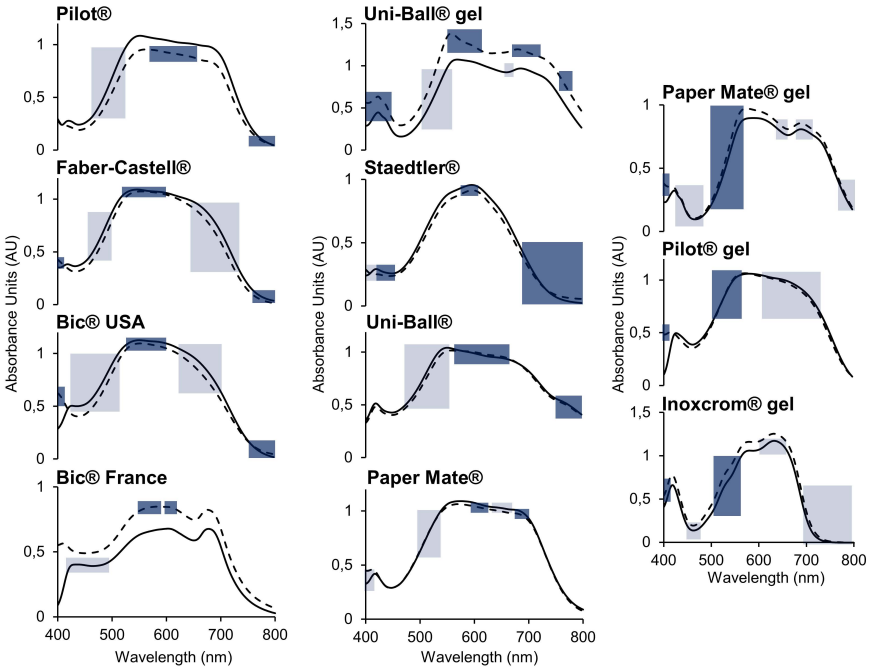

Figure 3. Spectra of young (solid line) and old (dashed line) ink of each writing tool. The spectrum ranges that characterise the young (light blue area) and old (dark blue area) ink are highlighted.

The young inks of the Bic®, Faber-Castell®, Staedtler® and Paper Mate® ballpoint pen brands and the Paper Mate® and Inoxcrom® gel pen brands were characterised by spectral modifications at 400 and 520 nm ascribed to the absorption of violet, blue and green. The inks of the Bic® from the USA, Faber-Castell® and Paper Mate® ballpoint pen brands and the Pilot®, Paper Mate®, Uni-Ball® and Inoxcrom® gel pen brands were also characterised by modifications in the red and purple region at 620-800 nm. In addition, the Pilot®, Paper Mate® and Uni-Ball® ballpoint and Uni-Ball®

gel inks were characterised by changes in the spectrum range between 440 and 580 nm attributed to the absorption of blue, green and yellow.

After ageing the inks of the Bic®, Faber-Castell®, Staedtler® and Paper Mate® ballpoint pen brands and the Pilot®, Paper Mate®, Uni-Ball® and Inoxcrom® gel pen brands were characterised by spectral changes in the range between 520 and 620 nm ascribed to the absorption of yellow, green and orange. The inks of the Bic®, Faber-Castell®, Staedtler®, Pilot®, Paper Mate® and Uni-Ball® ballpoint pen brands and the Uni-Ball® gel pen brands were also characterised by modifications in the orange, red and purple region at 580-800 nm. The inks of the Bic® from the USA, Faber-Castell® and Staedtler® ballpoint pen brands and the Pilot®, Paper Mate®, Uni-Ball® and Inoxcrom® gel pen brands were characterised by changes in the absorption of violet and blue in the range of 400-440 nm. In addition, the Pilot® ballpoint pen brand was characterised by modifications in the spectrum range between 580 and 680 nm attributed to the absorption of yellow, orange and red.

To sum up, the inks of the Bic® from France, Staedtler®, Pilot®, Paper Mate® and Uni-Ball ballpoint pen brands and the Inoxcrom® and Uni-Ball® gel pen brands were characterised over time by spectral modifications that shifted towards higher wavelengths, while those of the Pilot®, Paper Mate® and Inoxcrom® gel pen brands shifted towards lower wavelengths. The inks of the Bic® from the USA and Faber-Castell® ballpoint pen brands were characterised over time by modifications in both the upper and lower wavelengths of the visible spectrum.

The younger inks of all ballpoint pen brands except Staedtler® were characterised by changes in the slopes of the absorption bands in the range of 470 to 520 nm, whereas the older inks were characterised by spectral modifications in the range between 580 and 610 nm. It is within

and close to the latter range that triarylmethane dyes, the most commonly used in ballpoint pens, have their maximum absorption bands [15]. Therefore, although the ink strokes were not exposed to light, triarylmethane dyes can be unstable in the dark and can undergo oxidation reactions with atmospheric oxygen to form diphenylmethane derivatives and phenol [20]. However, due to the fact that the ballpoint pen inks are made up of a mixture of dyes, some of them could have their maximum absorption band very close to each other and, therefore, the degradation reactions that occurred in each of them could be suppressed due to competitive absorption [16]. Moreover, the younger inks of all gel pen brands except Uni-Ball® were characterised by spectral modifications in the range from 630 to 750 nm ascribed to the absorption maxima of red and purple absorbing components, while the older inks were characterised by those in the range between 500 and 550 nm attributed to the absorption maxima of green and yellow absorbing components. Although it was not possible to determine to which dyes these modifications were associated, the inks of the Paper Mate® and Uni-Ball® gel pen brands were known to be made up of pigments. Previous research has shown that pigment-based inks are more stable [20] and, therefore, the degradation of Paper Mate® and Uni-Ball® gel inks may not have been as strong as that of other pen brands, as pigments can act as degradation quenching agents [16].

The ballpoint pen inks therefore underwent modifications in characteristic ranges of the visible spectrum throughout ageing that differed from those of the gel pen inks, with the exception of the Uni-Ball® gel ink, which had similarities to ballpoint pen inks. This fact hinders the obtaining of a universal OPLS model.

4.3.2 Application to questioned documents

The feasibility of the method for dating case documents was assessed following the steps indicated in the flow graph shown in Figure 4.

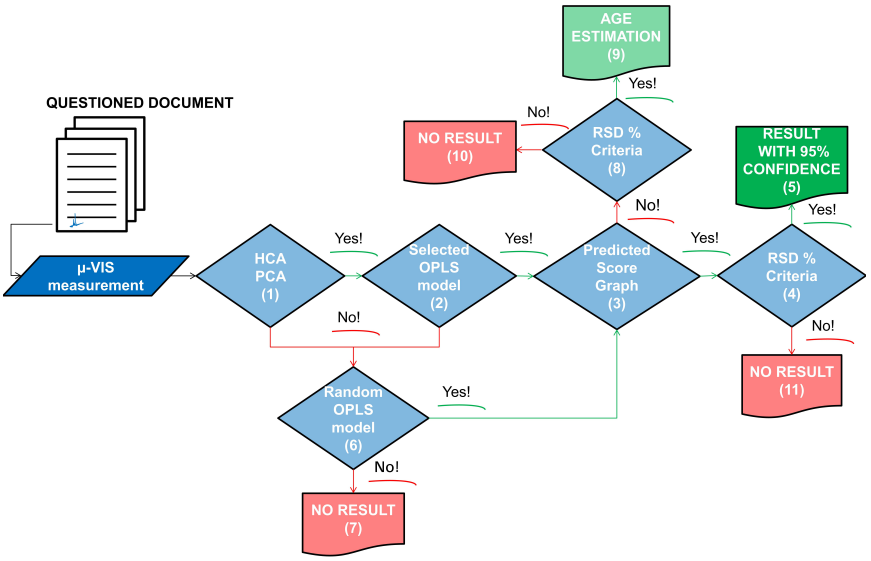

Figure 4. Flow graph used in the study of case documents.

The spectroscopic data recorded from the blind samples were applied to the PCA and/or HCA model to determine the pen brand used in each of them (step 1) and thus decide which predictive model to apply (step 2). In cases where the samples were not classified nor clustered with their respective pen brand, a random OPLS model was selected from the pen brands with which they were closest classified and/or clustered (step 6). In addition, the predicted score graph of the OPLS model was used (step 3), which establishes with 95% confidence an accurate age prediction for the ink samples within the ellipse.

The precision error of the results obtained for the replicas of each document was calculated by the relative standard deviation (RSD) using the Eq. 4 (steps 4 and 5):

$$\text{RSD (\%)} = \frac{S}{\bar{X}} x\ 100 \qquad \text{(Eq. 4)}$$

Where, *S* is the standard deviation and $\bar{X}$ the mean of the data. RSD values that were less than the accuracy error obtained in the validation of the OPLS models of each brand were taken as valid criteria.

4.3.2.1 Intercomparison study

The ink samples from documents F12018 and SDG-Q7 were clustered in the PCA model with the Bic® ballpoint pen brand from the USA (step 1), as shown in Figure 5A. The OPLS model of the Bic® ballpoint pen brand placed the two replicas of each document within the ellipse of the predicted score graph (steps 2 and 3), as illustrated in Figure 5B. An average age prediction of 476 days with an accuracy error of 17% was obtained for the document F12018, whereas that of the document SDG-Q7 was 622 days with an accuracy error of 14% (steps 4 and 5), as indicated in Table 3.

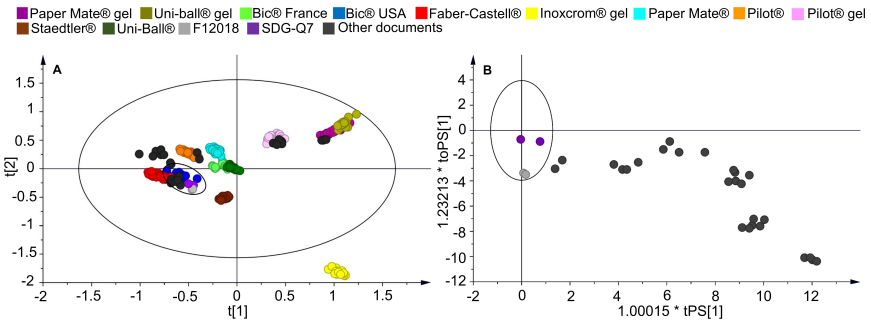

Figure 5. A. Ink samples from documents F12018 and SDG-Q7 clustered with the Bic® ballpoint pen brand in the scores graph of the PCA model. B. Two replicas of the documents F12018 and SDG-Q7 inside the ellipse of the predicted score graph of the OPLS model of the Bic® ballpoint pen brand.

Table 3. Data obtained from case documents used in the intercomparison study.

	Document	Classification	Date (days)	Predicted date (days)	Accuracy error (%)	Elimination step	Comments
Intercomparison study	F12018	Bic® USA	574	476	17	None	Well classified Within the range of application Two replicas within the ellipse RSD criterion met
	SDG-Q7	Bic® USA	548	622	14	None	
	SDG-Q7	Pilot®	548	535	2	None	Not classified Within the range of application Two replicas within the ellipse RSD criterion met
	F22018	Pilot® gel	574	No result		8 and 10	Well classified Within the range of application None of the replicas within the ellipse RSD criterion not met
	F42018	Pilot® gel	574	No result		8 and 10	
	F32018	Bic® USA	574	No result		8 and 10	
	SDG-Q6	Faber-Castell® Bic® USA Pilot®	152	No result		7	Not classified Within the range of application None of the replicas within the ellipse RSD criterion not met
	SDG-Q8	Faber-Castell® Bic® USA Pilot®	608	No result		7	
	SDG-Q9	Faber-Castell® Bic® USA Pilot®	61	No result		7	Not classified Out the application range None of the replicas within the ellipse RSD criterion not met

Moreover, although the ink samples were classified within the Bic® ballpoint pen brand, the Pilot® brand group was also found to be close to the ink used in the SDG-Q7 document (steps 1 and 6). Therefore, the OPLS model of the Pilot® ballpoint pen brand was also applied to the SDG-Q7 document, giving an average prediction of 535 days with an accuracy error of 2% (steps 4 and 5), as shown in Table 3. The ink samples from the SDG-Q7 document in addition to being placed very close to the Pilot® ballpoint pen brand in the PCA model, the two replicas were placed inside the ellipse of the predicted score graph (step 3) and were within the temporal application range of the OPLS model.

As can be observed, two OPLS models (Bic® USA and Pilot®) have correctly predicted the age of the same ink brand used in the questioned document (SDG-Q7). This implies that the same OPLS model of a pen ink brand may respond not only to ink strokes of the same brand, but also to other strokes made with a similar ink formulation. This finding could be positive for the future universal applicability of this methodology. Thus, OPLS models would not be needed for all commercial pen inks, but for the most representative and/or those that fit the largest number of different brands. The greater the number of different OPLS models, the greater the possibility that the ink stroke of the document in question will fit one of them. Likewise, OPLS models of other pen brands could be applied as a cross-checking tool for predicting the age of inks with a formulation similar to theirs, whenever the two ink replicas are placed inside the ellipse of the predicted score graph, the age of the ink is within the temporal application range of the OPLS model and the ink is close to any of the classes of the pen brands studied. Moreover, although the conditions to which the documents were exposed differed from those applied in the study, accurate predictions could be obtained. Therefore, when these differences are not large, the OPLS models are able to overcome them. In addition, accurate predictions were obtained, despite the fact that the type of paper

used in the documents was different from that used in the study, so the background correction of the support made before the measurement of the ink stroke was enough to eliminate its influence.

The ink samples from documents F22018 and F42018 were grouped with the Pilot® gel pen brand in the PCA model (step 1). Although the 574-day ink strokes were within the temporal application range of the OPLS model (step 2), which was 8 months to 2 years, the two replicas of each document were placed outside the ellipse of the predicted score graph (step 3) and thus inaccurate predictions were obtained (steps 8 and 10). That was also the case for the ink samples from document F32018 that were classified with the Bic® ballpoint pen brand from the USA. The 574-day ink stroke was within the temporal application range of the OPLS model, which was 5 months to 2 years, but the two replicas were placed outside the ellipse of the predicted score graph, resulting in inaccurate predictions. Although all the samples in the intercomparison study have been in the same conservation conditions, it is possible that these samples have suffered slight differences, which has led to inaccurate predictions. It must be highlighted that these documents (invoices) have been consulted on different occasions and, therefore, exposed in different ways and at different times to the light.

The ink samples from documents SDG-Q6 and SDG-Q8 were not classified in any of the pen brands studied (step 1). The Faber Castell®, Bic® from the USA and Pilot® ballpoint pen brands were the closest to them and thus their OPLS models were selected to carry out a trial prediction of the ink samples (step 6). Although the ink strokes were within the temporal application range of the OPLS models, neither of them placed the two replicas of each document inside the ellipse of the predicted score graph and, therefore, inaccurate predictions were obtained (step 7). This may be due to the fact that the ink formulation in the writing tools studied

differs from that used to make the ink strokes and, therefore, an exact age of the ink samples cannot be established if the ink cannot be classified with one of the pen brands studied. The lack of predictability due to this type of mismatch could be minimised by increasing the number of ink prediction OPLS models in the near future.

Another case was that of the ink samples from document SDG-Q9 which were also not classified in any of the pen brand groups studied, so the Faber Castell®, Bic® from the USA and Pilot® ballpoint pen brands which were closest to them were selected (step 1 and 6). The ink stroke was 2 months old and did not fall within the temporal application range of any of the OPLS models, so the two replicas were placed outside the ellipse and inaccurate predictions were obtained (step 7).

4.3.2.2 Case documents out of time range

Due to the last case above, the feasibility of the OPLS models to detect case documents out of their temporal application range was assessed, since being able to determine the time ranges bellow or above which a ink sample could be placed also provides very useful information.

The ink samples of all documents were well clustered with their respective pen brands in the PCA model (step 1), as shown in Table 4. In all cases, the two or one of the replicas of each document was placed outside the ellipse of the predicted score graph of the OPLS model (steps 2 and 3), resulting in inaccurate predictions as expected (steps 8 and 10). The OPLS models were able to detect all the ink samples that were out of their temporal application range, as at least one of the replicas placed it outside the ellipse.

Table 4. Data obtained from case documents out the time range of the method.

	Document	Classification	Date (days)	Elimination step	Comments
Out of time range	F12019	Paper Mate® gel	29	8 and 10	Well classified Out the application range Replicas out and at the limit of the ellipse RSD criterion not met **Correctly removed by the OPLS model**
	F22019	Paper Mate® gel	29	8 and 10	
	F12017	Pilot®	933	8 and 10	Well classified Out the application range Replicas out and within the ellipse RSD criterion not met **Correctly removed by the OPLS model**
	F32017	Bic® USA	933	8 and 10	Well classified Out the application range None of the replicas within the ellipse RSD criterion not met **Correctly removed by the OPLS model**
	F42017	Bic® USA	933	8 and 10	
	F5 2017	Pilot® gel	814	8 and 10	

A major problem could have been if the method had tried to estimate the date of any ink stroke, irrespective of its age (over-fitting). The use of partial least squares models could involve this risk [27]. In this methodology, this would imply the impossibility of knowing if the analysed ink sample is within the measurement range or not, in addition to obtaining poor results. However, as noted above, the OPLS models were able to identify ink samples that were not within their temporal application range with 95% confidence, whenever the ink samples were correctly clustered in the PCA model and/or classified in the HCA model with one of the pen brands studied. In these cases, one of the two ink replicas was placed outside the ellipse of the predicted score graph and thus the ink samples were temporarily above or below the application limit of the OPLS model of the corresponding pen brand.

4.3.3 Remarks

This study presents a non-invasive methodology for the dating of ink strokes on paper made with both ballpoint pen and gel pen brands by applying Vis-microspectrophotometry combined with orthogonal partial least squares regression. Besides being a fast and non-invasive technique that does not require any treatment of the sample, it was possible to apply it to micro surfaces, such as ink strokes, and thus applicable to real cases of document forgery, overcoming the disadvantage of the UV-Vis-NIR spectrophotometric technique.

The OPLS models of each writing tool were achieved by trial-and-error method until the optimal model was reached. First, different spectral filters and scaling were applied and combined, possible non-informative **X** variables were studied for their elimination and outlier detection was performed. It was then checked that the values of the statistical parameters (R^2, Q^2 and RMSE) obtained in the training and test sets applying these

pre-treatments were within the established limits, achieving the minimum accuracy error and the maximum predictive capacity.

Moreover, the classification of the inks enabled us to subsequently assign an optimal OPLS model for age prediction in each case. The OPLS model was able to predict an exact date with an accuracy error lower than 25% whenever: (i) the two replicas were placed inside the ellipse of the predicted score graph, (ii) the ink age was within the temporal application range of the OPLS model, and (iii) the ink was well classified in one of the groups of the pen brands studied. The intercomparison study showed that the ink samples that met these requirements and an age prediction could be obtained were those that (i) were made with an ink that fitted one of the OPLS models and (ii) were stored under conditions not too different from those applied in this study. These conditions will obviously not always be met and, therefore, there will always be a ratio of samples of questioned documents with no date estimate. What was promising is that it has been demonstrated that the age prediction was always performed with a 95% confidence rate and a high degree of accuracy and precision. Moreover, the response ratio could increase considerably as new ink models are added to the methodology, making it increasingly universal. Likewise, the OPLS model was capable of detecting with 95% confidence those inks out of its temporal application range, whenever the ink samples were correctly clustered in the PCA model and/or classified in the HCA model with one of the pen brands studied, but one of the two ink replicas was placed outside the ellipse of the predicted score graph. Thus, the methodology used cannot only accurately date the inks within its scope, but also determine with 95% confidence which ink samples are temporarily placed above or below the application limit of the OPLS model of the corresponding pen brand, providing very useful information.

Finally, the fact that the ink has a slower degradation kinetics in dark conditions made it impossible to visually detect significant spectral modifications in the dyes present within the inks. However, the chemometric model was able to detect spectral modifications depending on the age and brand of pen ink analysed. These modifications may be due to oxidation reactions with atmospheric oxygen in which dyes and/or pigments compete with each other [16, 20].

4.4 Conclusions

Multivariate analysis was shown to be a powerful tool for monitoring the spectral modifications during the ageing process of the dyes present in the pen ink composition. The methodology is capable of predicting the age of documents made with different pen ink brands and exposed to the same or slightly different storage conditions than those applied in the study as long as the established requirements are met, as well as detecting those documents that are above or below its temporal application range. Moreover, the method is a major advance in the field of ink dating, since it is applicable to cases of document forgery of up to 2 years by analysing the ink strokes kept in the darkness at a micro level without damaging the integrity of the document and provides accurate ink age predictions with 95% reliability with which to make a firm decision in court cases. As noted, with the current predictive models not all the ink samples analysed meet the requirements for an accurate age prediction. The rejection rate will decrease as the number of OPLS models increases with new inks, new ink batches and/or new inks with different storage conditions.

Acknowledgments

The authors would like to thank Xabier Rementeria, Head of the Documentoscopy and Graphistics Section of the Forensic Science Unit of the Basque Country Police Department (Ertzaintza), for providing case documents and related information. The authors also thank the University of the Basque Country (UPV/EHU) (Project GIU16/04) for the financial support and the Advanced Research Facilities (SGIker) of the UPV/EHU for the human support in the development of this work. The Coimbra Chemistry Centre (CQC) is supported by the Fundação para a Ciência e a Tecnologia (FCT), through the Projects UIDB/00313/2020 and UIDP/00313/2020. Finally, L. Ortiz-Herrero thanks UPV/EHU for the pre-doctoral fellowship.

References

[1] A.C.A Assis, End User Commentary on Emerging Approaches in the Analysis of Inks on Questioned Documents, in: S. Francese (Eds.), Emerging Technologies for the Analysis of Forensic Traces, Advanced Sciences and Technologies for Security Applications, Springer, Cham, 2019, pp. 179-182. https://doi.org/10.1007/978-3-030-20542-3_12.

[2] C. Weyermann, J. Almog, J. Bügler, A.A. Cantu, Minimum requirements for application of ink dating methods based on solvent analysis in casework, *Forensic Sci. Int.* 210 (1) (2011) 52-62. https://doi.org/10.1016/j.forsciint.2011.01.034.

[3] A. Koenig, S. Magnolon, C. Weyermann C, A comparative study of ballpoint ink ageing parameters using GC/MS, *Forensic Sci. Int.* 252 (2015) 93-106. https://doi.org/10.1016/j.forsciint.2015.03.027.

[4] C. Weyermann, D. Kirsch, C. Vera, B. Splenger, A GC/MS study of the drying of ballpoint pen ink on paper, *Forensic Sci. Int.* 168 (2007) 119-127. https://doi.org/10.1016/j.forsciint.2006.06.076.

[5] A. Koenig, J. Bügler, D. Kirsch, F. Köhler, C. Weyermann, Ink dating using thermal desorption and gas chromatography/mass spectrometry: Comparison of results obtained in two laboratories, *J. Forensic Sci.* 60 (2015) 52-61. https://doi.org/10.1111/1556-4029.12603.

[6] O. Díaz-Santana, F. Conde-Hardisson, D. Vega-Moreno, Comparison of the main dating methods for six ballpoint pen inks, *Microchem. J.* 138 (2018) 550-561. https://doi.org/10.1016/j.microc.2018.01.045.

[7] A. Koenig, C. Weyermann, Ink dating part II: Interpretation of results in a legal perspective, *Sci. Justice* 58 (2018) 31-46. http://dx.doi.org/10.1016/j.scijus.2017.08.003.

[8] M. Calcerrada, C. García-Ruiz, Analysis of questioned documents: A review, *Anal. Chim. Acta* 853 (2015) 143-166. https://doi.org/10.1016/j.aca.2014.10.057.

[9] R. Petry Gorziza, C.M. Bello de Carvalho, M. González, L. Borba Leal, T. Korndörfer, R. Scorsatto Ortiz, T. Trejos, R. Pereira Limberger, Blue and black ballpoint pen inks: A systematic review for ink characterization and dating analysis, *Brazilian Journal of Forensic Sciences, Medical Law and Bioethics* 8 (3) (2019) 113-138. http://dx.doi.org/10.17063/bjfs8(3)y2019113.

[10] A. Koenig, C. Weyermann, Ink dating, part I: Statistical distribution of selected ageing parameters in a ballpoint inks reference population, *Sci. Justice* 58 (2018) 17-30. https://doi.org/10.1016/j.scijus.2017.08.002.

[11] C.M. Bello de Carvalho, R. Scorsatto Ortiz. R. Pereira Limberger, Figures of merit evaluation of GC/MS method for quantification of 2-phenoxyethanol from ballpoint pen ink lines and determination of the influence of support paper on solvent extraction, *Quim. Nova* 42 (1) (2019) 42-48. https://doi.org/10.21577/0100-4042.20170308.

[12] J. Bügler, H. Buchner, A. Dallmayer, Age determination of ballpoint pen ink by thermal desorption and gas chromatography–mass spectrometry, *J. Forensic Sci.* 53 (4) (2008) 982-988. https://doi.org/10.1111/j.1556-4029.2008.00745.x.

[13] I. San Román, L. Bartolomé, M.L. Alonso, R.M. Alonso, M. Ezcurra, DATINK pilot study: An effective methodology for ballpoint pen ink dating in questioned documents, *Anal. Chim. Acta* 892 (2015) 105-114. http://dx.doi.org/10.1016/j.aca.2015.08.038.

[14] J.S. Seixas de Melo, The molecules of colour and Art. Molecules with history and modern applications, in: A. Albini, S. Prodi (Eds.), Photochemistry, RSC: London, 2020, Vol. 47, pp. 196-216. https://doi.org/10.1039/9781788016520-00196.

[15] K.O. Gorshkova, I.I. Tumkin, L.A. Myund, A.S. Tverjanovich, A.S. Mereshchenko, M.S. Panov, V.A. Kochemirovsky, The investigation of dye ageing dynamics in writing inks using Raman spectroscopy, *Dyes Pigm.* 131 (2016) 239-245. http://dx.doi.org/10.1016/j.dyepig.2016.04.009.

[16] C. Weyermann, D. Kirsch, C. Costa Vera, B. Spengler, Evaluation of the photodegradation of Crystal Violet upon light exposure by mass spectrometric and spectroscopic methods, *J. Forensic Sci.* 54 (2) (2009) 339-345. https://doi.org/10.1111/j.1556-4029.2008.00975.x.

[17] O. Díaz-Santana, D. Vega-Moreno, F. Conde-Hardisson, Gas chromatography-mass spectrometry and high-performance liquid chromatography-diode array detection for dating of paper ink, *J. Chromatogr. A* 1515 (2017) 187-195. https://doi.org/10.1016/j.chroma.2017.07.093.

[18] N.M. Grechukha, K.O. Gorshkova, M.S. Panov, I.I. Tumkin, E.O. Kirillova, V.V. Lukianov, N.P. Kirillova, V.A. Kochemirovsky, Analysis of the ageing processes of writing ink: Raman spectroscopy versus gas chromatography aspects, *Appl. Sci.* 7 (10) (2017) 991. https://doi.org/10.3390/app7100991.

[19] V. Sharma, R. Kumar, Dating of ballpoint pen writing inks via spectroscopic and multiple linear regression analysis: A novel approach, *Microchem. J.* 134 (2017) 104-113. https://doi.org/10.1016/j.microc.2017.05.014.

[20] G. Sauzier, J. McGann, S.W. Lewis, W. van Bronswijk, A study into the ageing and dating of blue ball tip inks on paper using in-situ visible spectroscopy with chemometrics, *Anal. Methods* 10 (2018) 5613-5621. https://doi.org/10.1039/c8ay01418c.

[21] L. Ortiz-Herrero, L. Bartolomé, I. Durán, I. Velasco, M.L. Alonso, M.I. Maguregui, M. Ezcurra, DATUVINK pilot study: A potential non-invasive methodology for dating ballpoint pen inks using multivariate chemometrics based on their UV–Vis-NIR reflectance spectra,

Microchem. J. 140 (2018) 158-166. https://doi.org/10.1016/j.microc.2018.04.019.

[22] M. Ezcurra, I. Velasco, J.M.G. Góngora, M.I. Maguregui, R.M. Alonso, Analysis of Bic Cristal Medium ballpoint pen inks, *J. Am. Soc. Quest. Doc. Exam.* 12 (2) (2009) 57-68.

[23] A.C. de Almeida Assis, F.I. Romano Inácio, J.S. Seixas de Melo, C. Farinha, Writing instruments inks: microspectrophotometry forensic analysis and characterisation, *European Police Science and Research Bulletin* 16 (2017) 187-207.

[24] L. Eriksson, T. Byrne, E. Johansson, J. Trygg, C. Vikström, Multi- and megavariate data analysis. Basic principles and applications, 3rd ed., Umetrics Academy, 2013.

[25] R.W. Kennard, L.A. Stone, Computer aided design of experiments, *Technometrics* 11 (1969) 137-148. https://doi.org/10.1080/00401706.1969.10490666.

[26] L. Ortiz-Herrero, I. Cardaba, S. Setien, L. Bartolomé, M.L. Alonso, M.I. Maguregui, OPLS multivariate regression of FTIR-ATR spectra of acrylic paints for age estimation in contemporary artworks, *Talanta* 205 (2019) 120114. https://doi.org/10.1016/j.talanta.2019.120114.

[27] B.C. Deng, Y.H. Yun, Y.Z. Liang, D.S. Cao, Q.S. Xu, L.Z. Yi, X. Huang, A new strategy to prevent over-fitting in partial least squares models based on model population analysis, *Anal. Chim. Acta* 880 (2015) 32-41. http://dx.doi.org/10.1016/j.aca.2015.04.045.

CHAPTER

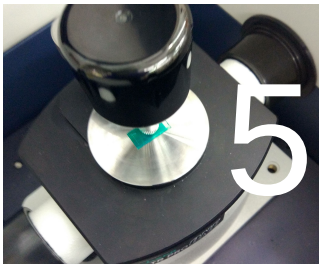

OPLS multivariate regression of FTIR-ATR spectra of acrylic paints for age estimation in contemporary artworks

L. Ortiz-Herrero, I. Cardaba, S. Setien, L. Bartolomé, M.L. Alonso, M.I. Maguregui

Talanta, **2019**; 205: 120114

Q1, IF: 5.339, 11/86, Chemistry, Analytical

Abstract

In recent years the interest and demand for artworks has been increasing, as they are an interesting commercial investment due to their growing value in the market. This explains the increasing number of counterfeits dealing with artworks that has led to the development of new methodologies for their characterisation. The material characterisation of these types of works can provide relevant information for both authentication and conservation/restoration. Thus, in this study multivariate chemometric methods were applied to FTIR-ATR spectroscopic data for artwork dating purposes. To that end, ageing prediction models were developed for Liquitex® and Hyplar® brands. Paint samples containing the green synthetic organic pigment (PG7) were exposed to artificial ageing and analysed with FTIR-ATR and Py-GC/MS for characterisation and monitoring of the main components. Although the OPLS ageing models were characterised primarily by the modifications undergone by the binder and surfactants, a universal model could not be developed due to differences in the modification trends of the different brands. The applicability of the OPLS modelling for artwork dating purposes was tested in artworks provided by internationally recognised contemporary Basque artists. For Liquitex® a significant correlation ($p < 0.05$) between natural and accelerated ageing could be established, in which approximately 50 h of accelerated ageing under the applied conditions were equivalent to one natural year. This correlation might have possible applications in the dating of artworks for up to at least 22 years. Thus, the study demonstrates that FTIR-ATR combined with chemometrics is a potential method for artwork dating and a valuable source of information about the chemical processes involved in paint ageing, which can be of great help in the conservation and restoration steps.

Keywords: Acrylic paint, artwork dating, FTIR-ATR, OPLS.

5.1 Introduction

The contemporary art market is very dynamic and its increasing demand involves hundreds of millions of dollars per year. However, several serious problems given within the art market are intensifying fraud and limiting its growth potential. Illicit art trade has become the third illegal market after drugs and weapons [1, 2]. Today there are many counterfeits present in museums and galleries that are sold, exchanged and exhibited among collectors and art institutions [3]; in fact, half of artworks currently in circulation may be counterfeits [4]. Hundred billions of dollars are spent worldwide on art every year and a great part of that is tainted by illegal and illicit activities causing damages in millions to museums, galleries and collectors [5].

Forgers are mainly copying artworks dated from the early to mid-20th century, as it is much easier to acquire authentic materials and modern paintings have increased in value in recent years [6]. Artistic reasons are also included that may affect the falsification. Contemporary art is easily copied, since in many cases the “exclusivity” of the design is not available, as many are serial works. In addition, the “manual dexterity” of the artists is not always evident (unlike old masters), since many of them are conceptual artworks. The massive production and short age of most of the works mean a vast amount of works with similar characteristics difficult to differentiate. Therefore, a correct material characterisation of these works aimed to the identification and precise dating of the materials used, could be of great help in detecting counterfeited or misattributed works.

The most widely used materials by contemporary artists are acrylic paints. Introduced to the market in the mid-1950s, acrylic emulsion paints use a synthetic resin dispersed in water as a binding medium. The acrylic medium is a dispersion of methyl methacrylate-ethyl acrylate (MMA-EA)

copolymer or methacrylate-n-butyl acrylate (MMA-nBA) copolymer. This type of paint has a fast drying, high resistance to chemicals and weathering and incredible flexibility [7]. Many brands of artist's acrylic paint are available; each consists of binders, pigments, extenders and a range of additives that will affect its performance and stability. In addition, the absorption of UV radiation and the oxygen diffusion in the paint cause photooxidation reactions, such as chain scission and cross-linking reactions, of the polymeric binder in acrylic paints, which firstly affect the uppermost layer of the paints. The polymer structure changes, and consequently the physical and mechanical properties and the chemical stability of the paints are modified. The additives and pigments added to the paint formulation can interfere with the photooxidation reactions. Therefore, by knowing the material composition of artworks and the degradation processes they undergo, appropriate conservation and restoration strategies can be developed and evaluated [8-11].

Therefore, material characterisation has also a big relevance in issues relating conservation strategies to be used with these contemporary works. In this context, the detection of the existence of diverse amounts of surfactants in the surface of acrylic paintings may determine the effectiveness of some treatments, such as cleaning. For instance, if a great lost in surfactants is identified in relation with the ageing process, an increase in the rigidity of the painting could be predicted, thus becoming more prone to crack in contact with humidity. On the contrary, in young paints or paints with no tendency to lose surfactants as they age, the surface may react differently when applying a cleaning solution.

In recent years, a number of techniques have been applied to deal with cases of counterfeiting and assist in the conservation and restoration of artworks. Non-destructive techniques, such as time resolved laser induced fluorescence (TR-LIF), X-ray fluorescence (XRF) [12], proton induced X-ray

emission (PIXE), neutron activation analysis (NAA), energy dispersive X-ray spectroscopy (EDX) [13], Raman spectroscopy [13-16], Fourier transform infrared spectroscopy (FTIR) [13], IR-hyperspectral imaging (IR-HSI) [17, 18], FTIR-attenuated total reflection (FTIR-ATR) [16, 19], IR reflection [20] and scanning electron microscopy-EDX (SEM-EDX) [16, 19], are used as a first option, as they do not damage the piece of art. Among the techniques, FTIR spectroscopy is widely used in the investigation of artworks, as it is a fast technique and requires a very small sample quantity, the latter being a very important factor when studying artwork constituents. There are now portable FTIRs adapted to heritage that do not require sampling [21]. In addition, its different modes of operation, such as ATR, have made this technique useful for the characterisation of artworks' materials [16, 19, 22] as well as for photostability studies and for the study of the influence of pigments on the photodegradation of acrylic paints [8-10, 23].

In most cases, non-destructive techniques are not enough to authenticate a work, so more invasive and destructive methods are required. These techniques imply damaging the artwork under examination, which is often restricted due to the high value and unique nature of the artworks. That is why the use of micro-destructive techniques, such as laser ablation-inductively coupled plasma/mass spectrometry (LA-ICP/MS) [24] and pyrolysis-gas chromatography/mass spectrometry (Py-GC/MS), is expanding in this field. Py-GC/MS has been applied for photo-oxidative ageing studies of artist's paints and for the characterisation and identification of the paint components employed by artists and those used in former restoration works in modern art materials, such as synthetic organic pigments, polymeric binders, varnishes and additives [19, 25-28]. This information is necessary to propose an appropriate preventive conservation treatment or assist during the restoration of an artwork [29, 30] and for authentication purposes [31].

Analytical techniques combined with statistical methods, such as multivariate chemometrics, have been widely used to extract the maximum and most representative information from the acquired data in an interpretable manner. Several applications of exploratory methods, such as principal component analysis (PCA) and hierarchical cluster analysis (HCA), have been reported in the conservation [32, 33] and forensic [34, 35] fields of artworks. In spite of the applications of partial least squares (PLS) for the quantification of paint components in the restoration of artworks [36, 37] as well as for the determination of their properties in quality control [38], no studies are available that apply this method to the dating of artworks. The applicability and effectiveness of this tool has been demonstrated in other forensic fields, such as in questioned documents' dating [39, 40].

In this study, FTIR-ATR and Py-GC/MS techniques were applied to the characterisation of artificially aged acrylic paints from six different manufacturers. The composition (binding medium, pigment and additives) of the paints was identified and the modifications undergone after the artificial ageing trials were studied. FTIR-ATR spectroscopic data of two of this paint brands were applied to multivariate chemometric tools, obtaining predictive models capable of dating paints. The applicability of the models developed for one of the acrylic paints was tested in artworks provided by the internationally well recognised contemporary Basque artists Jesús Mari Lazkano and Luis Candaudap.

5.2 Materials and methods

5.2.1 Reference paint samples and preparation

The acrylic paint was obtained from commercial paint tubes of six different brands. Five of them were purchased in 2015-2016: Liquitex Acrylic Paint® (United States (USA)), Royal Talens Van Gogh® (Netherlands), Titan Arts – Acrílico Extrafino (Spain), Vallejo Acrylic Artist Color® (Spain) and Golden Heavy Body® (USA). The last paint, Hyplar Acrylic Colors® (USA), was obtained from a painting tube purchased in the 80´s. All of them contained chlorinated copper phthalocyanine green (PG7) synthetic organic pigment. The choice of colour and manufacturers was made on the basis of interviews with artists and oral sources to identify the colours and brands preferred by contemporary Basque artists.

0.6 µm thick free paint films were applied over 180 µm plastic sheets with the help of a monitored film applicator (4340 Automatic Film Applicator, Elcometer, United Kingdom (UK)), prior to drying at room conditions for approximately 8 months. A paint sample set containing 48 samples of each brand was gradually aged under controlled accelerated ageing conditions and subsequently characterised by Py-GC/MS and FTIR-ATR and used for carrying out the dating study.

5.2.2 Accelerated ageing

The ageing procedure consisted in exposing the reference paint films (1 x 2 cm) to artificial solar radiation under controlled temperature, humidity and irradiance conditions, as reported in a previous work [39]. A Solarbox 1500e RH equipment (Neurtek Instruments, Spain) was used, with a Xenon Lamp, which provided radiation with wavelengths between 300 and 800 nm and a nominal irradiance of 600 W m^{-2}. The camera was equipped with

an indoor 310 nm UV filter and set to a black panel temperature of 55 ºC and 50% humidity. The accelerated ageing was carried out under isochronous sampling up to a maximum of 1426 h.

5.2.3 Py-GC/MS analysis

Py-GC/MS was performed to characterise the organic components, such as binders, pigments and additives, present in the artificially aged reference paint films of the six brands studied.

A 5250 pyrolyzer unit (CDS Analytical, USA) combined with a 5975C GC/MSD System with Triple-Axis Detector (Agilent Technologies, USA) equipped with a ZB-WAX capillary column (30 m x 0.25 mm x 0.25 µm) (Agilent Technologies, USA) was used. The pyrolysis temperature was set at 600 °C, since previous research studies have shown that this temperature is effective for the analysis of acrylic emulsion paints by achieving the fragmentation of the synthetic organic pigments and the acrylic paint binder [19, 28, 30]. The temperature of the pyrolysis interface was 300 °C and that of the injector 300 °C. The GC column temperature program was: initial temperature of 40 °C, kept for 2 min, increased up to 250 °C with 12 °C min^{-1} heating rate and held for 10 min. The helium gas flow was set at 1.7 mL min^{-1}. Mass spectra were recorded under electron impact (EI) ionisation at 70 eV. The ion source temperature of the mass spectrometer was 230 °C. The split ratio was 1:10 and the m/z spectrum was fixed between 40 and 550. The identification of the compounds was carried out using NIST 11 Mass Spectral Library and the similarity index (SI) was as high as 90% for most compounds.

The paint samples were scratched from the plastic sheets with a scalpel after artificial ageing. Approximately 10-20 µg (Sartorius SE2 Micro

Balance, Sartorius Stedim Biotech, Germany) of each paint were used for measurement. Blanks were run after every 5 samples.

5.2.4 FTIR-ATR analysis

FTIR-ATR was employed for the analysis of the samples obtained from the selected artworks and for the characterisation of both organic and inorganic paint components, including the binder, pigments and inorganic fillers and extenders present in the artificially aged reference paint films of Hyplar® and Liquitex® brands.

No sample preparation was required for ATR measurements. For the FTIR-ATR investigations FT/IR-4100 instrument with an ATR-PRO ONE unit (JASCO International Co., Ltd., Japan) equipped with a triglicine sulphate (TGS) detector and a diamond crystal was used. Spectra were acquired with 128 scans in the spectral range of 4000-400 cm^{-1} at 2.0 cm^{-1} resolution. Measurements were performed on one spot directly at the surface of the paint films and artwork samples. A background of air was recorded before every measurement and all spectra were corrected against the background spectrum by using Spectra Manager Software v.2 prior to chemometric analysis.

5.2.5 Chemometrics

For statistical analysis, SIMCA 14.1 Umetrics® (Umeå, Sweden) was used. Orthogonal partial least squares (OPLS) was applied to construct mathematical models for the two paint brands, Liquitex® and Hyplar®, that relate the spectroscopic data (**X** matrix) to the accelerated ageing time (**Y** vector). The models were used to predict the age of acrylic paints in artworks. OPLS is an extension of PLS that splits the systematic variation in the **X** block into two parts, one that models the correlation between **X**

and **Y** (predictive) and another that shows the systematic **X** variation not related (orthogonal) to **Y**. Orthogonalisation can reduce the complexity of the model, as it eliminates the systematic variation in the **X** matrix that is not correlated with the property to predict [41].

The **X** matrix was formed by spectroscopic data of the artificially aged reference paint samples for each brand. In the first step, the full sample set (48 samples per brand) was used for the development of each model (Table 1). Pre-processing methodologies, such as Savitzky-Golay, multiplicative scatter correction (MSC), standard normal variate (SNV), row center, exponentially weighted moving average (EWMA) and first and second derivatives, were tested to find models with better performance. The **X** variables were scaled to unit variance and the **Y** variable was transformed to logarithmic function.

Table 1. Accelerated ageing times applied to paint samples of Liquitex® and Hyplar® brands.

Sample number	Accelerated ageing time (h)	Sample number	Accelerated ageing time (h)
1	1426	**25**	427
2	1379	**26**	403
3	1331	**27**	379
4	1263	**28**	355
5	1216	**29**	331
6	1168	**30**	255
7	1097	**31**	236
8	1048	**32**	211
9	1000	**33**	184
10	929	**34**	165
11	905	**35**	140
12	881	**36**	116
13	859	**37**	93
14	833	**38**	88
15	762	**39**	84
16	738	**40**	71
17	714	**41**	65
18	682	**42**	60
19	666	**43**	46
20	594	**44**	42
21	571	**45**	37
22	546	**46**	22
23	519	**47**	18
24	499	**48**	12

In the second step, two prediction models were developed for each brand, based on the distribution of the paints as they age: one consisting of paint samples with a short-term ageing and another one of samples with a long-term ageing. The short-term ageing model for the Liquitex® brand consisted of 31 samples (sample no. 18 to 48), while the long-term ageing model was made up of 17 samples (no. 1 to 17). In the case of Hyplar®, the short-term ageing model consisted of 28 samples (no. 21 to 48) and the long-term one of 20 samples (no. 1 to 20). The **X** matrix was split into two sets, calibration samples (training set) and validation samples (test set), using Kennard-Stone algorithm [42]. The training set was used for building the OPLS model. The number of latent variables (LVs) was optimised by internal validation with cross-validation method. The main statistical parameters used for evaluating this step were the root mean square error of cross-validation (RMSECV) and the coefficient of determination of cross-validation (R^2 CV). RMSECV is calculated using Eq. 1:

$$\text{RMSECV} = \sqrt{\frac{\sum_{i=1}^{n}(y_i - \hat{y}_i)^2}{n}} \qquad \text{(Eq. 1)}$$

Where y_i is the measured value (accelerated ageing time), $\hat{y}_i$ is the value predicted by the model, and n is the total number of samples used in the training set. The external validation of the model was carried out using the spectra of the validation samples as a set, and then the predictive ability was evaluated by the RMSE of prediction (RMSEP) and the R^2 of prediction (R^2 P). The RMSEP was calculated using Eq. 2:

$$\text{RMSEP} = \sqrt{\frac{\sum_{i=1}^{n_t}\left(y_{t,i} - \hat{y}_{t,i}\right)^2}{n_t}} \qquad \text{(Eq. 2)}$$

Where $y_{t,i}$ is the measured value (accelerated ageing time), $\hat{y}_{t,i}$ is the age predicted by the model, and n_t is the number of samples in the test set. RMSEP expresses the average error to be expected in future predictions when the calibration model is applied to unknown samples [39, 41].

Taking into account the above statistical parameters, the optimal model would have high R^2 and Q^2 values as well as low RMSECV and RMSEP values and a small difference between the last two statistical parameters. A large difference between RMSECV and RMSEP indicates the possibility that too many LVs are used in the model (over-fitting) and noise is modelled. The number of LVs is intended to be as low as possible, as larger number of LVs may include some irrelevant information. The R^2 parameter varies from 0 to 1, indicating the degree of adjustment to perfect fitting, and the Q^2 parameter shows the robustness and predictive capacity of the model, being good when $Q^2 > 0.5$ and excellent when $Q^2 > 0.9$ [39, 41]. The Hotelling's T2 and distance-to-model tests with a 95% confidence level were applied to check for outliers.

5.2.6 Artwork description and sampling

The method developed needed to be tested on real artworks. The complexity of contemporary works respond, among other reasons, to the vast variety of materials and brands employed by contemporary painters. Moreover, it is not always easy to know which are the exact products used in a given artwork, since in many cases this is not relevant for the artist itself. We can find both, artists who thoroughly and carefully select the materials they use and artists whose experimental degree is higher in terms of materiality. Thereby, we were granted access to the complete collection of two well-known Basque painters who represent both cases and who kindly provided the samples needed: Jesús Mari Lazkano and Luis Candaudap. The former, characterised by its meticulous, detailed and

impeccable figurative technique, who carefully selects and documents the paints he uses [43]. On the other hand, Luis Candaudap is more experimental in his artistic practice, but also keeps record of the paint brands he has used throughout his artistic career.

Sampling was carried out over selected works painted by Jesús Mari Lazkano and Luis Candaudap in different years (Appendix A Figure A.1 and A.2). The selection was made based on the colour and paint brands used. The selected samples were analysed by FTIR-ATR and applied to the dating study. A total of 9 samples were taken from four different artworks. The first artwork was “Paisaje de Busturia” by Jesús Mari Lazkano, dating from 1996. The paint sample (code LPBV) was taken by manually scratching the surface of the green paint of the back of the artwork with a scalpel. The second painting was “Marina” by J. M. Lazkano, from 2015. 3 paint samples were obtained by scraping the green paint layer of the back (code LMV1), the stretcher (code LMV2) and the border (code LMV3) of the artwork. The third artwork was “Robin” by Luis Candaudap, which dates from 1997. The paint sample (code LCRV) was removed by scratching the layer of the green paint of the front of the artwork. The last artwork was “Pequeña Dignidad” by L. Candaudap, dating from 1998. Paint samples were taken by cutting with scissors the green (codes LCPDV1, LCPDV2 and LCPDV3) and purple (code LCPVM) painted canvas of the back of the artwork.

5.3 Results and discussion

5.3.1 Characterisation by Py-GC/MS

Under the applied pyrolysis conditions, the acrylic resins undergo depolymerisation reactions that cause the breakage of the polymer chain in its constituent monomers. In Table 2, the main pyrolysis products attributed to the binder of a recent paint sample of the Liquitex® brand are shown. The most intense peaks observed in the pyrogram (Figure 1A) were due to the polymer monomers. Methyl methacrylate (MMA) at RT 3.79 min (m/z 39, **41**, 69 and 100) and n-butyl acrylate (nBA) at RT 6.15 min (m/z **55**, 56 and 73) monomers were detected, with the corresponding sesquimer, dimer and trimer fractions at higher RTs: nBA-MMA sesquimer, nBA-MMA dimer, nBA sesquimer, nBA-nBA dimer, two isomers of nBA-nBA-MMA trimer, nBA-MMA-nBA trimer and nBA-nBA-nBA trimer, what would be in accordance with data reported by other authors [44]. The masses at m/z 56 and 73 observed in the nBA mass spectrum indicate the formation of butene and protonated acrylic acid, respectively [26]. The pyrograms of Talens®, Titan®, Vallejo® and Golden® brands were dominated by the same polymer monomers as Liquitex® (Table 2 and Appendix A Figure A.3).

Table 2. Pyrolysis products attributed to the binder, pigment and additives of a recent paint marked with an x and of a paint aged at an accelerated rate of 330 h marked with an * of the six brands studied with their corresponding compound name, retention time (RT (min)) and mass to charge ratio (m/z).

Compound	RT (min)	Paint brand						m/z
		Golden®	Talens®	Liquitex®	Hyplar®	Vallejo®	Titan®	
Binder								
Trans butene	1.41	x*	x*	x*	x	x*	x*	55, **56**
Methyl acrylate	3.01	x*	x*	x*	x	x*	x*	27, **55**, 85
Ethyl acrylate	3.63	x*		*	x*	x*	x*	27, 56, **55**
Methyl methacrylate	3.79	x*	x*	x*	x*	x*	x*	39, **41**, 69, 100
Ethyl methacrylate	4.33	x*	x*	*	x*	x*	x*	39, 41, **69**
N-butyl acetate	4.70	x*	x*	x*				41, **43**, 56, 73
N-butanol	5.71	x*	x*	x*		x*	x*	27, 31, 41, 43, **56**
N-butyl acrylate	6.15	x*	x*	x*	x*	x*	x*	**55**, 56, 73
N-butyl methacrylate	6.85	x*	x*	x*		x*	x*	39, 41, 56, **69**, 87
Styrene	7.23	x*	x*	x*	x*	x*	x*	51, 78, 103, **104**
Sec butyl cyclobutanecarboxylate	7.89	x*	x*	*		x*	x*	**55**, 83, 101
Acrylic acid	12.13	x*	x*	x*	x*	x*	x*	26, 27, 45, 55, **72**
Methacrylic acid	12.53	x*	x*	x*	x*	x*	x*	39, **41**, 86
EA-MMA sesquimer	12.78				x*			**128**, 143, 157
EA-MMA dimer	12.99				x*			**140**
EA sesquimer	13.29				x*			**143**
EA-EA dimer	13.80				x*			**98**
nBA-MMA sesquimer	14.54	x*	x*	x*		x*	x*	55, 83, 85, 101, 115, 129,**143**, 156
nBA-MMA dimer	14.67	x*	x*	x*		x*	x*	67, 95, **112**, 126, 141
nBA sesquimer	16.62	x*	x*	x*		x*	x*	57, 87, **115**, 142, 171, 189
nBA-nBA dimer	16.99	x*	x*	x*		x*	x*	57, 98, 120, **127**, 183, 140, 141
EA-EA-MMA trimer	18.69				x*			31, 45, **222**, 255, 269
EA-EA-MMA trimer	19.01				x*			31, 45, **166**, 255, 269
EA-EA-EA trimer	19.58				x*			**134**
nBA-nBA-MMA trimer	21.07	x*	x*	x*		x*	x*	57, 93, 139, 148, **195**, 250, 283, 325
nBA-nBA-MMA trimer	21.46	x*	x*	x*		x*	x*	57, 93, 120, 139, 148, 167, **195**, 250, 283, 325
nBA-MMA-nBA trimer	23.24	x*	x*	x*		x*	x*	57, 93, 149, 167, 195, **228**, 255, 283, 325
nBA-nBA-nBA trimer	24.45	x*	x*	x*		x*	x*	57, 134, 152, **181**, 236, 255, 282, 311

Pigment									
1-clorobutane	2.20	x*	x*	x*		x*	x*	x*	41, 43, **56**
Toluene	4.24	x*	x*	x*	x*	x*	x*	x*	**91**, 92
Ethyl benzene	5.45	x*	x*	x*	*	x*	x*	x*	**91**, 106
xylene	5.63	x*	x*	x*		x	*		**91**, 105, 106
Chlorobenzene	6.66		*	x*	x*	x*			77, **112**
Benzenedicarbonitrile	19.16		x*		*	*	*		50, 59, 75, 101, **128**, 129
Additive									
1H-imidazole-4-carboxilic acid	9.45	x*	x*	x*		*	x*		67, 94, 95, **112**
2,3,5-trimethyl phenol	15.39	x*	x*	x*	x*	x*	x*		67, 91, 97, **121**, 136
4,5,7-trimethyl coumarine	20.26	x*	x*	x*	x*	x*	x*		65, 115, 145, **188**
Surfactant									
p-tert-octylphenol	20.34	x*	x*	x*	x*	x*	x*		57, 77, 91, **135**, 107, 206

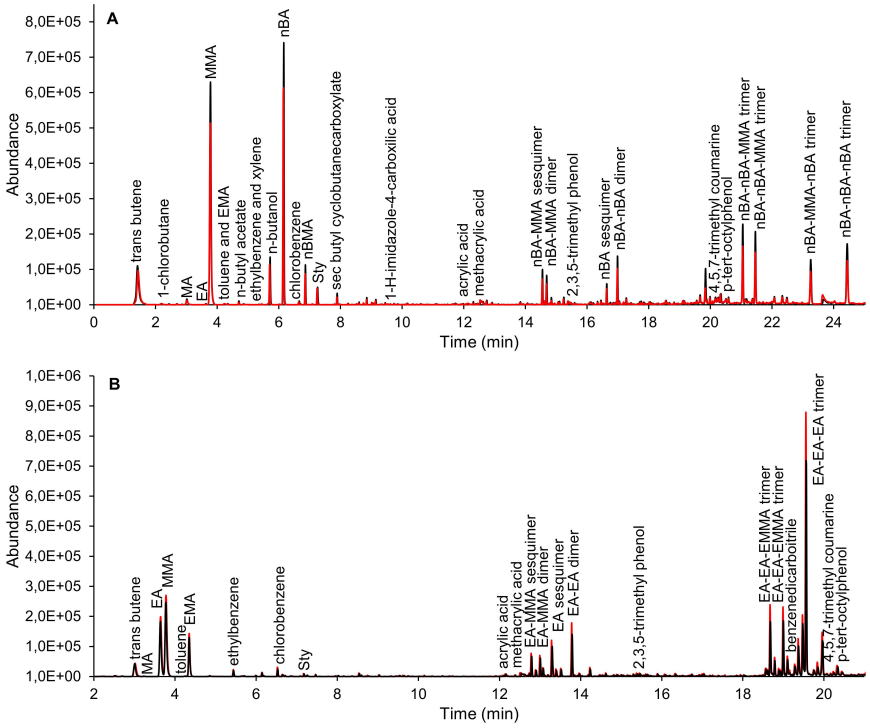

Figure 1. Pyrograms corresponding to a recent paint (red line) and to a paint with 330 h of accelerated ageing (black line) of Liquitex® (A) and Hyplar® (B) brands. The abundances of the chromatographic peaks were normalised with the sample mass.

In the Hyplar® brand, however, besides the characteristic peaks of MMA, ethyl acrylate (EA) monomer at RT 3.63 min (m/z 27, **55** and 56) was identified as a main peak (Figure 1B), while in the other brands only trace amounts of EA were added. The mass spectra of EA is characterised by a peak of m/z 55 that corresponds to the loss of an ethoxy (OC_2H_5) group to create a CH_2CHCO^+ fragment ion [26]. Ethyl methacrylate (EMA) at RT 4.33 min (m/z 39, 41 and **69**) was observed as a pyrolysis product of EA [26]. In addition to the peaks of the polymer monomers, the pyrogram of the acrylic binder is also characterised by the formation of sesquimers, dimmers and trimers at higher RTs: EA-MMA sesquimer, EA-MMA dimer, EA sesquimer, EA-EA dimer, two isomers of EA-EA-MMA trimer and EA-EA-EA trimer [44,

[45]. Polyacrylates contain tertiary hydrogen atoms along their polymer chain, which are prone to abstraction. If the polymer chain is not in a linear arrangement tertiary hydrogen atoms can be abstracted and the formation of free radicals not in the terminal carbon would initiate the formation of oligomers [26]. That is, sesquimers, dimers and trimers are recombinations or fragments of the polymer backbone composed of its monomers in different proportions [46]. The peak observed at RT 7.23 min was attributed to styrene (Sty) (m/z 51, 78, 103 and **104**). The area of this peak was significantly less intense than that of the MMA, nBA and EA monomers, indicating that a small quantity of styrene was added to paint formulations. This may explain why no styrene oligomers were detected. The presence of styrene is not linked to the pigment nor to any other additive present in the paints [19]. Thus, styrene comes from the binder. Styrene is used in paint formulations to decrease the cost of the acrylic resin and improve paint performance by enhancing its hardness and resistance to weathering, water and alkali [19, 29]. Therefore, an acrylic styrene-n-butyl acrylate-methyl methacrylate (sty-nBA-MMA) copolymer was used as binder for Liquitex®, Talens®, Titan®, Vallejo® and Golden® paints, whereas Hyplar® paint was characterised as an emulsion of poly(styrene-ethyl acrylate-methyl methacrylate) (p(sty-EA-EMA)). Acrylic paint formulations have been modified over the past few years, as styrene had not been previously detected with nBA-MMA copolymer in either Liquitex® nor Talens® paints [19, 45]. Other pyrolysis products related to nBA-MMA copolymer were methyl acrylate (MA), n-butanol, n-butyl acetate, n-butyl methacrylate (nBMA), trans butene and sec butyl cyclobutanecarboxylate [19, 29]. The peaks with m/z 86 and 72 were attributed to methacrylic acid and acrylic acid, respectively, detected in all paint brands (Table 2). These acids are used in the polymerisation process to increase the mechanical stability of the wet latex and reduce the surfactant content [19].

In the pyrograms peaks attributed to the pyrolysis products of the additives incorporated in the paints were detected, such as 1H-imidazole-4-carboxilic acid, 2,3,5-trimethyl phenol and 4,5,7-trimethyl coumarine (Table 2). These pyrolysis fragments come from additives used as biocides and antifouling agents, antioxidants and optical brighteners, respectively [19]. P-tert-octylphenol associated with the pyrolysis of the non-ionic alkylaryl poly(ethoxylated) type surfactant (octylphenyl-poly(ethylene oxide) (octylphenyl-PEO)) was identified in all paint brands. In the mass spectrum the molecular ion (m/z 206) and the base peak $[C_9H_{11}O]^+$ (m/z 135) resulting from the benzylic bond cleavage of that ion were detected [46].

Toluene, xylene, 1-chlorobutane, ethyl benzene, benzenedicarbonitrile and chlorobenzene characteristic of PG7 green pigment were also detected (Table 2) [19, 47]. Some of the pigment fragments could not be detected in all the paint brands, either because of the low concentration added in the commercial paint formulations [8] or because it could not be identified at the applied pyrolysis temperature, needing temperatures above 700 ºC [31, 47].

After the initial characterisation, the influence of the accelerated ageing over the six paint brands was studied by analysing samples taken at the end of the complete ageing cycle. An increase in monomers and oligomers caused by side- and main-chain scission reactions of the acrylic binder as photooxidation products was detected in Liquitex® and Titan® brands (Figure 1A and Appendix A Figure A.3E). This indicates a decrease in the thermal stability of the binder after exposure to accelerated ageing [8]. Hyplar®, Golden®, Talens® and Vallejo® brands (Figure 1B and Appendix A Figure A.3C, D and F) showed a decrease in the abundance of peaks attributed to the binder. No changes were detected for the surfactant under the applied accelerated ageing conditions in any of the brands studied. A larger number of peaks related to the pigment were detected in all paint

brands (Table 2), indicating a decrease in its thermal stability after exposure to the ageing conditions used. The observed decrease in thermal stability of this type of paintings as they age might imply extra care in their conservation as well as in any restoration intervention.

5.3.2 Characterisation by FTIR-ATR

Liquitex® and Hyplar® paintings were further characterised by FTIR-ATR, as they were representative of the two types of binders studied. In Figure 2A the FTIR-ATR spectrum of a non-aged Liquitex® paint is shown. The characteristic IR absorption of acrylic resins is ascribed to the strong band at 1725 cm^{-1} corresponding to the carbonyl (-C=O) stretching vibration [11]. The absorption band at 2952 cm^{-1} is attributed to C-H bond stretching vibrations. Another band of acrylic copolymers was that of C-H bending at 1448 cm^{-1}. Bands at 2878 and 1095 cm^{-1} are characteristic of PEO-type surfactant [19]. No characteristic bands of styrene, such as the absorptions in the range between 3100 and 2800 cm^{-1} attributed to =C-H aromatic stretching, the absorptions ascribed to C=C aromatic stretching between 1650 and 1450 cm^{-1} or the absorptions between 761 and 702 cm^{-1} attributed to C-H rocking of the aromatic ring [19], were detected in the FTIR-ATR spectra. Bands of the phthalocyanine green pigment were present at 1391, 1306, 1211 and 1160 cm^{-1} corresponding to C-H in-plane vibrations [8, 19].

The FTIR-ATR spectrum of a non-aged paint of Hyplar® brand is shown in Figure 2B. Two peaks characteristic of acrylic resins were identified: a strong and sharp absorption at 1725 cm^{-1} that corresponds to the carbonyl (-C=O) stretching vibration, followed with a strong absorption at 1150 cm^{-1}, which is related to the stretching vibration of the ester groups (-C-C(=O)-O-) [11]. The absorption band at 2954 cm^{-1} is attributed to C-H bond stretching vibrations of EA-MMA resins. Other bands of the acrylic

copolymer were those of C-H bending at 1448 and 1383 cm^{-1} and C-O and C-C stretching at 1237 and 1022 cm^{-1}. The spectrum indicates that there is a high abundance of a PEO-type surfactant on the paint surface by the bands at 1112 cm^{-1} and the C-H stretching region at 2895 cm^{-1}. The band at 1344 cm^{-1} is also ascribed to PEO type additive [11]. Neither extenders nor characteristic bands of styrene were detected in the FTIR-ATR spectra due to the low quantity in the binder. Bands of the phthalocyanine green pigment were present at 1305 and 1211 cm^{-1}, corresponding to C-H in-plane vibrations [8, 19].

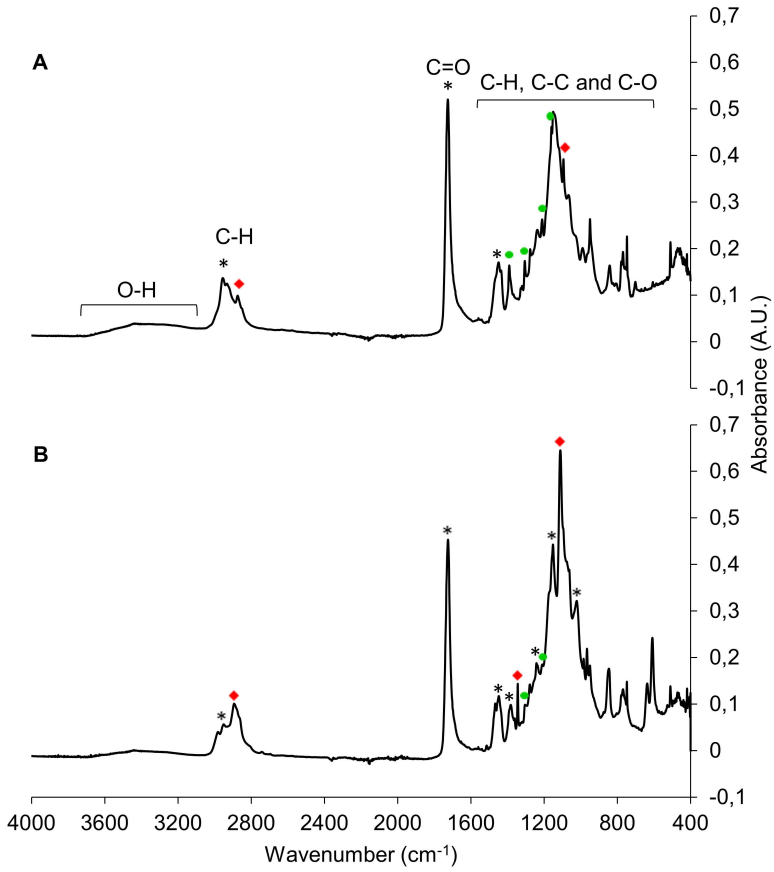

Figure 2. FTIR-ATR spectra of a non-aged paint sample of Liquitex® (A) and Hyplar® (B) brands. The characteristic IR bands assigned to the acrylic copolymer (*), PG7 pigment (green •) and PEO surfactant (red ♦) are marked.

The FTIR-ATR spectra of the aged acrylic paints were examined. The changes detected in Liquitex® brand after exposure to accelerated ageing are shown in Figure 3. The carbonyl absorption at 1725 cm^{-1} attributed to nBA-MMA copolymer decreased and broadened with 1097 h of ageing due to side-chain scission reactions that led to the loss and volatilisation of the side butyl groups of the polymer and the formation of gamma-lactones [8, 10, 11, 48]. The C-H(CH_2) stretching band at 2952 cm^{-1} decreased due to main-chain scission reactions [8]. Thus, the modifications in the spectra indicate photooxidation instability of the binder under the applied artificial ageing conditions. Besides, the increased presence of PEO type surfactant was observed on the surface of the paint within 571 h of accelerated ageing, as shown in the increase of the peak at 1095 cm^{-1} [9]. The absorptions at 2878 and 1095 cm^{-1} attributed to PEO showed alterations after 1097 h of ageing, with a tendency to decrease in intensity that may be associated with the degradation of the hydrocarbon fraction and with the oxidation of the PEO molecules that cause the excision of poly(oxyethylene) chains, respectively [11]. In addition, a decrease in the absorptions attributed to the phtalocyanine green pigment was observed, which indicates that the pigment is affected by light. The paint, however, showed an increase in the absorption bands assigned to the binder, PEO surfactant and PG7 pigment under the maximum conditions of accelerated ageing applied. This can be explained by the rearrangement of the broken bonds that may result in the recovery of the materials or in the creation of new ones.

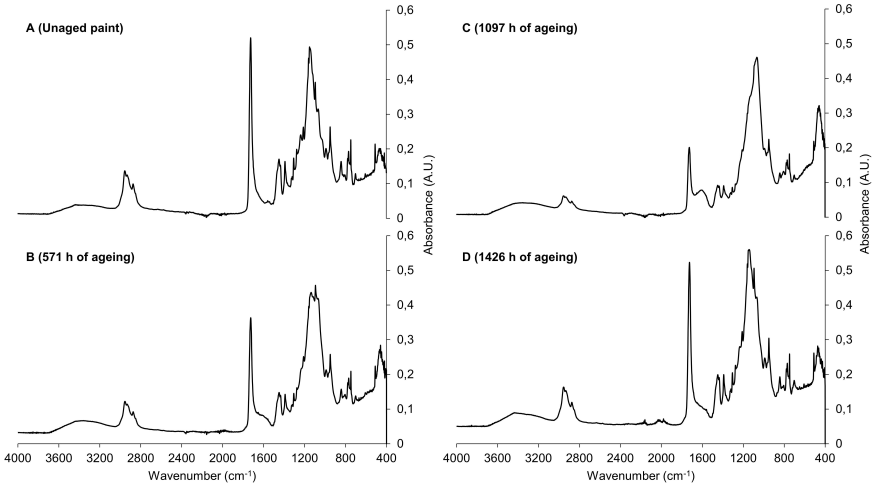

Figure 3. FTIR-ATR spectrum of a non-aged paint sample of Liquitex® brand (A) as well as samples with an accelerated ageing of 571 (B), 1097 (C) and 1426 (D) h.

Hyplar® FTIR-ATR spectra obtained after the accelerated ageing trials are shown in Figure 4. After an increase in the absorption band attributed to the –C=O stretching of the EA-MMA binder at 1725 cm^{-1} in the first 12 h, the band showed a moderate decrease as well as a broadening during the rest of the ageing. As in the previous case, the reason could be chain-breaking reactions that cause the loss and volatilisation of low molecular weight compounds and the formation of gamma-lactones [9, 48]. The fact that the carbonyl peak showed a slight decrease (almost remains constant) may also be explained by the fact that the loss of part of the carbonyl ester group is compensated by the formation of new oxidation products that absorb in the same region [48]. A limited increase in absorption ascribed to the C-O stretching vibration of the ester group at 1237 cm^{-1} was also detected, while the -CH region at 3000-2800 cm^{-1} was unaffected. Therefore, the bands attributed to the binder remain almost unaltered, indicating that p(EA-MMA) could have greater stability to light compared to p(nBA-MMA) [29]. The bands at 2895 and 1344 cm^{-1} attributed to the PEO surfactant could not be detected, while a decrease of the band at 1112 cm^{-}

[1] was observed after the first hours of accelerated ageing. This can be explained either by the thermal ageing that causes surface surfactant to melt and migrate back into the bulk film or by the accelerated light ageing that causes an enhanced photodegradation of the surface surfactant [49]. This last case may explain the increase in the absorption band of the EA-MMA copolymer at 1725 cm^{-1}, as the excision of the surfactant's poly(oxyethylene) chains during oxidation may result in the formation of short chains that may be compatible with the polymer, so they can diffuse back into the polymer [50]. The band at 1112 cm^{-1} attributed to PEO increased moderately with more hours of accelerated ageing due to the increased coalescence of the film that enhances the mobility of the surfactant within the film and brings it back to the paint surface [49]. The absorptions attributed to PG7 pigment showed a slight decrease under the accelerated ageing conditions applied.

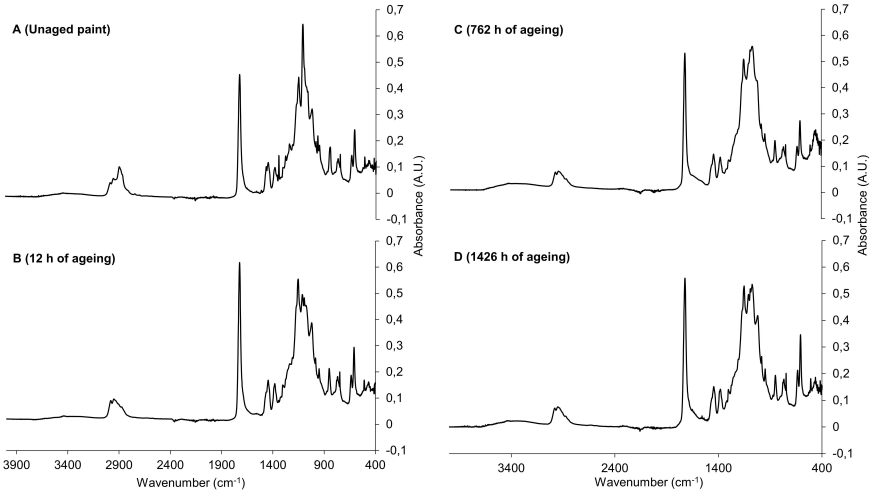

Figure 4. FTIR-ATR spectrum of a non-aged paint sample of Hyplar® brand (A) as well as samples with an accelerated ageing of 12 (B), 762 (C) and 1426 (D) h.

5.3.3 OPLS model development

Reference Liquitex® and Hyplar® paint films applied over plastic and artificially aged for 1426 h were isochronously sampled for the development of OPLS models. A full sample set consisting of 48 samples of Liquitex® brand paint films was first used for model development. The unwanted contributions to FTIR-ATR spectra can be overcome by applying different types of spectral pretreatments, such as Savitzky-Golay, MSC, SNV, row center, EWMA and first and second derivatives. Using the values of RMSECV and R^2 and the number of LVs to optimise and justify the type of spectral pretreatment to be applied, different OPLS models were built (Table 3). Tests were carried out using the full range and specific regions of the IR spectrum to try to reduce the influence of spectral noise. The application of the first derivative function with 15 points for the wavenumber range 4000-400 cm^{-1} showed the best statistical parameters. This is observed in the high correlation obtained with a minimum number of LVs and in the low values of RMSEE and RMSECV, indicating this model has a good fit to the data set.

The scores graph (Figure 5A) showed a displacement of the paint samples over the accelerated ageing time, resulting in two groups: one consisting of paint samples with a short-term ageing that moves to the right in the predictive component and another one of samples with a long-term ageing that moves down in the orthogonal component. Thus, the next step was to develop an OPLS model for each group.

Table 3. Data obtained from OPLS models of Liquitex® and Hyplar® using UV scaling and different spectral filters based on the full spectrum range and on specific regions.

Spectral range (cm^{-1})	Spectral filter	Liquitex® brand						Hyplar® brand					
		LV	R^2 Y	Q^2	RMSEE	RMSECV	R^2 CV	LV	R^2 Y	Q^2	RMSEE	RMSECV	R^2 CV
4000-400	No spectral filter	1+6	0.96	0.92	0.13	0.16	0.96	1+2	0.87	0.82	0.21	0.24	0.87
	1st derivative transformation (15 points in filter and quadratic order polynomial fit)	1+3	0.99	0.84	0.07	0.22	0.99	1+1	0.94	0.87	0.14	0.21	0.94
	1st derivative transformation (5 points in filter and quadratic order polynomial fit)	1+3	0.99	0.78	0.04	0.26	0.99	1+2	0.98	0.63	0.08	0.34	0.98
	2nd derivative transformation (15 points in filter and quadratic order polynomial fit)	1+3	0.99	0.73	0.05	0.30	0.99	1+3	0.99	0.39	0.04	0.45	0.99
	MSC	1+5	0.97	0.91	0.11	0.17	0.97	1+3	0.95	0.90	0.13	0.18	0.95
	SNV	1+5	0.96	0.91	0.12	0.17	0.96	1+3	0.95	0.90	0.13	0.18	0.95
	Row Center	1+6	0.94	0.88	0.15	0.20	0.94	1+3	0.95	0.91	0.14	0.17	0.94
	Savitzky-Golay	1+6	0.96	0.92	0.13	0.16	0.96	1+2	0.87	0.82	0.21	0.24	0.87
	EWMA	1+6	0.96	0.92	0.13	0.16	0.96	1+2	0.87	0.82	0.21	0.24	0.87
4000-600	1st derivative transformation (15 points in filter and quadratic order polynomial fit)	1+3	0.99	0.85	0.07	0.21	0.98	1+1	0.94	0.87	0.14	0.21	0.94
	2nd derivative transformation (15 points in filter and quadratic order polynomial fit)	1+3	0.99	0.74	0.05	0.29	0.99	1+2	0.98	0.64	0.08	0.34	0.98

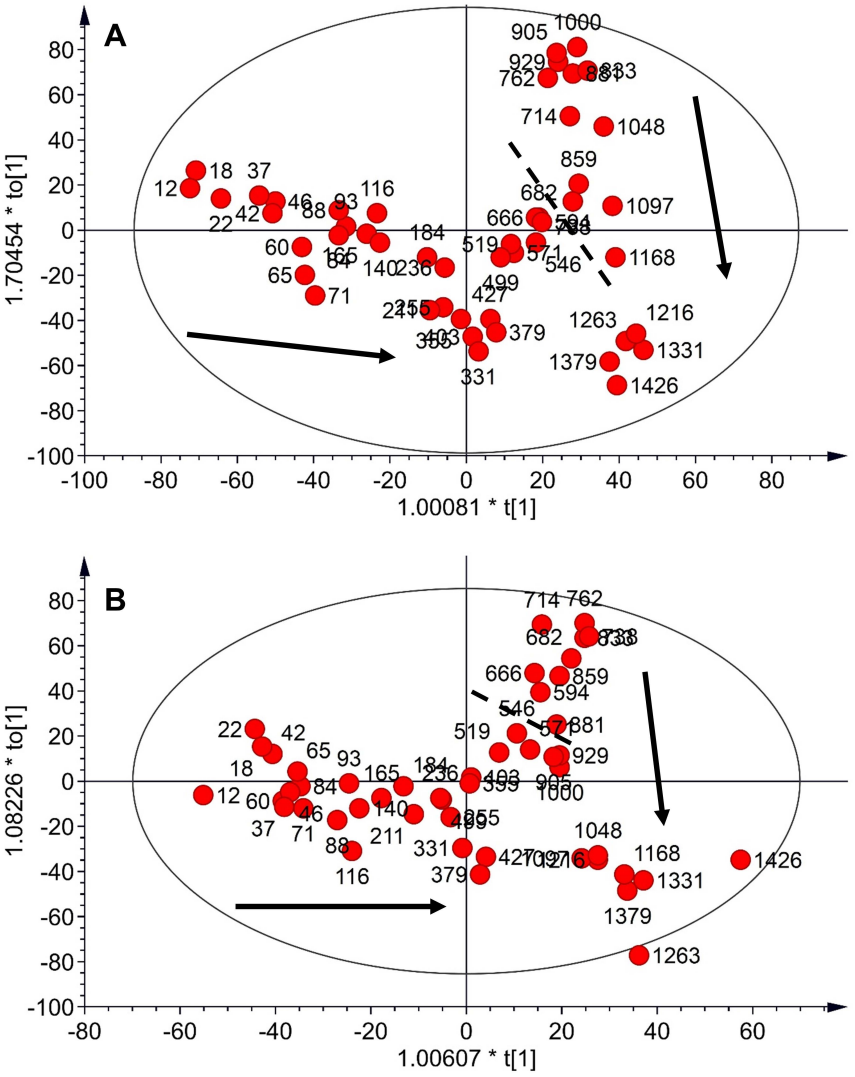

Figure 5. Score graph of the first predictive (t1) and orthogonal (to1) component, with Hotelling's T2 control ellipse (95% of confidence), for Liquitex® (A) and Hyplar® (B) brands. Each sample (red points) is represented with its accelerated ageing time in hours.

The model of short-term ageing consisted of 31 samples that were split into 21 for the calibration set and 10 for the validation set by using the Kennard-Stone algorithm. The model was selected with 4 LVs. No outliers

were found in the distance-to-model graph or Hotelling's T2 control graph with 95% confidence level. Besides, values of 0.28 for RMSECV and 0.99 for R^2 CV were achieved. The small value of RMSECV is indicative of the model's good predictive accuracy. The model was then applied to the validation set to check its prediction ability and its performance. A value of 0.19 for RMSEP was achieved using the external validation test set, exhibiting an acceptable predictive capacity with R^2 P values higher than 0.85. Likewise, an accuracy error of 32% was obtained in the predictions.

The long-term ageing model was made up of 17 samples split into 12 for the calibration set and 5 for the validation set using the Kennard-Stone algorithm. The model was set with 5 LVs. No outliers were found in either the distance-to-model graph or Hotelling's T2 control graph with a 95% confidence level. In addition, values of 0.05 for RMSECV and 1 for R^2 CV were obtained that indicate the model's high predictive accuracy. The model was then applied to the validation set, exhibiting excellent predictability and performance with values of 0.04 for RMSEP and 0.89 for R^2 P. High prediction accuracy with 8% error was obtained.

The wavenumbers of the absorption bands attributed to the Liquitex® paint components that define the prediction models were studied using the loadings graph. The aim was to highlight the most relevant physico-chemical processes under ageing. The younger paints of both models were characterised by modifications in the range between 2875-2805 cm^{-1} attributed to the PEO surfactant. The paints showed a decrease in the intensity of this band that may be associated with the degradation of the hydrocarbon fraction of the PEO. The paints were also characterised throughout the applied ageing trials by modifications in the range 1795-1765 cm^{-1} and 1680-1555 cm^{-1} attributed to the carbonyl group of the nBA-MMA acrylic resin. As the paint ages in the model of short-term ageing, the band widens due to formation of oxidised species, such as carboxyl acids,

ketones and aldehydes, and also decreases due to chain-breaking reactions that cause the loss and volatilisation of low molecular weight compounds [9]. Particularly the progressive absorptions at 1773, 1600 and 1710 cm^{-1} could indicate the formation of a γ-lactone structure [10, 11]. In contrast, the long-term model paints undergo an increase and a sharpening of the band as they age. That may indicate that oxidised species disappear and that a rearrangement of the broken bonds takes place that can lead to the recovery of the materials or the creation of new ones. Recent studies showed that nBA-MMA formulation exhibits prevailing cross-linking reactions in the long-term [7, 11]. Thus, the models were established by the changes undergone by the binder and surfactant as they age. These results are consistent with those observed visually in the characterisation of the spectra of Liquitex® paints.

The same procedure was followed to develop the different models for the Hyplar® brand. The full set of Hyplar® samples was first used to choose the best pretreatments for model development. The 1st derivative function with 15 points for the full range of FTIR-ATR spectra was used for model optimisation. The model was set with 2 LVs, explaining 94% for R^2Y and predicting 87% for Q^2 of the data variation that indicates that the model has a high fitting and prediction capacity (Table 3). Besides, low values of RMSEE and RMSECV were obtained, indicating the good predictive accuracy of the model.

As with the Liquitex® brand, the score graph (Figure 5B) showed two different displacements of the paint samples over the accelerated ageing time: short-term aged paints moved to the right in the predictive component, while long-term aged paints moved down in the orthogonal component. Thus, a model was developed for each group.

The model of short-term ageing consisted of 28 samples split into 18 samples for training set that was used to construct the model and 10 samples for validation set that was used to validate it. The model was established with 3 LVs. No outliers were found in either the distance-to-model graph or Hotelling's T2 control graph with a 95% confidence level. Besides, the model exhibited good predictive accuracy with values of 0.27 for RMSECV and 0.99 for R^2 CV. Values of 0.26 for RMSEP and 0.73 for R^2 P were obtained in the external validation, indicating an acceptable predictive capacity. An accuracy error of 31% was obtained in the predictions.

The long-term ageing model consisting of 20 samples was divided into 12 for the calibration set and 8 for the validation set using the Kennard-Stone algorithm. The model was set with 4 LVs and no outliers were found in either the distance-to-model graph or Hotelling's T2 control graph with a 95% confidence level. Values of 0.05 for RMSECV and 1 for R^2 CV were obtained, indicating the high predictive accuracy of the model. The external validation showed an excellent prediction ability and performance of the model with values of 0.05 for RMSEP and 0.95 for R^2 P. High predictive accuracy with 10% error was obtained. Thus, higher prediction accuracies were achieved for both brands within the long-term ageing models.

The wavenumbers of the absorption bands attributed to the Hyplar® paint compounds that define the prediction models were studied using the loadings graph. As in Liquitex® models, the ageing of the paint films were also characterised by modifications in the ranges 1790-1750 cm^{-1} and 1715-1590 cm^{-1} attributed to EA-MMA acrylic resin. Unlike the previous study, in the first hours of accelerated ageing the absorption band increases. This may be explained by the excision of the surfactant's poly(oxyethylene) chains during oxidation, leading to the formation of short chains that can be compatible with the polymer, so they can diffuse back

into the polymer [50]. As the paint ages the band decreases moderately due to chain-breaking reactions as well as broadens due to formation of further oxidised species, as mentioned earlier. The paint films within short-term ageing model were characterised by modifications in the range between 1100-1050 cm^{-1} attributed to the PEO surfactant. Initially the band decreased in intensity, and then started to grow up. This loading effect was only found in Hyplar® prediction model paints. The initial decrease may be associated with the oxidation of the PEO molecules that cause the excision of poly(oxyethylene) chains. Moreover, some studies have confirmed that substantial amounts of surfactants can be present on EA-MMA paintings after natural and thermal ageing. Ageing initially seems to cause surface surfactant to melt and migrate back into the bulk film; however, the migration rate post-ageing appears to accelerate due to increased polymer coalescence induced by ageing regime and/or increased mobility resulting from thermal degradation of the surfactant within the bulk film [48, 49]. In addition, Hyplar® paint films within the long-term ageing model were also characterised by modifications in the range between 1335-1295 cm^{-1} attributed to phtalocyanine green pigment. Thus, the models were established by the changes suffered mainly by the surfactant and, to a lesser extent, by the binder and the pigment.

From the study of the loadings of the OPLS models, relevant information could be extracted. First, the models that fit to the ageing of the Liquitex® brand paints (nBA-MMA copolymer) were mainly influenced by the ageing processes of the binder, following by those of the surfactants to a much lesser extent. In the case of Hyplar® (EA-MMA copolymer), the most relevant influences were the degradation and migration of the surfactants and, secondly, the degradation processes of the binder and pigments. Moreover, although both brands' models were characterised by modifications of the same paint components, PEO type surfactants underwent different reactions in its chemical structure in each brand. Thus,

it was not possible to set a single OPLS prediction model for the two paint brands.

Furthermore, two different OPLS models needed to be established for each brand's short and long term ageing predictions, as shown in Figure 5A and B. In the case of Liquitex® paints, the short-term model was mainly influenced by the degradation of the binder, which induced modifications (decreasing and broadening) in the characteristic band of the carbonyl group (1725 cm^{-1}) of the nBA-MMA acrylic resin. While, in the long-term samples, the growth and narrowing (just the opposite) of the same band was the main influence in the OPLS model due to prevalence of the cross-linking reactions and the disappearance of the oxidised species. In the case of Hyplar® acrylic paints, the change in the influence of the prediction models was less obvious than for the Liquitex® samples. The influence in the short-term model was related, among others, to the disappearance of the surfactant on the paint film surface due to degradation/migration processes, being just the opposite in the case of the long-term model because of the migration of the surfactants back to the paint film surface.

Finally, as mentioned above, higher prediction accuracies were calculated within the long-term ageing models (8-10% accuracy error) than within the short-term ones (31-32%) for both paint brands. Once the different influences and loadings weights in each of the models have been studied, the improvement in estimation accuracy could be due to the decrease in the number of influential ageing processes in the long-term models. For example, while the short-term Liquitex® model was influenced by binder and surfactant modifications, in the case of the long-term model, the cross-linking process link to the binder ageing was only the most relevant influence. Something similar was observed with Hyplar®, where the migration of the surfactant back to the surface of the paint film became the most influential process in the long-term model.

5.3.4 Application of OPLS models to artwork dating

The predictive models developed for the Liquitex® brand were applied to paint samples obtained from different artworks, dated from 1996 to 2015, provided by the artists Jesús Mari Lazkano and Luis Candaudap. These samples were used to determine the correlation between artificial ageing and its equivalent to natural ageing. The model for short-term ageing was used to predict the equivalent accelerated age of the most recent artworks (LMV1, LMV2 and LMV3 codes), while the long-term ageing model was used for the samples coming from the oldest artworks (LCPDM, LCPDV1, LCPDV2, LCPDV3, LCRV and LPBV codes). The predicted age was represented against the real age of the artworks by obtaining a regression line. It must be mentioned that the prediction models were developed with paints that already had undergone one year of natural drying. Thus, the real age of the artworks was corrected by subtracting one natural year from the predicted age. In most cases, the exact paint brand used by a given artist is unknown, as they explore and experiment with different brands and colour mixtures. In this case, only the artist Jesús Mari Lazkano was able to confirm the use of Liquitex® brand in his artworks, while Luis Candaudap sensed that he could have used it. Moreover, the storage conditions of the artworks cannot be specified because of their multiple locations (studio, exhibition halls, etc.). Some of the samples obtained from artworks by Luis Candaudap, coded LCPDV1, LCPDV2 and LCPDV3, showed a large deviation not matching the regression line, maybe due to the experimental character of his artistic practice, which might have implied the use of different acrylic paint brands as well as pigments and additives. Although organic pigments have shown no influence on the Liquitex® model, the influence of inorganic pigments must be taken into account, as other studies have demonstrated their influence on the chemical behaviour and stability of acrylic paints [10]. The samples taken from the artworks by Jesús Mari Lazkano fitted all except for those with LMV1 and LMV3 codes,

corresponding to duplicate samples taken from 2 of the 4 artworks. Thus, a sample from each artwork (LCPDM, LCRV, LPBV and LMV2) was successfully applied to the regression line. The purple pigment sample (LCPDM code) fitted well into the regression line, indicating that pigment type and its modifications during ageing are not a determining factor in the model, as shown in the study of the loadings graph (OPLS model development section). The correlation was determined by the equation in Figure 6, in which approximately 50 h of accelerated ageing under the applied conditions are equivalent to one natural year. This regression could be used to date artworks up to 22 years at least, preserved under comparable conditions and created with the same Liquitex® paint formulation. Due to the difficulty to obtain real samples from artworks made exclusively with Liquitex®, each of the five samples used to construct the regression line, which was obtained from long- and short-term ageing models, was taken as a real sample. To this end, each sample was excluded one by one and the age of these samples was predicted from the regression equation obtained with the remaining four samples. As shown in Figure 6, an acceptable predicted date (red triangle) was calculated with accuracy error values between 1% and 4%.

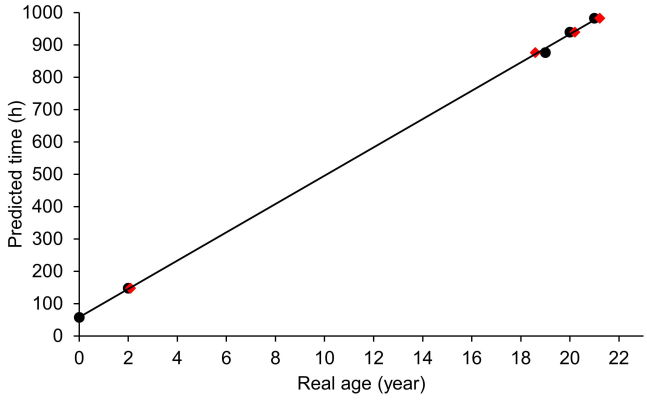

Figure 6. Graph of the real age (year) against the predicted ageing time (h) for Liquitex® brand. Equation Y = 43.75 X + 58.46, R^2 = 0.99. The red triangle represents the predicted date from the regression obtained with the dataset (n = 4) leaving out the test sample.

5.4 Conclusions

In this study, six commercial acrylic emulsion paints from different manufacturers were characterised by Py-GC/MS and two of them further studied by FTIR-ATR. Two different types of acrylic copolymer were identified as the binding medium: p(nBA/MMA) in Liquitex®, Talens®, Titan®, Golden® and Vallejo® brands and p(EA/MMA) in Hyplar® brand, with low amounts of styrene in both formulations. This indicates that the paint formulations have undergone modifications, as styrene had not been previously detected in brands, such as Liquitex® and Talens®. Therefore, the presence of styrene in a Liquitex® or Talens® acrylic binding medium could provide an evidence for artwork dating within the last years. In addition, all paint brands showed common constituents in their formulation, such as a non-ionic PEO type surfactant.

The results of the accelerated ageing trials showed alterations in the paint constituents as well as the formation of new photooxidation products. Py-GC/MS analysis revealed a decrease in the thermal stability of the pigment and acrylic binders after accelerated ageing, which could affect their conservation and the treatments that can be applied for their restoration.

Prediction models were developed for two of the studied brands, Liquitex® and Hyplar®, based on the distribution of the paints as they age. The models for Liquitex® and Hyplar® brands were mainly characterised by the modifications undergone by both the binder and the surfactant as they aged and moderately by the pigment in the Hyplar® acrylic paints. Although both brands' models are characterised by modifications of the same paint materials, PEO type surfactants undergo different reactions in its chemical structure in each brand. Moreover, the two brands showed different ageing trends that may be due to different binder composition and surfactant content in their formulation. While Liquitex® paints (nBA-MMA

copolymer) undergo surfactant modifications due to the excision of the hydrocarbon chains, Hyplar® paints (EA-MMA copolymer) exhibit the excision of the poly(oxyethylene) chain. Although this fact precludes the possibility of finding a universal model, the OPLS models developed for the Liquitex® acrylic paints could potentially be applied to other brands of acrylic paints with the same copolymer (nBA-MMA), such as Talens®, Titan®, Vallejo® or Golden®. This conclusion should be corroborated in the near future with further studies. In any case, this information can already be of great help for the development of appropriate conservation-restoration methodologies for these types of paints.

A correlation between natural and accelerated ageing could be established for the Liquitex® models, in which approximately 50 h of accelerated ageing under the applied conditions were equivalent to one natural year. This regression could be used to date artworks up to 22 years preserved under comparable conditions and created with the same paint formulation. Despite the lack of universality of the prediction models, they could be applicable to different Liquitex® paint colours, since pigment modifications during age seemed not to be a determining factor in the OPLS models. In addition, it must be taken into account that not all the samples taken from the same artwork fit into the models. This may be due to the use of paint mixtures that the artist employs in his working method. In conclusion, this methodology could be a first step to dating contemporary artworks by the application of multivariate chemometrics to spectroscopic data.

Acknowledgments

The authors would like to thank the artists Jesús Mari Lazkano and Luis Candaudap for providing the artworks and the information related to them. Authors also thank the General Research Services (SGIker) of the

UPV/EHU for the technological support in the development of this work. Finally, L. Ortiz-Herrero thanks UPV/EHU for the pre-doctoral fellowship.

References

[1] The Contemporary Art Market Report 2018 - Artprice, General synopsis. Contemporary Art's market performance. https://www.artprice.com/artprice-reports/the-contemporary-art-market-report-2018, 2018 (accessed 3 January 2019).

[2] The Art Black Market - Carré d'artistes. https://www.carredartistes.com/en/blog/the-art-black-market-n188 (accessed 3 January 2019).

[3] J., A. Draghici, The Fake Legal Art Market, A View of an Art Historian and a Lawyer. https://www.mmrecht.com/artlaw/the_fake_legal_art_market.php, 2016 (accessed 3 January 2019).

[4] S. Schlackman, These Techniques Can Detect Art Forgery, Art Theft & Fraud, Art Law Journal. https://alj.artrepreneur.com/techniques-art-forgery/, 2018 (accessed 3 January 2019).

[5] B. Ryder Howe, The Surprising Truth About Fake Art and How to Avoid Being Scammed, Town & Country. https://www.townandcountrymag.com/leisure/arts-and-culture/a12108723/fake-art-how-to-avoid-scams/, 2017 (accessed 3 January 2019).

[6] A. Dickson, A.I. and the Art of Spotting Fakes, Medium. https://medium.com/s/story/a-i-and-the-art-of-spotting-fakes-6a674b0bdfef, 2018 (accessed 3 January 2019).

[7] T. Learner, P. Smithen, J.W. Krueger, M.R. Schilling (Eds.), Modern Paints Uncovered Symposium, Tate Modern, London, 16-19 May 2006.

[8] M. Anghelone, D. Jembrih-Simbürger, V. Pintus, M. Schreiner, Photostability and influence of phthalocyanine pigments on the photodegradation of acrylic paints under accelerated solar radiation,

Polym. Degrad. Stab. 146 (2017) 13-23. https://doi.org/10.1016/j.polymdegradstab.2017.09.013.

[9] M. Anghelone, V. Stoytschew, D. Jembrih-Simbürger, M. Schreiner, Spectroscopic methods for the identification and photostability study of red synthetic organic pigments in alkyd and acrylic paints, *Microchem. J.* 139 (2018) 155-163. https://doi.org/10.1016/j.microc.2018.02.029.

[10] V. Pintus, S. Wei, M. Schreiner, Accelerated UV ageing studies of acrylic, alkyd, and polyvinyl acetate paints: Influence of inorganic pigments, *Microchem. J.* 124 (2016) 949-961. http://dx.doi.org/10.1016/j.microc.2015.07.009.

[11] M.F. Silva, Analytical study of accelerated light ageing and cleaning effects on acrylic and PVAc dispersion paints used in Modern and Contemporary Art, Universitat Politècnica de València, PhD Thesis (2011).

[12] M. Marinelli, A. Pasqualucci, M. Romani, G. Verona-Rinati, Time resolved laser induced fluorescence for characterisation of binders in contemporary artworks, *J. Cult. Herit.* 23 (2017) 98-105. http://dx.doi.org/10.1016/j.culher.2016.09.005.

[13] M. Ortega-Avilés, P. Vandenabeele, D. Tenorio, G. Murillo, M. Jiménez-Reyes, N. Gutiérrez, Spectroscopic investigation of a 'Virgin of Sorrows' canvas painting: A multi-method approach, *Anal. Chim. Acta* 550 (2005) 164-172. http://dx.doi.org/10.1016/j.aca.2005.06.059.

[14] S. Saverwyns, Russian avant-garde. . . or not? Amicro-Raman spectroscopy study of six paintings attributed to Liubov Popova, *J. Raman Spectrosc.* 41 (2010) 1525-1532. https://doi.org/10.1002/jrs.2654.

[15] I. Żmuda-Trzebiatowska, M. Wachowiak, A. Klisińska-Kopacz, G. Trykowski, G. Śliwiński, Raman spectroscopic signatures of the yellow and ochre paints from artist palette of J. Matejko (1838–1893),

Spectrochim. Acta A Mol. Biomol. Spectrosc. 136 (2015) 793-801. http://dx.doi.org/10.1016/j.saa.2014.09.096.

[16] M.R. López-Ramírez, N. Navas, L.R. Rodríguez-Simón, J.C. Otero, E. Manzano, Study of modern artistic materials using combined spectroscopic and chromatographic techniques. Case study: painting with the signature “Picasso”, *Anal. Methods* 7 (2015) 1499-1508. http://dx.doi.org/10.1039/c4ay02365j.

[17] G. Capobianco, M.P. Bracciale, D. Sali, F. Sbardella, P. Belloni, G. Bonifazi, S. Serranti, M.L. Santarelli, M.C. Guidi, Chemometrics approach to FT-IR hyperspectral imageing analysis of degradation products in artwork cross-section, *Microchem. J.* 132 (2017) 69-76. http://dx.doi.org/10.1016/j.microc.2017.01.007.

[18] A. Polak, T. Kelman, P. Murray, S. Marshall, D.J.M. Stothard, N. Eastaugh, F. Eastaugh, Hyperspectral imageing combined with data classification techniques as an aid for artwork authentication, *J. Cult. Herit.* 26 (2017) 1-11. http://dx.doi.org/10.1016/j.culher.2017.01.013.

[19] T. Fardi, V. Pintus, E. Kampasakali, E. Pavlidou, M. Schreiner, G. Kyriacou, Analytical characterisation of artist’s paint systems based on emulsion polymers and synthetic organic pigments, *J. Anal. Appl. Pyrolysis* 135 (2018) 231-241. https://doi.org/10.1016/j.jaap.2018.09.001.

[20] F. Rosi, A. Daveri, P. Moretti, B.G. Brunetti, C. Miliani, Interpretation of mid and near-infrared reflection properties of synthetic polymer paints for the non-invasive assessment of binding media in twentieth-century pictorial artworks, *Microchem. J.* 124 (2016) 898-908. http://dx.doi.org/10.1016/j.microc.2015.08.019.

[21] IPERION CH. Integrated Platform for the European Research Infrastructure ON Cultural Heritage. http://www.iperionch.eu/ (accessed 3 January 2019).

[22] V. Pintus, M. Schreiner, Characterisation and identification of acrylic binding media: influence of UV light on the ageing process, *Anal.*

Bioanal. Chem. 399 (2011) 2961-2976. https://doi.org/10.1007/s00216-010-4357-5.

[23] M. Anghelone, D. Jembrih-Simbürger, M. Schreiner, Influence of phthalocyanine pigments on the photo-degradation of alkyd artists' paints under different conditions of artificial solar radiation, *Polym. Degrad. Stab.* 134 (2016) 157-168. http://dx.doi.org/10.1016/j.polymdegradstab.2016.10.007.

[24] K. Smith, K. Horton, R.J. Watling, N. Scoullar, Detecting art forgeries using LA-ICP-MS incorporating the in situ application of laser-based collection technology, *Talanta* 67 (2005) 402-413. http://dx.doi.org/10.1016/j.talanta.2005.06.030.

[25] G. Chiavari, S. Prati, Analytical Pyrolysis as Diagnostic Tool in the Investigation of Works of Art, *Chromatographia* 58 (2003) 543-554. https://doi.org/10.1365/s10337-003-0094-7.

[26] T. Learner, The analysis of synthetic paints by pyrolysis–gas chromatography–mass spectrometry (PyGCMS), *Stud. Conserv.* 46 (2001) 225-241. http://dx.doi.org/10.1179/sic.2001.46.4.225.

[27] L. Osete-Cortina, M.T. Doménech-Carbó, Characterisation of acrylic resins used for restoration of artworks by pyrolysis-silylation-gas chromatography/mass spectrometry with hexamethyldisilazane, *J. Chromatogr. A* 1127 (2006) 228-236. https://doi.org/10.1016/j.chroma.2006.05.081.

[28] J. Peris-Vicente, U. Baumer, H. Stege, K. Lutzenberger, J.V. Gimeno Adelantado, Characterisation of Commercial Synthetic Resins by Pyrolysis-Gas Chromatography/Mass Spectrometry: Application to Modern Art and Conservation, *Anal. Chem.* 81 (2009) 3180-3187. https://doi.org/10.1021/ac900149p.

[29] P. Schossler, I. Fortes, Jr. J.C. D'Ars de Figueiredo, F. Carazza, L.A. Cruz Souza, Acrylic and Vinyl Resins Identification by Pyrolysis-Gas Chromatography/Mass Spectrometry: A Study of Cases in Modern Art

Conservation, *Anal. Lett.* 46 (2013) 1869-1884. http://dx.doi.org/10.1080/00032719.2013.777925.

[30] T. Fardi, V. Pintus, E. Kampasakali, E. Pavlidou, K.G. Papaspyropoulos, M. Schreiner, G. Kyriacou, A novel methodological approach for the assessment of surface cleaning of acrylic emulsion paints, *Microchem. J.* 141 (2018) 25-39. https://doi.org/10.1016/j.microc.2018.04.033.

[31] J. Russell, B.W. Singer, J.J. Perry, A. Bacon, The identification of synthetic organic pigments in modern paints and modern paintings using pyrolysis-gas chromatography–mass spectrometry, *Anal. Bioanal. Chem.* 400 (2011) 1473-1491. https://doi.org/10.1007/s00216-011-4822-9.

[32] E. Marengo, M.C. Liparota, E. Robotti, M. Bobba, Monitoring of paintings under exposure to UV light by ATR-FT-IR spectroscopy and multivariate control graphs, *Vib. Spectrosc.* 40 (2006) 225-234. https://doi.org/10.1016/j.vibspec.2005.09.005.

[33] S. Carlesi, M. Picollo, M. Ricci, M. Becucci, The ageing of model pigment/linseed oil systems studied by means of vibrational spectroscopies and chemometrics, *Vib. Spectrosc.* 99 (2018) 86-92. https://doi.org/10.1016/j.vibspec.2018.09.001.

[34] D. Lambert, C. Muehlethaler, P. Esseiva, G. Massonnet, Combining spectroscopic data in the forensic analysis of paint: Application of a multiblock technique as chemometric tool, *Forensic Sci. Int.* 263 (2016) 39-47. http://dx.doi.org/10.1016/j.forsciint.2016.03.049.

[35] C. Muehlethaler, G. Massonnet, P. Esseiva, The application of chemometrics on Infrared and Raman spectra as a tool for the forensic analysis of paints, *Forensic Sci. Int.* 209 (2011) 173-182. http://dx.doi.org/10.1016/j.forsciint.2011.01.025.

[36] P.A. Hayes, S. Vahur, I. Leito, ATR-FTIR spectroscopy and quantitative multivariate analysis of paints and coating materials,

Spectrochim. Acta A Mol. Biomol. Spectrosc. 133 (2014) 207-213. http://dx.doi.org/10.1016/j.saa.2014.05.058.

[37] E. Marengo, M.C. Liparota, E. Robotti, M. Bobba, Multivariate calibration applied to the field of cultural heritage: Analysis of the pigments on the surface of a painting, *Anal. Chim. Acta* 53 (2005) 111-122. http://dx.doi.org/10.1016/j.aca.2005.07.061.

[38] F.M.V. Pereira, M.I.M.S. Bueno, Calibration of paint and varnish properties: Potentialities using X-ray Spectroscopy and Partial Least Squares, *Chemom. Intell. Lab. Syst.* 92 (2008) 131-137. http://dx.doi.org/10.1016/j.chemolab.2008.02.003.

[39] L. Ortiz-Herrero, L. Bartolomé, I. Durán, I. Velasco, M.L. Alonso, M.I. Maguregui, M. Ezcurra, DATUVINK pilot study: A potential non-invasive methodology for dating ballpoint pen inks using multivariate chemometrics based on their UV–Vis-NIR reflectance spectra, *Microchem. J.* 140 (2018) 158-166. https://doi.org/10.1016/j.microc.2018.04.019.

[40] L. Ortiz-Herrero, M.E. Blanco, C. García-Ruiz, L. Bartolomé, Direct and indirect approaches based on paper analysis by Py-GC/MS for estimating the age of documents, *J. Anal. Appl. Pyrolysis* 131 (2018) 9-16. https://doi.org/10.1016/j.jaap.2018.02.018.

[41] L. Eriksson, T. Byrne, E. Johansson, J. Trygg, C. Vikström, Multi- and Megavariate Data Analysis. Basic Principles and Applications, third ed., Umetrics Academy, 2013.

[42] R.W. Kennard, L.A. Stone, Computer Aided Design of Experiments, *Technometrics* 11 (1969) 137-148. http://dx.doi.org/10.1080/00401706.1969.10490666.

[43] Jesús Mari Lazkano: “Decidí ser un pintor realista cuando nadie quería serlo”. Deia. https://www.deia.eus/2016/07/17/ocio-y-cultura/decidi-ser-un-pintor-realista-cuando-nadie-queria-serlo#Loleido, 2016 (accessed 15 February 2019).

[44] D. Scalarone, O. Chiantore, Separation techniques for the analysis of artists' acrylic emulsion paints, *J. Sep. Sci.* 27 (2004) 263-274. http://dx.doi.org/10.1002/jssc.200301638.

[45] O. Chiantore, D. Scalarone, T. Learner, Characterisation of Artists' Acrylic Emulsion Paints, *Int. J. Polym. Anal. Ch.* 8 (2003) 67-82. http://dx.doi.org/10.1080/10236660304884.

[46] M.F. Silva, M.T. Doménech-Carbó, L. Osete-Cortina, Characterisation of additives of PVAc and acrylic waterborne dispersions and paints by analytical pyrolysis–GC–MS and pyrolysis–silylation–GC–MS, *J. Anal. Appl. Pyrolysis* 113 (2015) 606-620. https://doi.org/10.1016/j.jaap.2015.04.011.

[47] G. Germinario, I.D. van der Werf, L. Sabbatini, Pyrolysis gas chromatography mass spectrometry of two green phthalocyanine pigments and their identification in paint systems, *J. Anal. Appl. Pyrolysis* 115 (2015) 175-183. https://doi.org/10.1016/j.jaap.2015.07.016.

[48] O. Chiantore, L. Trossarelli, M. Lazzari, Photooxidative degradation of acrylic and methacrylic polymers, *Polymer* 41 (2000) 1657-1668. https://doi.org/10.1016/S0032-3861(99)00349-3.

[49] B. Ormsby, E. Kampasakali, C. Miliani, T. Learner, An FTIR-based exploration of the effects of wet cleaning treatments on artists' acrylic emulsion paint films, e-PS 6 (2009) 186-195.

[50] M.T. Doménech-Carbó, M.F. Silva, E. Aura-Castro, L. Fuster-López, S. Kröner, M.L. Martínez-Bazán, X. Más-Barberá, M.F. Mecklenburg, L. Osete-Cortina, A. Doménech, J.V. Gimeno-Adelantado, D.J. Yusá-Marco, Study of behaviour on simulated daylight ageing of artists' acrylic and poly(vinyl acetate) paint films, *Anal. Bioanal. Chem.* 399 (2011) 2921–2937. https://doi.org/10.1007/s00216-010-4294-3.

Appendix A. Supplementary data

Figure A.1. “Paisaje de Busturia” (A) and “Marina” (B) artworks by Jesús Mari Lazkano from 1996 and 2015, respectively.

Figure A.2. “Pequeña Dignidad” (front (C) and back (D)) and “Robin” (E) artworks by Luis Candaudap from 1998 and 1997, respectively**.**

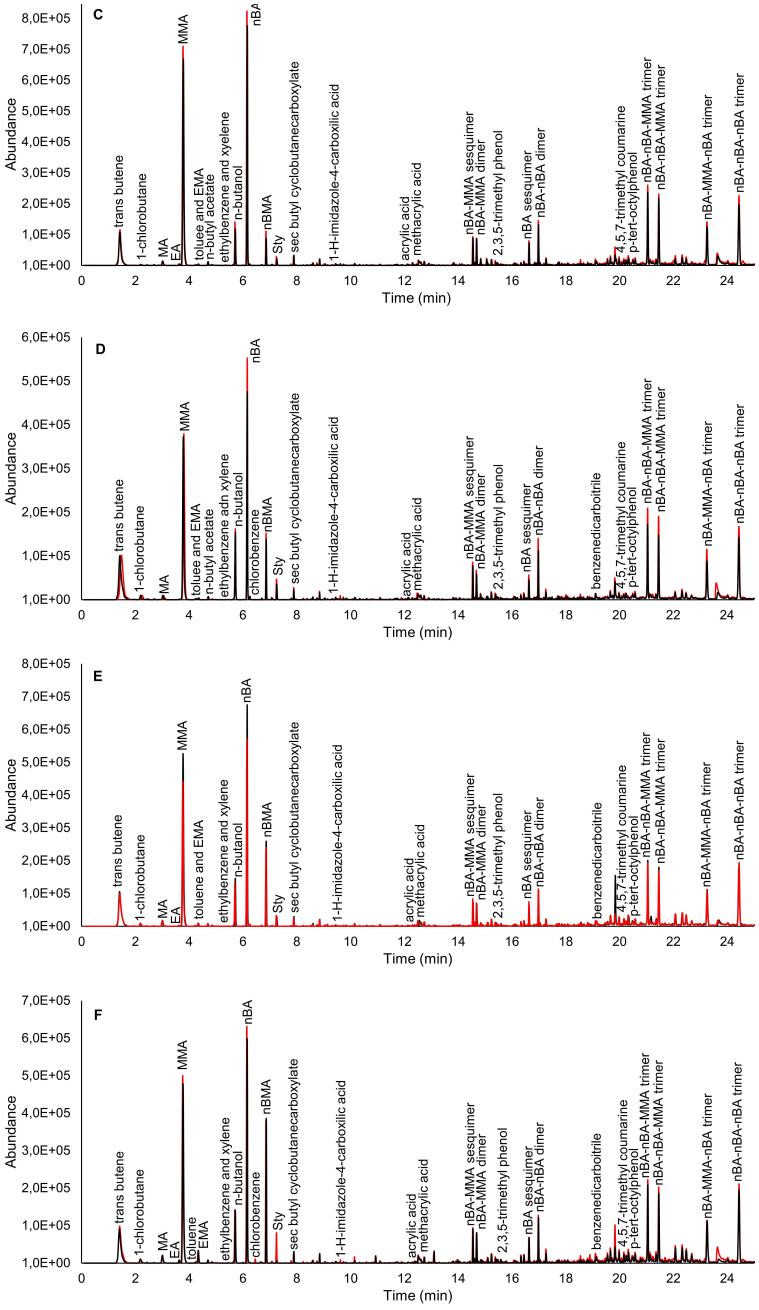

Figure A.3. Pyrograms corresponding to a recent paint (red line) and to a paint with 330 hours of accelerated ageing (black line) of Golden® (C), Talens® (D), Titan® (E) and Vallejo® (F) brands. The abundances of the chromatographic peaks were normalised with the sample mass.

CHAPTER

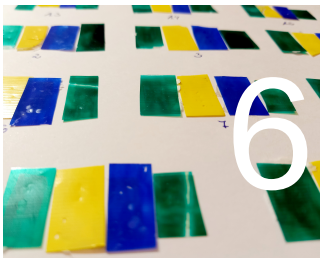

Extension study of a statistical age prediction model for acrylic paints

L. Ortiz-Herrero, I. Cardaba, L. Bartolomé, M.L. Alonso, M.I. Maguregui

Polymer Degradation and Stability, **2020**; 179: 109263

Q1, IF: 4.032, 13/89, Polymer Science

Abstract

In this work, the robustness and potential applicability of statistical age prediction models applied to the dating of different acrylic paints were studied. The FTIR-ATR analysis of three acrylic colours (Hansa yellow, phthalocyanine green and ultramarine blue) from two manufacturers (Liquitex® and Vallejo®) subjected to accelerated ageing was carried out. The acrylic paints were characterised and the modifications of their FTIR-ATR spectra throughout ageing were studied. Predictive models developed with the Liquitex® brand containing phthalocyanine green (PG7) pigment were then applied to other colour and brands of acrylic paints and their robustness and feasibility were studied based on calculated accuracy error values. The influence of the pigment on the ageing of the paint components, the type and quantity of additives present in the acrylic paint as well as the ageing conditions to which it was subjected were decisive in the short-term predictive model, which explains the low accuracy values obtained for all the acrylic paints analysed. However, the slower degradation processes taking place in the longer term and the stabilisation of the acrylic paints at higher stages of ageing made them fit successfully into the long-term model, obtaining an error of between 14 and 23%. Thus, the predictive statistical model is robust and feasible to be used for different colours of the same brand of acrylic paint as well as for acrylic paints of different brands that have been long-term aged under slightly different conditions of accelerated ageing. In conclusion, this methodology could be a promising tool in the field of dating contemporary artworks of a certain age.

Keywords: acrylic paint, dating, FTIR-ATR, OPLS.

6.1 Introduction

The contemporary art market is experiencing an unprecedented level of buying and selling activity that generates millions of dollars worldwide. As art prices rise, art-related crime is on the increase, making counterfeiting a multi-million dollar enterprise. The uncovering of fake artworks has a negative impact on the entire art market. That is why new technologies are being used to detect counterfeits that have already entered the art market as well as to prevent their sale and acquisition [1, 2].

Non-destructive techniques, such as Raman spectroscopy [3-6], Fourier transform infrared spectroscopy (FTIR) [3], IR-hyperspectral imaging (IR-HSI) [7, 8], FTIR-attenuated total reflection (FTIR-ATR) [6, 9], IR reflection [10] and scanning electron microscopy-energy dispersive X-ray spectroscopy (SEM-EDX) [6, 9], are usually used as first option, as they do not damage the artwork [3, 6, 9]. Among the techniques, FTIR-ATR spectroscopy is widely used for the characterisation of artwork materials [6, 9, 11] and for the study of the influence of pigments on the photodegradation of acrylic paints [12-15].

In some cases, non-destructive techniques are not enough, so analytical techniques combined with statistical methods, such as multivariate chemometrics, have been widely used to extract the maximum and most representative information from the acquired data in an interpretable manner. Partial least squares (PLS) is an X→Y regression methodology typically used for either predictive purposes or control monitoring. Despite the applications of PLS for the quantification of paint components in the restoration of artworks [16] as well as for the determination of their properties in quality control [17], there are not many studies that apply this method to the dating of artworks, although the applicability and effectiveness of this tool has been demonstrated in other forensic fields [18, 19]. An important

challenge that the PLS has to face is the eventual lack of robustness of the models when they want to be used for universal applications [20]. Since the setup of an optimal FTIR-ATR multivariate model is costly, once it has been developed it is expected to be valid for a long period of time.

In previous research by Ortiz-Herrero *et al.* [21], a non-destructive paint dating methodology was developed for the authentication of acrylic paints used in contemporary artworks. A multivariate chemometric method (orthogonal partial least squares (OPLS)) was applied to FTIR-ATR spectroscopic data acquired from aged Liquitex® brand paints containing PG7 pigment in order to develop age prediction models split into two temporal ranges (short- and long-term). The applicability of the predictive models was tested in artworks created with the Liquitex® brand by internationally recognised contemporary Basque artists. The correlation obtained between natural ageing and its equivalent to the accelerated one may have possible applications in the dating of artworks for up to at least 22 years, preserved under comparable conditions and created with the same paint formulation as those in the study. In addition, the loadings graph allows studying which variables influence the predictive models. From this graph, the ageing processes of the paint constituents by which the predictive models were characterised were studied. The short-term model was influenced by the degradation of the acrylic binder due to chain-scission reactions and oxidation phenomena as well as by the non-ionic polyethylene oxide surfactant due to the excision of the hydrocarbon chains. The long-term model was only characterised by the modifications undergone by the acrylic binder due to the disappearance of oxidised species and cross-linking reactions. Thus, it was concluded that the predictive models could potentially be applied to other brands of acrylic paints with the same n-butyl acrylate-methyl methacrylate (nBA-MMA) copolymer as well as to different Liquitex® brand paint colours, as pigment

modifications during ageing seemed not to be a determining factor in the predictive models.

The aim of this work was to corroborate the above facts and to study the robustness and potential applicability of the predictive models in different acrylic paint colours and brands. For this purpose, three Liquitex® paint colours and a Vallejo® paint that shared the same organic pigment and acrylic resin as the paint used in the previous research were selected. The paints were exposed to slightly modified conditions of accelerated ageing, analysed by FTIR-ATR and subsequently applied to the predictive models in order to determine their robustness and feasibility based on the accuracy error values obtained for each paint sample. The acrylic paints were also characterised and the evolution of their FTIR-ATR spectra throughout ageing was studied.

6.2 Materials and methods

6.2.1 Paint samples and preparation

The choice of manufacturers and paint colours was made on the basis of publications and interviews with contemporary artists to find out the most studied and widely used materials. Different pigments were selected to check whether the type and colour of the pigment influenced the chemical behaviour and stability of the acrylic paints and, therefore, whether they could affect the applicability of the predictive models. Commercial acrylic paints from Liquitex Acrylic Paint® (United States (USA)) containing Hansa Yellow 10G (PY3) and Phthalocyanine Green BS (PG7) organic pigments and Ultramarine Blue (PB29) inorganic pigment were used. The selection of this commercial brand was based on the fact that it is one of the most widely used brands worldwide as well as being the brand used in almost all the acrylic studies on which our research has been based [9, 22]. The

predictive models were also tested to determine if they were applicable to acrylic paint brands other than Liquitex® that shared the n-butyl acrylate-methyl methacrylate (nBA-MMA) copolymer. Vallejo Acrylic Artist Colour® brand paint (Spain) containing PG7 organic pigment was selected to that end. This commercial brand is widely used by contemporary Basque artists.

0.6 µm thick free paint films were applied over 180 µm plastic sheets with the help of a monitored film applicator (4340 Automatic Film Applicator, Elcometer, United Kingdom (UK)). The paint films were dried under room conditions for approximately 24 months in order to ensure the curing of the paint prior to being subjected to accelerated ageing. The paints used were water-based in which the binder is a polymer dispersion in water. The drying period applied to the paint allowed the water to evaporate and the polymer particles to come together and intermingle to form a continuous film. This way, the paint film coalesces. In addition, the natural cross-linking of the polymer could be achieved, increasing the hardness, resistance and mechanical properties of the paint film [23, 24]. After curing the paint, a sample set containing 15 samples of each type of paint was gradually aged under controlled accelerated ageing conditions and subsequently analysed by FTIR-ATR.

6.2.2 Accelerated ageing

The ageing procedure consisted in exposing the paint films (1 x 2 cm) to artificial solar radiation under controlled temperature, humidity and irradiance conditions. A Solarbox 1500e RH equipment (Neurtek Instruments, Spain) was used with a Xenon Lamp, which provided radiation with wavelengths between 300 and 800 nm and a nominal irradiance of 600 W m^{-2}. The camera was equipped with an indoor 310 nm UV filter and set to a black panel temperature of 50 ºC and 40% humidity.

These conditions were slightly different from the previous study (55 ºC, 50% humidity and an old 310 nm UV filter was used) to check the robustness and potential applicability of the predictive models [21]. The accelerated ageing was carried out under isochronous sampling up to a maximum of 1232 h.

6.2.3 FTIR-ATR analysis

No sample preparation was required for ATR measurements. For the FTIR-ATR investigations FT/IR-4100 instrument with an ATR-PRO ONE unit (JASCO International Co., Ltd., Japan) equipped with a triglycine sulphate (TGS) detector and a diamond crystal was used. Spectra were acquired with 128 scans in the spectral range of 4000-400 cm^{-1} at 2.0 cm^{-1} resolution. Measurements were performed on one spot directly at the surface of the paint films on two different days. A background of air was recorded before every measurement and all spectra were corrected against the background spectrum by using Spectra Manager Software v.2 prior to chemometric analysis.

6.2.4 Chemometrics

SIMCA 14.1 Umetrics® (Umeå, Sweden) was used for statistical analysis. Two predictive models were previously developed and validated by Ortiz-Herrero *et al.* [21] using OPLS regression to FTIR-ATR spectra of Liquitex® brand paint samples containing PG7 pigment. The predictive models correlated the spectroscopic data (**X** matrix) to the accelerated ageing time (**Y** vector). The **X** variables were scaled to unit variance and the **Y** variable was transformed to logarithmic function. The unwanted contributions to FTIR-ATR spectra were overcome by applying the first derivative function with 15 points for the entire spectrum range. The main characteristics of both OPLS models are shown in Table 1.

Table 1. Main characteristics of the short- and long-term models.

OPLS model	Number of samples	Application range	Statistical values					
			LV	RMSECV	R^2 CV	RMSEP	R^2 P	E %
Short-term	21 for calibration 10 for validation	From 0 to 14 years old	4	0.28 (1.91 h)	0.99	0.19 (1.55 h)	0.85	32
Long-term	12 for calibration 5 for validation	From 14 to 29 years old	5	0.05 (1.12 h)	1	0.04 (1.10 h)	0.89	8

* LV (latent variable), RMSECV (root mean square error of cross-validation), RMSEP (root mean square error of prediction), R^2 CV (coefficient of determination of cross-validation), R^2 P (coefficient of determination of prediction) and E (accuracy error).
* Data obtained from a previous study by Ortiz-Herrero *et al.* [21].

The two predictive models were applied to predict the accelerated age of the paint samples and thus check its applicability and robustness in the different brands and pigment colours. 10 paint samples coded 15 to 6 with accelerated ageing of 24, 48, 132, 180, 227, 310, 322, 394, 536 and 680 h were applied to the short-term model and 5 paint samples coded 5 to 1 with accelerated ageing of 728, 868, 948, 1064 and 1232 h were used in the long-term model. The paint films had a two-year drying period prior to accelerated ageing, so the correlation obtained by Ortiz-Herrero *et al.* [21], in which approximately 50 h of accelerated ageing under the applied conditions was one natural year, was taken into account to correct the deviation from the prediction. The average value of the predictions was calculated for each paint analysed on the two different days. The accuracy error was calculated according to the following equation (Eq. 1):

$$\text{Error (\%)} = \left(\frac{(y_r - y_p)}{y_r}\right) x\ 100 \qquad \text{(Eq. 1)}$$

Where, y_p is the accelerated ageing value predicted by the model for the paint sample and y_r the real value.

6.3 Results and discussion

6.3.1 Characterisation by FTIR-ATR

The characterisation of FTIR-ATR spectra of Liquitex® paints containing PY3 and PB29 pigments was performed (Figure 1). The characterisation of Liquitex® paint with PG7 pigment was previously carried out by Ortiz-Herrero *et al.* [21]. The two Liquitex® paints gave a characteristic nBA-MMA copolymer profile. A strong band at around 1727 cm^{-1} ascribed to the carbonyl stretching vibration was observed. The absorption bands at about 2955, 2934 and 2874 cm^{-1} were attributed to C–H bond stretching

vibrations. Another band of the acrylic copolymer was that of C-H bending at around 1449 cm^{-1} [9, 25]. The bands at around 1236, 1144 and 1159 cm^{-1} were assigned to C-O stretching [12]. The stretching vibrations of the polyethoxylated non-ionic surfactant were observed at about 1112 cm^{-1}. No characteristic styrene bands were detected in either of the spectra of the two Liquitex® paints. This can be explained by the very low concentration of styrene present in the paints and the consequent overlapping of their absorption bands by the acrylic polymer, pigments and fillers. The monoarylide yellow paint had a medium intensity carbonyl peak at around 1671 cm^{-1} consistent with the ketohydrazone structure with strong intramolecular hydrogen bonding. The band at 1593 cm^{-1} was attributed to the -C=N- bond and the bands at 1479 and 1338 cm^{-1} were ascribed to the aromatic nitro group. An absorbance at 1036 cm^{-1} attributed to the aromatic chloro group of PY3 was also observed [9, 26, 27]. The ultramarine blue pigment used in the Liquitex® paint masked in some infrared regions the detection of the acrylic binding media with its strong infrared absorption. The spectrum showed overlapping Al, $Si-O_4$ stretching bands between 850 and 1100 cm^{-1}. These bands mask the C-O/C-C skeletal vibrations of the acrylic binder (1200-900 cm^{-1}). Moreover, weaker absorption bands were observed at 688 and 656 cm^{-1} [11, 15, 22]. The paint had a high blue pigment content compared to the intensity of the bands of the other paint constituents.

The FTIR-ATR characterisation of the Vallejo® brand was also performed, as shown in Figure 1. The characteristic IR absorptions of nBA-MMA acrylic resin were identified. The strong and sharp absorption at 1725 cm^{-1} corresponded to the –C=O stretching vibration and the bands at 2956, 2933 and 2874 cm^{-1} were attributed to C–H stretching. Another band of the acrylic copolymer was that of C–H bending at 1448 cm^{-1} [9, 25]. The bands at 1236, 1143 and 1159 cm^{-1} were assigned to C-O stretching [12]. The band at 1112 cm^{-1} was characteristic of polyethylene oxide (PEO)

surfactant. Neither extenders nor characteristic bands of styrene were detected in the FTIR-ATR spectrum. The phthalocyanine green pigment showed an absorption band at 1564 cm^{-1} attributed to C=N aromatic stretching. The bands at 1391, 1306, 1277, 1211, 1093 and 948 cm^{-1} were ascribed to C-H in-plane vibrations. The band assigned to C-H out-of-plane/C-N stretching vibrations at 748cm^{-1} was also observed [9, 12].

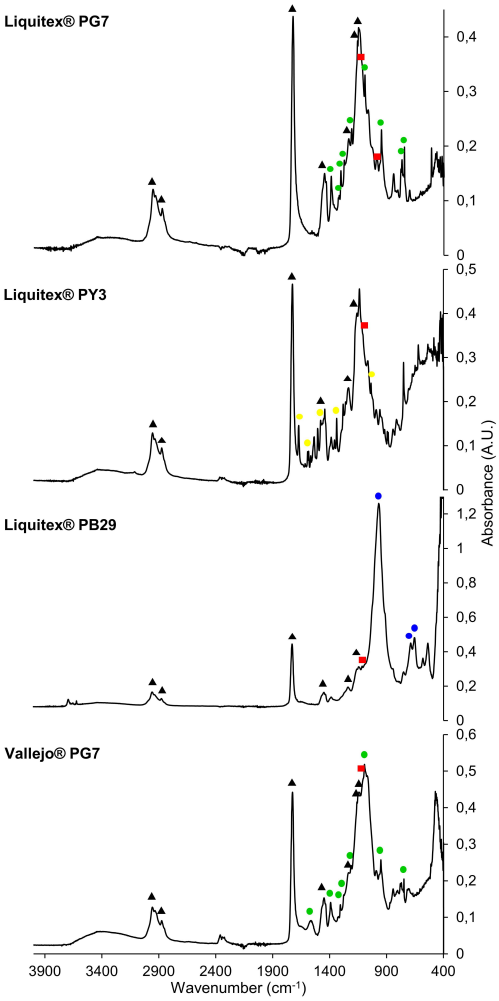

Figure 1. FTIR-ATR spectra of Liquitex® (PG7, PY3 and PB29) and Vallejo® (PG7) with an accelerated ageing of 24 h. The characteristic IR bands assigned to the acrylic copolymer (triangle), pigment (circle with different colours depending on the pigment) and PEO surfactant (square) are marked.

The FTIR-ATR spectra of aged acrylic paints were examined and their evolution throughout the ageing trials was discussed. The FTIR-ATR spectra of Liquitex® with PY3 pigment at different accelerated ageing stages (Figure 2) showed the photodegradation processes of paint constituents. The absorption bands exhibited an oscillating trend throughout the 868 h of ageing. This oscillatory trend may be due to the influence of PY3 pigment on the acrylic binder and surfactant [28]. The carbonyl band of the acrylic binder at 1726 cm^{-1} displayed a moderate decreased with 948 h of ageing due to side-chain scission reactions that cause the loss and volatilisation of low molecular weight compounds, such as the side butyl ester groups of the nBA-MMA copolymer [12, 15, 22, 29]. Moreover, the band showed a widening attributed to oxidation processes and formation of oxidised species, such as carboxyl acids, ketones, aldehydes, open chain anhydrides and gamma-lactones [15, 28, 29]. The $CH(CH_2)$ stretching bands at 2954, 2934 and 2875 cm^{-1} exhibited a slight decrease due to main-chain scission reactions that leads to formation of volatile species [12, 13]. The band at 1449 cm^{-1} ascribed to C-H bending also decreased moderately. This phenomenon may be caused by hydrogen abstraction from backbone CH_2 groups [28]. Moreover, the bands at 1234 and 1159 cm^{-1} assigned to the stretching vibration of the –C-C(=O)-O bonds in the ester groups showed a limited decrease in their intensity. The slight decrease of the non-ionic polyethylene oxide surfactant band at 1110 cm^{-1} may be associated with the oxidation of the PEO molecules that cause the excision of poly(oxyethylene) chains [24, 30]. The absorption bands assigned to the acrylic binder and PEO surfactant showed no change in intensity and shape over the maximum applied ageing time. The bands ascribed to the PY3 pigment displayed a decrease in intensity and disappeared after 948 h of ageing.

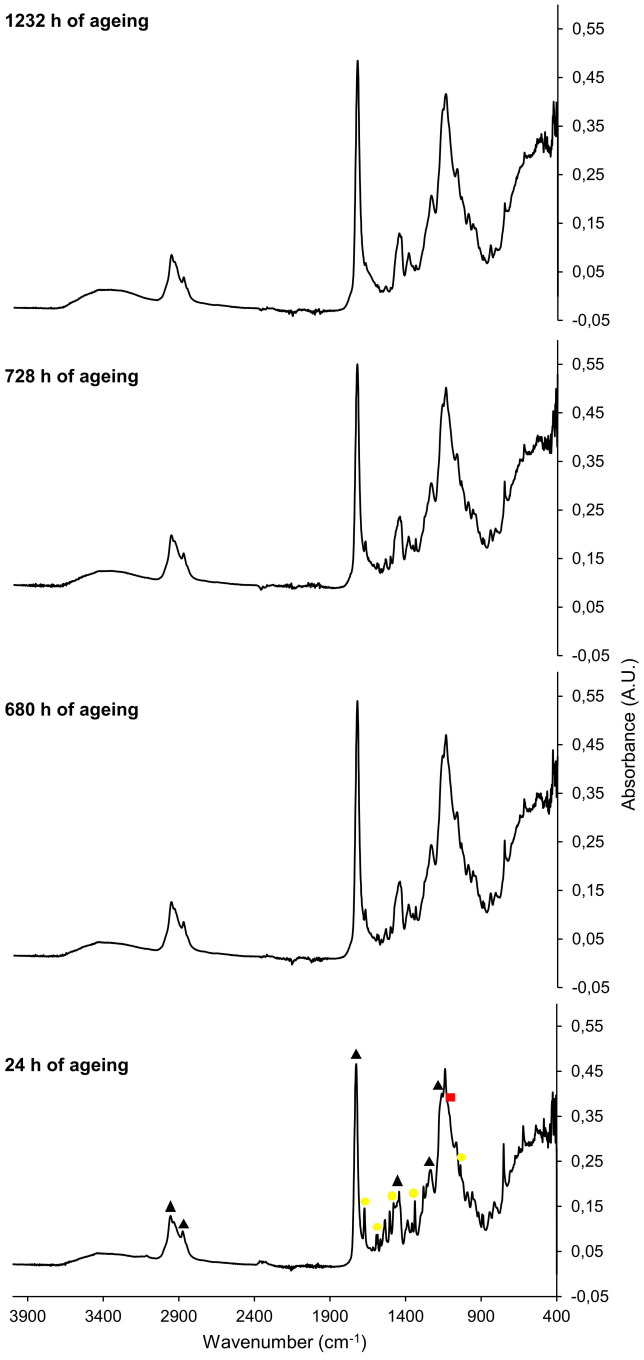

Figure 2. FTIR-ATR spectra of Liquitex® (PY3) with an accelerated ageing of 24, 680, 728 and 1232 h.

The differences in the FTIR-ATR spectra recorded between the unaged and aged Liquitex® paint containing PB29 pigment were also examined (Figure 3). An oscillating trend was observed throughout the 536 h of ageing. The bands assigned to the PB29 pigment became more pronounced compared to those of the acrylic binder with 948 h of ageing. This may be due to degradation of the organic part of the paint caused by photooxidative reactions, such as chain excision and Norrish reactions, which produce low molecular weight fractions volatilised from the acrylic binder and make the paint surface relatively enriched in pigment content [12, 13, 15]. The carbonyl band ascribed to the acrylic binder at 1728 cm^{-1} showed a moderate increase that may be explained by the fact that the loss of part of the carbonyl ester group is compensated by the formation of new oxidation compounds that absorb in the same region [29]. In addition, a widening attributed to oxidation processes and the formation of oxidised species was observed. The surface polyethoxylated non-ionic surfactant also increased. Thermal ageing initially caused the surface surfactant to melt and migrate to the bulk film. However, the migration rate post-ageing accelerated significantly due to the increased polymer coalescence induced by the ageing regime and/or the increased mobility resulting from the thermal degradation of the surfactant within the bulk film that caused the PEO surfactant to migrate back to the paint/air interface [30, 31]. The FTIR-ATR spectrum was significantly altered at 1064 h of aging with a decrease in the C-O stretching bands at 1237, 1159, 1144 cm^{-1}. These modifications may suggest the loss of an ester group consistent with the reduction of C=O band and to the fast oxidative chain scission of the polyethoxylated surfactant [15]. The presence of PB29 pigment was also decreased, either because it was degrading or because other species were migrating to the surface and, therefore, the relative PB29 content was reduced. In contrast, most of the principal absorptions increased when the paint was exposed to the maximum accelerated ageing time.

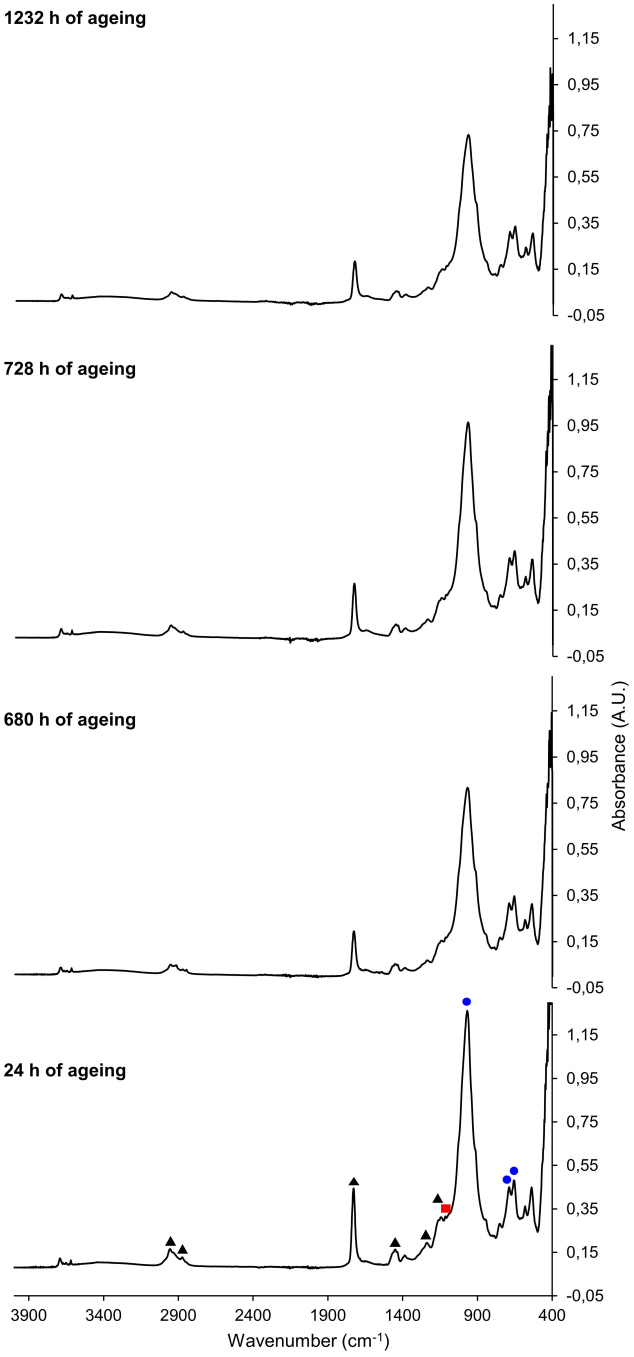

Figure 3. FTIR-ATR spectra of Liquitex® (PB29) with an accelerated ageing of 24, 680, 728 and 1232 h.

The changes detected in Liquitex® paint containing PG7 pigment after exposure to accelerated ageing are shown in Figure 4. The absorption bands followed an oscillating trend throughout the 322 h of ageing. The carbonyl absorption at 1725 cm^{-1} attributed to the nBA-MMA copolymer increased with 728 h of ageing due to the formation of oxidised species absorbing in that region [11, 29]. The C–H stretching, C-H bending and C-O stretching bands also increased moderately. UV radiation induced PEO surfactant to migrate from the inside of the film to the paint surface, causing an increase in its absorption bands [24, 30]. An enrichment of the PG7 pigment was also observed. The absorption bands showed a new oscillating trend in the FTIR-ATR spectrum up to the maximum ageing time applied.

The modifications recorded in the FTIR-ATR spectrum of the Vallejo® brand after accelerated ageing trials were discussed (Figure 5). The absorption bands of the paint showed an increase in the first 48 h of exposure. The carbonyl band ascribed to the acrylic binder at 1725 cm^{-1} increased. As explained above, the loss of part of the carbonyl ester group can be compensated by the formation of new oxidation compounds that absorb in the same region [29]. In addition, the bands assigned to C-O stretching showed an increase in their intensity. The presence of the PEO surfactant also became more prominent, as the increased coalescence of the film enhances the mobility of the compound within the film and brings it back to paint surface [30]. An enrichment of the PG7 pigment reflected in the increase of its band at 1093 cm^{-1} was also observed. The absorption bands showed slight oscillations up to the maximum of accelerated ageing applied without remarkable modifications.

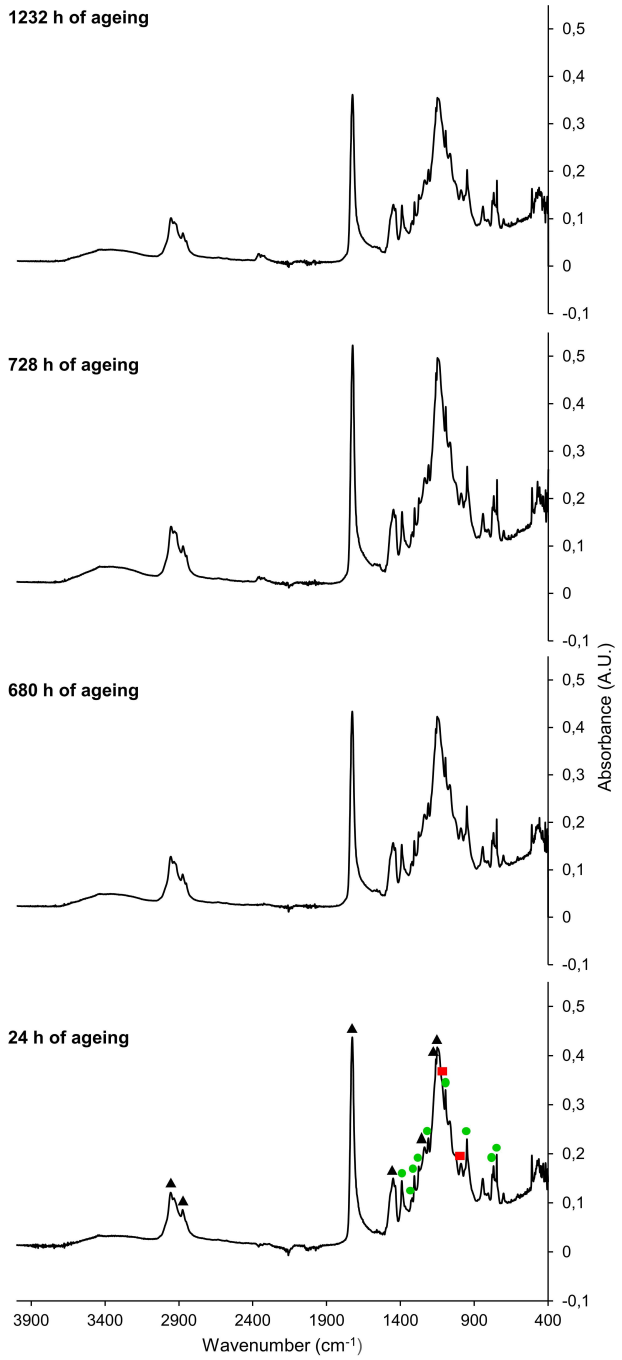

Figure 4. FTIR-ATR spectra of Liquitex® (PG7) with an accelerated ageing of 24, 680, 728 and 1232 h.

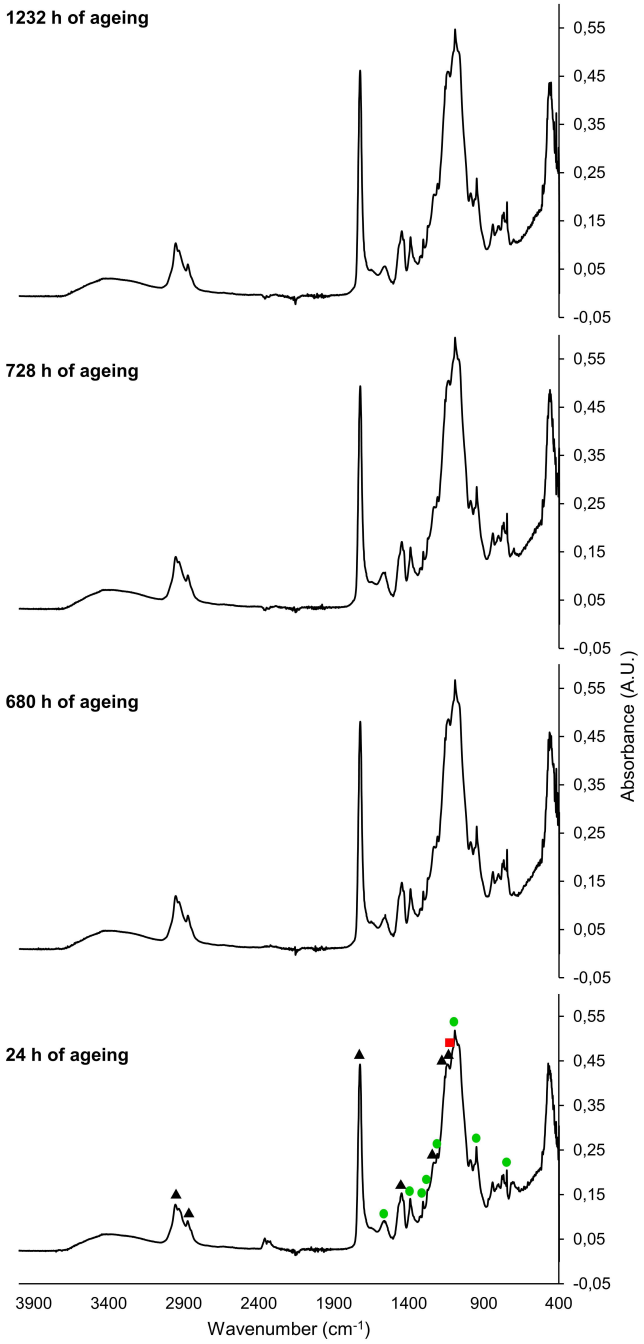

Figure 5. FTIR-ATR spectra of Vallejo® (PG7) with an accelerated ageing of 24, 680, 728 and 1232 h.

6.3.2 Application of OPLS models: Potential applicability and robustness

In the previous research, the loadings graph of the predictive models was studied from which relevant information was extracted [21]. First, the predictive models were influenced mainly by the ageing processes of the acrylic binder and, to a lesser extent, by those of the PEO surfactant. Moreover, two different predictive models needed to be established for short- and long-term ageing predictions. The short-term model was mainly influenced by the degradation of the acrylic binder that induced modifications (decrease and widening) in the characteristic band of the carbonyl group (1725 cm^{-1}) of the nBA-MMA copolymer. In the long-term paint samples, however, the increase and narrowing of that band due to cross-linking reactions and the disappearance of oxidised species was the main influence on the predictive model.

The two OPLS models were used in the prediction of the analysed paint samples in order to determine their potential applicability to other acrylic paint brands and pigment colours as well as to study their robustness to slightly different ageing conditions.

None of the paints aged between 24 and 680 h fitted the short-term model, exhibiting a large deviation in the predictive results obtained (accuracy error values above 50%, results not shown).

Each pigment in the Liquitex® paint influenced the degradation processes of the pictorial film in a specific way, showing a different evolution of the FTIR-ATR spectrum when exposed to accelerated ageing (Figure 2 and Figure 3). For instance, the intensity of the carbonyl band was characterised by an oscillatory trend for the paints containing PY3 and PB29 pigments due to the simultaneity of side-chain loss and oxidation

phenomena [29, 32], but with a different extent for the different pigments. In the case of PY3 the band ended up increasing when the paint was exposed to 680 h of ageing. For PB29 the trend was less clear, displaying ascending and descending movements for each accelerated time tested. The PEO surfactant was characterised by the same trend as that detected for the acrylic polymer for each paint colour, driven by migration and oxidation processes. Thus, the FTIR-ATR spectra show that the short-term model cannot be applied to different colours of the same brand of acrylic paint, since each particular pigment induces characteristic reactions with the paint constituents under accelerated ageing exposure, displaying specific spectral modifications for each acrylic paint and explaining the large deviation obtained in the predictive results. This fact can be supported by research that has demonstrated that the degradation processes in pictorial films are influenced by the pigments, which may act as retarders or promoters of the ageing processes of the paint constituents [12, 22, 28].

The short-term model also failed when applied to Vallejo® brand paint samples. The spectral modifications upon exposure to accelerated ageing were different from those observed with the Liquitex® brand, despite sharing the same acrylic binder, surfactant and organic pigment (Figure 5). The FTIR-ATR spectra showed mild oscillations with a slight trend towards increased band intensities up to 680 h of ageing. The bands assigned to the carbonyl group of the acrylic binder increased due to oxidation processes as well as those of the PEO surfactant due to its migration towards the paint surface. The variations in the ageing conditions to which Vallejo® paints were exposed may be the reason why they show a different ageing to that of the Liquitex® brand. In addition, the different modifications of the FTIR-ATR spectra observed between the Vallejo® brand and the one of Liquitex® with PG7 pigment analysed in this work may imply that each acrylic paint brand has its characteristic ageing and depends on a greater number of processes, being the type and quantity of components

that make up the paint decisive in this first ageing stage. Thus, the short-term model is not applicable to different brands of acrylic paint.

Moreover, the Liquitex® samples with phthalocyanine green pigment belonging to the same brand with which the short-term model was developed did not fit the model. This may be due to the fact that the analysed paint samples and those used in the model showed different spectral modifications under the exposure to slightly different accelerated ageing conditions. While an oscillatory trend was observed in the samples analysed, those used in the short-term model were characterised by a constant downward trend. The model samples showed modifications ascribed to the C=O stretching of the nBA-MMA copolymer by a widening of the band due to the formation of oxidised species and a decrease due to chain excision reactions that cause the loss and volatilisation of low molecular weight compounds. The model was also characterised by changes in the C-H stretching band associated with the degradation of the hydrocarbon fraction of the PEO surfactant [21]. The discrepancies between the two sets of samples, as mentioned above, may be due to the fact that ageing was not conducted under exactly the same conditions as in the previous case, which affected the short-term prediction results. Therefore, the predictive model is not robust for predicting the age of acrylic paints that have been exposed to uncontrolled ageing conditions.

In contrast, all acrylic paints aged between 728 and 1232 h fitted the long-term model, obtaining an average error between 15 and 20% for each brand (Table 2). Although the accuracy errors were slightly higher than that obtained in the model validation (8% error) [21], they were still acceptable. Some of the paint samples of Liquitex® brand containing the PB29 pigment and Vallejo® brand showed an accuracy error greater than 20%, possibly because they were at the lower and upper limits of the model's application range and, therefore, did not fit the model well.

Table 2. Accelerated and natural ageing time values predicted by the long-term model and accuracy error in absolute value calculated for each paint sample. The predicted natural ageing time was calculated using the correlation found by Ortiz-Herrero *et al.* [21].

Acrylic paint	Sample code	Accelerated ageing time (h)	Predicted accelerated ageing time (h)	Predicted natural ageing time (year)	Accuracy error (%)
Liquitex® (PY3)	1	1232	989	20	20
	2	1064	990	20	7
	3	948	990	20	4
	4	868	1034	21	19
	5	728	880	18	21
Liquitex® (PB29)	1	1232	807	16	34
	2	1064	746	15	30
	3	948	908	18	4
	4	868	789	16	9
	5	728	855	17	17
Liquitex® (PG7)	1	1232	998	20	19
	2	1064	1122	22	5
	3	948	861	17	9
	4	868	1068	21	23
Vallejo® (PG7)	1	1232	1006	20	18
	2	1064	1032	21	3
	3	948	990	20	4
	4	868	1017	20	17
	5	728	964	19	32

The long-term ageing model was only characterised by modifications associated with the carbonyl band of the acrylic binder caused by a sharpening due to the disappearance of oxidised species and an increase due to cross-linking reactions [21]. The fact that the model was influenced by fewer ageing processes may be the reason why all the acrylic paints analysed fitted the model. Moreover, in the case of the Liquitex® yellow paint, the FTIR-ATR spectrum showed a decrease in the absorption bands from 948 h of ageing with a tendency to remain constant up to the maximum applied ageing time (Figure 2). Vallejo® paint showed slight modifications at this stage of ageing (Figure 5). These minor modifications in the FTIR-ATR spectra indicate that the paints reach stability, which may explain why the type of pigment and the brand of acrylic paint are not decisive when using the long-term model. The fact that the accuracy error values for the Liquitex® green paint samples aged under slightly different conditions were acceptable may also suggest that the conditions to which the acrylic paints are exposed at this stage of ageing are not determinant. Thus, the statistical predictive model can be considered robust and feasible to be used for different colours of the same brand of acrylic paint as well as for acrylic paints of different brands that have been long-term aged under not completely identical accelerated ageing conditions.

6.4 Conclusions

In this study, four commercial acrylic paints from two different manufacturers were characterised by FTIR-ATR. Each acrylic paint showed characteristic modifications of its FTIR-ATR spectra throughout the accelerated ageing in spite of sharing the same paint constituents, such as the acrylic binder, the surfactant and in two of the cases the organic pigment.

Pigments were found to influence the short-term stability of acrylic paints when exposed to accelerated ageing, as they can act as promoters or inhibitors of the degradation of binders and surfactants depending on their chemical structure and colour. Furthermore, the formulation of each brand of acrylic paint, i.e. the type and quantity of components that make up the paint, have a significant importance in its ageing, as has been observed among green paints of the Liquitex® and Vallejo® brands. This would explain the non-fitting of the analysed paints to the short-term model, making it impossible to obtain acceptable accuracy values. Thus, the short-term model is not applicable to different pigments of the same brand of acrylic paint nor to different brands of acrylic paint. This implies that if one were to estimate the age of a contemporary artwork made with acrylic paint less than 14 years old, one would have to use a specific model for each brand and pigment. The accelerated ageing conditions to which the acrylic paints were subjected were also decisive in this stage of ageing. Therefore, it is concluded that the model is not robust and that the ageing conditions must be set precisely in order to obtain reproducible predictive results.

However, the fewer processes occurring at higher stages of ageing as well as the stabilisation of acrylic paints, such as the Liquitex® yellow paint and the Vallejo® green paint, allowed acceptable accuracy error values to be obtained with the long-term model. Thus, the predictive statistical model can be feasible to be used for different colours of the same brand of acrylic paint as well as for acrylic paints of different brands with the same copolymer (nBA-MMA), such as Talens®, Titan®, Vallejo® or Golden®. Moreover, the model is robust to predict the age of acrylic paints that have been aged under slightly different conditions. This indicates that the long-term model could be applied to the dating of contemporary artworks from 14 to at least 22 years old, created with acrylic paints without regard to the brand or paint colour used by the artist or the conditions under which the work has been preserved. Further studies would be needed to extend the

range of application of the predictive model to artworks older than 22 years. In conclusion, this study reaffirms the dating of relatively old contemporary artworks by the application of multivariate chemometrics to spectroscopic data.

Acknowledgments

The authors would like to thank the General Research Services (SGIker) of the UPV/EHU for the technological support. Authors also thank to Omaira de la Hera of the Faculty of Science and Technology of the UPV/EHU for her useful discussion. L. Ortiz-Herrero thanks UPV/EHU for the pre-doctoral fellowship.

References

[1] General synopsis. Contemporary Art's market performance. The Contemporary Art Market Report 2018 – Artprice, https://www.artprice.com/artprice-reports/the-contemporary-art-market-report-2018/general-synopsis-contemporary-arts-market-performance (2018), Accessed date: 25 August 2019.

[2] M. Durkee, WYWH: Tricking the Art Market – On Forgery, Beltracchi, and Scientific Technology. Center for art law, https://itsartlaw.org/2018/12/18/wywh-tricking-the-art-market-on-forgery-beltracchi-and-scientific-technology/ (2018), Accessed date: 25 August 2019.

[3] M. Ortega-Avilés, P. Vandenabeele, D. Tenorio, G. Murillo, M. Jiménez-Reyes, N. Gutiérrez, Spectroscopic investigation of a 'Virgin of Sorrows' canvas painting: a multi-method approach, *Anal. Chim. Acta* 550 (2005) 164-172. https://doi.org/10.1016/j.aca.2005.06.059.

[4] S. Saverwyns, Russian avant-garde. . . or not? A micro-Raman spectroscopy study of six paintings attributed to Liubov Popova, *J. Raman Spectrosc.* 41 (2010) 1525-1532. https://doi.org/10.1002/jrs.2654.

[5] I. Żmuda-Trzebiatowska, M. Wachowiak, A. Klisińska-Kopacz, G. Trykowski, G. Śliwiński, Raman spectroscopic signatures of the yellow and ochre paints from artist palette of J. Matejko (1838–1893), *Spectrochim. Acta A Mol. Biomol. Spectrosc.* 136 (2015) 793-801. https://doi.org/10.1016/j.saa.2014.09.096.

[6] M.R. López-Ramírez, N. Navas, L.R. Rodríguez-Simón, J.C. Otero, E. Manzano, Study of modern artistic materials using combined spectroscopic and chromatographic techniques. Case study: painting with the signature "Picasso", *Anal. Methods* 7 (2015) 1499-1508. https://doi.org/10.1039/c4ay02365j.

[7] G. Capobianco, M.P. Bracciale, D. Sali, F. Sbardella, P. Belloni, G. Bonifazi, S. Serranti, M.L. Santarelli, M.C. Guidi, Chemometrics approach to FT-IR hyperspectral imageing analysis of degradation products in artwork cross-section, *Microchem. J.* 132 (2017) 69–76. https://doi.org/10.1016/j.microc.2017.01.007.

[8] A. Polak, T. Kelman, P. Murray, S. Marshall, D.J.M. Stothard, N. Eastaugh, F. Eastaugh, Hyperspectral imageing combined with data classification techniques as an aid for artwork authentication, *J. Cult. Herit.* 26 (2017) 1-11. https://doi.org/10.1016/j.culher.2017.01.013.

[9] T. Fardi, V. Pintus, E. Kampasakali, E. Pavlidou, M. Schreiner, G. Kyriacou, Analytical characterisation of artist's paint systems based on emulsion polymers and synthetic organic pigments, *J. Anal. Appl. Pyrolysis* 135 (2018) 231-241. https://doi.org/10.1016/j.jaap.2018.09.001.

[10] F. Rosi, A. Daveri, P. Moretti, B.G. Brunetti, C. Miliani, Interpretation of mid and near-infrared reflection properties of synthetic polymer paints for the non-invasive assessment of binding media in twentieth-century pictorial artworks, *Microchem. J.* 124 (2016) 898–908. https://doi.org/10.1016/j.microc.2015.08.019.

[11] V. Pintus, M. Schreiner, Characterisation and identification of acrylic binding media: influence of UV light on the ageing process, *Anal. Bioanal. Chem.* 399 (2011) 2961–2976. https://doi.org/10.1007/s00216-010-4357-5.

[12] M. Anghelone, D. Jembrih-Simbürger, V. Pintus, M. Schreiner, Photostability and influence of phthalocyanine pigments on the photodegradation of acrylic paints under accelerated solar radiation, *Polym. Degrad. Stabil.* 146 (2017) 13-23. https://doi.org/10.1016/j.polymdegradstab.2017.09.013.

[13] M. Anghelone, V. Stoytschew, D. Jembrih-Simbürger, M. Schreiner, Spectroscopic methods for the identification and photostability study of red synthetic organic pigments in alkyd and acrylic paints,

Microchem. J. 139 (2018) 155–163. https://doi.org/10.1016/j.microc.2018.02.029.

[14] M. Anghelone, D. Jembrih-Simbürger, M. Schreiner, Influence of phthalocyanine pigments on the photo-degradation of alkyd artists' paints under different conditions of artificial solar radiation, *Polym. Degrad. Stabil.* 134 (2016) 157-168. https://doi.org/10.1016/j.polymdegradstab.2016.10.007.

[15] V. Pintus, S. Wei, M. Schreiner, Accelerated UV ageing studies of acrylic, alkyd, and polyvinyl acetate paints: Influence of inorganic pigments, *Microchem. J.* 124 (2016) 949–961. https://doi.org/10.1016/j.microc.2015.07.009.

[16] P.A. Hayes, S. Vahur, I. Leito, ATR-FTIR spectroscopy and quantitative multivariate analysis of paints and coating materials, *Spectrochim. Acta Mol. Biomol. Spectrosc.* 133 (2014) 207–213. https://doi.org/10.1016/j.saa.2014.05.058.

[17] F.M.V. Pereira, M.I.M.S. Bueno, Calibration of paint and varnish properties: potentialities using X-ray spectroscopy and partial least squares, *Chemom. Intell. Lab. Syst.* 92 (2008) 131-137. https://doi.org/10.1016/j.chemolab.2008.02.003.

[18] L. Ortiz-Herrero, L. Bartolomé, I. Durán, I. Velasco, M.L. Alonso, M.I. Maguregui, M. Ezcurra, DATUVINK pilot study: a potential non-invasive methodology for dating ballpoint pen inks using multivariate chemometrics based on their UV–Vis-NIR reflectance spectra, *Microchem. J.* 140 (2018) 158-166. https://doi.org/10.1016/j.microc.2018.04.019.

[19] L. Ortiz-Herrero, M.E. Blanco, C. García-Ruiz, L. Bartolomé, Direct and indirect approaches based on paper analysis by Py-GC/MS for estimating the age of documents, *J. Anal. Appl. Pyrolysis* 131 (2018) 9-16. https://doi.org/10.1016/j.jaap.2018.02.018.

[20] R. Balabin, S. Smirnov, Interpolation and extrapolation problems of multivariate regression in analytical chemistry: benchmarking the

robustness on near-infrared (NIR) spectroscopy data, *Analyst* 137 (2012) 1604-1610. https://doi.org/10.1039/c2an15972d.

[21] L. Ortiz-Herrero, I. Cardaba, S. Setien, L. Bartolomé, M.L. Alonso, M.I. Maguregui, OPLS multivariate regression of FTIR-ATR spectra of acrylic paints for age estimation in contemporary artworks, *Talanta* 205 (2019) 120114. https://doi.org/10.1016/j.talanta.2019.120114.

[22] V. Pintus, S. Wei, M. Schreiner, UV ageing studies: evaluation of lightfastness declarations of commercial acrylic paints, *Anal. Bioanal. Chem.* 402 (2012) 1567-1584. https://doi.org/10.1007/s00216-011-5369-5.

[23] E. Jablonski, T. Learner, J. Hayes, M. Golden, Conservation Concerns for Acrylic Emulsion Paints: A Literature Review, TATE PAPERS, ISSN 1753-9854.

[24] M.T. Doménech-Carbó, M.F. Silva, E. Aura-Castro, L. Fuster-López, S. Kröner, M.L. Martínez-Bazán, X. Más-Barberá, M.F. Mecklenburg, L. Osete-Cortina, A. Doménech, J.V. Gimeno-Adelantado, D.J. Yúsa-Marco, Study of behaviour on simulated daylight ageing of artists' acrylic and poly(vinyl acetate) paint films, *Anal. Bioanal. Chem.* 399 (2011) 2921-2937. https://doi.org/10.1007/s00216-010-4294-3.

[25] M.F. Silva, Analytical study of accelerated light ageing and cleaning effects on acrylic and PVAc dispersion paints used in Modern and Contemporary Art, PhD Thesis Universitat Politècnica de València, 2011.

[26] J. Russell, A study of the materials and techniques of Francis Bacon (1909-1992), Doctoral thesis, Northumbria University, 2010.

[27] T. Learner, P. Smithen, J.W. Krueger, M.R. Schilling (Eds.), Modern Paints Uncovered Symposium, Tate Modern, London, May 2006, pp. 16-19.

[28] A. Ciccola, M. Guiso, F. Domenici, F. Sciubba, A. Bianco, Azo-pigments effect on UV degradation of contemporary art pictorial film:

A FTIR-NMR combination study, *Polym. Degrad. Stabil.* 140 (2017) 74-83. http://dx.doi.org/10.1016/j.polymdegradstab.2017.04.004.

[29] O. Chiantore, L. Trossarelli, M. Lazzari, Photooxidative degradation of acrylic and methacrylic polymers, *Polymer* 41 (2000) 1657–1668. https://doi.org/10.1016/S0032-3861(99)00349-3.

[30] B. Ormsby, E. Kampasakali, C. Miliani, T. Learner, An FTIR-based exploration of the effects of wet cleaning treatments on artists' acrylic emulsion paint films, e-PS 6 (2009) 186–195.

[31] T. Fardi, E. Kampasakali, Z. Terzopoulou, V. Pintus, E. Pavlidou, M. Schreiner, D. Bikiaris, G. Kyriacou, A preliminary study on the physicochemical properties of pigmented Sty/nBA/MMA emulsion films: The effect of thermal ageing, *Polym. Degrad. Stabil.* 158 (2018) 157-167. https://doi.org/10.1016/j.polymdegradstab.2018.11.001.

[32] A. Ciccola, I. Serafini, M. Guiso, F. Ripanti, F. Domenici, F. Sciubba, P. Postorino, A. Bianco, Spectroscopy for contemporary art: Discovering the effect of synthetic organic pigments on UVB degradation of acrylic binder, *Polym. Degrad. Stabil.* 159 (2019) 224-228. https://doi.org/10.1016/j.polymdegradstab.2018.11.027.

CHAPTER 7

Estimation of the post-mortem interval of human skeletal remains using Raman spectroscopy and chemometrics

L. Ortiz-Herrero, B. Uribe, L. Hidalgo Armas, M.L. Alonso, A. Sarmiento, J. Irurita, R.M. Alonso, M.I. Maguregui, F. Etxeberria, L. Bartolomé

Forensic Science International, **2021** (under review)

Q1, IF: 2.108, 4/16, Medicine, Legal

Abstract

An important demand exists in the field of forensic analysis to objectively determine the post-mortem interval (PMI) when human skeletal remains are discovered. It is widely known that bones undergo different chemical and physical processes after death, mainly due to their interaction with the environment in which they are found, although it is not known exactly what these processes consist of. Multiple techniques have been used so far to follow up these and other post-mortem changes and thus establish the time elapsed since the individual's death, but they present important drawbacks in terms of reliability and accuracy. The aim of this research was to propose an analytical methodology capable of determining the PMI by using non-destructive Raman spectroscopy measurements of human skeletal remains. The recorded Raman spectra provided valuable and potentially useful information from which a multivariate study was performed by means of orthogonal partial least squares regression (OPLSR) in order to correlate the PMI with the detected spectral modifications. A collection of 53 real human skeletal remains with known PMI (15 years ≤ PMI ≤ 87 years) was analysed and used for building and validating the OPLS model. The PMI of 10 out of 14 validation samples could be determined with an accuracy error of less than 30%, demonstrating the adequate predictive performance of the OPLS model even in spite of the large inter-individual variability it handled. This opens up the possibility of applying the OPLS model in combination with non-destructive techniques to the determination of the PMI of human skeletal remains that have been buried in conditions similar or equal to those of cemetery niches and in a geographic location with a Mediterranean climate, which is an important achievement for forensic medicine and anthropology.

Keywords: human bones, PMI, Raman spectroscopy, OPLSR.

7.1 Introduction

Multiple studies have shown the importance of achieving a methodology for establishing exactly how long the remains of a human body have been buried. This aim, which is an important demand for many researchers in the field of forensic science, is justified by anthropological and legal interests.

The time for a case to be relevant (not legally prescribed) varies according to each country's legal system. In the Spanish legal system, the knowledge of the PMI is fundamental in criminal law, since the Organic Law 10/1995 of 23 November 1995 establishes a maximum of 20 years for the prescription of a case, in which the judicial sentence is 15 years or more [1, 2]. In Germany, the evidence is considered relevant when the PMI is less than 30 to 50 years [3], whereas for the jurisdiction of England and Wales the samples are legally valid if the human skeletal remains are not older than 75 years [4, 5].

Most of the studies carried out so far agree on the justification for the lack of these methods, referring to the difficulty of establishing a reliable method to accurately determine the PMI, as Nagy *et al.* cited in their research study “Dating human skeletal remains is one of the most important and yet unreliable aspects of forensic medicine” [6]. The cause of this difficulty lies in the complex degradation processes undergone by the bones. These degradation processes known as diagenesis consists of a set of chemical, physical and biological interaction processes between bones and the environment in which they are found (water, soil, humidity, gases, suspended particles, pH and/or bacteria). The complexity and variety of these processes make this type of degradation not exactly known, in addition to being complicated to simplify these degradation processes to a few [7].

Based on the characteristics and chemical composition of the bone, it is important to note its different parts. Inside the bone, a medullary part called the organic phase can be observed, in which components such as collagen, lipids, proteins, etc. are found. The outer part, the cortical, is that which contains organic elements and minerals, such as magnesium and hydroxyapatite crystals, which provide hardness to the bone. The cortical area is therefore made up of an inorganic phase embedded in an organic one [1, 8, 9]. This research will focus on this area, since it presents an inorganic phase that will take longer to degrade and an organic phase that, being the first to degrade, can potentially be more informative in forensic contexts [7].

The factors mentioned above that influence degradation can be classified as internal and external [1, 10]. The internal factors are those specific to the person, such as age, diseases suffered or the diet followed [1]. The externals are those factors related to the environment and the surroundings, i.e. temperature, humidity, insects, and above all, the characteristics of the soil where the body is buried [10]. These processes are called diagenetics and are not fully and accurately known, but affect both the organic and mineral phases. They can be related to the loss of collagen and, therefore, to a decrease in nitrogen and amino acids, among many other phenomena [11].

In recent years, the forensic field has expanded rapidly as a branch of analytical chemistry, both in research on PMI calculation and in the different areas that this science raises [7]. Besides empirical principles based on the examiner's experience and subjective comparisons [12], multiple techniques have been applied to determine the time elapsed since death of skeletal remains, such as luminol chemiluminescent reaction [2, 3, 12-14], radioisotope measurements [5, 12, 15], proteomics [16, 17], metabarcoding [15, 18], high performance liquid chromatography-tandem mass spectrometry

(HPLC/MS/MS) [19], X-ray diffraction (XRD) [1], UV-Vis spectroscopy [8, 20, 21], UV-Vis-induced fluorescence [22], stereomicroscopy and digital imaging [23], Fourier transform infrared (FTIR) spectroscopy [6, 21, 24-26] and Raman spectroscopy [7, 25, 26]. In addition to the lack of objectivity of several of the methods mentioned, some of them are of a destructive nature. For this reason, among others, Raman spectroscopy has established itself as a very versatile technique for the analysis of bone tissue composition [27]. The Raman spectrum of skeletal remains not only provides us with extensive information about the structure and composition of their minerals and collagen, but also with a complete examination of their diagenesis [9, 28-30]. Moreover, Raman spectroscopy has demonstrated its application in determining the PMI of bones and teeth by studying their dynamic chemical modifications and correlating them with the time of burial [7, 25, 26, 28]. Further advantages of Raman spectroscopy are that it is microscopic, fast and non-destructive, which are of utmost importance in cases of forensic or anthropological analysis [10], in addition to the fact that it can be portable [7, 9, 27, 31].

In spite of the use of Raman spectroscopy and a wide variety of other analytical techniques in the determination of the PMI, only few research studies have applied them in combination with chemometrics. Chemometrics transforms the recorded data into more useful and interpretable information with which a predictive model can be built. This predictive model relates several variables or parameters allowing the examination of the hidden information in a set of data related to each other but influenced by numerous variables. With these chemometric treatments, useful information is extracted from the trends in the multivariate data set [27, 32]. Wang *et al.* [24] used FTIR spectroscopy together with chemometrics to date human skeletal remains of up to 552 days. Predictions with a root mean square error of 50.93 days for buried bones and 71.03 days for unburied bones were obtained using the genetic algorithm combined with

partial least squares (GA-PLS). In addition, the modifications that occur in the most significant FTIR regions and that are potentially applicable to the estimation of the PMI were identified and interpreted. However, this study did not take into account the influence of inter-individual differences on the FTIR spectrum variations and, even more important, the mathematical model was built from samples subjected to two controlled experimental burial conditions, which will differ from the natural ones, so the prediction set could have been giving by far over-optimistic results. Woess *et al.* [26] tested the suitability of various IR and Raman microscopic imaging techniques to draw conclusions about the PMI of human skeletal remains. The techniques were combined with multivariate imaging analysis (MIA) and principal component analysis (PCA) for a more sophisticated characterisation of the bone material as well as to differentiate between forensic and archaeological remains. Issues such as the impact of environmental factors still need to be explored and future studies will have to consider a larger sample size to further narrow down the PMI. Moreover, Longato *et al.* [33] used micro-computed tomography (micro-CT), mid-infrared (MIR) microscopic imaging and energy dispersive X-ray (EDS) mapping to investigate bone density, analyse organic and mineral components, determine elemental composition and, finally, apply and compare the results obtained by these analytical techniques together with PLSR to determine the PMI of human skeletal remains. The results obtained proved to be usable to predict the Ca/C ratio and bone volume (BV) over total volume (TV) for the estimation of the PMI. Future research will have to consider more individuals in order to develop a PMI screening tool based on the outcome of this multidimensional approach.

The aim of this research was to model the Raman spectral modifications experienced by human skeletal remains in relation to the PMI (15 years ≤ PMI ≤ 87 years) in order to provide a reliable method of quantifying the PMI. Likewise, the methodology was intended to be an invaluable tool for

the identification and characterisation of the most influential spectral regions throughout the burial period, which could provide important additional information for the dating of the PMI. Furthermore, in order to fulfil these scopes and be applicable in real scenarios, the OPLS model was externally validated with bone samples coming from cemetery niches with a large inter-individual variability.

7.2 Materials and methods

7.2.1 Fieldwork

A collection of 53 human skeletal remains with known PMI (15 years ≤ PMI ≤ 87 years) was used in this study. The sampling for the collection of human skeletal remains with defined PMI was carried out from niches of the San José (Granada, Andalucía, Spain) and Lucena (Córdoba, Andalucía, Spain) burial sites. The bone collection from the San José's burial site began to be exhumed in 1991 and was completed in 2010, while the collection from Lucena's burial site was fully gathered in 2018. The skeletal remains were kept piled up in bags in a warehouse at the cemetery. The exact date of their exhumation was unknown. It must be emphasised that since the human skeletal remains were buried in niches, they did not come into contact with the soil, nor were they exposed to adverse climatic conditions, thus minimising the diagenetic processes that occur after burial [1, 19].

Both cities have a Mediterranean climate characterised by being warm and temperate with higher precipitation in winter than in summer. The mean annual temperature in Córdoba is 17.8 °C with a mean rainfall of 612 mm, whereas in Granada, the mean annual temperature is 15.5 °C with a mean rainfall of 450 mm [34].

7.2.2 Sample pre-treatment

The chemical treatment applied to the bones was a water bath with sodium hypochlorite and a brushing of each bone in order to eliminate the fungi and bacteria that had or could attack them in their storage causing an accelerated degradation of the bone. This treatment was carried out as a way to preserve both the organic and inorganic properties of the bone, avoiding bacterial growth and microbiological action. Once the pre-treatment of the samples was carried out, they were kept at a constant temperature (20-25 ºC) inside wooden boxes for their conservation, being only removed for analysis. The latency time until research was added to the known PMI. It is worth noting that all procedures in this study meet the requirements of local laws and institutional guidelines and were approved and supervised by the Ethics Committee of the University of Granada.

7.2.3 Bone subsampling

Long bones are mainly selected for sampling due to their relative size and strength as well as being more resistant to diagenesis [8, 20, 25]. The left tibias of 37 individuals (50% male and 50% female) from Lucena's burial site and 15 individuals (60% male and 40% female) from San José's burial site with age at death ranging between 32 and 100 years (mean 70 years; standard deviation 18) were collected. The skeletal remains had a PMI ranging from 15 to 87 years (mean 37 years, standard deviation 14) at the time of analysis. Anthropological data and burial sites of all measured human skeletal remains are shown in Table 1.

Sample code	Sex	Burial Site	Age at death (year)	PMI (year)
LU3	Male	Lucena	-	49
LU7	Male	Lucena	46	27
LU11	Male	Lucena	57	17
LU13	Male	Lucena	-	43
LU21	Female	Lucena	-	53
LU22	Male	Lucena	71	29
LU24	Male	Lucena	73	20
LU27	Male	Lucena	74	15
LU29	Female	Lucena	89	34
LU33	Female	Lucena	-	48
LU36	Male	Lucena	-	65
LU39	Male	Lucena	-	53
LU43	Male	Lucena	71	25
LU44	Female	Lucena	81	21
LU52	Female	Lucena	82	31
LU54	Male	Lucena	66	22
LU59	Male	Lucena	81	33
LU65	Male	Lucena	67	33
LU70	Male	Lucena	-	50
LU71	Female	Lucena	-	48
LU76	Female	Lucena	-	41
LU78	Male	Lucena	-	51
LU84	Male	Lucena	54	38
LU89	Male	Lucena	74	36
LU91	Male	Lucena	77	35
LU101	Female	Lucena	75	37
LU103	Female	Lucena	75	33
LU105	Female	Lucena	-	42
LU111	Female	Lucena	91	19
LU114	Female	Lucena	-	44
LU115	Female	Lucena	100	15
LU136	Female	Lucena	90	28
LU148	Female	Lucena	81	26
LU161	Male	Lucena	-	45
LU186	Female	Lucena	-	57
LU193	Female	Lucena	-	39
LU197	Female	Lucena	99	25
G14	Female	San José	73	51
G15	Male	San José	90	58
G56	Male	San José	75	51
G64	Female	San José	61	44
G67	Female	San José	41	44
G69	Male	San José	61	46
G170A	Female	San José	-	87
G261	Female	San José	81	22
G427	Male	San José	94	20
G490	Male	San José	32	18
G497	Female	San José	68	31
G498	Male	San José	33	31
G523	Male	San José	41	30
G528	Male	San José	65	24
G531	Male	San José	34	29

Table 1. Description of the human skeletal remains sampled.

The measurements were performed in the diaphysis of the tibia in an area where the anthropometric measurements required by Anthropologists and Forensic Doctors were unaffected. An electric drill (Dremel® MultiPro®, United States (USA)) was used to scrape a region measuring approximately 5 mm wide, 10 mm long and 1-2 mm deep from the cortical surface of each bone. This way, any contaminants, such as the minerals deposited superficially in the outer layers of the bone and the residual haemoglobin in the bone tissue, which may be responsible for the emission of fluorescence and thus make the Raman spectra qualitatively and quantitatively unusable, could be removed quickly and in an almost non-destructive manner [31].

7.2.4 Raman spectroscopy measurements

The measuring equipment was a NRS-5100 Dispersive Raman Spectrometer (JASCO Analítica Spain S.L., Spain) equipped with a confocal microscope, using an x100 objective, and a 785 nm excitation wavelength laser, operating at 100% power. The scan range was 3200-200 cm^{-1}. The measurement conditions were set to 3 scans of 20 seconds of acquisition per spectrum. Due to the high fluorescence radiated by the bones, a 3-minute photobleaching was performed prior to recording the spectrum, thus minimising the fluorescence background [9, 35]. Three randomly selected points were measured in the scraped area of each sample to overcome bone heterogeneity. Cosmic rays were removed and the baseline was subtracted by applying a polynomial fit of order 3. The 3 recorded spectra were averaged to obtain a final Raman spectrum that was representative of a wide part of the cortical zone of each bone. The range of the Raman spectrum employed for the chemometric processing was 2000-350 cm^{-1}. The software used for system control, data acquisition and data analysis were the Spectra Manager II and WiRE 3 Renishaw® (Gloucestershire, United Kingdom (UK)).

7.2.5 Chemometrics

SIMCA 15.0.2 Umetrics® (Umeå, Sweden) was used for multivariate analysis. A preliminary exploratory analysis was performed by PCA using the data of various ratios and mineral crystallinity calculated from the 53 samples of the set. PCA is a multivariate projection method designed to extract and display systematic variation in an **X** data matrix. The most important use of PCA is to represent a multivariate data table as a low-dimensional plane so that an overview of the data is obtained. This overview can uncover groups of observations, trends, relationships between observations and variables and outliers [32]. The detection of the latter was the objective of this exploratory analysis. Once the potential outliers were detected and eliminated, the modelling of the PMI was performed by means of OPLSR. OPLS is an extension of PLS that splits the systematic variation in the **X** block into two parts, one that models the correlation between **X** and **Y** (predictive) and another that shows the systematic variation in **X** not related to **Y** (orthogonal). Orthogonalisation can reduce the complexity of the model, as it eliminates the systematic variation in the **X** matrix that is not correlated with the property to predict [32]. Therefore, an OPLS model was built correlating the Raman spectra of the various bones (**X** matrix) with the known PMI of each of them (**Y** vector). This model will be used to predict the unknown PMI of new human skeletal remains from their spectroscopic data. To this end, the total sample set, reduced to 47 samples after the elimination of outliers, was split into three groups depending on their PMI: 15 years ≤ PMI ≤ 30 years (17 samples), 30 years < PMI ≤ 50 years (23 samples) and 50 years < PMI ≤ 87 years (7 samples). To construct the **X** matrix, the intensity values of the Raman shifts of the entire spectrum range of each bone sample were used. The **X** matrix was split into two sample sets using the Kennard-Stone algorithm [36]: a training set (calibration samples) consisting of 70% of the samples from each group and a test set (validation samples) consisting of 30% of

them. The training set was used for the construction of the OPLS model. For its optimisation, the **X** matrix was scaled and transformed by applying different mathematical treatments, such as Savitzky-Golay, multiplicative scatter correction (MSC), standard normal variate (SNV), row center, exponentially weighted moving average (EWMA) and first and second derivatives. The **Y** variable (PMI) was transformed to a logarithmic function due to its non-normal distribution. In addition, the Raman spectrum was examined for non-informative and noisy **X** variables responsible for interfering with those that were determinant for the PMI modelling. The number of latent variables (LVs) constituting the model was set by internal validation with the cross-validation method. The statistical parameters used for evaluating this step were the root mean square error of cross-validation (RMSECV) and the coefficient of determination of cross-validation (R^2 CV). RMSECV was calculated using Eq. 1:

$$\text{RMSECV} = \sqrt{\frac{\sum_{i=1}^{n}(y_i - \hat{y}_i)^2}{n}} \qquad \text{(Eq. 1)}$$

Where y_i is the known PMI value, $\hat{y}_i$ is the PMI value predicted by the model and *n* is the total number of samples used in the training set. The external validation of the OPLS model was subsequently performed using the test set. To this end, the RMSE of prediction (RMSEP) and the R^2 of prediction (R^2 P) were assessed. The RMSEP was calculated with Eq. 2:

$$\text{RMSEP} = \sqrt{\frac{\sum_{i=1}^{n_t}(y_{t,i} - \hat{y}_{t,i})^2}{n_t}} \qquad \text{(Eq. 2)}$$

Where $y_{t,i}$ is the known PMI value, $\hat{y}_{t,i}$ is the PMI value predicted by the model and n_t is the number of samples in the test set. The RMSEP expresses the average error to be expected in future predictions when the

OPLS model is applied to unknown human skeletal remains. In addition, the predictive accuracy error was calculated for the test set using Eq. 3:

$$\text{Error (\%)} = \left(\frac{(y_r - y_p)}{y_r}\right) x\ 100 \qquad \text{(Eq. 3)}$$

Where, y_p is the PMI value predicted by the OPLS model and y_r the known PMI value of the bone. Taking into account the above statistical parameters, the optimal model would have to have high R^2 and Q^2 values, low RMSECV and RMSEP values as well as a small difference between these last two statistical parameters. A large difference between RMSECV and RMSEP would indicate the possibility that too many LVs were being used in the model (over-fitting) and that the noise was being modelled. The number of LVs was intended to be as low as possible, as larger number of LVs might include some irrelevant information. The R^2 parameter varies from 0 to 1, indicating the degree of adjustment to perfect fitting, and the Q^2 parameter shows the robustness and predictive capacity of the model, being good when $Q^2 > 0.5$ and excellent when $Q^2 > 0.9$ [32, 37]. In this way, it was possible to check which of the treatments obtained the best and most reliable model with the lowest error rate to date the PMI.

7.3 Results and discussion

7.3.1 Characterisation of the Raman spectrum

Human skeletal remains are composite materials containing a 20-30 wt.% organic fraction embedded in a 70-80 wt.% inorganic phase of hydroxyapatite ($Ca_{10}(PO_4)_6(OH)_x$) partially substituted by carbonate (approx. 7 wt.%) at both the hydroxyl (A-type) and phosphate (B-type) sites [24, 30]. Taking this into account, the identified characteristic bands of the Raman spectrum of a human bone are shown in Figure 1.

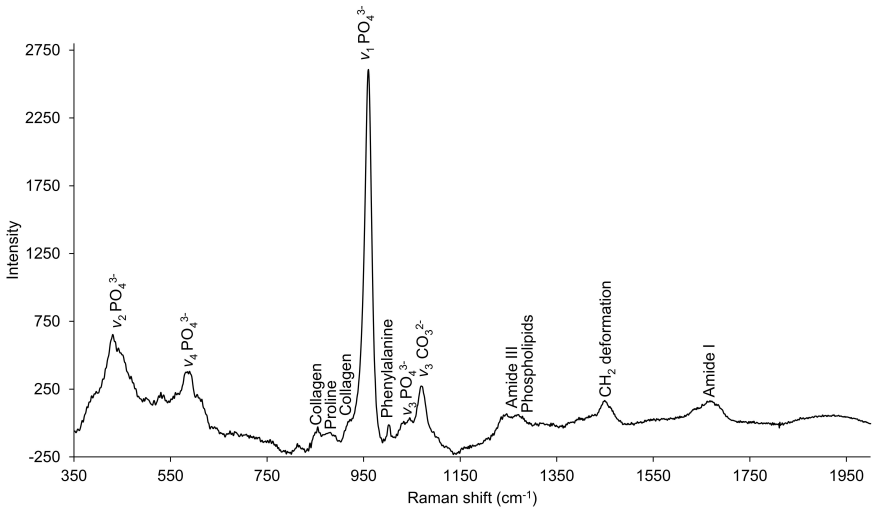

Figure 1. Raman spectrum of the LU27 bone sample with the baseline subtracted by applying a polynomial fit of order 3. The characteristic Raman bands are identified.

The amide I band between 1605 and 1720 cm^{-1} was mainly due to the C=O stretching within the collagen polypeptide [7]. The δ N-H vibration of amide III within the protein α-helix was detected in the region between 1215 and 1360 cm^{-1}, while the CH_2 deformation of proteins was identified between 1410 and 1500 cm^{-1} [7, 26, 38]. The proline band assigned to the *v* C-C vibrational mode was detected at 880 cm^{-1} and was surrounded by two collagen bands attributed to the δ CCH (855 cm^{-1}) and *v* C-C (923 cm^{-1}) vibrational modes [9, 38]. The phenylalaline band at 1003 cm^{-1} may be due to the breathing mode of the ring [9]. In addition to the organic Raman bands, those of the phosphate ions (PO_4^{3-}) corresponding to hydroxyapatite, which constitutes the inorganic phase of the bone, were detected [25, 29]. The strongest and narrowest band at 925-992 cm^{-1} was assigned to the v_1 vibrational mode of PO_4^{3-}, whereas the bands at 400-490 cm^{-1} and 550-615 cm^{-1} were attributed to the v_2 and v_4 vibrational modes of PO_4^{3-}, respectively [7, 26]. The carbonate ion (CO_3^{2-}) band in the region between 1015 and 1095 cm^{-1} was due to the v_3 vibrational mode

and may result from the substitution of these ions into the phosphate positions in the hydroxyapatite mineral lattice [9, 29]. Furthermore, the bones had a minimal fat composition with the δ CH vibrations of phospholipids being barely detectable at 1295 cm^{-1} [7].

7.3.2 Outliers detection through PCA

The carbonate-to-phosphate ratio (v_3 CO_3^{2-} band (1070 cm^{-1})/v_1 PO_4^{3-} band (960 cm^{-1})), the mineral-to-matrix ratio (v_1 PO_4^{3-} band/amide I band (1605-1720 cm^{-1})), the collagen crosslinking ratio (amide I band (1675 cm^{-1})/amide I band (1645 cm^{-1})) and the mineral crystallinity (1/v_1 PO_4^{3-} band width) were calculated. Ratios and mineral crystallinity have previously been used in other research studies to define bone quality. Such studies have reported anomalies in bone composition and, consequently, in the values of ratios and mineral crystallinity calculated from individuals with genetic disorders, osteoporosis, fractures, etc. [6, 10, 38], so that exploratory analysis of ratios and mineral crystallinity would allow us to detect outliers in the data set available. The intensities of the corresponding bands of the Raman spectrum of each bone sample were used to calculate the ratios due to the fact that they were more reproducible and less influenced by instrumental variations than those calculated from the integrated areas. The calculated ratios and mineral crystallinity were used as **X** variables in the PCA. Subsequent to being scaled to unit variance (UV), the Hotelling's T2 and distance-to-model plots at 95% confidence were used for outlier detection.

The sample set consisted of 53 samples, 6 of which (LU36, LU186, LU21, LU115, G69, G261) were detected as outliers, exceeding the critical limits (level 0.05) of the Hotelling's T2 and distance-to-model plots of the PCA (Figure 2) and, therefore, eliminated from the set. Due to the large inter-individual variability (sex, age, diet, body size, etc.) of the analysed human

skeletal remains, it was not possible to establish the cause of the anomalous and different behaviour of these outliers. This way, the training set eventually included 33 samples, while the test set included 14.

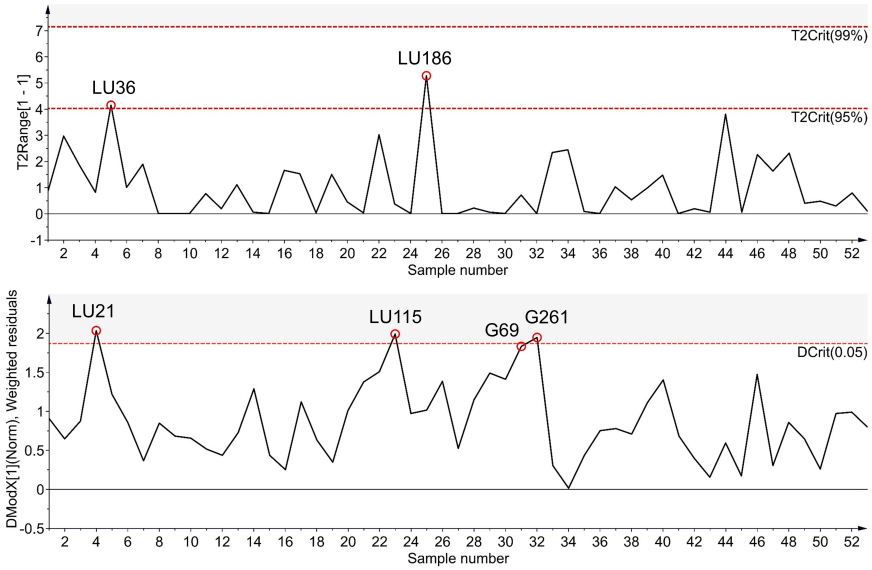

Figure 2. Outliers detected in the Hotelling's T2 and distance-to-model plots at 95% confidence.

7.3.3 OPLS model construction and validation

The UV scaling and the second derivative transformation of the **X** matrix were the mathematical treatments selected for the optimisation of the OPLS model. The aim of the second derivative transformation was to resolve the overlapping bands, which allowed for improved qualitative and quantitative data [24]. **X** variables with values between -0.04 and 0.04 in the loadings plot were eliminated, which resulted in an **X** matrix consisting of 295 variables, thus improving the robustness and performance of the OPLS model. The model was established with 3 LVs, explaining 43% for R^2X and 89% for R^2Y and predicting 67% for Q^2 of the variance of the population data within the training set, which indicates that the OPLS

model had a valid fit and predictive ability. In addition, values of 0.10 (1.25 years) for RMSECV and 0.89 for R^2 CV were obtained. The low RMSECV value as well as the R^2 CV value close to 1 highlight the high predictive accuracy and the adequate fit of the OPLS model. It also had a great predictability, obtaining a value of 0.17 (1.48 years) for the RMSEP within the validation set. The RMSECV and RMSEP values were of the same magnitude, which demonstrates the robustness of the model.

7.3.4 OPLS model application to PMI estimation

The OPLS model was used to determine the PMI of the 14 samples of the test set. Predictions with an accuracy deviation of less than 30% were obtained for 10 of the samples studied, as shown in Table 2. The fact that it was possible to accurately predict 71% of the samples in the total set demonstrated the adequate predictive performance of the OPLS model. The large deviation of the remaining 29% of the bone samples (results not shown) could be justified due to the high inter-individual variability introduced, which could affect the chemical content of the bones and, therefore, lead to variations in the Raman spectra characteristic of each individual, thus not fitting well into the OPLS model. Nevertheless, the use of human skeletal remains with large inter-individual variability and exposed to uncontrolled burial conditions as calibration and validation samples enabled the OPLS model to be applied to the identification and determination of the PMI of skeletons encountered in real forensic scenarios and to the potential distinction between these and the archaeological ones, while ensuring the reliability and acceptable error rate of the predictions provided. In addition, the optimistic predictions that would have been obtained if the OPLS model had been built and validated with bone samples of certain inter-individual characteristics, non-human or buried under controlled experimental conditions are avoided. However, future studies will have to check whether the OPLS model could be applied

to human skeletal remains from another geographical location and exposed to different burial conditions than those used in this study.

Sample code	PMI (year)	Predicted PMI (year)	Accuracy error (%)
LU3	49	39	20
LU22	29	31	7
LU33	48	44	7
LU65	33	38	15
LU70	50	41	18
LU71	48	35	28
LU78	51	36	29
LU84	38	29	23
G497	31	30	2
G523	30	38	27

Table 2. PMI estimates and accuracy errors given in absolute value for the test set samples using the OPLS model.

Moreover, the regions of the Raman spectra of human skeletal remains that were most significantly modified as a function of their PMI and, therefore, had the greatest contribution to the PMI modelling, were examined using the loadings plot. To understand these modifications, in addition to Raman studies, we have relied on those of FTIR performed on bone, since Raman spectroscopy researchers are known to have used and modified infrared correlations in order to be able to interpret Raman spectra of bone [38].

The degradation of human skeletons is a complicated and multivariate process that begins immediately after the death of the individual and is highly dependent on the external conditions to which the body is exposed [29]. It has been reported that the PO_4^{3-} bands are not meaningfully modified within the first few years of post-mortem [7, 24, 25]. In the present research study, the human skeletal remains with a PMI greater than 15 years underwent changes in the Raman bands assigned to the v_2 and v_4 vibrational modes of PO_4^{3-} (Figure 3), which may be due to the environmental factors to which the skeletons have been exposed and which have caused their inorganic phase to dissolve, leach, exchange ions, precipitate minerals and/or recrystallize [24]. In relation to the latter,

modifications in the phosphate bands can be attributed to changes in the crystallinity index (C.I.), as reported by Patonai *et al.* [39]. Such authors found that forensic human skeletal remains had a poorly crystallised apatite content, while at higher PMI the C.I. index increased, undergoing modifications in the apatite and resulting in a more ordered and larger crystal structure. Likewise, the loss of organic matter in the post-mortem degradation process of the skeletons, as will be discussed below, can also cause an increase in the degree of crystallinity of the hydroxyapatite [1]. It is worth recalling that the human skeletal remains from the present research study had a PMI between 15 and 87 years and, therefore, modifications in the v_2 PO_4^{3-} and v_4 PO_4^{3-} bands were detected in skeletons with up to the aforementioned PMI. Nevertheless, Woess *et al.* [26] reported that such modifications (reduction in the intensity of Raman bands) continue to be experienced in archaeological remains with a PMI of up to 1260 years. Moreover, in the present research study the skeletal remains with a PMI between 15 and 50 years underwent changes in the PO_4^{3-} Raman band attributed to the v_1 vibrational mode, however, those with a PMI greater than 50 years remained unchanged, as shown in Figure 3. It is worth mentioning that Woess *et al.* [26] reported that this phosphate band was minimally modified in forensic samples with a PMI between 1 day and 85 years and in archaeological samples with a PMI between 650 and 1260 years. Nonetheless, King *et al.* [29] observed changes in the position and full width at half the maximum height (FWHM) of the primary phosphate band (v_1 PO_4^{3-}) of the Raman spectrum of prehistoric skeletal remains due to the substitution of foreign ions from the soil in which they were buried and the adverse climatic conditions to which they were exposed. The human skeletons from the present research study were buried in niches and, therefore, were less susceptible to foreign ion substitutions into the mineral lattice, not undergoing such significant modifications and shifts in the v_1 PO_4^{3-} band. Furthermore, Woess *et al.* [26] found that archaeological human skeletal remains had a more prominent

and sharp IR band at 1042 cm^{-1} compared to the forensic ones due to the mineralisation of the bones. Although this band may be less obvious in forensic remains, in the present research study, the OPLS model was able to detect modifications in the Raman range from 1040 to 1048 cm^{-1}, except in those skeletons with a PMI between 30 and 50 years, as shown in Figure 3.

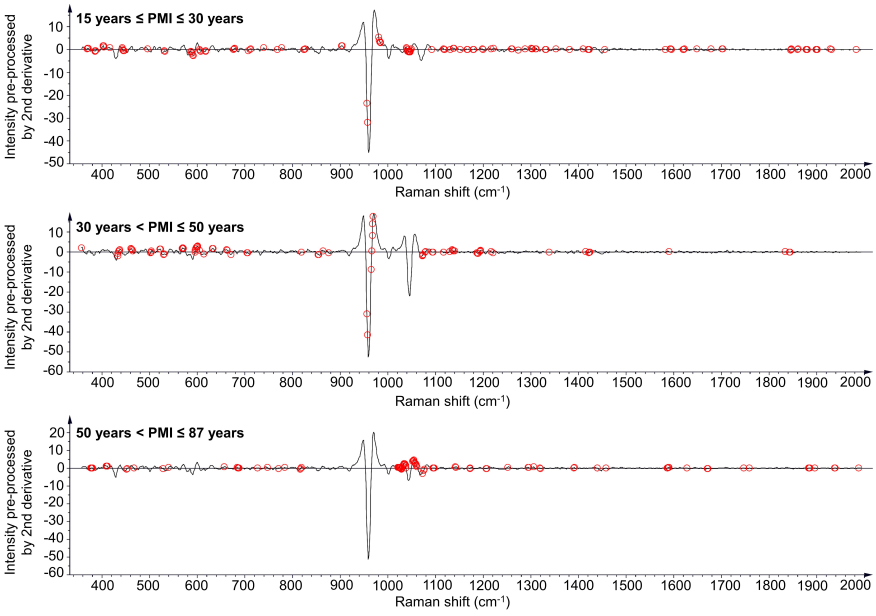

Figure 3. Red-rounded regions of the second derivative Raman spectrum that undergo modifications throughout the burial period and that most influence the modelling of the PMI.

Moreover, according to several scientific papers that report the alteration of the organic matrix (decrease of IR and Raman bands) in the skeletal remains with a PMI of up to a few years [7, 24, 26], the modifications in the Raman bands of the CH_2 deformation of proteins and of the amide I and III continued to be observed in the present research study up to the 87 years of PMI (Figure 3). Due to the decay of human skeletal remains, organic matter undergoes a complex process of disintegration, resulting in

the formation of simple chemical substances [1]. Therefore, forensic bone samples would be expected to have more organic bands in their spectra compared to archaeological ones [26, 33, 39]. Amide I and III regions are highly prone to changes in the secondary structure of proteins. More specifically, alterations in the amide I band may be due to a structural change in collagen [7]. In this regard, it has been reported that skeletal remains buried in the soil have suffered collagen loss with increasing PMI, either by chemical breakdown or enzymatic digestion by bacteria followed by leaching [7, 23, 24]. Wang *et al.* [24] observed large differences between the FTIR spectra of bones buried in soil and those not buried and exposed to air, with the former undergoing a higher rate of degradation. As mentioned above, the human skeletal remains from the present research study were buried in niches and, therefore, less prone to attack by bacteria and fungi that could accelerate the removal of organic matter and weaken the structural integrity of the bone. In spite of this, human skeletons experienced modifications in the organic matrix consistent with those reported by Pérez-Martínez *et al.* [19], who observed a loss of collagen in the remains buried in niches, with a significant decrease in the number of peptides of Collagen type I in those with a PMI equal to or greater than 20 years. All the modifications observed during the period of burial in the present research study (15 years ≤ PMI ≤ 87 years) could be extrapolated and applied as indicative information to real cases with circumstances similar to those of human skeletons buried in niches, such as open-air burials, e.g. coffins and bodies found in caves.

7.4 Conclusions

The combination of Raman spectroscopy with OPLSR has proved to overcome the inefficiency of single analytical techniques in the study of the diagenetic processes to which human skeletal remains are subjected during burial by enabling the visualisation and interpretation of the

modifications experienced in the spectra of human skeletons according to their PMI. Moreover, even though the coupling of such techniques had previously demonstrated its effectiveness in the determination of the PMI from the modelling of the modifications experienced by synthetic laboratory samples, it has also turned out to be successful when applied to real human skeletal remains, presenting itself as an additional and/or complementary tool to those already existing for the determination of the PMI. In spite of a previous exploratory analysis for the detection of outliers and a pre-processing of the analytical signals, the great inter-individual variability of the skeletons and the large number of external and internal factors that influence their diagenesis have been decisive to fail in the construction of an OPLS model capable of estimating with acceptable accuracy the PMI of all the samples in the validation set. Nevertheless, the estimates were highly promising for those samples to which the OPLS model was able to respond, opening up the possibility of determining the PMI of human skeletal remains (15 years ≤ PMI ≤ 87 years) that have been buried in similar or equal conditions to those of the cemetery niches and in a geographic location with a Mediterranean climate. The results obtained in this research could be improved by increasing in the future the number of real skeleton samples with which the OPLS model is built and validated. Therefore, the non-destructive and confirmatory nature, versatility, portability, selectivity, accuracy and the ability to provide an estimated error associated with the result provided via chemometrics, make Raman spectroscopy in combination with the OPLSR method a promising technique for determining the PMI in forensic settings where only human skeletal remains are available for analysis.

Acknowledgments

The authors would like to thank the technician Bendición Funes from the Centre for Scientific Instrumentation (CIC) of the University of Granada for

the technological support with the Raman equipment. The authors also thank the Advanced Research Facilities (SGIker) of the University of the Basque Country (UPV/EHU) for the human and technological support as well as the UPV/EHU (project GIU19/068) and Professor Ramón J. Barrio, director of the Doctorate Program in Forensic Analysis at the UPV/EHU, for the funds provided. L. Ortiz-Herrero thanks the UPV/EHU for the pre-doctoral fellowship.

References

[1] M. Prieto-Castelló, J.H. del Rincón, C. Pérez-Sirvent, P. Alvarez-Jimenez, M. Pérez-Cárceles, E. Osuna, A. Luna, Application of biochemical and X-ray diffraction analyses to establish the postmortem interval, *Forensic Sci. Int.* 172 (2-3) (2007) 112–118. https://doi.org/10.1016/j.forsciint.2006.12.014.

[2] J.A. Hernández Sarabia, C. Pérez-Martínez, J.P. Hernández del Rincón, A. Luna, Study of chemiluminescence measured by luminometry and its application in the estimation of postmortem interval of bone remains, *Leg. Med.* 33 (2018) 32–35. https://doi.org/10.1016/j.legalmed.2018.05.001.

[3] F. Ramsthaler, K. Kreutz, K. Zipp, M.A. Verhoff, Dating skeletal remains with luminol-chemiluminescence. Validity, intra- and interobserver error, *Forensic Sci. Int.* 187 (1) (2009) 47–50. https://doi.org/10.1016/j.forsciint.2009.02.015.

[4] B. Swift, I. Lauder, S. Black, J. Norris, An estimation of the post-mortem interval in human skeletal remains: a radionuclide and trace element approach, *Forensic Sci. Int.* 117 (1) (2001) 73-87. https://doi.org/10.1016/s0379-0738(00)00451-5.

[5] B. Swift, Dating human skeletal remains: Investigating the viability of measuring the equilibrium between 210Po and 210Pb as a means of estimating the post-mortem interval, *Forensic Sci. Int.* 98 (1) (1998) 119–126. https://doi.org/10.1016/s0379-0738(98)00141-8.

[6] G. Nagy, T. Lorand, Z. Patonai, G. Montsko, I. Bajnoczky, A. Marcsik, L. Mark, Analysis of pathological and non-pathological human skeletal remains by FT-IR spectroscopy, *Forensic Sci. Int.* 175 (1) (2008) 55–60. https://doi.org/10.1016/j.forsciint.2007.05.008.

[7] G. McLaughlin, I.K. Lednev, Potential application of Raman spectroscopy for determining burial duration of skeletal remains, *Anal.*

Bioanal. Chem. 401 (8) (2011) 2511–2518. https://doi.org/10.1007/s00216-011-5338-z.

[8] A. Boaks, D. Siwek, F. Mortazavi, The temporal degradation of bone collagen: A histochemical approach, *Forensic Sci. Int.* 240 (2014) 104-110. http://dx.doi.org/10.1016/j.forsciint.2014.04.008.

[9] G. McLaughlin, I.K. Lednev, Spectroscopic Discrimination of Bone Samples from Various Species, *Am. J. Anal. Chem.* 3 (2012) 161-167. http://dx.doi.org/10.4236/ajac.2012.32023.

[10] J.L. Prieto, C. Magaña, D.H. Ubelaker, Interpretation of Postmortem Change in Cadavers in Spain, *J. Forensic Sci.* 49 (5) (2004) 918-923. http://dx.doi.org/10.1520/JFS2003337.

[11] G.S. Mandair, M.D. Morris, Contributions of Raman spectroscopy to the understanding of bone strength, *BoneKEy Rep.* 4 620 (2015). http://dx.doi.org/10.1038/bonekey.2014.115.

[12] A. Cappella, D. Gibelli, E. Muccino, V. Scarpulla, E. Cerutti, V. Caruso, E. Sguazza, D. Mazzarelli, C. Cattaneo, The comparative performance of PMI estimation in skeletal remains by three methods (C-14, luminol test and OHI): analysis of 20 cases, *Int. J. Legal Med.* 132 (4) (2015) 1215-1224. http://dx.doi.org/10.1007/s00414-015-1152-z.

[13] F. Introna, G. Di Vella, C.P. Campobasso, Determination of postmortem interval from old skeletal remains by image analysis of luminol test results, *J. Forensic Sci.* 44 (3) (1999) 535–538. http://dx.doi.org/10.1520/JFS14505J.

[14] F. Ramsthaler, S.C. Ebach, C.G. Birngruber, M.A. Verhoff, Postmortem interval of skeletal remains through the detection of intraosseal hemin traces. A comparison of UV-95 fluorescence, luminol, Hexagon-OBTI®, and Combur® tests, *Forensic Sci. Int.* 209 (2011) 59-63. http://dx.doi.org/10.1016/j.forsciint.2010.12.011.

[15] I. Szelecz, S. Lösch, C.V.W. Seppey, E. Lara, D. Singer, F. Sorge, J. Tschui, M.A. Perotti, E.A.D. Mitchell, Comparative analysis of bones,

mites, soil chemistry, nematodes and soil micro-eukaryotes from a suspected homicide to estimate the post-mortem interval, *Sci Rep.* 8 (2018). http://dx.doi.org/10.1038/s41598-017-18179-z.

[16] N. Procopio, A. Williams, A.T. Chamberlain, M. Buckley, Forensic proteomics for the evaluation of the post-mortem decay in bones, *J. Proteomics* 177 (2018) 21–30. http://dx.doi.org/10.1016/j.jprot.2018.01.016.

[17] G. Prieto-Bonete, M.D. Pérez-Cárceles, A. Maurandi-López, C. Pérez-Martínez, A. Luna, Association between protein profile and postmortem interval in human bone remains, *J. Proteomics* 192 (2019) 54-63. https://doi.org/10.1016/j.jprot.2018.08.008.

[18] N. Procopio, S. Ghignone, A. Williams, A. Chamberlain, A. Mello, M. Buckley, Metabarcoding to investigate changes in soil microbial communities within forensic burial contexts, *Forensic Sci. Int. Genet.* 39 (2019) 73-85. https://doi.org/10.1016/j.fsigen.2018.12.002.

[19] C. Pérez-Martínez, M.D. Pérez-Cárceles, I. Legaz, G. Prieto-Bonete, A. Luna, Quantification of nitrogenous bases, DNA and Collagen type I for the estimation of the postmortem interval in bone remains, *Forensic Sci. Int.* 281 (2017) 106-112. https://doi.org/10.1016/j.forsciint.2017.10.039.

[20] F. Kanz, C. Reiter, D.U. Risser, Citrate Content of Bone for Time since Death Estimation: Results from Burials with Different Physical Characteristics and Known PMI, *J. Forensic Sci.* 59 (3) (2014) 613-620. http://dx.doi.org/10.1111/1556-4029.12341.

[21] H.P. Schwarcz, K. Agur, L.M. Jantz, A new method for determination of postmortem interval: citrate content of bone, *J. Forensic Sci.* 55 (6) (2010) 1516-1522. http://dx.doi.org/10.1111/j.1556-4029.2010.01511.x.

[22] V. Sterzik, T. Jung, K. Jellinghaus, M. Bohnert, Estimating the postmortem interval of human skeletal remains by analyzing their

optical behavior, *Int. J. Legal Med.* 130 (2016) 1557-1566. http://dx.doi.org/10.1007/s00414-016-1395-3.

[23] K. Jellinghaus, P.K. Urban, C. Hachmann, M. Bohnert, G. Hotz, W. Rosendahl, U. Wittwer-Backofen, Collagen degradation as a possibility to determine the post-mortem interval (PMI) of human bones in a forensic context – A survey, *Leg. Med.* 36 (2019) 96-102. https://doi.org/10.1016/j.legalmed.2018.11.009.

[24] Q. Wang, Y. Zhang, H. Lin, S. Zha, R. Fang, X. Wei, S. Fan, Z. Wang, Estimation of the late postmortem interval using FTIR spectroscopy and chemometrics in human skeletal remains, *Forensic Sci. Int.* 281 (2017) 113–120. https://doi.org/10.1016/j.forsciint.2017.10.033.

[25] D. Creagh, A. Cameron, Estimating the Post-Mortem Interval of skeletonized remains: The use of Infrared spectroscopy and Raman spectro-microscopy, *Radiat. Phys. Chem.* 137 (2017) 225–229. http://dx.doi.org/10.1016/j.radphyschem.2016.03.007.

[26] C. Woess, S.H. Unterberger, C. Roider, M. Ritsch-Marte, N. Pemberger, J. Cemper-Kiesslich, P. Hatzer-Grubwieser, W. Parson, J. Dominikus Pallua, Assessing various Infrared (IR) microscopic imaging techniques for post-mortem interval evaluation of human skeletal remains, *PLoS One* 12 (3) (2017). https://doi.org/10.1371/journal.pone.0174552.

[27] K.C. Doty, C.K. Muro, J. Bueno, L. Halámková, I.K. Lednev, What can Raman spectroscopy do for criminalistics?, *J. Raman Spectrosc.* 47 (2016) 39-50. https://doi.org/10.1002/jrs.4826.

[28] M. Raghavan, Investigation of Mineral and Collagen Organization in Bone Using Raman Spectroscopy, University of Michigan, Thesis (2011).

[29] C.L. King, N. Tayles, K.C. Gordon, Re-examining the chemical evaluation of diagenesis in human bone apatite, *J. Archaeol. Sci.* 38 (2011) 2222-2230. https://doi.org/10.1016/j.jas.2011.03.023.

[30] M.P.M. Marques, D. Gonçalves, A.I.C. Amarante, C.I. Makhoul, S.F. Parkerf, L.A.E. Batista de Carvalho, Osteometrics in burned human skeletal remains by neutron and optical vibrational spectroscopy, *RSCAdv.* 6 (2016) 68638-68641. https://doi.org/10.1039/C6RA13564A.

[31] M. Chikhani, R. Wuhrer, H. Green, Optimization of Sample Preparation Processes of Bone Material for Raman Spectroscopy, *J. Forensic Sci.* 63 (6) (2018) 1809-1812. https://doi.org/10.1111/1556-4029.13782.

[32] L. Eriksson, T. Byrne, E. Johansson, J. Trygg, C. Vikström, Multi- and megavariate data analysis. Basic principles and applications, 3rd ed., Umetrics Academy, 2013.

[33] S. Longato, C. Wöss, P. Hatzer-Grubwieser, C. Bauer, W. Parson, S.H. Unterberger, V. Kuhn, N. Pemberger, A.K. Pallua, W. Recheis, R. Lackner, R. Stalder, J.D. Pallua, Post-mortem Interval Estimation of Human Skeletal Remains by Micro-Computed Tomography, Mid-Infrared Microscopic Imaging and Energy Dispersive X-ray Mapping, *Anal. Methods* 7 (2015) 2917-2927. http://dx.doi.org/10.1039/c4ay02943g.

[34] Climate-data.org. https://es.climate-data.org/europe/espana/andalucia-252/ (accessed 3 January 2021).

[35] K. Golcuk, G.S. Mandair, A.F. Callender, N. Sahar, D.H. Kohn, M.D. Morris, Is photobleaching necessary for Raman imaging of bone tissue using a green laser?, *Biochim. Biophys. Acta - Biomembranes* 1758 (7) (2006) 868-873. https://doi.org/10.1016/j.bbamem.2006.02.022.

[36] R.W. Kennard, L.A. Stone, Computer aided design of experiments, *Technometrics* 11 (1969) 137-148. https://doi.org/10.1080/00401706.1969.10490666.

[37] L. Ortiz-Herrero, A.C. de Almeida Assis, L. Bartolomé, M.L. Alonso, M.I. Maguregui, R.M. Alonso, J.S. Seixas de Melo, A novel, non-

invasive, multi-purpose and comprehensive method to date inks in real handwritten documents based on the monitoring of the dye ageing processes, *Chemom. Intell. Lab. Syst.* 207 (2020) 104187. https://doi.org/10.1016/j.chemolab.2020.104187.

[38] M.D. Morris, G.S. Mandair, Raman Assessment of Bone Quality, *Clin. Orthop. Relat. Res.* 469 (2011) 2160-2169. https://doi.org/10.1007/s11999-010-1692-y.

[39] Z. Patonai, G. Maasz, P. Avar, J. Schmidt, T. Lorand, I. Bajnoczky, L. Mark, Novel dating method to distinguish between forensic and archaeological human skeletal remains by bone mineralization indexes, *Int. J. Legal Med.* 127 (2013) 529-533. https://doi.org/10.1007/s00414-012-0785-4.

CHAPTER 8

General discussion and prospects

8.1 General discussion

Forensic laboratories are equipped with state-of-the-art techniques and methodologies to meet the challenges posed by forensics, with special emphasis on those in the field of dating. However, they may not be sufficient to make a final decision due to the multidimensional and complex data that forensic experts have to deal with. In recent years, multivariate regression methods are revolutionising forensic dating by improving the performance of laboratories through the rapid and optimal handling and processing of such data with which meaningful and objective results on which to rely are being achieved [1, 2]. Their recent incorporation to this field, the limited statistical knowledge of forensic experts and the lack of standardised chemometric procedures, though, make their potential and optimal use practically unknown and, therefore, their acceptance continues to be a challenge with their implementation being available only in a few forensic laboratories [2, 3]. This thesis tries to reverse this situation by focusing on the important applicability of a multivariate linear regression method called PLSR to the field of forensic dating.

The major technological development undertaken in this thesis has been the implementation of multiple chemometric-based dating methodologies able to model the modifications experienced by the components of different forensic evidences throughout the ageing process, i.e. direct dating. Focusing on the field of questioned documents, **Chapter 2** presents a micro-destructive methodology for dating documents of up to 30 years old, stored under comparable conditions and manufactured with the same or similar type of paper as that of the study. Likewise, **Chapters 3 and 4** describe various methodologies for dating questioned documents containing handwritten ink strokes. With the first methodology, ballpoint pen inks of up to 5 years old, preserved under conditions comparable to those of the study and manufactured with the same ink formulation as

Inoxcrom®, could be dated non-destructively. Thus, ballpoint pen inks with a chromatographic profile equivalent to Inoxcrom®, such as Milan® and Paper Mate® brand pens, could be dated with an accuracy error of 25%. The second method made possible the non-invasive dating of counterfeit documents of up to 2 years of age, written with different pen ink brands and exposed to the same or slightly different storage conditions than those of the study. These methodologies are a breakthrough within the field of questioned document dating and constitute an outstanding alternative to the current ink dating methodologies, based on the analysis of volatile components, which are destructive and basically restricted to documents of up to 2 years old [4-6]. Referring to the field of art forgery, **Chapter 5** presents a non-destructive methodology for dating paintings of up to at least 22 years old, preserved under comparable conditions and created with the same brand of paint as that of the study. Subsequently, the extension study in **Chapter 6** would demonstrate that 14 to 22 years old paintings could be successfully dated with the long-term ageing OPLS model of the Liquitex® paint brand, despite the brands used in those paintings. However, artworks younger than 14 years would require exclusively tailored OPLS models. This was due to the fact that the paints underwent slower ageing processes at longer stages, which enabled them to fit the long-term ageing OPLS model (14-23% error), in spite of the differences in their formulation and the moderately different ageing conditions to which they were exposed. It is worth noting that this methodology represents an important technological progress, since until now there was no chemometric-based methodology that could be applied to the dating of contemporary artworks and that, therefore, it could provide invaluable data for authentication purposes. With regard to the field of medico-legal death investigation, **Chapter 7** describes a non-destructive methodology for estimating the PMI of human skeletons constrained at present to situations with similar conditions to the studied ones. Those of cemetery niches in a Mediterranean climate region. The implementation of

such a more refined methodology could complement or replace PMI determinations made on an empirical basis from the examiner's experience and base on subjective comparisons with previously documented cases showing similar characteristics and on morphological and histological analyses [7, 8].

On the other hand, since in **Chapters 2, 3 and 5** artificially aged samples were used for the construction of the chemometric models, the correlation between accelerated ageing and its equivalent to natural ageing had to be established so that these methodologies could have real applicability. Thus, it was possible to establish correlations for each matrix and temporal range. Approximately 5 hours of artificially ageing a document's paper under the set conditions were equivalent to one natural year under police custody conditions. Besides, approximately one hour of artificially ageing the ink deposited on a document under the established conditions proofed to be equivalent to 143 hours of natural ageing. In the case of the paints used in contemporary art, it was possible to determine an approximate equivalence of one year of natural ageing to 50 hours of accelerated ageing under the conditions studied. In addition to giving real applicability to the methodologies, the correlations established are of utmost importance for other purposes. For example, the latter would provide important information in the field of preventive conservation in Cultural Heritage with regard to addressing the durability and ageing performance issues of Liquitex® like acrylic paints. Likewise, the effectiveness of the materials used for the restoration and conservation of contemporary paintings could be tested with that correlation.

While this thesis has focused mainly on direct dating, a further method exists, which is indirect dating, based on the analysis of the composition of forensic evidence and its subsequent comparison with reference samples from collections [9]. Complementing both dating methods would add

information and ratify the results obtained by direct dating. This goal was reached in **Chapter 2**. 4-hydroxybutanoic acid and 2-hydroxy-3,4-dimethyl-2-cyclopentane-1-one were identified as characteristic compounds for a set of documents with ages between 1991 and 2011, except for that of 1986. Propanoic acid was detected in the three oldest documents and 4-hydroperoxy-1-phenyl-1-cyclohexene, 2-methyl benzofuran and naphthalene were characteristic of the 1986 document. Monitoring the presence or absence of these compounds would indirectly locate the questioned document within an approximate period of time, thus confirming the results provided by direct dating.

A further important point to highlight is that all the chemometric-based methodologies developed in the different chapters of the present thesis have employed micro- or non-destructive techniques, with none or minimal sampling and no sample pre-treatment. This underlines the ability of multivariate regression methods to couple with any analytical technique currently at the forefront of forensics. Great advantage since the techniques to which they will be coupled must preserve the integrity of the proof, often due to the legal relevance of forensic evidence and the need for counter-analysis [3].

Moreover, state-of-the-art techniques applied together with multivariate regression methods that have demonstrated great potential but lack of practical applicability, have been adapted by coupling them to a microscope, thus making them suitable for real forensic scenarios. **Chapters 3 and 4** reflect such flexibility of chemometrics. The former presents a non-destructive methodology for dating ballpoint pen inks using UV-Vis-NIR spectroscopy together with PLSR. However, the implementation of this methodology to real scenarios required adapting it to a microspectrophotometric technique, which has a smaller sample aperture and is therefore representative of handwritten strokes. Hence, the

study in Chapter 4 refers to a non-invasive methodology for dating inks in handwritten documents using Vis-MSP together with multivariate classification and regression methods.

Likewise, in relation to **Chapter 4**, it is worth mentioning that thanks to the statistical basis of multivariate regression methods, data handling and processing has been done in such a way that prediction error has been reduced to a minimum, thus providing reliable results with which to make objective decisions. Indispensable, since forensic evidence is often legally relevant, so inconsistencies in the results provided would have serious social and economic consequences, among others. Furthermore, reliable and firmly grounded results are a mandatory requirement for acceptance in a trial [10, 11]. In this regard, the methodology was systematised with the help of a flow chart, showing the various stages and statistical criteria to be met in order to confidently make an accurate age prediction for a questioned document with an error of less than 25%. The methodology also allowed for an easy detection of any document out of its applicability time range, thus out of the scope of the method. Whatever the case may be, the methodology gives rise to reliable results with a 95% confidence.

An additional useful chemometric tool presented in this thesis is the loadings plot, which has not only functioned as a filter-method for the selection of variables in **Chapter 7**, but has also allowed to determine which **X** variables are the most influential in the modelling of time throughout all chapters of this thesis. The identification of these variables has been facilitated when using the OPLSR method, since the horizontal axis of the loadings plot is represented by the predictive component [12]. Each of the **X** variables is associated with a certain wavelength/wavenumber corresponding to an area of the band or with a certain retention time corresponding to an area of the chromatographic peak and, therefore, to a specific compound in the forensic sample that is

modified during ageing. This knowledge is of utmost importance for a thorough understanding of the physical-chemical modifications that sample compounds undergo over time and which is of value to the criminal enquiry, in addition to providing supplementary information for other areas outside of forensics, as was the case in **Chapter 5**. From the loadings plot it was found that the short- and long-term ageing OPLS models of the Liquitex® paint brand were basically characterised by the modifications of the p(nBA-MMA) copolymer over time, which constitutes the binder in this type of paint formulation. The modifications of the PEO surfactant contributed to a lesser extent. On the contrary, the OPLS models of the Hyplar® paint brand were characterised by the degradation and migration of the PEO surfactant and, to a lesser extent, by the modifications of the PG7 pigment and the p(EA-MMA) copolymer which constitutes the binder. Knowing these differences in formulations and modifications throughout ageing is key to developing appropriate methodologies for the conservation and restoration of contemporary works of art.

Furthermore, the crime scenes the forensic experts face on a daily basis are widely diverse, so each of them will involve a specific type of evidence. This implies the need to build robust chemometric models with wide applicability. Since the majority of these methods are built from synthetic tailor made laboratory samples aged under controlled conditions, one would expect them to have a unique application and, therefore, each forensic scenario would need its own custom-made chemometric model. **Chapters 4 and 6**, however, have demonstrated that this is not always the case and that the same OPLS model can respond not only to the same sample nature used in its modelling, but also to those that meet certain requirements. Thus, we would not need an OPLS model for each possible evidence encountered at a crime scene, but for the most representative, fitting a larger number of them.

It is also worth noting the ability of coupling cutting-edge techniques with multivariate regression methods in the modelling of the modifications experienced by real case evidence throughout natural ageing, as it was the case in **Chapter 7.** Human skeletons buried in niches with a large inter-individual variability were used, enabling the construction of reliable age quantification models. This demonstrates the great potential of such models to cope with the complex and changeable conditions that real forensic cases may present, despite the fact that these variable conditions might affect the process of global physicochemical changes in forensic samples. This is of great importance, since, as mentioned above, OPLS models are often built under stable and controlled experimental conditions that may not be equal to natural conditions, so the data may fit the mathematical models too optimistically [13].

The results of each chapter in this thesis are presented as the basis to justify and promote the need of the forensic community to continue investigating the possibilities that chemometric tools may offer to forensics, in addition to encouraging the implementation of these tools in forensic laboratories in order to provide reliable answers to the questions posed to forensic experts at crime scenes.

8.2 Prospects

As modern technology advances, researchers are pursuing new smaller, portable, non-destructive and easy-to-use equipment. The popularity of hyperspectral imaging (HSI) systems and smartphone cameras is expected to increase rapidly in forensics in the near future. HSI combines the advantages of conventional spectroscopic techniques with those of imaging techniques, obtaining both spectral and spatial information, so researchers can analyse the chemical composition of forensic evidence and simultaneously visualise its spatial distribution. The HSI's fast

scanning system enables a wide area of evidence to be recorded in a few seconds, which addresses the representativeness issues that spectroscopic techniques present. Moreover, the portability of both HSI systems and smartphone cameras allows the forensic expert to transport them to the crime scene, where forensic evidence can be analysed and interpreted in the original context almost instantly. Thus, rapid data acquisition, ease of automation, portability, high system resolution, reduction of human error, non-destructiveness and non-contact analysis make HSI and smartphone cameras the future frontier of forensics [14]. However, these technologies as such do not fully exploit the large amount of data they provide, so these data will need to be chemometrically processed to select useful chemical information and improve the visual quality of the images with which to perform a detection, visualisation and identification of forensic evidence or even provide temporal information about it [15-19]. With regard to the latter utility, Thanakiatkrai *et al.* [19] hypothesised that the colour change in bloodstains due to their decay process could be quantitatively detectable by their digital images captured from smartphone cameras. This digital image is formed when an image sensor converts reflected light that has passed through three colour filters — red, green and blue (RGB) — into digital signals. The intensity of the RGB values determines the final colour of each pixel. These values and their counterparts —cyan, magenta, yellow and key (CMYK) — could be plotted against the time elapsed since the bloodstain was deposited to generate a calibration curve. Just as for the age estimation of bloodstains, this approach could be implemented similarly to other forensic evidence encountered at crime scenes, thus directing forensic dating towards emerging imaging techniques coupled with chemometrics.

References

[1] M. Bovens, B. Ahrens, I. Alberink, A. Nordgaard, T. Salonen, S. Huhtala, Chemometrics in forensic chemistry — Part I: Implications to the forensic workflow, *Forensic Sci. Int.* 301 (2019) 82–90. https://doi.org/10.1016/j.forsciint.2019.05.030.

[2] R. Kumar, V. Sharma, Chemometrics in forensic science, *TrAC Trends Anal. Chem.* 105 (2018) 191-201. https://doi.org/10.1016/j.trac.2018.05.010.

[3] C.S. Silva, A. Braz, M.F. Pimentel, Vibrational Spectroscopy and Chemometrics in Forensic Chemistry: Critical Review, Current Trends and Challenges, *J. Braz. Chem. Soc.* 30 (11) (2019) 2259-2290. http://dx.doi.org/10.21577/0103-5053.20190140.

[4] V.N. Aginsky, Dating and characterizing writing, stamp pad and jet printer inks by gas chromatography/mass spectrometry, *Int. J. Forensic Doc. Examiners* 2 (2) (1996) 103-116.

[5] J. Bügler, H. Buchner, A. Dallmayer, Age determination of ballpoint pen ink by thermal desorption and gas chromatography–mass spectrometry, *J. Forensic Sci.* 53 (4) (2008) 982-988. https://doi.org/10.1111/j.1556-4029.2008.00745.x.

[6] C. Weyermann, D. Kirsch, C. Vera, B. Splenger, A GC/MS study of the drying of ballpoint pen ink on paper, *Forensic Sci. Int.* 168 (2007) 119-127. https://doi.org/10.1016/j.forsciint.2006.06.076.

[7] J.L. Prieto, C. Magaña, D.H. Ubelaker, Interpretation of Postmortem Change in Cadavers in Spain, *J. Forensic Sci.* 49 (5) (2004) 918-923. http://dx.doi.org/10.1520/JFS2003337.

[8] A. Cappella, D. Gibelli, E. Muccino, V. Scarpulla, E. Cerutti, V. Caruso, E. Sguazza, D. Mazzarelli, C. Cattaneo, The comparative performance of PMI estimation in skeletal remains by three methods (C-14, luminol test and OHI): analysis of 20 cases, *Int. J. Legal Med.*

132 (4) (2015) 1215-1224. http://dx.doi.org/10.1007/s00414-015-1152-z.

[9] M. Calcerrada, C. García-Ruiz, Analysis of questioned documents: a review, *Anal. Chim. Acta* 853 (2015) 143-166. https://doi.org/10.1016/j.aca.2014.10.057.

[10] C. Weyermann, O. Ribaux, Situating forensic traces in time, *Sci. Justice* 52 (2012) 68-75. http://dx.doi.org/10.1016/j.scijus.2011.09.003.

[11] A.C.A. Assis, End user commentary on emerging approaches in the analysis of inks on questioned documents, in: S. Francese (Ed.), Emerging Technologies for the Analysis of Forensic Traces, Advanced Sciences and Technologies for Security Applications, Springer, Cham, 2019, pp. 179-182. https://doi.org/10.1007/978-3-030-20542-3_12.

[12] L. Eriksson, T. Byrne, E. Johansson, J. Trygg, C. Vikström, Multi- and Megavariate Data Analysis. Basic Principles and Applications, third ed., Umetrics Academy, 2013.

[13] Q. Wang, Y. Zhang, H. Lin, S. Zha, R. Fang, X. Wei, S. Fan, Z. Wang, Estimation of the late postmortem interval using FTIR spectroscopy and chemometrics in human skeletal remains, *Forensic Sci. Int.* 281 (2017) 113-120. https://doi.org/10.1016/j.forsciint.2017.10.033.

[14] G.J. Edelman, E. Gaston, T.G. van Leeuwen, P.J. Cullen, M.C.G. Aalders, Hyperspectral imaging for non-contact analysis of forensic traces, *Forensic Sci. Int.* 223 (2012) 28-39. http://dx.doi.org/10.1016/j.forsciint.2012.09.012.

[15] B. Li, P. Beveridge, W.T. O'Hare, M. Islam, The age estimation of blood stains up to 30 days old using visible wavelength hyperspectral image analysis and linear discriminant analysis, *Sci. Justice* 53 (2013) 270-277. http://dx.doi.org/10.1016/j.scijus.2013.04.004.

[16] G. Edelman, T.G. van Leeuwen, M.C.G. Aalders, Hyperspectral imaging for the age estimation of bloodstains at the crime scene,

Forensic Sci. Int. 223 (2012) 72-77. http://dx.doi.org/10.1016/j.forsciint.2012.08.003.

[17] C. Woess, S.H. Unterberger, C. Roider, M. Ritsch-Marte, N. Pemberger, J. Cemper-Kiesslich, P. Hatzer-Grubwieser, W. Parson, J. Dominikus Pallua, Assessing various Infrared (IR) microscopic imaging techniques for post-mortem interval evaluation of human skeletal remains, *PLoS One* 12 (3) (2017). https://doi.org/10.1371/journal.pone.0174552.

[18] P. Tramini, B. Bonnet, R. Sabatier, L. Maury, A method of age estimation using Raman microspectrometry imaging of the human dentin, *Forensic Sci. Int.* 118 (2001) 1-9. https://doi.org/10.1016/S0379-0738(00)00352-2.

[19] P. Thanakiatkrai, A. Yaodam, T. Kitpipit, Age estimation of bloodstains using smartphones and digital image analysis, *Forensic Sci. Int.* 233 (2013) 288-297. http://dx.doi.org/10.1016/j.forsciint.2013.09.027.

.

CHAPTER 9

Conclusions

Conclusions

The most important conclusions of this thesis are summarised below.

1. Multivariate regression models built from both natural and accelerated ageing samples have succeeded in being applied to the dating of evidence from various forensic fields.

2. Multivariate regression methods can be successfully coupled with any analytical technique that is at the forefront of forensics.

3. The preparation of synthetic tailor made laboratory samples aged under accelerated conditions has enabled the building of (O)PLS models in a field such as forensics where obtaining real samples is extremely difficult. These samples have also allow for wider dating time interval methods, which would be very time-consuming and difficult to achieve by using naturally aged samples.

4. Several of the developed methodologies have improved and overcome the disadvantages or objectives not reached by the preceding methodologies.

5. The age estimation models built in this work can be easily updated as new samples are added, rendering more robust and reliable models.

6. The developed chemometric-based dating methodologies have been able to respond to real-life claims that conventional methodologies fail to cope with.

7. The statistical basis of chemometrics has made it possible to provide reliable and objective age estimates, indispensable for acceptance and decision-making in the courts.

8. A clear guideline has been provided to the forensic community with the steps to be followed for the optimal application of multivariate regression methods to the dating of any forensic evidence that may be encountered in future scenarios.

9. The testing for the applicability of the developed methodologies to real-life scenarios has involved the participation of scientific police units, academic institutions and artists, as it should be the case.

Annex

List of scientific publications included in this thesis

L. Ortiz-Herrero, M.E. Blanco, C. García-Ruiz, L. Bartolomé, Direct and indirect approaches based on paper analysis by Py-GC/MS for estimating the age of documents, *J. Anal. Appl. Pyrolysis* 131 (2018) 9-16. https://doi.org/10.1016/j.jaap.2018.02.018.

L. Ortiz-Herrero, L. Bartolomé, I. Durán, I. Velasco, M.L. Alonso, M.I. Maguregui, M. Ezcurra, DATUVINK pilot study: A potential non-invasive methodology for dating ballpoint pen inks using multivariate chemometrics based on their UV–vis-NIR reflectance spectra, *Microchem. J.* 140 (2018) 158-166. https://doi.org/10.1016/j.microc.2018.04.019.

L. Ortiz-Herrero, I. Cardaba, S. Setien, L. Bartolomé, M.L. Alonso, M.I. Maguregui, OPLS multivariate regression of FTIR-ATR spectra of acrylic paints for age estimation in contemporary artworks, *Talanta* 205 (2019) 120114. https://doi.org/10.1016/j.talanta.2019.120114.

L. Ortiz-Herrero, I. Cardaba, L. Bartolomé, M.L. Alonso, M.I. Maguregui, Extension study of a statistical age prediction model for acrylic paints, *Polym. Degrad. Stab.* 179 (2020) 109263. https://doi.org/10.1016/j.polymdegradstab.2020.109263.

L. Ortiz-Herrero, A.C. de Almeida Assis, L. Bartolomé, M.L. Alonso, M.I. Maguregui, R.M. Alonso, J.S. Seixas de Melo, A novel, non-invasive, multi-purpose and comprehensive method to date inks in real handwritten documents based on the monitoring of the dye ageing processes, *Chemom. Intell. Lab. Syst.* 207 (2020) 104187. https://doi.org/10.1016/j.chemolab.2020.104187.

Journal of Analytical and Applied Pyrolysis 131 (2018) 9–16

Contents lists available at ScienceDirect

Journal of Analytical and Applied Pyrolysis

journal homepage: www.elsevier.com/locate/jaap

Direct and indirect approaches based on paper analysis by Py-GC/MS for estimating the age of documents

L. Ortiz-Herrero[a,*], M.E. Blanco[a], C. García-Ruiz[b,c], L. Bartolomé[d]

[a] Analytical Chemistry Department, Faculty of Science and Technology, University of the Basque Country (UPV/EHU), Barrio Sarriena S/N, 48940 Leioa, Bizkaia, Spain
[b] University Institute of Research in Police Sciences, University of Alcalá, Ctra. Madrid-Barcelona Km. 33.600, 28871 Alcalá de Henares, Madrid, Spain
[c] Department of Analytical Chemistry, Physical Chemistry and Chemical Engineering, Edificio Polivalente de Química, University of Alcalá, Ctra. Madrid-Barcelona Km. 33.600, 28871 Alcalá de Henares, Madrid, Spain
[d] Advances Research Facilities (SGIker), Faculty of Science and Technology, University of the Basque Country (UPV/EHU), Barrio Sarriena S/N, 48940 Leioa, Bizkaia, Spain

ARTICLE INFO

Keywords:
Questioned document
Paper
Py-GC/MS
Age estimation
Multivariate regression

ABSTRACT

The age of a relatively old document is one of the pending issues to be resolved in the field of forensic documentary examination. Although nowadays there are a variety of analytical methodologies focused in the analysis of inks for dating documents, the paper analysis has attained little attention. This work aims to develop two complementary approaches for estimating the age of documents based on paper analysis employing the pyrolysis technique coupled to gas chromatography with detection by mass spectrometry (Py-GC/MS): (i) a direct approach using the pyrolytic fingerprints and multivariate regression with artificially aged samples, and (ii) an indirect approach based on the identification of compounds characteristic of the document period. The direct approach has successfully allowed the age estimation of relatively old documents under police custody (up to 30 years of age) and the determination of a relation between the natural and the accelerated aging of paper under the used conditions. This approach is applicable to papers that have the same (or similar) composition and have been stored under comparable storage conditions. Additionally, the indirect approach is presented as an interesting perspective to ratify valuable information of the document age.

1. Introduction

The analysis of documents is a matter of great interest in the forensic analysis field. From handwritten texts and signatures to printed papers, a broad range of document types may be subject to analysis (e.g. to identity certifying documents, commercial documents or industrial and intellectual property documents). These are commonly legal documents of mandatory compliance and/or with economic, administrative, labour and social implications. The wide variety and complexity of documents hinders their analysis and, therefore, several aspects of the forensic science aimed to study documents (named as documentoscopy) remain so far unsolved. The estimation of the age of a document is one of these pending issues to be resolved [1–3].

Although the body of a document may be constituted of many different materials—as for example granodiorite in the famous Rosetta Stone—for many centuries paper has been the principal component used in documentation all over the world [4]. Since the first paper made in China before the year 105 CE, composed of fragments of cloth or silk threads, different materials have been used. In 751, Arabs varied and improved the composition of paper to reduce the cost of manufacture, employing mixtures of linen, hemp and cotton. In the 10th century, a mixture of linen seeds was used in the Armenian paper [5]. In 1450, the supply problems that emerged with the invention of the printing press spurred the production of new types of paper, mainly based in the use of plants. Nowadays, paper is primarily manufactured with fibres of cellulose and hemicelluloses and wood fibres, with several impurities such as lignin, pectins, traces of resins, tannins, carbohydrates and waxes [2,4,6,7]. In addition, small amounts of organic and inorganic additives like inks, adhesives, fillers and bleaches are commonly added to improve the properties of the paper.

By analysing its composition, it is possible to characterize the origin of a paper through their trace elements, which can differ from one manufacturer to another [6,7]. By this way, a unique chemical fingerprint can be identified for each batch or sheet of paper [4]. Therefore, paper could provide crucial information about the production of manuscripts that may not be found in any other kind of evidence [2,4,7–9].

Nevertheless, paper does not remain unchanged over time [10] as it

* Corresponding author.
E-mail addresses: laura.ortiz@ehu.eus (L. Ortiz-Herrero), maria.blanco@iit.it (M.E. Blanco), carmen.gruiz@uah.es (C. García-Ruiz), luis.bartolome@ehu.eus (L. Bartolomé).

https://doi.org/10.1016/j.jaap.2018.02.018
Received 29 September 2017; Received in revised form 16 February 2018; Accepted 18 February 2018
Available online 21 February 2018
0165-2370/

Microchemical Journal 140 (2018) 158–166

Contents lists available at ScienceDirect

Microchemical Journal

journal homepage: www.elsevier.com/locate/microc

DATUVINK pilot study: A potential non-invasive methodology for dating ballpoint pen inks using multivariate chemometrics based on their UV–vis-NIR reflectance spectra

L. Ortiz-Herrero[a,*], L. Bartolomé[b], I. Durán[a], I. Velasco[a], M.L. Alonso[a], M.I. Maguregui[c], M. Ezcurra[d]

[a] Analytical Chemistry Department, Faculty of Science and Technology, University of the Basque Country (UPV/EHU), Barrio Sarriena S/N, 48940 Leioa, Bizkaia, Spain
[b] Advances Research Facilities (SGIker), Faculty of Science and Technology, University of the Basque Country (UPV/EHU), Barrio Sarriena S/N, 48940 Leioa, Bizkaia, Spain
[c] Painting Department, Faculty of Fine Arts, University of the Basque Country (UPV/EHU), Barrio Sarriena S/N, 48940 Leioa, Bizkaia, Spain
[d] LEYAS Investigaciones Forenses Documentales S.L., 31011 Pamplona, Spain

ARTICLE INFO

Keywords:
Ballpoint pen ink
Diffuse reflectance
Ink dating
Multivariate regression

ABSTRACT

The main methods for dating ballpoint pen inks in questioned documents used up to day are based mainly on the analysis of ink volatile components. These methods have some limitations still unresolved, such as the impossibility for dating documents older than two to five years and the destruction in part or totally of the questioned document after the analysis. This study aims to overcome these drawbacks by exploring the feasibility of dating inks based on their spectroscopic UV–vis-NIR diffuse reflectance spectra monitoring combined with a Partial Least-Squares (PLS) multivariate modelling. Inoxcrom® ink samples were exposed to artificial aging, their reflectance spectra were measured and a multivariate calibration was applied. Mathematical pretreatments of the spectroscopic data were carried out to enhance the prediction ability of the models and the qualitative interpretation of the spectra. The best PLS model was obtained after SNV spectral filter. Accurate predictions (RSD of 25%) were obtained for two of the five pen inks analysed and a correlation between the natural aging and the accelerated artificial aging could be established. Moreover, the spectra region more closely related to the ink aging process could be delimited, in which younger inks were characterized by modifications in the visible and NIR spectra region, while after aging the most influential region was the NIR spectrum. The mismatch with the other three pen inks tested could be attributed to consistent differences in ink formulations. Inks sharing a common chromatographic profile proved to fit correctly in the predictive model indicating that the methodology shows a great potential for future applications in the field of questioned documents dating.

1. Introduction

In the forensic field of documents, most of the analyses are focused on documents made up of paper and ink. A huge number of studies have been carried out both on the printing system and on the handwriting tool [1,2]. One of the main arising problems is the need for dating questioned documents, either by determining the time an ink has been deposited on a paper or by comparing the relative dates of different constituents within the document [1,3,4]. Currently, only partial solutions have been found to this problem mainly due to the large number of factors involved in the ink aging process [5–9]. In addition, an added difficulty is that practically all of the dating methods developed until now are destructive, removing total or partially the test sample [10–15].

Most ink dating studies have been carried out with viscous ink writing tools, like ballpoint pens. Ink is a complex homogeneous medium, made up of solvents, pigments, dyes, resins, lubricants, solubilizers, surfactants, particulate matters or fluorescers among other constituents [1]. In the last decade, several methods for ink dating have been developed based on different components of ink formulations. However, nowadays the most used methods focus on the loss of ink volatile components by applying Gas Chromatography/Mass Spectrometry (GC/MS) technique. These compounds diminish over time and most of them will evaporate in a few minutes after being deposited on

* Corresponding author.
E-mail addresses: laura.ortiz@ehu.eus (L. Ortiz-Herrero), luis.bartolome@ehu.eus (L. Bartolomé), marialuz.alonso@ehu.eus (M.L. Alonso), itxaso.maguregui@ehu.eus (M.I. Maguregui), mezcurra@leyas.es (M. Ezcurra).

https://doi.org/10.1016/j.microc.2018.04.019
Received 26 October 2017; Received in revised form 15 April 2018; Accepted 15 April 2018
Available online 17 April 2018

Talanta 205 (2019) 120114

Contents lists available at ScienceDirect

Talanta

journal homepage: www.elsevier.com/locate/talanta

OPLS multivariate regression of FTIR-ATR spectra of acrylic paints for age estimation in contemporary artworks

L. Ortiz-Herrero[a,*], I. Cardaba[b], S. Setien[a], L. Bartolomé[c], M.L. Alonso[a], M.I. Maguregui[b]

[a] Analytical Chemistry Department, Faculty of Science and Technology, University of the Basque Country (UPV/EHU), Barrio Sarriena S/N, 48940, Leioa, Bizkaia, Spain
[b] Painting Department, Faculty of Fine Arts, University of the Basque Country (UPV/EHU), Barrio Sarriena S/N, 48940, Leioa, Bizkaia, Spain
[c] Advances Research Facilities (SGIker), Faculty of Science and Technology, University of the Basque Country (UPV/EHU), Barrio Sarriena S/N, 48940, Leioa, Bizkaia, Spain

ARTICLE INFO

Keywords:
Acrylic paint
Artwork dating
FTIR-ATR
OPLS

ABSTRACT

In recent years the interest and demand for artworks has been increasing as they are an interesting commercial investment due to their growing value in the market. This explains the increasing number of counterfeits dealing with artworks that has led to the development of new methodologies for their characterization. The material characterization of these types of works can provide relevant information for both authentication and conservation/restoration. Thus, in this study multivariate chemometric methods were applied to FTIR-ATR spectroscopic data for artwork dating purposes. To that end, ageing prediction models were developed for Liquitex® and Hyplar® brands. Paint samples containing the green synthetic organic pigment (PG7), were exposed to artificial ageing and analysed with FTIR-ATR and Py-GC/MS for characterization and monitorization of the main components (binding medium, pigment and additives). Although the OPLS ageing models were mainly characterized by the modifications suffered by both the binder and the surfactants, a universal model could not be developed due to differences in the modification trends of the different brands. The applicability of the OPLS modelling for artwork dating purposes was tested in artworks provided by internationally recognized contemporary Basque artists. For Liquitex® a significant correlation ($p < 0.05$) between natural and accelerated ageing could be established, in which approximately 50 h of accelerated ageing under the applied conditions were equivalent to one natural year. This correlation might have possible applications in the dating of artworks for up to at least 22 years. Thus, the study demonstrates that FTIR-ATR combined with chemometrics is a potential method for artwork dating and a valuable source of information about the chemical processes involved in paint ageing, which can be of great help in the conservation and restoration steps.

1. Introduction

The contemporary art market is very dynamic and its increasing demand involves hundreds of millions of dollars per year. However, several serious problems given within the art market are intensifying fraud and limiting its growth potential. Illicit art trade has become the third illegal market after drugs and weapons [1,2]. Today there are many counterfeits present in museums and galleries that are sold, exchanged and exhibited among collectors and art institutions [3]; in fact, half of artworks currently in circulation may be counterfeits [4]. Hundred billions of dollars are spent worldwide on art every year and a great part of that is tainted by illegal and illicit activities causing damages in millions to museums, galleries and collectors [5].

Forgers are mainly copying artworks dated from the early to mid-20th century, as it is much easier to acquire authentic materials and modern paintings have increased in value in recent years [6]. Artistic reasons are also included that may affect the falsification. Contemporary art is easily copied since in many cases the "exclusivity" of the design is not available as many are serial works. In addition, the "manual dexterity" of the artists is not always evident (unlike old masters), since many of them are conceptual artworks. The massive production and short age of most of the works mean a vast amount of works with similar characteristics difficult to differentiate. Therefore a correct material characterization of these works aimed to the identification and precise dating of the materials used, could be of great help in detecting counterfeited or misattributed works.

The most widely used materials by contemporary artists are acrylic paints. Introduced to the market in the mid-1950s, acrylic emulsion

* Corresponding author.
E-mail addresses: laura.ortiz@ehu.eus (L. Ortiz-Herrero), irene.cardaba@ehu.eus (I. Cardaba), luis.bartolome@ehu.eus (L. Bartolomé), marialuz.alonso@ehu.eus (M.L. Alonso), itxaso.maguregui@ehu.eus (M.I. Maguregui).

https://doi.org/10.1016/j.talanta.2019.120114
Received 12 April 2019; Received in revised form 1 July 2019; Accepted 2 July 2019
Available online 03 July 2019

Polymer Degradation and Stability 179 (2020) 109263

Contents lists available at ScienceDirect

Polymer Degradation and Stability

journal homepage: www.elsevier.com/locate/polydegstab

Extension study of a statistical age prediction model for acrylic paints

L. Ortiz-Herrero [a, *], I. Cardaba [b], L. Bartolomé [c], M.L. Alonso [a], M.I. Maguregui [b]

[a] Analytical Chemistry Department, Faculty of Science and Technology, University of the Basque Country (UPV/EHU), Barrio Sarriena S/N, 48940, Leioa, Bizkaia, Spain
[b] Painting Department, Faculty of Fine Arts, University of the Basque Country (UPV/EHU), Barrio Sarriena S/N, 48940, Leioa, Bizkaia, Spain
[c] Advances Research Facilities (SGIker), Faculty of Science and Technology, University of the Basque Country (UPV/EHU), Barrio Sarriena S/N, 48940, Leioa, Bizkaia, Spain

ARTICLE INFO

Article history:
Received 20 February 2020
Received in revised form
20 May 2020
Accepted 6 June 2020
Available online 8 June 2020

Keywords:
Acrylic paint
Dating
FTIR-ATR
OPLS

ABSTRACT

In this work, the robustness and potential applicability of statistical age prediction models applied to the dating of different acrylic paints were studied. The FTIR-ATR analysis of three acrylic colours (Hansa yellow, phthalocyanine green and ultramarine blue) from two manufacturers (Liquitex® and Vallejo®) subjected to accelerated ageing was carried out. The acrylic paints were characterised and the modifications of their ATR spectra throughout ageing were studied. Predictive models developed with the Liquitex® brand containing phthalocyanine green pigment were then applied to other colour and brands of acrylic paints and their robustness and feasibility were studied based on calculated accuracy error values. The influence of the pigment on the ageing of the paint components, the type and quantity of additives present in the acrylic paint as well as the ageing conditions to which it was subjected were decisive in the short-term predictive model, which explains the low accuracy values obtained for all the acrylic paints analysed. However, the slower degradation processes taking place in the longer term and the stabilisation of the acrylic paints at higher stages of ageing made them fit successfully into the long-term model, obtaining an error of between 14 and 23%. Thus, the predictive statistical model is robust and feasible to be used for different colours of the same brand of acrylic paint as well as for acrylic paints of different brands that have been long-term aged under slightly different conditions of accelerated ageing. In conclusion, this methodology could be a promising tool in the field of dating contemporary artworks of a certain age.

1. Introduction

The contemporary art market is experiencing an unprecedented level of buying and selling activity that generates millions of dollars worldwide. As art prices rise, art-related crime is on the increase, making counterfeiting a multi-million dollar enterprise. The uncovering of fake artworks has a negative impact on the entire art market. That is why new technologies are being used to detect counterfeits that have already entered the art market as well as to prevent their sale and acquisition [1,2].

Non-destructive techniques such as Raman spectroscopy [3–6], Fourier transform infrared spectroscopy (FTIR) [3], IR hyper spectral imaging (IR-HIS) [7,8], FTIR-attenuated total reflection (FTIR-ATR) [6,9], IR reflection [10] and scanning electron microscopy-energy dispersive X-ray spectroscopy (SEM-EDX) [6,9] are usually used as first option as they do not damage the work of art [3,6,9]. Among the techniques, FTIR-ATR spectroscopy is widely used for the characterisation of artwork materials [6,9,11] and for the study of the influence of pigments on the photodegradation of acrylic paints [12–15].

In some cases, non-invasive techniques are not enough, so analytical techniques combined with statistical methods, such as multivariate chemometrics, have been widely used to extract the maximum and most representative information from the acquired data in an interpretable manner. Partial Least Squares (PLS) is an X→y regression methodology typically used for either predictive purposes or control monitoring. Despite the applications of partial least squares (PLS) for quantification of paint components in the restoration of artworks [16] as well as for the determination of their properties in quality control [17], there are not many studies that

* Corresponding author.
E-mail addresses: laura.ortiz@ehu.eus (L. Ortiz-Herrero), irene.cardaba@ehu.eus (I. Cardaba), luis.bartolome@ehu.eus (L. Bartolomé), marialuz.alonso@ehu.eus (M.L. Alonso), itxaso.maguregui@ehu.eus (M.I. Maguregui).

https://doi.org/10.1016/j.polymdegradstab.2020.109263
0141-3910/

Chemometrics and Intelligent Laboratory Systems 207 (2020) 104187

Contents lists available at ScienceDirect

Chemometrics and Intelligent Laboratory Systems

journal homepage: www.elsevier.com/locate/chemometrics

A novel, non-invasive, multi-purpose and comprehensive method to date inks in real handwritten documents based on the monitoring of the dye ageing processes

L. Ortiz-Herrero [a,*], A.C. de Almeida Assis [b], L. Bartolomé [c], M.L. Alonso [a], M.I. Maguregui [d], R.M. Alonso [a], J.S. Seixas de Melo [e]

[a] Analytical Chemistry Department, Faculty of Science and Technology, University of the Basque Country (UPV/EHU), Barrio Sarriena S/N, 48940, Leioa, Bizkaia, Spain
[b] Scientific Police Laboratory, Judiciary Police, Rua Gomes Freire, 174, 1169-007, Lisbon, Portugal
[c] Advances Research Facilities (SGIker), Martina Casiano Technology Platform, University of the Basque Country (UPV/EHU), Barrio Sarriena S/N, 48940, Leioa, Bizkaia, Spain
[d] Painting Department, Faculty of Fine Arts, University of the Basque Country (UPV/EHU), Barrio Sarriena S/N, 48940, Leioa, Bizkaia, Spain
[e] Coimbra Chemistry Centre, Department of Chemistry, University of Coimbra, Rua Larga, 3004-535, Coimbra, Portugal

ARTICLE INFO

Keywords:
Ballpoint pen
Gel pen
Ink dating
Dyes
Vis-microspectrophotometry
OPLS
Forensic chemistry
Questioned documents

ABSTRACT

Blue ink strokes belonging to 11 types of writing tools from 7 different brands were naturally aged in the darkness for 2 years and characterised by Vis-microspectrophotometry (Vis-MSP). Ink clustering and classification was performed by applying principal component analysis (PCA) and hierarchical cluster analysis (HCA) in order to subsequently assign an optimal orthogonal partial least squares (OPLS) model capable to predict the age of different inks. This method was found applicable to the exact dating of forged documents with ink strokes of up to 2 years old. The method was tested with blind samples supplied by the Forensic Science Unit of the Basque Country Police Department. Age predictions ($p < 0.05$) with an accuracy error below 25% were obtained whenever: (i) the two ink replicas were placed inside the ellipse of the predicted score graph, (ii) the age of the ink was within the temporary application range of the OPLS model, and (iii) the ink was found to fit correctly in any of the classifications of the pen brands studied. The OPLS model was also able to detect those inks out of its temporary application range, if the ink samples were correctly clustered in the PCA model and/or classified in the HCA model with one of the pen brands studied, but one of the two ink replicas was placed outside the ellipse of the predicted score graph. Thus, these inks were temporarily above or below the application limit of the OPLS model of the corresponding pen brand.

1. Introduction

Forgery of documents and the fight against this type of illegal activity is an everyday reality which is increasing and can have serious and far-reaching negative implications for companies, individuals and political entities. This crime is not only for profit, but may also constitute a means to other ends, such as terrorism, smuggling of migrants and trafficking in persons. The different units of law enforcement agencies have therefore been forced to collaborate and develop new methodologies to deal with these crimes [1].

Counterfeit material may consist of contracts, wills, titles and deeds, bank checks, suicide notes, agreements, ID cards, handwritten correspondence, etc. The study of these materials implies their chemical analysis as well as the use of physical and optical techniques either to determine their authorship, the alterations made to them or to date them. The dating of documents is one of the most studied tasks, but also one of the most challenging due to the great variety of pen brands and ink formulations on the market. Moreover, the lack of knowledge of the conditions under which the documents were exposed and the lack of inter-laboratory validation and applicability assessment of the methodologies developed are also critical issues in the reliability of the results [2–6], and rightfully questioned when presented in court cases [7].

The most commonly used writing tools are ballpoint pens, which contain viscous oil-based inks, as well as rollerball pens, containing

* Corresponding author.
E-mail addresses: laura.ortiz@ehu.eus (L. Ortiz-Herrero), ana.assis@pj.pt (A.C. de Almeida Assis), luis.bartolome@ehu.eus (L. Bartolomé), marialuz.alonso@ehu.eus (M.L. Alonso), itxaso.maguregui@ehu.eus (M.I. Maguregui), rosamaria.alonso@ehu.eus (R.M. Alonso), sseixas@ci.uc.pt (J.S. Seixas de Melo).

https://doi.org/10.1016/j.chemolab.2020.104187
Received 22 April 2020; Received in revised form 17 September 2020; Accepted 22 October 2020
Available online 24 October 2020

eman ta zabal zazu

Universidad del País Vasco

Euskal Herriko Unibertsitatea

CAMPUS OF INTERNATIONAL EXCELLENCE